离子液体与光电子能谱

Ionic liquids and photoelectron spectroscopy

（英文版）

刘艳辉　门　爽　高景龙　著

Liu Yanhui　Men Shuang　Gao Jinglong

電子工業出版社

Publishing House of Electronics Industry

北京・BEIJING

内容简介

本书从光电子能谱的角度，揭示了结构与性能间的相互关系，对离子液体进行了系统、详细的阐述。同时对离子液体中的催化剂体系进行了简要介绍。

本书共 6 章，介绍了离子液体主要物理化学性质、离子液体合成、X 射线光电子能谱，还从光电子能谱角度研究了离子液体体系和离子液体中催化剂体系等。

本书既注重理论知识的传授，又强调实际应用。本书可作为有关技术人员的参考用书，也可供高等学校材料类、化学类或其他相关专业参考使用。

图书在版编目（CIP）数据

离子液体与光电子能谱 = Ionic liquids and photoelectron spectroscopy：英文/刘艳辉，门爽，高景龙著. —北京：电子工业出版社，2017.12
ISBN 978-7-121-33370-5

Ⅰ. ①离… Ⅱ. ①刘… ②门… ③高… Ⅲ. ①离子－液体－研究－英文 ②光电子谱法－研究－英文 Ⅳ. ①O646.1 ②O657.39

中国版本图书馆 CIP 数据核字（2017）第 322964 号

责任编辑：杨秋奎
印　　刷：
装　　订：
出版发行：电子工业出版社
　　北京市海淀区万寿路 173 信箱　邮编 100036
开　　本：787×1092　1/16　印张：11　字数：268 千字
版　　次：2017 年 12 月第 1 版
印　　次：2017 年 12 月第 1 次印刷
定　　价：49.00 元

凡所购买电子工业出版社图书有缺损问题，请向购买书店调换。若书店售缺，请与本社发行部联系，联系及邮购电话：（010）88254888，88258888。

质量投诉请发邮件至 zlts@phei.com.cn，盗版侵权举报请发邮件至 dbqq@phei.com.cn。

本书咨询联系方式：（010）88254694。

Preface

This book is written based upon the research work being conducted by Dr. Yanhui Liu, Prof. Jinglong Gao and myself (all from Shenyang Ligong University). The commencement of this project dates back to the year of 2008, when I firstly joined the Nottingham Ionic Liquids group. Throughout the whole of my Ph.D study, many attempts had been made with the view of demonstrating the electronic environment of ionic liquids by the state-of-the-art ultra high vacuum technique, X-ray photoelectron spectroscopy. I was a bit of luck to have finally systematically investigated three families of ionic liquids, including imidazolium, pyrrolidinium and pyridinium, as well as directly probed the interaction of solute-solvent and solute-ligand in ionic liquids. I was delighted to see these studies had made this field expanded and matured.

It was in the year of 2012, when Dr. Liu and I founded the Ionic Liquid Group at Shenyang Ligong University. I am fortunate to have collaborated with Dr. Liu, who has shown strong background in theory and great intelligence in doing research. With her tremendous helps, I am flattered to see we could add something to this research area. The recent publishing of the paper about the impact of the cation acidity on the cation-anion interaction in ionic liquids inspires us to finish this book, which summarily describes all aspects of our research with reference to ionic liquids.

Herein, we bring all results together in a coherent and smooth account of the field in simple words. *Chapter 1* and *Chapter 2*, which briefly introduce the basic aspects of ionic liquids and the XPS technique respectively, were written by Dr. Liu. One of the results chapters, *Chapter 5*, was also written by Dr. Liu. I wrote two of the results chapters, *Chapter 3* and *Chapter 4*. The

Appendix, which demonstrates XP spectra for all ionic liquids studied in this book was written by Prof. Gao. We hope some may read this book for basic understanding, some for further improvement and some for enjoyment.

So many people helped me in this project, whom if I do not show my appreciation, I will be failing in my duty. To Prof. Peter Licence who is my academic Ph.D supervisor and the person I respect the most, I owe my biggest debt grateful. His wisdom and encouragement is always a constant source of motivation throughout the whole of my research life. Furthermore, I am on behalf of Dr. Liu to acknowledge the International Cooperation Project (F16-214-6-00) from the Department of Science and Technology of City of Shenyang for financial support. Last but not least, I must thank Dr. Liu and Prof. Gao once again, for spending several months with me in front of the laptop preparing this book.

Men Shuang

November 19th 2017

前　言

离子液体主要是指完全由有机阳离子及无机或有机阴离子组成的，在室温或接近室温的温度下呈现出液体状态的熔融盐类。离子液体具有不易挥发、无污染、不易燃、易与产物分离、易回收、可循环使用及使用方便等优点，是传统有机溶剂的理想替代品。它有效地避免了传统有机溶剂造成的环境污染、健康问题、安全隐患及设备腐蚀等问题，是名副其实的、环境友好的“绿色溶剂”，适应清洁技术和可持续发展的要求。

近年来，离子液体的应用已经处于工业试验阶段，即将进入工业应用；因为离子液体种类繁多，每一种化学反应在离子液体中进行都有可能取得与传统方法不同的、令人惊异的结果，这一巨大的化学新宝藏有待我们去开发。

笔者所在课题组近几年来以咪唑类离子液体为突破口，一直从事离子液体的合成、提纯、表征及应用研究。本书不仅介绍了课题组成员的大量研究结果，也介绍了相关的基本知识。

本书共 5 章，第 1 章、第 2 章和第 5 章由沈阳理工大学刘艳辉博士编写，第 3 章和第 4 章由沈阳理工大学门爽博士编写，附录由沈阳理工大学高景龙教授编写。本书的出版得到了沈阳理工大学学科发展规划处学术专著基金和沈阳市科技局国际合作处国际合作项目（F16-214-6-00）的共同资助。在本书的编写过程中，英国诺丁汉大学 Peter Licence 教授给予了指导和支持，电子工业出版社有关同志为本书的顺利出版付出了辛勤的劳动，在此一并表示诚挚的谢意！

由于离子液体领域的研究正在蓬勃发展，知识体系更新迅速，而且以 X 射线光电子能谱手段研究离子液体的结构性能是一种崭新的技术，加上笔者所在的课题组成员水平所限，书中不足之处，敬请广大读者批评指正。

刘艳辉

2017 年 12 月

于沈阳理工大学

目录 / Contents

Chapter 1

Ionic Liquids

Over the past decade, ionic liquids have attracted an expanding interest from not only academic but also industrial sources.[1, 2] The widespread investigation of ionic liquids now provides opportunities to understand in more depth, many processes, *e.g.* catalysis. The ultra high vacuum (UHV) technique, *i.e.* X-ray photoelectron spectroscopy (XPS), is now accepted as a reliable method for the study of ionic liquid-based systems.[3] This method, based upon offering information on the electronic environment of metal catalysts, allows further design of catalytic systems with the aim to enhance catalytic reactions. It is the primary goal of this research.

To allow design of catalytic systems, a key consideration is the tuning of the metal centre to achieve the desired reaction performance. Varying the electronic environment at the metal centre appears to be the general idea of such topic. However, there is relatively little experimental data about how the electronic environment of the metal centre is influenced by either the solvent or the ligand. In principle, the necessary information can be derived from XPS such that a valid comparison and correlation can be made between the XPS data and the reaction performance. Unfortunately, common molecular solvents used in catalysis suffer rapid evaporation under UHV conditions. As ionic liquids have negligible volatility, they can offer the opportunity to explore this correlation in a new approach. However, such a correlation between XPS data and the reaction performance is actually difficult to obtain due to reasons such as the low solubility of the metal catalyst in ionic liquids and difficult identification of subtle electronic changes at the metal centre. Moreover, even after a proper understanding of such a correlation, to finally design a metal catalytic system with the aim to enhance a catalytic reaction is also not trivial.

What makes this book a significant improvement upon the previous work is that the influence of both the ligand and the solvent on the electronic environment of the metal centre is investigated systematically. The correlation between XPS data and the reaction performance is also made for two such systems. This correlation is then used to design a metal catalytic system to enhance a selected reaction. To the best of our knowledge, it is the first time that XPS has been applied as a tool to enhance a catalytic reaction conducted in ionic liquids.[4]

Chapter 1 introduces the basic aspects of ionic liquids. The XPS technique employed is presented in *Chapter 2*. *Chapter 3* describes the use of XPS to study a range of pure ionic liquids and some simple ionic liquid mixtures, employing imidazolium-, pyrrolidinium- and pyridinium-based cations with common anions. These investigations are used to define a series of robust C 1s fitting models and therefore to identify the aliphatic carbon component ($C_{aliphatic}$ 1s) which is used as a common charge reference point. Moreover, charge correction methods are discussed in detail for different cation-based ionic liquids, to allow accurate measurement of reliable binding energies for solutes in ionic liquid-based solutions. In *Chapters 4* and *5*, XPS is used to probe the electronic environment of a solute metal centre. *Chapter 4* focuses on interactions between solute and solvent; *Chapter 5* illustrates the investigation of metal-ligand interactions.

This chapter reports the basic structure and properties of ionic liquids, reviews the application of ionic liquids to catalysis and briefly introduces the synthesis of ionic liquids. A more thorough introduction of each part of this work is presented in the subsequent results *Chapters* (*3*, *4* and *5*).

1.1 Ionic liquids

1.1.1 Definition

Ionic liquids are salts with melting points below 100℃. They are generally composed of large and asymmetric cations and simple anions.[5] To date, a large range of cation and anion combinations have been used to generate ionic liquids. However, the main stream of research has focused upon combinations of imidazolium-, pyrrolidinium- and pyridinium-based cations with inorganic anions, see Figure 1.1. Ionic liquids that are liquid at room temperature or below are also

commonly referred to as room temperature ionic liquids (RTILs).

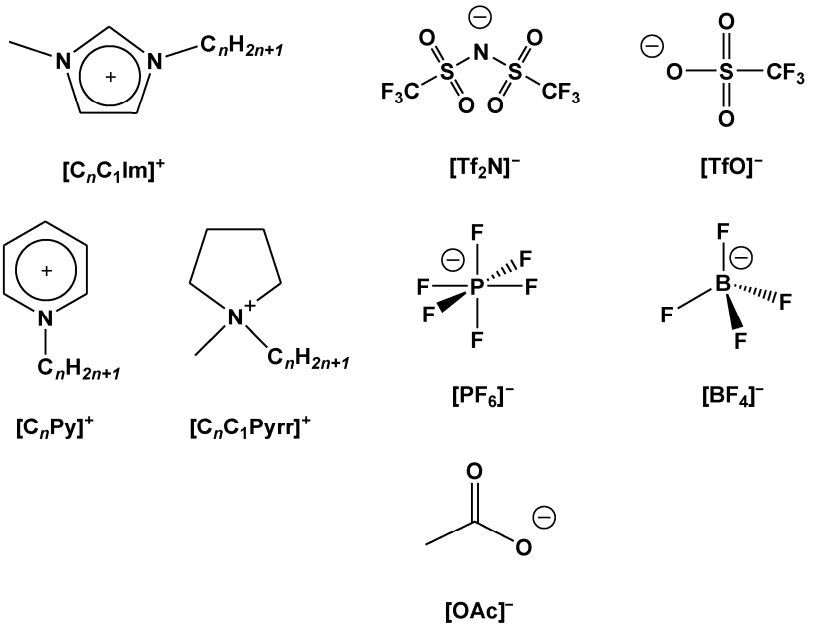

Figure1.1 Commonly used cations and anions of ionic liquids. There are a vast number of cation-anion combinations which can form over 10^6 possible primary ionic liquids and at least 10^{12} binary and 10^{18} ternary ionic liquids respectively[2]

1.1.2 A brief history of ionic liquids

The investigation of ionic liquids dates back to at least the year of 1914, when Walden studied ethylammonium nitrate. [1] However, the first boom in ionic liquid research was stimulated by the development of chloroaluminate-based ionic liquids in the 1960s. [6, 7] These ionic liquids are both air and water sensitive and thus were found to have restricted applications.

At the end of the 20th century, the second boom in ionic liquid research occurred, with the development of air- and water-stable ionic liquids.[2, 8, 9] Due to their negligible volatility and non-flammability, ionic liquids were employed as potential alternatives for the replacement of organic solvents. [10] More recently, by varying the functionality of either the cation or the anion, the potential to tune physico-chemical properties of ionic liquids was realised, which consequently, led to the development of functionalised ionic liquids or "task-specific" ionic liquids. [11]

1.2 Properties of ionic liquids

Ionic liquids exhibit many advantageous properties when compared to commonly used organic solvents, making them desirable alternatives for the application in a large range of research areas. [1, 2]This section will focus on the properties which are relevant to the investigation presented in this book, *i.e.* ionic liquids under UHV conditions. [12, 13]

1.2.1 Why are ionic liquids liquid?

What makes an ionic liquid distinctive from a common inorganic salt is that, ionic liquids have much lower melting points. The melting points of some ionic liquids have been found to be as low as 255 K. [14] The large asymmetric ions with flexible non-charge carrying groups and weakly coordinated anions lead to low lattice enthalpies; whilst the highly charge delocalised cations increase the entropy difference between the solid and liquid state. These two factors give rise to negative Gibbs free energies of fusion under ambient conditions, which results in the liquid state of ionic liquids to be thermodynamically favoured. [15]

1.2.2 Viscosity

In general, ionic liquids are more viscous than water (1 cP) and other commonly used organic solvents, with their viscosities ranging from 10 cP to more than 2000 cP at room temperature.[1] The choice of the anion can significantly influence the viscosity of ionic liquids; however, the alkyl chain length of the cation can also be used to more finely tune the viscosity. It has been shown that the viscosities of ionic liquids increase with the increasing of the alkyl chain length.[1] The viscosities of representative ionic liquids can be found in Table 1.1.

Table 1.1 Available melting point/glass transition, viscosity and conductivity values for the ionic liquids used to prepare metal catalyst-containing solutions in this book

Ionic liquids	Melting point/glass transition/K	Viscosity/cP(298 K)	Conductivity/ms. cm^{-1} (298 K)
$[C_8C_1Im][OAc]$	200.1①②	701①	
$[C_8C_1Im]Cl$	186.1[16]②	2087[17]	
$[C_8C_1Im][BF_4]$	194.7[18]②	220[19]	0.58[20]

（To be continued）

Continued table

Ionic liquids	Melting point/glass transition/K	Viscosity/cP(298 K)	Conductivity/ms. cm^{-1} (298 K)
$[C_8C_1Im][TfO]$	268.1[21]	390①	
$[C_8C_1Im][PF_6]$	203.2[22]②	690[23]	0.26[20]
$[C_8C_1Im][Tf_2N]$	193.1[24]②	90[24]	1.30[24]
$[C_8C_1Pyrr][Tf_2N]$	258.5[25]	128①	
$[C_8C_1Pyrr][BF_4]$	302.9①		
$[C_8Py][BF_4]$	248.0[26]	721①	

① data measured in this book

② glass transition

1.2.3 Low volatility

Initially, ionic liquids were considered to have no detectable vapour pressure although theoretical simulations and estimations had been conducted with regards to the vapour pressure of ionic liquids. [27] It was thought that the decomposition of ionic liquids would occur before the temperature of evaporation was achieved. [28] However, more recently, it has been indicated that several ionic liquids have appreciable volatility, specifically under reduced pressure and high temperature. [29]

To date, a wide range of ionic liquids have been vaporised[27, 30] and even distilled. A large amount of work conducted in this field at the University of Nottingham was shown that spectroscopically pure distillates can be produced especially in the case of $[Tf_2N]^-$-based ionic liquids, where the $\Delta_{vap}H$ is the smallest. Where $\Delta_{vap}H$ is large, sometimes competing reaction can occur. An excellent example has been found in both $[BF_4]^-$- and $[PF_6]^-$-based ionic liquids, where at high temperature, a carbene-based product can be yielded, see Figure 1.2. [31, 32]

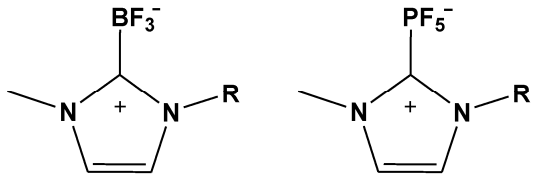

Figure 1.2 Structures of borate- and phosphonate-based carbene adducts according to ref [32]

Above all, ionic liquids possess very low vapour pressures at room temperature and therefore can be transferred into a UHV chamber, *i.e.* XPS chamber, without leading to a noticeable increase in instrument-base pressure. [33] It allows the analysis of ionic liquids at room temperature by XPS, and thus the commencement of this work.

1.2.4 Conductivity

Ionic liquids conduct *via* ion mobility. Typical conductivity values for ionic liquids are between 0.1 and 3 $ms \cdot cm^{-1}$,[34] although some ionic liquids with conductivities up to 110 $ms \cdot cm^{-1}$ have also been prepared.[35] However, ionic liquids are not as conducting as one might expect. [36] The conductivities of ionic liquids are similar to the non-aqueous electrolytes but are considerably lower than those of concentrated aqueous electrolytes.[37]

Moreover, it has been reported that conductivity and viscosity can be correlated with each other. The relatively high viscosity[38] causes the lower conductivities observed for pure ionic liquids.

In general, an increase in the alkyl chain length of the cation usually results in a large decrease in conductivity.[39]

1.2.5 Solvation properties

There are a huge number of different ionic liquids, each with their own solvation properties. They can dissolve a variety of materials, *e.g.* aromatic and aliphatic organic compounds,[40] inorganic compounds,[41] transition metal catalysts,[42] nanoparticles,[43] polymers,[44] biomaterials[45] and enzymes.[46] By modifying their chemical structures, the solvation properties of ionic liquids can be altered.[47] Generally, ionic liquids are immiscible with commonly used non-polar solvents, *e.g.* toluene; whilst miscible with polar or protic solvents, *e.g.* acetontrile and methanol.[48] Consequently, ionic liquids can find application in biphasic systems such as solvent-solvent separations and extractions.[49]

The solubility of a metal catalyst in an ionic liquid depends upon the nature of ionic liquid and the solute-solvent interaction involved. Neutral metal compounds are generally found to be poorly soluble in ionic liquids and therefore leach out of catalytic systems. This problem can be overcome by either employing charged metal complexes or by adding functional ligands to enhance the solubility of neutral metal compounds.[50]

1.3 Synthesis of ionic liquids

Ionic liquids used for the analysis discussed in this book were all prepared using a variety of methods. The experiments presented in the following sections are based upon literature methods. Ionic liquids can be synthesised in two steps from simple organic starting materials. The first step is N-Alkylation to make several types of basic ionic liquids, for example imidazolium-based ionic liquids, *i.e.* $[C_8C_1Im]Cl$, see Scheme 1.1.

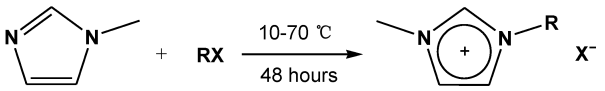

Scheme 1.1 Alkylation of 1-methylimidazole with an alkylation agent; R = ethyl, butyl, hexyl, octyl, decayl or dodecyl; X = Cl, Br or I.

The second step is the salt metathesis of the basic ionic liquids to yield the desired ionic liquid containing commonly used anions, *i.e.* $[Tf_2N]^-$, $[PF_6]^-$, $[TfO]^-$, $[BF_4]^-$ and $[OAc]^-$,see scheme 1, 2.

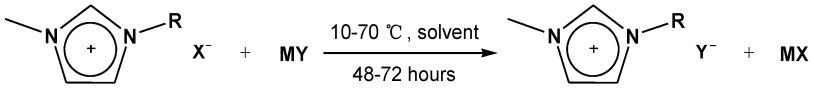

Scheme 1.2 Salt metathesis reaction for the preparation of ionic liquids; M = H^+, Na^+, Li^+ and Ag^+; Y = $[PF_6]^-$, $[BF_4]^-$, $[Tf_2N]^-$, $[TfO]^-$ and $[OAc]^-$. The reaction solvent is H_2O.

1.3.1 Materials

1-Methylimidazole was distilled over calcium hydride prior to use. 1-Methylpyrrolidine, pyridine and all other chemicals were obtained from Sigma-Aldrich or Alfa Aesar and were used as received. Lithium bis[(trifluoromethane)sulfonyl]imide was obtained from 3M and also used as received.

1.3.2 Instrumentation

The purity of ionic liquids can influence their properties or even reactivity for catalysis.[13, 51] Consequently, the characterisation of the locally prepared ionic liquids became curial. In this book,

all ionic liquids were characterised by ESI-MS using Bruker MicroTOF, as well as ^{1}H and ^{13}C NMR spectra recorded using a Bruker DPX-300 spectrometer at 300 and 75MHz respectively as solutions in $CDCl_3$, CD_3OD and DMSO-d_6. Thermal data was determined by DSC (Q2000 V24.4 Build 116).

Ionic liquids are hygroscopic and thus able to absorb moisture from the atmosphere.[52, 53] In this work, water was removed under high vacuum at 60℃ for at least 12h for all ionic liquids samples. However, even by this treatment, water is still present at ppm level. Karl Fischer analysis (Mitsubishi CA-100 Moisturemeter) was used to determine the water concentrations and they were all found to be approximately 40 ppm. Moreover, as has been found by the Nottingham Ionic Liquids group, no water presents in $[C_8C_1Im][BF_4]$ at～10^{-9} mbar above～245K.[54] Since the pressure in the main XPS chamber remained≤1×10^{-8} mbar during all XPS measurements, it suggests that all volatile impurities, *i.e.* water, are removed, leading to high purity samples.[31, 54]

Anion chromatography (Dionex, ICS-3000, IonPack AS15, 4mm×250mm analytical column) was used to determine the halide concentration when salt metathesis was one of the synthetic steps. The eluent is a mixture of Millipore Milli-Q 18 MΩ ultrapure water, 100mm NaOH aqueous solution and acetonitrile in a 60:15:25 volume ratio and the flow rate is 0.2 ml/min. Specifically for acetate-based ionic liquids, halide concentrations were found to be between 36 and 1010 ppm due to the difficult post reaction separations of the starting materials and the products. However, it should be noted that no halide signal was observed during XPS analysis for any acetate-based samples, *i.e.* the concentration was below the limit of detection in all cases. For other cases, the halide concentrations were all below 10 ppm. Anion retention times associated with the anion chromatography experiment are shown in Table 1.2.

Table 1.2 Standard retention times for different anions during anion chromatography measurements

Anion	Time/min	Anion	Time/min	Anion	Time/min
$[OAc]^-$	4.5	$[TfO]^-$	8.5	$[PF_6]^-$	22.5
Cl^-	5.1	$[BF_4]^-$	9.1	$[Tf_2N]^-$	30.9
Br^-	6.5	I^-	10.5		

1.3.3 Imidazolium-based ionic liquids

1.3.3.1 $[C_2C_1Im]Br$

1-Methylimidazole (20g, 0.24mol) was placed in a round-bottomed flask fitted with a water

condenser equipped with a drying tube so as to avoid moisture penetration. Bromoethane (1.2 molar equivalents) was added drop wise with stirring at 70℃. The reaction time was 48-72h. When ^{1}HNMR analysis of the lower phase showed no 1-methylimidazole remained, the upper phase, containing unreacted bromoethane, was separated using a separating funnel. The lower phase, containing the desired product $[C_2C_1Im]Br$, was dried under rotary evaporator and then under high vacuum(~10^{-1} mbar) at 60℃ for 12 h to yield the desired product, $[C_2C_1Im]Br$, as a white solid. Yield: 70%

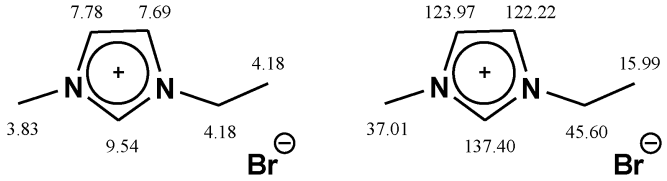

^{1}H NMR δ_H (300 MHz, $CDCl_3$), 1.39 (t, *J*=7.4 Hz, 3H), 3.83 (s, 3H), 4.18 (t, *J*=7.4 Hz, 2H), 7.69 (s, 1H), 7.78 (s, 1H), 9.54 (s, 1H). ^{13}C NMR δ_C (75 MHz, $CDCl_3$), 15.99, 37.01, 45.60, 122.22, 123.97, 137.40.

These data are consistent with those reported in literature.[55]

1.3.3.2 $[C_4C_1Im]Cl$

A similar procedure to that outlined for $[C_2C_1Im]Br$ was used to yield $[C_4C_1Im]Cl$ as a white solid. Yield: 65%

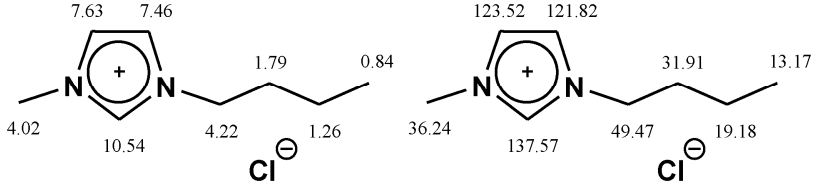

^{1}H NMR δ_H (300 MHz, $CDCl_3$), 0.84 (t, *J*=7.3 Hz, 3H), 1.26 (m, 2H), 1.79 (m, 2H), 4.02 (s, 3H), 4.22 (t, *J*=7.3 Hz, 2H), 7.46 (d, *J*=1.8 Hz, 1H), 7.63 (d, *J*=1.8 Hz, 1H), 10.54 (s, 1H). 13C NMR δ_C (75 MHz, $CDCl_3$), 13.17, 19.18, 31.91, 36.24, 49.47, 121.82, 123.52, 137.57.

These data are consistent with those reported in literature.[16]

1.3.3.3 $[C_8C_1Im]Cl$

1-Methylimidazole (20g, 0.24mol) was placed in a two necked round-bottomed flask fitted with a water condenser topped with a blue silica tube. 1-Chlorooctane (1.2 molar equivalents) was added drop wise with stirring at 70℃. The reaction was allowed to preceed for 48-72h. The unreacted 1-methylimidazole and 1-chlorooctane impurities were then removed by washing the

mixture with ethyl acetate (30 ml) three times. The desired product, $[C_8C_1Im]Cl$, was firstly dried using a rotary evaporator and then under high vacuum at 60℃ for 12 h to yield a pale yellow liquid. Yield: 68%

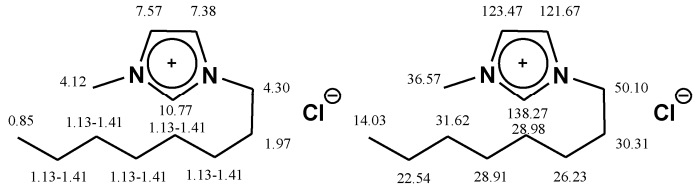

^{1}H NMR δ_H (300 MHz, CD_3Cl), 0.85 (m, 3H), 1.13-1.41 (m, 10H), 1.97 (m, 2H), 4.12 (s, 3H), 4.30 (t, J=7.4 Hz, 2H), 7.38 (s, 1H), 7.57 (s, 1H), 10.77 (s, 1H). ^{13}C NMR δ_C (75 MHz, CD_3Cl) 14.03, 22.54, 26.23, 28.91, 28.98, 30.31, 31.62, 36.57, 50.10, 121.67, 123.47, 138.27.

These data are consistent with those reported in literature.[16]

1.3.3.4 $[C_{12}C_1Im]Cl$

1-Methylimidazole (20g, 0.24mol) was placed in a round-bottomed flask fitted with a water condenser topped with a blue silica tube. 1-Chlorododecane (0.9 molar equivalents) was added drop wise, with stirring, at 70℃. The reaction was allowed to preceed for 48-72h. After recrystallising from acetonitrile/ethyl acetate, the desired $[C_{12}C_1Im]Cl$ was firstly dried using a rotary evaporator and then under high vacuum at 60℃ for 12 h to yield a white solid. Yield: 78%

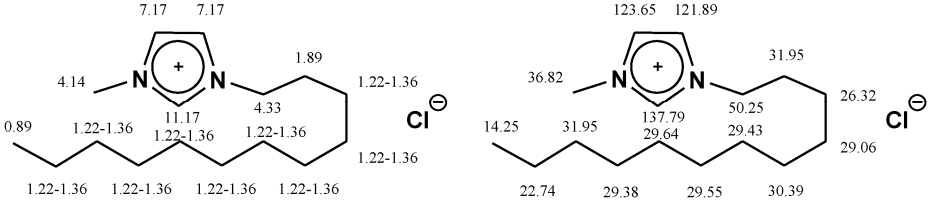

^{1}H NMR δ_H (300 MHz, $CDCl_3$), 0.89 (m, 3H), 1.22-1.36 (m, 18H), 1.89 (br. s., 2H), 4.14 (s, 3H), 4.33 (t, J=7.4 Hz, 2H), 7.17 (d, J=7.6 Hz, 2H), 11.17 (s, 1H). ^{13}C NMR δ_C (75 MHz, $CDCl_3$), 14.25, 22.74, 26.32, 29.06, 29.38, 29.43, 29.55, 29.64, 30.39, 31.95, 36.82, 50.25, 121.89, 123.65, 137.79.

These data are consistent with those reported in literature.[16]

1.3.3.5 $[C_8C_1Im][NTf_2]$

$[C_8C_1Im]Cl$ (27.7g, 0.12mol) was transferred to a round bottomed flask and dissolved in 100 ml deionised H_2O. A water condenser was set up and the solution was stirred at 70℃. $Li(NTf_2)$ (1.2 molar equivalents) was dissolved in deionised H_2O (50ml) and added to the reaction drop wise. Instantly, two phases formed where the lower phase was $[C_8C_1Im][NTf_2]$ and the upper phase was

aqueous LiCl. After 12h, the upper phase was removed, and the lower phase was washed with deionised H_2O (30ml)three times to remove LiCl. The desired product $[C_8C_1Im][NTf_2]$ was then dried under high vacuum at 60℃ for 12h to yield a colourless liquid. Yield: 85%

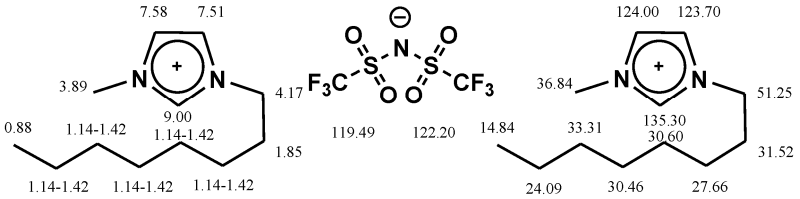

^{1}H NMR δ_H (300 MHz, CD_3OH), 0.88 (t, J = 6.8 Hz, 3H), 1.14-1.42 (m, 10H), 1.85 (m, 2H), 3.89 (s, 3H), 4.17 (t, J = 7.4 Hz, 2H), 7.51 (d, J = 1.8 Hz, 1H), 7.58 (d, J = 1.8 Hz, 1H), 9.00 (s, 1H). ^{13}C NMR δ_C (75 MHz, CD_3OH) 14.84, 24.09, 27.66, 30.46, 30.60, 31.52, 33.31, 36.84, 51.25, 119.49, 122.22, 123.70, 124.00, 135.30. $[Cl]_{IC}$ < 10 ppm.

These data are consistent with those reported in literature.[56]

1.3.3.6 $[C_8C_1Im][PF_6]$

$[C_8C_1Im]Cl$ (27.7g, 0.12mol) was transferred to a round bottomed flask and dissolved in 50 ml of deionised H_2O. An aqueous solution of 60% HPF_6 (1.2 molar equivalents) was added drop wise using a plastic syringe (HPF_6 can be glass corrosive) while stirring $[C_8C_1Im]Cl$ in an ice bath. After reacted for 12 h, the upper phase was removed and the lower phase was washed with deionised H_2O (30 ml) until the pH was *ca.* 7. Finally, the desired $[C_8C_1Im][PF_6]$ was dried firstly under rotary evaporator and then under high vacuum at 60℃ for 12 h. The desired $[C_8C_1Im][PF_6]$ was a colourless liquid. Yield: 87%

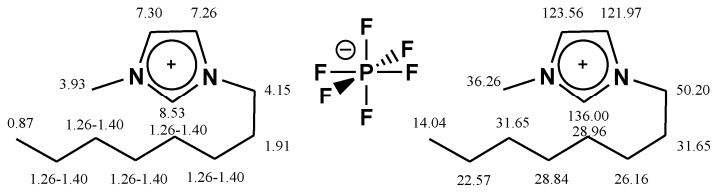

^{1}H NMR δ_H (300 MHz, $CDCl_3$), 0.87 (t, J = 6.8 Hz, 3H), 1.26-1.40 (m, 10H), 1.91 (m, 2H), 3.93 (s, 3H), 4.15 (t, J = 7.4 Hz, 2H), 7.26 (t, J = 1.8 Hz, 1H), 7.30 (t, J = 1.8 Hz, 1H), 8.53 (s, 1H). ^{13}C NMR δ_C (300 MHz, $CDCl_3$) 14.04, 22.57, 26.16, 28.84, 28.96, 29.90, 31.65, 36.26, 50.20, 121.97, 123.56, 136.00. $[Cl]_{IC}$ < 10 ppm.

These data are consistent with those reported in literature.[16]

1.3.3.7 $[C_8C_1Im][TfO]$

$[C_8C_1Im]Cl$ (27.7g, 0.12mol) was transferred to a round-bottomed flask and dissolved in 50 ml deionised H_2O. A water condenser was set up and the solution was stirred at 70℃. Li(TfO) (1.2 molar equivalents) was dissolved in deionised H_2O (50 ml) and added to the reaction drop wise. The reaction

was continued for 48-72h. The reaction mixture was allowed to cooled and the lower phase was washed with cold deionised H_2O (30 ml) by three times to remove LiCl and unreacted Li(TfO). The desired $[C_8C_1Im][TfO]$ was dried firstly in a rotary evaporator and then under high vacuum at 60 ºC for 12 h to give the desired product $[C_8C_1Im][TfO]$ as a pale yellow liquid. Yield: 59%

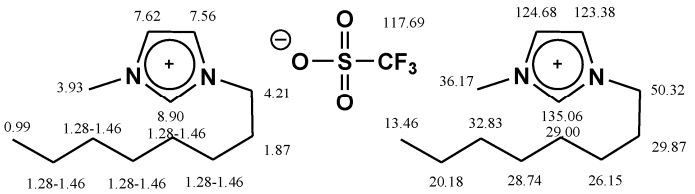

^{1}H NMR δ_H (300 MHz, CD_3OD), 0.99 (t, *J*=7.4 Hz, 3H), 1.28-1.46 (m, 10H), 1.87 (m, 2H), 3.93 (s, 3H), 4.21 (t, *J*=7.3 Hz, 2H), 7.56 (d, *J*=1.9 Hz, 2H), 7.62 (d, *J*=1.9 Hz, 2H), 8.90 (br. s., 1H). ^{13}C NMR δ_C (75 MHz, CD_3OD), 13.46, 20.18, 26.15, 28.74, 29.00, 29.87, 32.83, 36.17, 50.32, 117.69, 123.38, 124.68, 135.06. $[Cl]_{IC}$ < 10 ppm.

These data are consistent with those reported in literature.[57]

1.3.3.8 $[C_8C_1Im][BF_4]$

$[C_8C_1Im]Cl$ (27.7g, 0.12 mol) was dissolved in 100 ml deionised water in a round bottomed flask. A water condenser was set up and the solution was stirred at 70℃. $NaBF_4$ (1.2 molar equivalents) was dissolved in deionised H_2O (50 ml) and added to the reaction drop wise. After 48-72h, the reaction mixture was allowed to cool down and the lower phase was washed with cold deionised water (30 ml) three times to remove NaCl and unreacted $NaBF_4$. The desired $[C_8C_1Im][BF_4]$ was dried using a rotary evaporator and then under high vacuum at 60℃ for 12 h to yield a colourless liquid. Yield: 63%

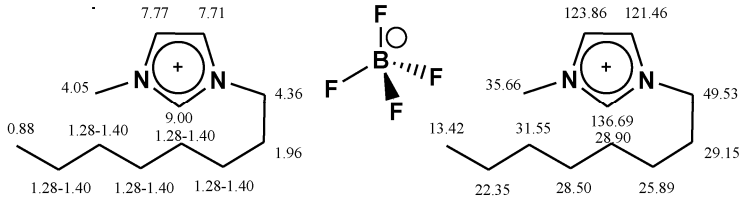

^{1}H NMR δ_H (300 MHz, $CDCl_3$), 0.88 (m, 3H), 1.28-1.40 (m, 10H), 1.96 (m, 2H), 4.05 (s, 3H), 4.36 (m, 2H), 7.71 (s, 1H), 7.77 (s, 1H), 9.00 (s, 1H). 13C NMR δ_C (75 MHz, $CDCl_3$), 13.42, 22.35, 25.89, 28.50, 28.90, 29.15, 31.55, 35.66, 49.53, 121.46, 123.86, 136.69. $[Cl]_{IC}$ < 10 ppm.

These data are consistent with those reported in literature.[58]

1.3.3.9 $[C_2C_1Im][OAc]$

$[C_2C_1Im]Br$ (22.9g, 0.12 mol) was transferred to a round-bottomed flask and dissolved in

deionised H_2O (50 ml). Sliver acetate (1.2 molar equivalents), $Ag(CH_3COO)$, was added and the mixture was stirred for 24 h at room temperature. The AgBr formed during the reaction was removed by filtration and the filtrate was evaporated using a rotary evaporator to remove H_2O. Acetone was then added to precipitate the unreacted $Ag(CH_3COO)$ in the ionic liquid. $Ag(CH_3COO)$ was removed by filtration and the acetone was removed firstly using a rotary evaporator and then under high vacuum at 60℃ for 12 h to give the desired product $[C_2C_1Im][OAc]$ as a colourless liquid. Yield: 51%

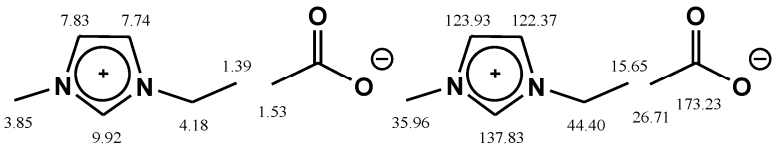

1H NMR δ_H (300 MHz, DMSO-d_6), 1.39 (t, *J*=7.3 Hz, 3H), 1.53 (s, 3H), 3.85 (s, 3H), 4.18 (m, 2H), 7.74 (s, 1H), 7.83 (s, 1H), 9.92 (s, 1H). ^{13}C NMR δ_C (75 MHz, DMSO-d_6), 15.65, 26.71, 35.96, 44.40, 122.37, 123.93, 137.83, 173.23. $[Br]I_C$ = 36 ppm.

These data are consistent with those reported in literature.[59]

1.3.3.10 $[C_4C_1Im][OAc]$

A similar procedure to that outlined for $[C_2C_1Im][OAc]$ was used to yield $[C_4C_1Im][OAc]$ as a colourless liquid. Yield: 58%

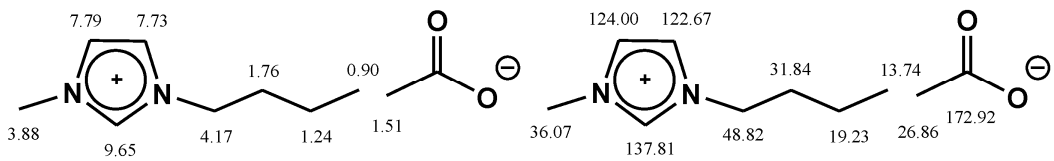

^{1}H NMR δ_H (300 MHz, DMSO-d_6), 0.90 (t, *J*=7.4 Hz, 3H), 1.24 (m, 2H), 1.51 (s, 3H), 1.76 (m, 2H), 3.88 (s, 3H), 4.17 (t, *J*=7.2 Hz, 2H), 7.73 (s, 1H), 7.79 (s, 1H), 9.65 (br. s., 1H). 13C NMR δ_C (75 MHz, DMSO-d_6), 13.74, 19.23, 26.86, 31.84, 36.07, 48.82, 122.67, 124.00, 137.81, 172.92. $[Cl]I_C$ = 665 ppm.

These data are consistent with those reported in literature.[59]

1.3.3.11 $[C_8C_1Im][OAc]$

A similar procedure to that outlined for $[C_2C_1Im][OAc]$ was used to yield $[C_8C_1Im][OAc]$ as a pale yellow liquid. Yield: 66%

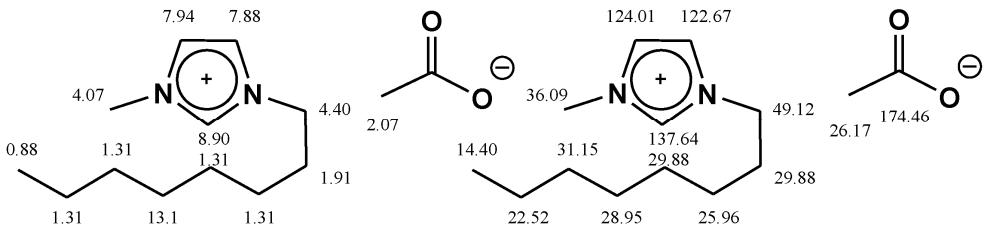

^{1}H NMR δ_H (300 MHz, DMSO-d_6), 0.88 (t, J=7.3 Hz, 3H), 1.31 (m, 10H), 1.91 (m, 2H), 2.07 (s, 3H), 4.07 (s, 3H), 4.40 (t, J=7.3 Hz, 2H), 7.88 (d, J=1.9 Hz, 1H), 7.94 (d, J=1.9 Hz, 1H), 8.90 (br. s., 1H). ^{13}C NMR δ_C (75 MHz, DMSO-d_6), 14.40, 22.52, 25.96, 26.17, 28.95, 29.88, 31.15, 31.62, 36.09, 49.12, 122.67, 124.01, 137.64, 174.46. $[Cl]_{IC}$ = 156 ppm. ESI-MS negative: 316.95 (1 cation plus 2 anions). ESI-MS positive: 195.19. T_g= 200.1 K.

1.3.3.12 $[C_{12}C_1Im][OAc]$

A similar procedure to that outlined for $[C_2C_1Im][OAc]$ was used to yield $[C_{12}C_1Im][OAc]$ as a yellow liquid. Yield: 43%

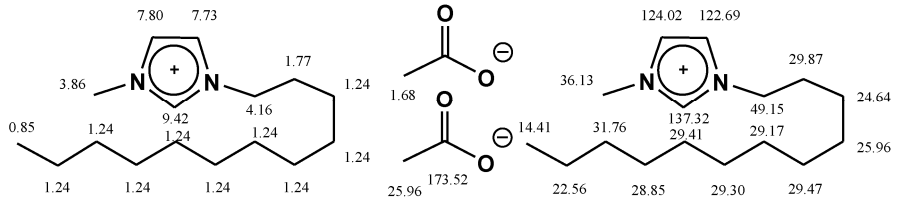

^{1}H NMR δ_H (300 MHz, DMSO-d_6), 0.85 (m, 3H), 1.24 (m, 18H), 1.68 (s, 3H), 1.77 (m, 2H), 3.86 (s, 3H), 4.16 (m, 2H), 7.73 (s, 1H), 7.80 (s, 1H), 9.42 (s, 1H). ^{13}C NMR δ_C (75 MHz, DMSO-d_6), 14.41, 22.56, 24.64, 25.96, 28.85, 29.17, 29.30, 29.41, 29.47, 29.87, 31.76, 36.13, 49.15, 122.69, 124.02, 137.32, 173.52. $[Cl]_{IC}$ = 1010 ppm. ESI-MS negative: 371.25 (1 cation plus 2 anions). ESI-MS positive: 251.25. T_m= 275.7 K.

1.3.4 Pyrrolidinium-based ionic liquids

1.3.4.1 $[C_2C_1Pyrr]Br$

1-Methylpyrrolidine (20.4g, 0.24mol) was placed in a round-bottomed flask fitted with a water condenser topped with a drying tube (to avoid moisture penetration). Bromoethane (1.2 molar equivalents) was added drop wise while stirring at 70℃. The reaction time was 24-72h. The desired product $[C_2C_1Pyrr]Br$ was recrystallised in acetonitrile/ethyl acetate and dried firstly using a rotary evaporator and then under high vacuum at 60℃ for 12 h to yield a white solid. Yield: 71%

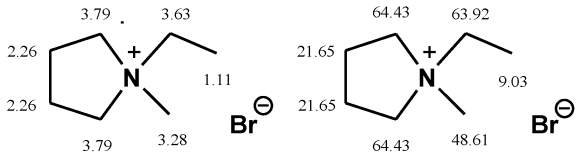

^{1}H NMR δ_H (300MHz, $CDCl_3$), 1.11 (m, 3H), 2.26 (br. s., 4H), 3.28 (s, 3H), 3.63 (m, 2H), 3.79 (m, 4H). ^{13}C NMR δ_C (75MHz, $CDCl_3$), 9.03, 21.65, 48.61, 63.92, 64.43.

These data are consistent with those reported in literature.[56]

1.3.4.2 [C_4C_1Pyrr]Br

A similar procedure to that outlined for [C_2C_1Pyrr]Br was used to yield [C_4C_1Pyrr]Br as a white solid. Yield: 70%

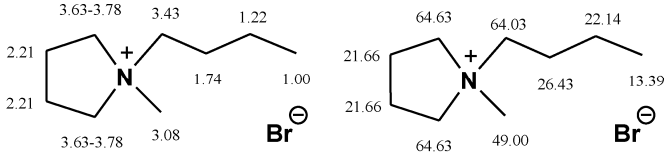

^{1}H NMR δ_H (300MHz, $CDCl_3$), 1.00 (m, 3H), 1.22 (m, 2H), 1.67-1.81 (m, 2H), 2.21 (br. s., 4H), 3.08 (s, 3H), 3.43 (m, 2H), 3.63-3.78 (m, 4H). ^{13}C NMR δ_C (75MHz, $CDCl_3$), 13.39, 21.66, 22.14, 26.43, 49.00, 64.03, 64.63.

These data are consistent with those reported in literature.[56]

1.3.4.3 [C_6C_1Pyrr]Br

A similar procedure to that outlined for [C_2C_1Pyrr]Br was used to yield [C_6C_1Pyrr]Br as a white solid. Yield: 79%

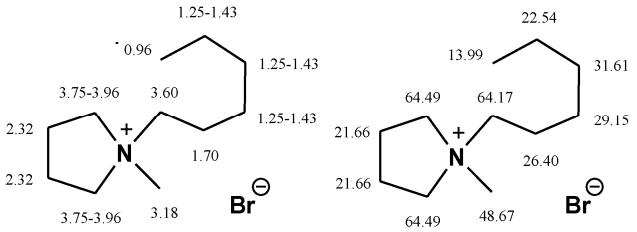

^{1}H NMR δ_H (300MHz, $CDCl_3$), 0.96 (m, 3H), 1.25-1.43 (m, 6H), 1.60-1.81 (m, 2H), 2.32 (br. s., 4H), 3.18 (s, 3H), 3.60 (m, 2H), 3.75-3.96 (m, 4H). ^{13}C NMR δ_C (75MHz, $CDCl_3$), 13.99, 21.66, 22.54, 26.40, 29.15, 31.61, 48.67, 64.17, 64.49.

These data are consistent with those reported in literature.[56]

1.3.4.4 [C_8C_1Pyrr]Br

A similar procedure to that outlined for [C_2C_1Pyrr]Br was used to yield [C_8C_1Pyrr]Br as a white solid. Yield: 88%

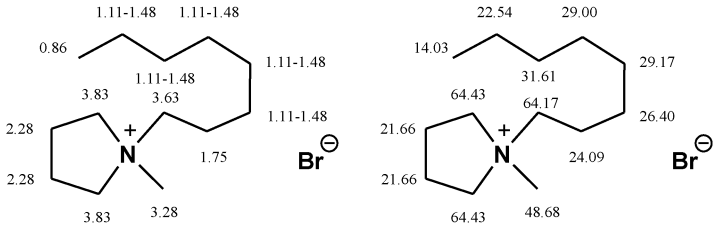

^{1}H NMR δ_H (300MHz, $CDCl_3$), 0.86 (m, 3H), 1.11-1.48 (m, 10H), 1.65-1.86 (m, 2H), 2.28 (br. s., 4H), 3.28 (s, 3H), 3.63 (m, 2H), 3.73-3.99 (m, 4H). ^{13}C NMR δ_C (75MHz, $CDCl_3$), 14.03, 21.66, 22.54, 24.09, 26.40, 29.00, 29.17, 31.61, 48.67, 64.17, 64.43.

These data are consistent with those reported in literature.[56]

1.3.4.5 [$C_{10}C_1$Pyrr]Br

A similar procedure to that outlined for [C_2C_1Pyrr]Br was used to yield [$C_{10}C_1$Pyrr]Br as a white solid. Yield: 85%

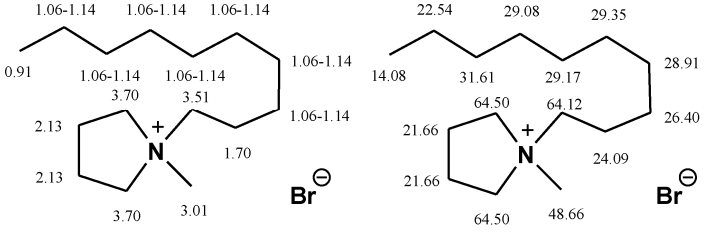

^{1}H NMR δ_H (300MHz, $CDCl_3$), 0.91 (m, 3H), 1.06-1.41 (m, 14H), 1.70 (m, 2H), 2.13 (br. s., 4H), 3.01 (s, 3H), 3.51 (m, 2H), 3.70 (br. s., 4H). ^{13}C NMR δ_C (75MHz, $CDCl_3$), 14.08, 21.66, 22.54, 24.09, 26.40, 28.91, 29.08, 29.17, 29.35, 31.61, 48.66, 64.12, 64.50.

These data are consistent with those reported in literature.[56]

1.3.4.6 [C_8C_1Pyrr]I

A similar procedure to that outlined for [C_2C_1Pyrr]Br was used to yield [C_8C_1Pyrr]I as a yellow solid. Yield: 62%

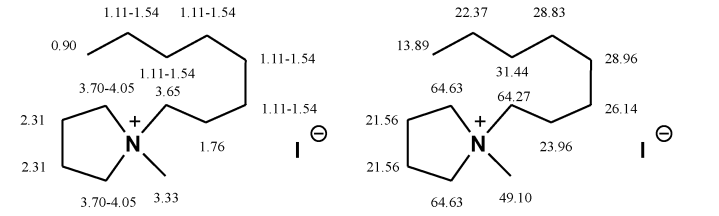

^{1}H NMR δ_H (300MHz, $CDCl_3$), 0.90 (t, J=6.9 Hz, 3H), 1.11-1.54 (m, 10H), 1.76 (m, 2H), 2.31 (br. s., 4H), 3.33 (s, 3H), 3.65 (m, 2H), 3.70-4.05 (m, 4H). ^{13}C NMR δ_C (75MHz, $CDCl_3$), 13.89, 21.56, 22.37, 23.96, 26.14, 28.83, 28.96, 31.44, 49.10, 64.27, 64.63. ESI-MS negative: 452.03 (1 cation plus 2 anions). ESI-MS positive: 198.22. T_m= 344.0 K.

1.3.4.7 $[C_2C_1Pyrr][Tf_2N]$

$[C_2C_1Pyrr]Br$ (23.3g, 0.12 mol) was transferred to a round-bottomed flask and dissolved in deionised H_2O (100 ml). A water condenser was set up and the solution was stirred at 70℃. $Li(NTf_2)$ (1.2 molar equivalents) was dissolved in deionised H_2O (50 ml) and added to the reaction drop wise. After 12h, the upper phase was separated, and the lower phase was washed with deionised water three times to remove LiCl. The desired product $[C_2C_1Pyrr][Tf_2N]$ was then dried firstly using a rotary evaporator and then under high vacuum at 60℃ for 12 h to yield a colourless liquid. Yield: 76%

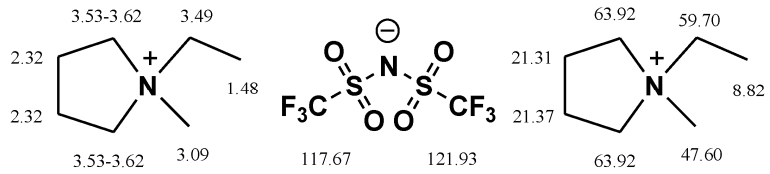

^{1}H NMR δ_H (300MHz, $CDCl_3$), 1.48 (t, J=7.3Hz, 3H), 2.32 (br. s., 4 H), 3.09 (s, 3 H), 3.43-3.52 (m, 2 H), 3.53-3.62 (m, 4 H). ^{13}C NMR δ_C (75MHz, $CDCl_3$), 8.82, 21.37, 47.60, 59.70, 63.92, 117.67, 121.93. $[Br]_{IC}$ < 10 ppm.

These data are consistent with those reported in literature.[56]

1.3.4.8 $[C_4C_1Pyrr][Tf_2N]$

A similar procedure to that outlined for $[C_2C_1Pyrr][Tf_2N]$ was used to yield $[C_4C_1Pyrr][Tf_2N]$ as a colourless liquid. Yield: 88%

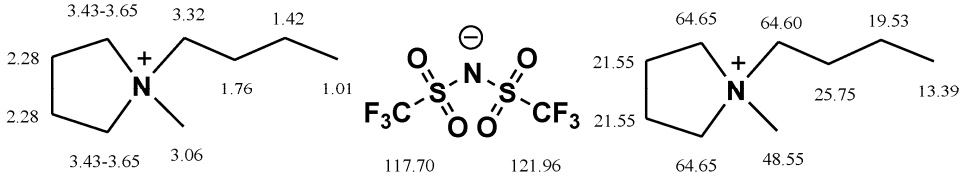

^{1}H NMR δ_H (300MHz, $CDCl_3$), 1.01 (t, J=7.3Hz, 3H), 1.34-1.52 (m, 2 H), 1.67-1.85 (m, 2 H), 2.28 (br. s., 4 H), 3.06 (s, 3H), 3.24-3.40 (m, 2 H), 3.43-3.65 (m, 4 H). ^{13}C NMR δ_C (75MHz, $CDCl_3$), 13.39, 19.53, 21.55, 25.75, 48.55, 64.60, 64.65, 117.70, 121.96. $[Br]_{IC}$ < 10 ppm.

These data are consistent with those reported in literature.[56]

1.3.4.9 $[C_6C_1Pyrr][Tf_2N]$

A similar procedure to that outlined for $[C_2C_1Pyrr][Tf_2N]$ was used to yield $[C_6C_1Pyrr][Tf_2N]$ as a colourless liquid. Yield: 82%

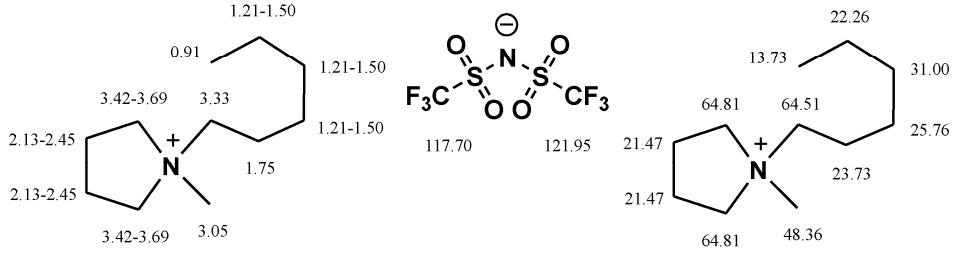

^{1}H NMR δ_H (300MHz, $CDCl_3$), 0.91 (m, 3H), 1.21-1.50 (m, 6 H), 1.75 (m, 2 H), 2.13-2.45 (m, 4 H), 3.05 (s, 3 H), 3.33 (m, 2 H), 3.42-3.69 (m, 4 H), ^{13}C NMR δ_C (75MHz, $CDCl_3$), 13.73, 21.47, 22.26, 23.73, 25.76, 31.00, 48.36, 64.51, 64.81, 117.70, 121.95. $[Br]_{IC}$ < 10 ppm.

These data are consistent with those reported in literature.[60]

1.3.4.10 $[C_8C_1Pyrr][Tf_2N]$

A similar procedure to that outlined for $[C_2C_1Pyrr][Tf_2N]$ was used to yield $[C_8C_1Pyrr][Tf_2N]$ as a colourless liquid. Yield: 82%

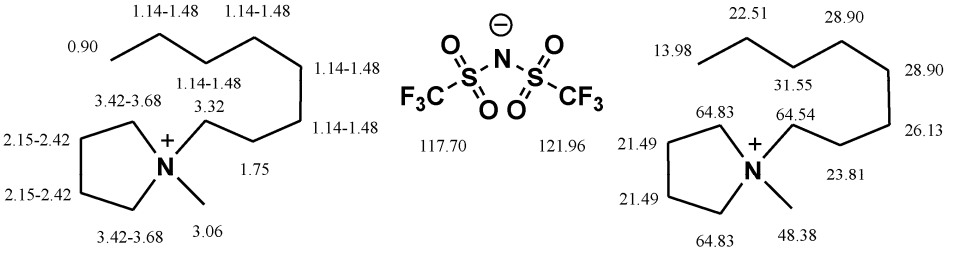

^{1}H NMR δ_H (300MHz, $CDCl_3$), 0.90 (t, J=7.0 Hz, 3H). 1.14-1.48 (m, 10H), 1.65-1.89 (m, 2 H), 2.15-2.42 (m, 4 H), 3.06 (s, 3 H), 3.22-3.40 (m, 2 H), 3.42-3.68 (m, 4 H). ^{13}C NMR δ_C (75MHz, $CDCl_3$), 13.98, 21.49, 22.51, 23.81, 26.13, 28.90, 31.55, 48.38, 64.54, 64.83, 117.70, 121.96. $[Br]_{IC}$ < 10 ppm. ESI-MS negative: 279.92. ESI-MS positive: 198.22. T_m= 258.5 K.

1.3.4.11 $[C_{10}C_1Pyrr][Tf_2N]$

A similar procedure to that outlined for $[C_2C_1Pyrr][Tf_2N]$ was used to yield $[C_{10}C_1Pyrr][Tf_2N]$ as a colourless liquid. Yield: 81%

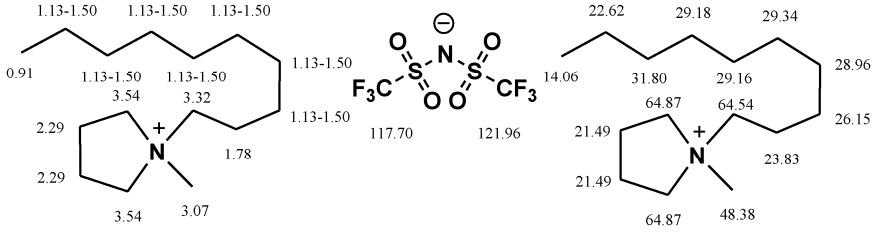

^{1}H NMR δ_H (300MHz, $CDCl_3$), 0.91 (t, J=7.0 Hz, 3H). 1.13-1.50 (m, 14 H), 1.78 (m, 2H), 2.29 (br. s., 4H), 3.07 (s, 3 H), 3.23-3.41 (m, 2 H), 3.54 (br. s., 4 H). ^{13}C NMR δ_C (75MHz, $CDCl_3$), 14.06, 21.49, 22.62, 23.83, 26.15, 28.96, 29.18, 29.26, 29.34, 31.80, 48.38, 64.54, 64.84, 117.70, 121.96. $[Br]_{IC}$ < 10 ppm. ESI-MS negative: 279.92. ESI-MS positive: 226.25. T_m= 262.0 K.

1.3.4.12 $[C_8C_1Pyrr][BF_4]$

A similar procedure to that outlined for $[C_8C_1Im][BF_4]$ was used to yield $[C_8C_1Pyrr][BF_4]$ as a white solid. Yield: 60%

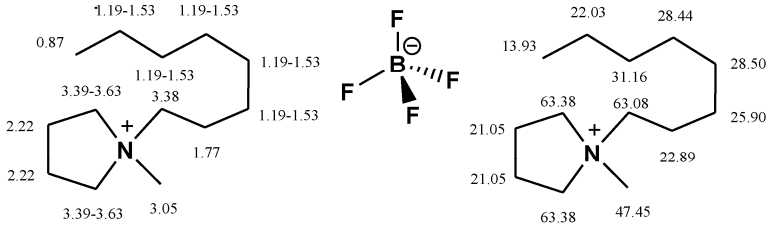

^{1}H NMR δ_H (300MHz, DMSO-d_6), 0.87 (t, J=6.9 Hz, 3H). 1.19-1.53 (m, 10 H), 1.77 (m, 2 H), 2.22 (br. s., 4 H), 3.05 (s, 3 H), 3.38 (m, 2H), 3.39-3.63 (m, 4 H). ^{13}C NMR δ_C (75MHz, DMSO-d_6), 13.93, 21.05, 22.03, 22.89, 25.90, 28.44, 28.50, 31.16, 47.45, 63.08, 63.38. $[Br]_{IC}$ < 10 ppm. ESI-MS negative: 372.23 (1 cation plus 2 anions). ESI-MS positive: 198.23. T_m= 302.9 K.

1.3.5 Pyridinium-based ionic liquids

1.3.5.1 $[C_2Py]Br$

1-Pyridine (19 g, 0.24mol) was placed in a round-bottomed flask fitted with a water condenser topped with a drying tube. Bromoctane (1.2 molar equivalents) was added drop wise while stirring at 70℃. After the reaction allowed to proceed for 24-72h, the desired product, $[C_2Py]Br$, was recrystallised in acetonitrile/ethyl acetate and dried firstly using a rotary evaporator and then under high vacuum at 60℃ for 12 h to yield a white solid. Yield: 72%

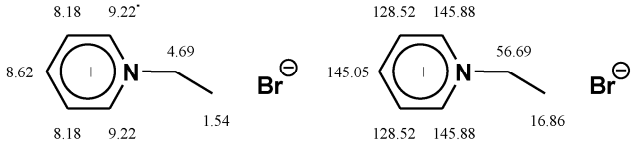

^{1}H NMR δ_H (300 MHz, DMSO-d_6), 1.54 (t, J=7.3 Hz, 3H), 4.69 (2H, m), 8.18 (2H, m), 8.62 (1H, m), 9.22 (d, J=5.9 Hz, 2H). ^{13}C NMR δ_C (75 MHz, DMSO-d_6), 16.86, 56.69, 128.52, 145.05, 145.88.

These data are consistent with those reported in literature.[61]

1.3.5.2 [C_4Py]Br

A similar procedure to that outlined for [C_2Py]Br was used to yield [C_4Py]Br as a white solid. Yield: 62%

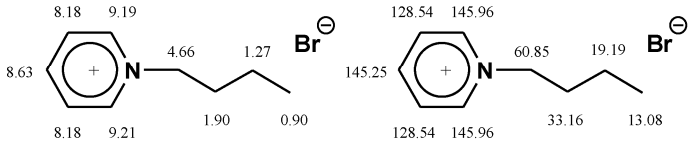

^{1}H NMR δ_H (300 MHz, $CDCl_3$), 0.90 (m, 3H), 1.27 (m, 2H), 1.90 (m, 2H), 4.66 (t, J=7.4 Hz, 2H), 8.18 (m, 2H), 8.63 (m, 1H), 9.19 (d, J=1.2 Hz, 1H), 9.21 (d, J=1.2 Hz, 1H). ^{13}C NMR δ_C (75 MHz, $CDCl_3$), 13.80, 19.19, 33.16, 60.85, 128.54, 145.25, 145.96.

These data are consistent with those reported in literature.[62]

1.3.5.3 [C_6Py]Br

A similar procedure to that outlined for [C_2Py]Br was used to yield [C_6Py]Br as a white solid. Yield: 79%

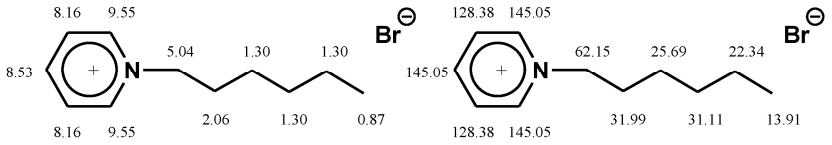

^{1}H NMR δ_H (300 MHz, $CDCl_3$), 0.87 (m, 3H), 1.30 (m, 6H), 2.06 (m, 2H), 5.04 (t, J=7.4Hz, 2H), 8.16 (t, J=6.9 Hz, 2H), 8.53 (m, 1H), 9.55 (d, J=6.0 Hz, 2H). ^{13}C NMR δ_C (75 MHz, $CDCl_3$), 13.91, 22.34, 25.69, 31.11, 31.99, 62.15, 128.38, 145.05.

These data are consistent with those reported in literature.[62]

1.3.5.4 [C_8Py]Br

A similar procedure to that outlined for [C_2Py]Br was used to yield [C_8Py]Br as a white solid. Yield: 78%

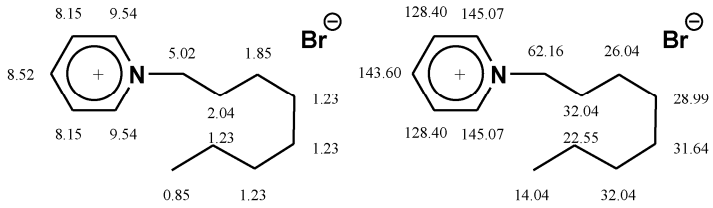

^{1}H NMR δ_H (300 MHz, $CDCl_3$), 0.85 (m, 3H), 1.23 (m, 8H), 1.85 (m, 2H), 2.04 (m, 2H), 5.02 (t, J=7.2Hz, 2H), 8.15 (t, J=6.8 Hz, 2H), 8.52 (m, 1H), 9.54 (d, J=6 Hz, 2H). ^{13}C NMR δ_C (75 MHz, $CDCl_3$), 14.04, 22.55, 26.04, 28.99, 31.64, 32.04, 62.16, 128.40, 143.60, 145.07.

These data are consistent with those reported in literature.[61]

1.3.5.5 $[C_{10}Py]Br$

A similar procedure to that outlined for $[C_2Py]Br$ was used to yield $[C_{10}Py]Br$ as a white solid. Yield: 89%

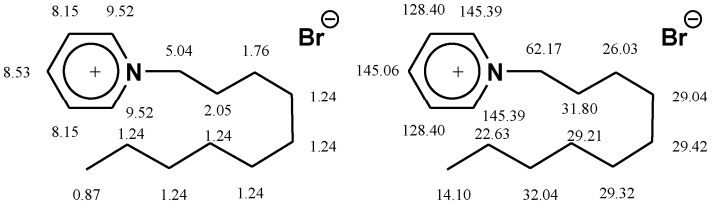

^{1}H NMR δ_H (300 MHz, $CDCl_3$), 0.87 (m, 3H), 1.24 (m, 12H), 1.76 (m, 2H), 2.05 (m, 2H), 5.04 (m, 2H), 8.15 (m, 2H), 8.53 (m, 1H), 9.52 (m, 2H). ^{13}C NMR δ_C (75 MHz, $CDCl_3$), 14.10, 22.63, 26.03, 29.04, 29.21, 29.32, 29.42, 31.80, 32.04, 62.17, 128.40, 145.06, 145.39.

These data are consistent with those reported in literature.[61]

1.3.5.6 $[C_2Py][Tf_2N]$

A similar procedure to that outlined $[C_8C_1Im][Tf_2N]$ was used to yield $[C_2Py][Tf_2N]$ as a colourless liquid. Yield: 75%

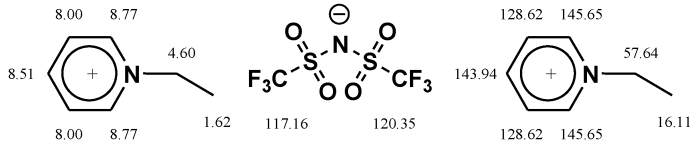

^{1}H NMR δ_H (300 MHz, $CDCl_3$), 1.62 (t, J=7.2 Hz, 3H), 4.60 (m, 2H), 8.00 (m, 2H), 8.51 (m, 1H), 8.77 (d, J=5.5 Hz, 2H). ^{13}C NMR δ_C (75 MHz, $CDCl_3$), 16.11, 57.64, 117.16, 120.35, 128.62, 143.94, 145.65. $[Br]_{IC}$ < 10 ppm.

These data are consistent with those reported in literature.[63]

1.3.5.7 $[C_4Py][Tf_2N]$

A similar procedure to that outlined for $[C_8C_1Im][Tf_2N]$ was used to yield $[C_4Py][Tf_2N]$ as a colourless liquid. Yield: 75%

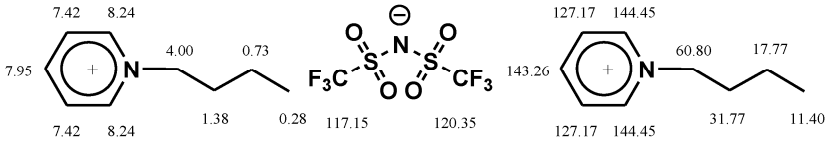

^{1}H NMR δ_H (300 MHz, DMSO-d_6), 0.28 (t, J=7.5 Hz, 3H), 0.73 (m, 2H), 1.38 (m, 2H), 4.00 (m, 2H), 7.42 (m, 2H), 7.95 (m, 1H), 8.24 (d, J=5.8 Hz, 2H). ^{13}C NMR δ_C (75 MHz, DMSO-d_6), 11.40, 17.77, 31.77, 60.80, 117.15, 120.35, 127.17, 143.26, 144.45. $[Br]_{IC}$ < 10 ppm.

These data are consistent with those reported in literature.[36]

1.3.5.8 $[C_6Py][Tf_2N]$

A similar procedure to that outlined $[C_8C_1Im][Tf_2N]$ was used to yield $[C_6Py][Tf_2N]$ as a colourless liquid. Yield: 85%

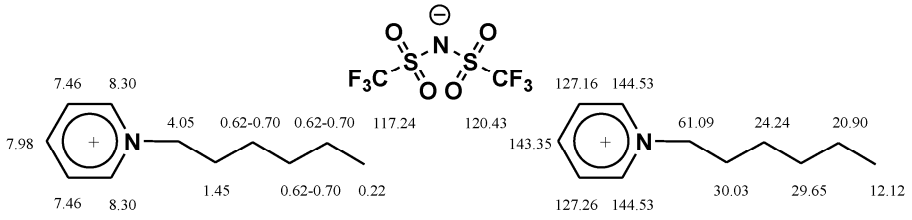

^{1}H NMR δ_H (300 MHz, DMSO-d_6), 0.22 (m, 3H), 0.62-0.70 (m, 6H), 1.45 (m, 2H), 4.05 (m, 2H), 7.46 (m, 2H), 7.98 (m, 1H), 8.30 (d, J=5.8 Hz, 2H). ^{13}C NMR δ_C (75 MHz, DMSO-d_6), 12.12, 20.90, 24.24, 29.65, 30.03, 61.09, 117.24, 120.43, 127.26, 143.35, 144.53. $[Br]_{IC}$ < 10 ppm.

These data are consistent with those reported in literature.[61]

1.3.5.9 $[C_8Py][Tf_2N]$

A similar procedure to that outlined $[C_8C_1Im][Tf_2N]$ was used to yield $[C_8Py][Tf_2N]$ as a colourless liquid. Yield: 82%

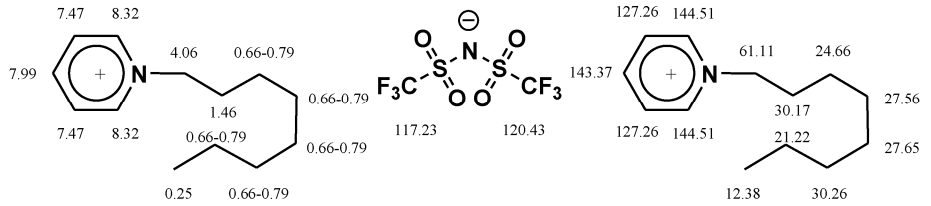

^{1}H NMR δ_H (300 MHz, DMSO-d_6), 0.25 (m, 3H), 0.66-0.79 (m, 10H), 1.46 (m, 2H), 4.06 (t, J=7.0 Hz, 2H), 7.47 (m, 2H), 7.99 (m, 1H), 8.32 (d, J=5.8 Hz, 2H). ^{13}C NMR δ_C (75 MHz, DMSO-d_6), 12.38, 21.22, 24.66, 27.56, 27.65, 30.17, 30.36, 61.11, 117.23, 120.43, 127.26, 143.37, 144.51. $[Br]_{IC}$ < 10 ppm.

These data are consistent with those reported in literature.[62]

1.3.5.10 $[C_{10}Py][Tf_2N]$

A similar procedure to that outlined for $[C_8C_1Im][Tf_2N]$ was used to yield $[C_{10}Py][Tf_2N]$ as a colourless liquid. Yield: 85%

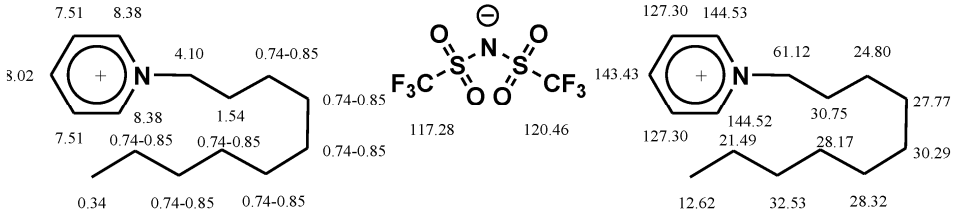

^{1}H NMR δ_H (300 MHz, DMSO-d_6), 0.34 (m, 3H), 0.74-0.85 (m, 14H), 1.54 (m, 2H), 4.10 (t, J=7.2 Hz, 2H), 7.51 (m, 2H), 8.02 (m, 1H), 8.38 (d, J=5.8 Hz, 2H). ^{13}C NMR δ_C (75 MHz, DMSO-d_6), 12.62, 21.49, 24.80, 27.77, 28.17, 28.32, 30.29, 30.75, 32.53, 61.12, 117.28, 120.46, 127.30, 143.43, 144.53. $[Br]_{IC}$ < 10 ppm.

These data are consistent with those reported in literature.[61]

1.3.5.11 $[C_8Py]I$

A similar procedure to that outlined for $[C_2Py]I$ was used to yield $[C_8Py]I$ as a yellow solid. Yield: 64%

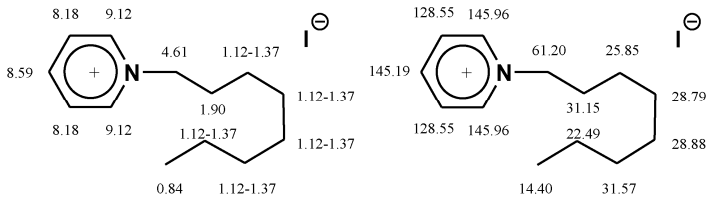

^{1}H NMR δ_H (300 MHz, DMSO-d_6), 0.84 (m, 3H), 1.12-1.37 (m, 10H), 1.90 (m, 2H), 4.61 (t, J=6.4 Hz, 2H), 8.18 (m, 2H), 8.59 (m, 1H), 9.12 (br. s., 2H). ^{13}C NMR δ_C (75 MHz, DMSO-d_6), 14.40, 22.49, 25.84, 28.79, 28.88, 31.15, 31.57, 61.20, 128.55, 145.19, 145.96. ESI-MS negative: 445.99 (1 cation plus 2 anions). ESI-MS positive: 192.18. T_m= 314.6 K.

1.3.5.12 $[C_8Py][BF_4]$

A similar procedure to that outlined for $[C_8C_1Im][BF_4]$ was used to yield $[C_8Py][BF_4]$ as a yellow liquid. Yield: 60%

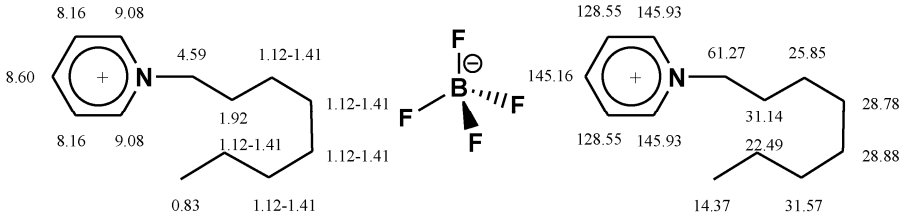

^{1}H NMR δ_H (300 MHz, DMSO-d_6), 0.83 (m, 3H), 1.12-1.41 (m, 10H), 1.92 (m, 2H), 4.59 (t, J=7.4 Hz, 2H), 8.16 (m, 2H), 8.60 (m, 1H), 9.08 (d, J=5.5 Hz, 2H). ^{13}C NMR δ_C (75 MHz, DMSO-d_6), 14.37, 22.49, 25.85, 28.78, 28.88, 31.14, 31.57, 61.27, 128.55, 145.16, 145.93. $[Br]_{IC}$ < 10 ppm. ESI-MS negative: 366.18 (1 cation plus 2 anions). ESI-MS positive: 192.18. T_m= 248.0 K.

1.3.5.13 $[C_8Py][TfO]$

A similar procedure to that outlined for $[C_8C_1Im][TfO]$ was used to yield $[C_8Py][TfO]$ as a white solid. Yield: 67%

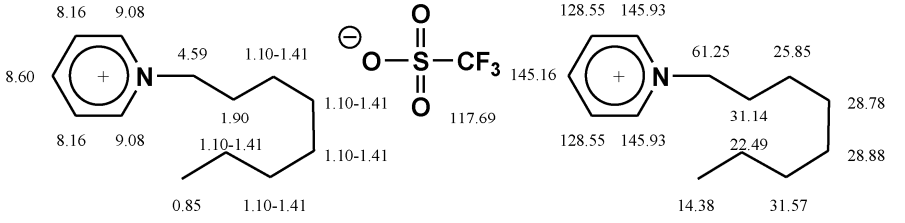

^{1}H NMR δ_H (300 MHz, DMSO-d_6), 0.85 (m, 3H), 1.10-1.41 (m, 10H), 1.90 (m, 2H), 4.59 (t, J=7.5 Hz, 2H), 8.16 (m, 2H), 8.60 (m, 1H), 9.08 (d, J=5.5 Hz, 2H). ^{13}C NMR δ_C (75 MHz, DMSO-d_6), 14.38, 22.49, 25.85, 28.78, 28.88, 31.14, 31.57, 61.25, 117.69, 128.55, 145.16, 145.93. $[Br]_{IC}$ < 10 ppm. ESI-MS negative: 490.08 (1 cation plus 2 anions). ESI-MS positive: 192.18. T_m= 345.9 K.

1.3.5.14 $[C_8Py][PF_6]$

A similar procedure to that outlined $[C_8C_1Im][PF_6]$ was used to yield $[C_8Py][PF_6]$ as a white solid. Yield: 60%

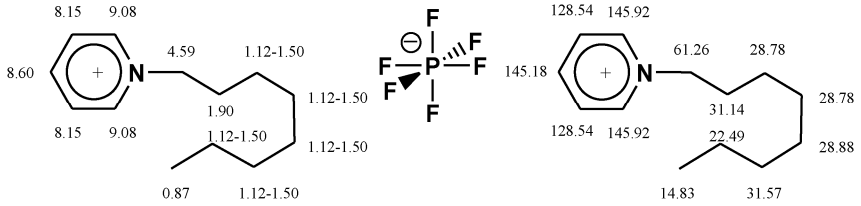

^{1}H NMR δ_H (300 MHz, DMSO-d_6), 0.87 (m, 3H), 1.12-1.50 (m, 10H), 1.90 (m, 2H), 4.59 (t, J=7.5 Hz, 2H), 8.15 (m, 2H), 8.60 (m, 1H), 9.08 (d, J=5.6 Hz, 2H). 13C NMR δ_C (75 MHz, DMSO-d_6), 14.83, 22.49, 25.85, 28.78, 28.88, 31.14, 31.57, 61.26, 128.54, 145.18, 145.92. $[Br]_{IC}$ < 10 ppm. ESI-MS negative: 482.11 (1 cation plus 2 anions). ESI-MS positive: 192.18. T_m= 338.2 K.

1.4 Dissolution of metal catalysts in ionic liquids

Unfortunately, the solubility of metal compounds[64] in ionic liquids is generally much lower than ionic metal complexes.[65] It presents difficulty in defining the peak area of X-ray Photoelectron Spectra (low signal to noise ratio) as well as acquiring the binding energy information. Consequently, a high concentration of the solute in ionic liquids is required. In order to achieve a high concentration for neutral metal compounds, different approaches have been successfully applied such as the use of task specific ionic liquids[64, 66] and the addition of different ligands.[50, 67] In this work, two main methods were used, the addition of phosphine ligands and the formation of phosphineimidazolylidene palladium complexes.

1.4.1 The addition of phosphine ligands

The solubility of the catalyst, *e.g.* a rhodium catalyst, can be improved by adding phosphine ligands. This procedure is supposed to avoid the leaching of the rhodium catalyst out of the reaction system. The rhodium catalyst, *i.e.* in this book (Acetylacetonato)dicarbonyl- rhodium(I) ([Rh(acac)($CO)_2$]), can react with the phosphine ligands and produce a species which is more soluble in ionic liquids.

In this book, Rh-containing ionic liquid-based solutions were prepared using 1,1′-Bis (diphenylphosphino)ferrocene (dppf) and Triphenylphosphine (PPh_3) as ligands and will be discussed in detail in *Chapter 5*.

Furthermore, since the rhodium catalyst shows limited and slow solubility in ionic liquids,

dichloromethane was added to the mixture to speed up solvation processes.[68, 69] The addition of dichloromethane allows full contact of the catalyst and ionic liquids as they are both dissolved in dichloromethane. Dichloromethane can then be removed completely, firstly under rotary evaporator and then under high vacuum at room temperature, to give Rh-containing ionic liquid based solutions.

1.4.2 The formation of phosphineimidazolylidene palladium complexes

Ionic liquids, when applied to catalysis, can act as 'innocent' solvents and co-catalysts or even as ligand sources for given reactions.[70] In particular, in the palladium catalysed Suzuki cross coupling reaction, due to the interaction of the palladium catalyst, Tetrakis(triphenyl phosphine)palladium(0) ($[Pd(PPh_3)_4]$), with ionic liquids, there is the formation of a new more active species in solution, *i.e.* phosphineimidazolylidene palladium complex.[71] The formation of the phosphineimidazolylidene palladium complex can give rise to an acceleration of the Suzuki cross coupling reaction.[72]

Moreover, the formation of the phosphineimidazolylidene palladium complex does indeed enhance the concentration of the palladium in the solution. The preparation of the Pd-containing ionic liquid-based solution is described as follows:

Into a mixture of NaCl (12 mg, 0.21 mmol), bromobenzene (13.1 ml, 0.125 mmol) and $[Pd(PPh_3)_4]$ (24 mg, 0.021mmol) in any ionic liquid used in this work (0.25 ml), a solution of Na_2CO_3 (26 mg, 0.25 mmol) in water (0.125 ml) was injected. The resulting solution was heated to 110℃ for 3h under an inert atmosphere to ensure complete dissolution of the organometallic species. Any undissolved material was removed by filtration and volatile compounds were removed under high vacuum. It must be noted that all ionic liquid solutions were prepared in a dry-box using pre-pumped and de-gassed ionic liquids. A more detailed discussion will be presented in *Chapter 4*.

1.5 Ionic liquids analysed in this book

In this book, imidazolium-, pyrrolidinium- and pyrinidnium-based ionic liquids are investigated and the nomenclature applied for these different cations is shown in Table 1.3.

Table 1.3 Cations studied in this book

Cation	Name
$[C_2C_1Im]^+$	1-ethyl-3-methylimidazolium
$[C_4C_1Im]^+$	1-butyl-3-methylimidazolium
$[C_8C_1Im]^+$	1-octyl-3-methylimidazolium
$[C_{12}C_1Im]^+$	1-dodecyl-3-methylimidazolium
$[C_2C_1Pyrr]^+$	1-ethyl-1-methylpyrrolidinium
$[C_4C_1Pyrr]^+$	1-butyl-1-methylpyrrolidinium
$[C_6C_1Pyrr]^+$	1-hexyl-1-methylpyrrolidinium
$[C_8C_1Pyrr]^+$	1-octyl-1-methylpyrrolidinium
$[C_{10}C_1Pyrr]^+$	1-decyl-1-methylpyrrolidinium
$[C_2Py]^+$	1-ethylpyridinium
$[C_4Py]^+$	1-butylpyridinium
$[C_6Py]^+$	1-hexylpyridinium
$[C_8Py]^+$	1-octylpyridinium
$[C_{10}Py]^+$	1-decylpyridinium

The number of anions available for the synthesis of ionic liquids is much smaller than the number of cations. However, the nature of the anion is found to be much more efficient at influencing the properties of the ionic liquids. Table 1.4 shows the anions studied in this book.

Table 1.4 Anions studied in this book

Anion	Name
$[Tf_2N]^-$	Bis[(trifluoromethane)sulfonyl]imide
$[PF_6]^-$	Hexafluorophosphate
$[I_3]^-$	Triiodide
$[TfO]^-$	Trifluoromethanesulfonate
$[IBr_2]^-$	Iododibromide
$[BF_4]^-$	Tetrafluoroborate
$[SnCl_3]^-$	Trichlorostannate(II)
$[Sn_2Cl_5]^-$	Pentachlorodistannate(II)
Cl^-	Chloride
Br^-	Bromide
I^-	Iodide
$[OAc]^-$	Acetate

1.6 Catalysis in ionic liquids

Due to their wide range of fascinating properties, ionic liquids have been used in a broad range of research fields such as organic/inorganic synthesis,[42, 70] electrochemistry,[73] and

catalysis.[74] Their intrinsic low-volatility also allows ionic liquids to act as potential solvents for the replacement of traditional organic solvents.[8, 75, 76] Ionic liquids can also play a role in the immobilisation of catalysts which allows ease of separation of products and possible recycle of the catalyst. For example, supported ionic liquids phases (SILPs) involve a catalyst which is immobilised within a thin-film of an ionic liquid adsorbed on a solid support and these have been applied to gas-phase catalysis.[77] A further modification of this technique, *i.e.* solid catalysts with ionic liquid layers (SCILLs), may even exhibit better reaction selectivity, as experimentally demonstrated in hydrogenation reactions.[78, 79]

Moreover, ionic liquid-catalyst interactions have been shown to occur in most of the common homogeneous catalytic processes, *e.g.* cross-coupling, hydroformylation and hydrogenation. It has been shown that both the cations and anions of ionic liquids can interact with a catalyst. The nature of the anion plays an important role in this interaction, *i.e.* more basic anions may bind directly to the metal centre.[80] Cations can also act as co-ligands *via e.g.* carbene formation at the C^2 position for imidazolium-based ionic liquids.[81] In some cases, this interaction can result in altered reactivity of the catalytic system and thus different reaction performance, such as reaction rates or selectivities.[82] A good understanding of these interactions in ionic liquids will be fundamental for the successful development of this technology.[12, 83]

References

[1] WASSERSCHEID P，WELTON T. Ionic Liquids in Synthesis[M]. Weinheim: WILEY-VCH，2007.

[2] PLECHKOVA N V，SEDDON K R. Applications of ionic liquids in the chemical industry[J]. Chemical Society Reviews，2008，37(1): 123-150.

[3] LOVELOCK K R J，VILLAR-GARCIA I J，MAIER F，et al. Photoelectron Spectroscopy of Ionic Liquid-Based Interfaces[J]. Chemical Reviews，2010，110(9): 5158-5190.

[4] MEN S，LOVELOCK K R J，LICENCE P. Directly probing the effect of the solvent on a catalyst electronic environment using X-ray photoelectron spectroscopy[J]. Rsc Advances，2015，5(45): 35958-35965.

[5] FORSYTH S A，PRINGLE J M，MACFARLANE D R. Ionic liquids - An overview[J].

Australian Journal of Chemistry，2004，57(2): 113-119.

[6] WILKES J S. A short history of ionic liquids - from molten salts to neoteric solvents[J]. Green Chemistry，2002，4(2): 73-80.

[7] GALE R J，GILBERT B，OSTERYOUNG R A. Raman-Spectra of Molten Aluminum-Chloride-1-Butylpyridinium Chloride Systems at Ambient-Temperatures[J]. Inorganic Chemistry，1978，17(10): 2728-2729.

[8] SEDDON K R. Ionic liquids for clean technology[J]. Journal of Chemical Technology and Biotechnology，1997，68(4): 351-356.

[9] ROGERS R D，SEDDON K R. Ionic liquids - Solvents of the future?[J]. Science，2003，302(5646): 792-793.

[10] CAPELLO C，FISCHER U，HUNGERBUHLER K. What is a green solvent? A comprehensive framework for the environmental assessment of solvents[J]. Green Chemistry，2007，9(9): 927-934.

[11] HOUGH W L，SMIGLAK M，RODRIGUEZ H，et al. The third evolution of ionic liquids: active pharmaceutical ingredients[J]. New Journal of Chemistry，2007，31(8): 1429-1436.

[12] CHIAPPE C，PIERACCINI D. Ionic liquids: solvent properties and organic reactivity[J]. Journal of Physical Organic Chemistry，2005，18(4): 275-297.

[13] SEDDON K R，STARK A，TORRES M J. Influence of chloride，water and organic solvents on the physical properties of ionic liquids[J]. Pure and Applied Chemistry，2000，72(12): 2275-2287.

[14] TOKUDA H，ISHII K，SUSAN M，et al. Physicochemical properties and structures of room-temperature ionic liquids. 3. Variation of cationic structures 10.1021/jpO53396f[J]. Journal of Physical Chemistry B，2006，110(6): 2833-2839.

[15] KROSSING I，SLATTERY J M，DAGUENET C，et al. Why are ionic liquids liquid? A simple explanation based on lattice and solvation energies [J]. Journal of the American Chemical Society，2007，129(36): 11296-11296.

[16] HUDDLESTON J G，VISSER A E，REICHERT W M，et al. Characterization and comparison of hydrophilic and hydrophobic room temperature ionic liquids incorporating the imidazolium cation[J]. Green Chemistry，2001，3(4): 156-164.

[17] CALVAR N，GOMEZ E，GONZALEZ B，et al. Experimental determination，correlation，and prediction of physical properties of the ternary mixtures ethanol plus water with 1-octyl-3-methylimidazolium chloride and 1-ethyl-3-methylimidazolium ethylsulfate[J].

Journal of Chemical and Engineering Data，2007，52(6): 2529-2535.

[18] HOLBREY J D，SEDDON K R. The phase behaviour of 1-alkyl-3-methylimidazolium tetrafluoroborates；ionic liquids and ionic liquid crystals[J]. Journal of the Chemical Society，Dalton Transactions: Inorganic Chemistry，1999(13): 2133-2139.

[19] SANMAMED Y A，GONZALEZ-SALGADO D，TRONCOSO J，et al. Viscosity-induced errors in the density determination of room temperature ionic liquids using vibrating tube densitometry[J]. Fluid Phase Equilibria，2007，252(1-2): 96-102.

[20] KANAKUBO M，HARRIS K R，TSUCHIHASHI N，et al. Effect of pressure on transport properties of the ionic liquid 1-butyl-3-methylimidazolium hexafluorophosphate[J]. Journal of Physical Chemistry B，2007，111(8): 2062-2069.

[21] PAPAICONOMOU N，YAKELIS N，SALMINEN J，et al. Synthesis and properties of seven ionic liquids containing 1-methyl-3-octylimidazolium or 1-butyl-4-methylpyridinium cations[J]. Journal of Chemical and Engineering Data，2006，51(4): 1389-1393.

[22] LAW G，WATSON P R. Surface tension measurements of N-alkylimidazolium ionic liquids[J]. Langmuir，2001，17(20): 6138-6141.

[23] PEREIRO A B，LEGIDO J L，RODRIGUEZ A. Physical properties of ionic liquids based on 1-alkyl-3-methylimidazolium cation and hexafluorophosphate as anion and temperature dependence[J]. Journal of Chemical Thermodynamics，2007，39(8): 1168-1175.

[24] TOKUDA H，TSUZUKI S，SUSAN M A B H，et al. How ionic are room-temperature ionic liquids? An indicator of the physicochemical properties[J]. Journal of Physical Chemistry B，2006，110(39): 19593-19600.

[25] MEN S，LOVELOCK K R J，LICENCE P. X-ray Photoelectron Spectroscopy of Pyrrolidinium-Based Ionic Liquids: Cation-Anion Interactions and a Comparison to Imidazolium-Based Analogues[J]. Physical Chemistry Chemical Physics，2011，13(33): 15244-15255.

[26] MEN S，MITCHELL D S，LOVELOCK K R J，et al. X-ray Photoelectron Spectroscopy of Pyridinium-Based Ionic Liquids: Comparison to Imidazolium- and Pyrrolidinium-Based Analogues[J]. Chemphyschem，2015，16(10): 2211-2218.

[27] REBELO L P N，CANONGIA LOPES J N，ESPERANCA J，et al. On the critical temperature，normal boiling point，and vapor pressure of ionic liquids[J]. Journal of Physical Chemistry B，2005，109(13): 6040-6043.

[28] FOX D M，GILMAN J W，DE LONG H C，et al. TGA decomposition kinetics of

1-butyl-2,3-dimethylimidazolium tetrafluoroborate and the thermal effects of contaminants[J]. Journal of Chemical Thermodynamics，2005，37(9): 900-905.

[29] LEAL J P，ESPERANCA J，DA PIEDADE M E M，et al. The nature of ionic liquids in the gas phase[J]. Journal of Physical Chemistry A，2007，111(28): 6176-6182.

[30] CREMER T，KILLIAN M，GOTTFRIED J M，et al. Physical Vapor Deposition of [EMIM][Tf2N]: A New Approach to the Modification of Surface Properties with Ultrathin Ionic Liquid Films[J]. Chemphyschem，2008，9(15): 2185-2190.

[31] TAYLOR A W，LOVELOCK K R J，DEYKO A，et al. High vacuum distillation of ionic liquids and separation of ionic liquid mixtures[J]. Physical Chemistry Chemical Physics，2010，12(8): 1772-1783.

[32] TAYLOR A W，LOVELOCK K R J，JONES R G，et al. Borane-substituted imidazol-2-ylidenes: syntheses in vacuo[J]. Dalton Transactions，2011，40(7): 1463-1470.

[33] MAIER F，GOTTFRIED J M，ROSSA J，et al. Surface enrichment and depletion effects of ions dissolved in an ionic liquid: an X-ray photoelectron spectroscopy study[J]. Angewandte Chemie-International Edition，2006，45(46): 7778-7780.

[34] TOCHIGI K，YAMAMOTO H. Estimation of ionic conductivity and viscosity of ionic liquids using a QSPR model[J]. Journal of Physical Chemistry C，2007，111(43): 15989-15994.

[35] HAGIWARA R，MATSUMOTO K，NAKAMORI Y，et al. Physicochemical properties of 1,3-dialkylimidazolium fluorohydrogenate room-temperature molten salts[J]. Journal of the Electrochemical Society，2003，150(12): D195-D199.

[36] TOKUDA H，TSUZUKI S，SUSAN M，et al. How ionic are room-temperature ionic liquids? An indicator of the physicochemical properties[J]. Journal of Physical Chemistry B，2006，110(39): 19593-19600.

[37] WIDEGREN J A，SAURER E M，MARSH K N，et al. Electrolytic conductivity of four imidazolium-based room-temperature ionic liquids and the effect of a water impurity[J]. Journal of Chemical Thermodynamics，2005，37(6): 569-575.

[38] XU W，COOPER E I，ANGELL C A. Ionic liquids: Ion mobilities，glass temperatures，and fragilities[J]. Journal of Physical Chemistry B，2003，107(25): 6170-6178.

[39] LEYS J，WUBBENHORST M，MENON C P，et al. Temperature dependence of the electrical conductivity of imidazolium ionic liquids[J]. Journal of Chemical Physics，2008，128(6): 064509.

[40] CHIAPPE C，PIERACCINI D，POMELLI C S. Ionic Liquids in Organic Synthesis[M]. Washington: American Chemical Society，2007.

[41] COCALIA V A，GUTOWSKI K E，ROGERS R D. The coordination chemistry of actinides in ionic liquids: A review of experiment and simulation[J]. Coordination Chemistry Reviews，2006，250(7-8): 755-764.

[42] PARVULESCU V I，HARDACRE C. Catalysis in ionic liquids[J]. Chemical Reviews，2007，107(6): 2615-2665.

[43] FONSECA G S，MACHADO G，TEIXEIRA S R，et al. Synthesis and characterization of catalytic iridium nanoparticles in imidazolium ionic liquids[J]. Journal of Colloid and Interface Science，2006，301(1): 193-204.

[44] THURECHT K J，GOODEN P N，GOEl S，et al. Free-radical polymerization in ionic liquids: The case for a protected radical[J]. Macromolecules，2008，41(8): 2814-2820.

[45] SWATLOSKI R P，SPEAR S K，HOLBREY J D，et al. Dissolution of cellose with ionic liquids[J]. Journal of the American Chemical Society，2002，124(18): 4974-4975.

[46] MONIRUZZAMAN M，NAKASHIMA K，KAMIYA N，et al. Recent advances of enzymatic reactions in ionic liquids[J]. Biochemical Engineering Journal，2010，48(3): 295-314.

[47] FREIRE M G，NEVES C，CARVALHO P J，et al. Mutual Solubilities of water and hydrophobic ionic liquids[J]. Journal of Physical Chemistry B，2007，111(45): 13082-13089.

[48] MARSH K N，DEEV A，WU A C T，et al. Room temperature ionic liquids as replacements for conventional solvents - A review[J]. Korean Journal of Chemical Engineering，2002，19(3): 357-362.

[49] BLANCHARD L A，HANCU D，BECKMAN E J，et al. Green processing using ionic liquids and CO_2[J]. Nature，1999，399(6731): 28-29.

[50] HINTERMAIR U，ZHAO G Y，SANTINI C C，et al. Supported ionic liquid phase catalysis with supercritical flow[J]. Chemical Communications，2007(14): 1462-1464.

[51] EARLE M J，GORDON C M，PLECHKOVA N V，et al. Decolorization of ionic liquids for spectroscopy[J]. Analytical Chemistry，2007，79(2): 758-764.

[52] TRAN C D，LACERDA S H D，OLIVEIRA D. Absorption of water by room-temperature ionic liquids: Effect of anions on concentration and state of water[J]. Applied Spectroscopy，2003，57(2): 152-157.

[53] DIMITRAKIS G，VILLAR-GARCIA I J，LESTER E，et al. Dielectric spectroscopy: a technique for the determination of water coordination within ionic liquids[J]. Physical Chemistry Chemical Physics，2008，10(20): 2947-2951.

[54] LOVELOCK K R J，SMITH E F，DEYKO A，et al. Water adsorption on a liquid surface[J]. Chemical Communications，2007(46): 4866-4868.

[55] BONHOTE P，DIAS A P，ARMAND M，et al. Hydrophobic，highly conductive ambient-temperature molten salts[J]. Inorganic Chemistry，1998，37(1): 166-166.

[56] MACFARLANE D R，MEAKIN P，SUN J，et al. Pyrrolidinium imides: A new family of molten salts and conductive plastic crystal phases[J]. Journal of Physical Chemistry B，1999，103(20): 4164-4170.

[57] BONHOTE P，DIAS A P，PAPAGEORGIOU N，et al. Hydrophobic，highly conductive ambient-temperature molten salts[J]. Inorganic Chemistry，1996，35(5): 1168-1178.

[58] SUAREZ P A Z，DULLIUS J E L，EINLOFT S，et al. The use of new ionic liquids in two-phase catalytic hydrogenation reaction by rhodium complexes[J]. Polyhedron，1996，15(7): 1217-1219.

[59] ZHANG Z，LI J，ZHANG Q，et al. Enthalpy of solution of amino acid ionic liquid 1-ethyl-3-methylimidazollum ammonioacetate[J]. Journal of Chemical and Engineering Data，2008，53(5): 1196-1198.

[60] MACFARLANE D R，MEAKIN P，AMINI N，et al. Structural studies of ambient temperature plastic crystal ion conductors[J]. Journal of Physics-Condensed Matter，2001，13(36): 8257-8267.

[61] PAPAICONOMOU N，SALMINEN J，LEE J M，et al. Physicochemical properties of hydrophobic ionic liquids containing 1-octylpyridinium，1-octyl-2-methylpyridinium，or 1-octyl-4-methylpyridinium cations[J]. Journal of Chemical and Engineering Data，2007，52(3): 833-840.

[62] CROSTHWAITE J M，MULDOON M J，DIXON J K，et al. Phase transition and decomposition temperatures，heat capacities and viscosities of pyridinium ionic liquids[J]. Journal of Chemical Thermodynamics，2005，37(6): 559-568.

[63] KATO R，GMEHLING J. Activity coefficients at infinite dilution of various solutes in the ionic liquids $[MMIM]^+[CH_3SO_4]^-$，$[MMIM]^+[CH_3OC_2H_4SO_4]^-$，$[MMIM]^+[(CH_3)_2PO_4]^-$，$[C_5H_5NC_2H_5]^+[(CF_3SO_2)_2N]^-$ and $[C_5H_5NH]^+[C_2H_5OC_2H_4OSO_3]^-$[J]. Fluid Phase Equilibria，2004，226: 37-44.

[64] NOCKEMANN P，THIJS B，PITTOIS S，et al. Task-specific ionic liquid for solubilizing metal oxides[J]. Journal of Physical Chemistry B，2006，110(42): 20978-20992.

[65] CHAUVIN Y，MUSSMANN L，OLIVIER H. A novel class of versatile solvents for two-phase catalysis: Hydrogenation，isomerization，and hydroformylation of alkenes catalyzed by rhodium complexes in liquid 1,3-dialkylimidazolium salts[J]. Angewandte Chemie-International Edition，1995，34(23-24): 2698-2700.

[66] LEE S G. Functionalized imidazolium salts for task-specific ionic liquids and their applications[J]. Chemical Communications，2006(10): 1049-1063.

[67] SELLIN M F，WEBB P B，COLE-HAMILTON D J. Continuous flow homogeneous catalysis: hydroformylation of alkenes in supercritical fluid-ionic liquid biphasic mixtures[J]. Chemical Communications，2001(8): 781-782.

[68] MACLEOD S，ROSSO R J. Hydrogenation of low molecular weight polymers in ionic liquids and the effects of added salt[J]. Advanced Synthesis & Catalysis，2003，345(5): 568-571.

[69] GIL W，TRZECIAK A M，ZIOLKOWSKI J J. Catalytic polymerization of phenylacetylene with dimeric $[Rh(OMe)(cod)]_2$ complex in ionic liquids[J]. Applied Organometallic Chemistry，2006，20(11): 766-770.

[70] WELTON T. Ionic liquids in catalysis[J]. Coordination Chemistry Reviews，2004，248(21-24): 2459-2477.

[71] MATHEWS C J，SMITH P J，WELTON T，et al. In situ formation of mixed phosphine-imidazolylidene palladium complexes in room-temperature ionic liquids[J]. Organometallics，2001，20(18): 3848-3850.

[72] MATHEWS C J，SMITH P J，WELTON T. Palladium catalysed Suzuki cross-coupling reactions in ambient temperature ionic liquids[J]. Chemical Communications，2000(14): 1249-1250.

[73] ENDRES F，MACFARLANE D R，ABBOTT A P. Electrodeposition from Ionic Liquids[M]. Weinheim: WILEY-VCH，2011.

[74] FALCIONI F，WALKER A J，BRUCE N C. Biocatalysis in novel functionalized ionic liquids[J]. Abstracts of Papers of the American Chemical Society，2006，231: 114.

[75] EARLE M J，SEDDON K R. Ionic liquids. Green solvents for the future[J]. Pure and Applied Chemistry，2000，72(7): 1391-1398.

[76] POLIAKOFF M，LICENCE P. Sustainable technology - Green chemistry[J]. Nature，2007，

450(7171): 810-812.

[77] MIKKOLA J P，VIRTANEN P，KORDAS K，et al. SILCA-supported ionic liquid catalysts for fine chemicals[J]. Applied Catalysis a-General，2007，328(1): 68-76.

[78] KERNCHEN U，ETZOLD B，KORTH W，et al. Solid catalyst with ionic liquid layer (SCILL) - A new concept to improve selectivity illustrated by hydrogenation of cyclooctadiene[J]. Chemical Engineering & Technology，2007，30(8): 985-994.

[79] STEINRUCK H P，LIBUDA J，WASSERSCHEID P，et al. Surface Science and Model Catalysis with Ionic Liquid-Modified Materials[J]. Advanced Materials，2011，23(22-23): 2571-2587.

[80] BOSMANN A，FRANCIO G，JANSSEN E，et al. Activation，tuning，and immobilization of homogeneous catalysts in an tonic liquid/compressed CO_2 continuous-flow system[J]. Angewandte Chemie-International Edition，2001，40(14): 2697-2699.

[81] OTT L S，CLINE M L，DEETLEFS M，et al. Nanoclusters in ionic liquids: Evidence for N-heterocyclic carbene formation from imidazolium-based ionic liquids detected by H-2 NMR[J]. Journal of the American Chemical Society，2005，127(16): 5758-5759.

[82] HERRMANN W A，BOHM V P W. Heck reaction catalyzed by phospha-palladacycles in non-aqueous ionic liquids[J]. Journal of Organometallic Chemistry，1999，572(1): 141-145.

[83] CHOWDHURY S，MOHAN R S，SCOTT J L. Reactivity of ionic liquids[J]. Tetrahedron，2007，63(11): 2363-2389.

Chapter 2

X-ray Photoelectron Spectroscopy

2.1 X–ray photoelectron spectroscopy

X-ray photoelectron spectroscopy (XPS) is a quantitative spectroscopic technique which provides a measurement of binding energy for the inelastic/non-scattered photoelectrons emitted from a sample when irradiated by incident X-ray in *vacuo*. This technique was firstly developed by Kai Siegbahn[1] in the 1960s and has since become a widely used analytical method in many research fields, for example heterogeneous catalysis, corrosion science and polymer science.[2, 3] XPS provides information regarding both elemental composition and the electronic environments of given elements in the near surface region of a sample.[2]

2.1.1 Principle

The photoelectric process is the basic principle upon which XPS operates.[3] When X-rays irradiate a sample, the incident photon causes the emission of photoelectrons. An inelastic emitted photoelectron has discrete kinetic energy which may be measured. The binding energy may be derived using Eq. (2.1).

$$\mathrm{KE} = h\nu - \mathrm{BE} - \Phi_s \qquad (2.1)$$

Where $h\nu$ is the energy of the incident photon, KE is the kinetic energy of the emitted photoelectron, BE is the binding energy of the atomic orbital from which the electrons originates

and Φ_s is the spectrometer work function. The binding energy is actually relative to the highest occupied quantum level (the Fermi level) of an atom and is regarded as the energy gap between the initial and final states of the photoelectron process. The work function refers to the minimum energy required when removing an electron from the Fermi level to the Vacuum level. A schematic of the photoelectron process is described in Figure 2.1.

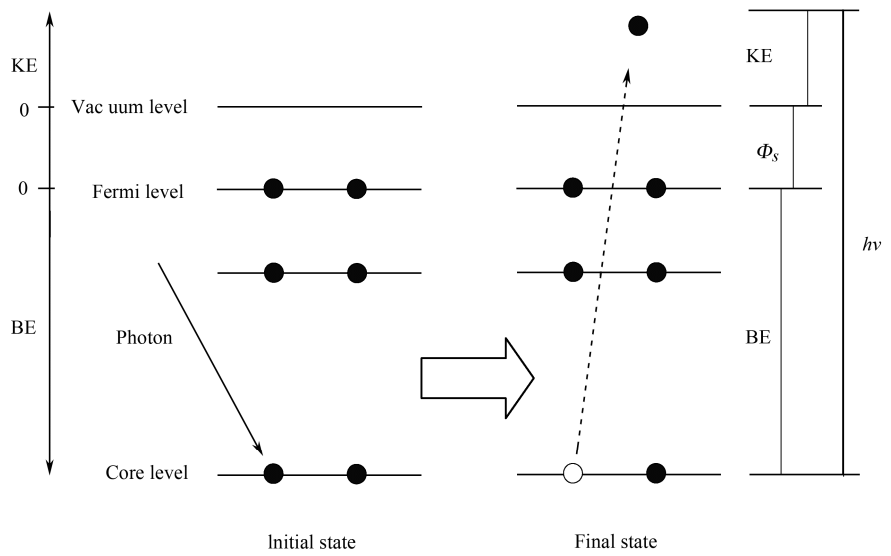

Figure 2.1 Photoemission process

X-ray photons can penetrate into a sample at a distance of the order of magnitude of several micrometres, resulting in photoemissions. Typically, the inelastic mean free path, λ, of photoelectrons in organic compounds is of the order 3 nm. At the kinetic energies measured here (800-1300 eV), the information depth (3λ), ID, defines a region from which 95% of the measured signal originates. This determines the detectable region of XPS is between 7 and 9 nm at the normal emission angle, θ = 0°. A more detailed introduction of ID will be reported in *Section 2.2.3*. However, it is worth emphasising that at this emission angle (θ), XPS data is indicative of the bulk of the sample.[4] More surface sensitive information can be derived from angle resolved X-ray photoelectron spectroscopy, ARXPS. For example, at emission angle (θ) of 80° (ID = 1-1.5 nm), 95% of the XPS signals originate from a surface depth of 1-1.5 nm, whereas 65% of the XPS signals come from the uppermost 0.3-0.5 nm of the sample which is even less than the width of a single molecule of many ionic liquids.[4, 5]

A typical XP spectrum is a plot of the number of photoelectrons (counts) versus binding

energy, see Figure 2.2. The photoelectrons emitted from a sample without any loss of energy form the main photoelectron lines; whilst those which suffer inelastic processes contribute to the background of an XP spectrum. A more detailed introduction of XP spectrum will be reported in *Section 2.1.5*.

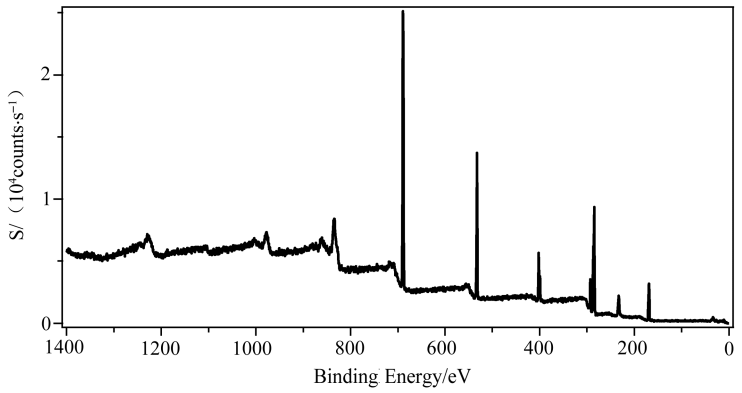

Figure 2.2 A typical XP spectrum

2.1.2 Experimental set-up

A schematic of the typical XPS experimental set-up used in this work is shown in Figure 2.3. X-rays are generated from an X-ray gun employing an aluminium targeted anode (for this work). The generated X-ray is then monochromated in an array of quartz crystals by selective diffraction. The application of a monochromator gives rise to better energy resolution which makes the measured peaks much narrower. It can also remove the interference from X-ray satellites and reduce the background signal due to the removal of Bremsstrahlung radiation. The existence of a monochromator also increases the distance between X-ray source and the sample which reduces the risk of sample damage or overheating. The emitted photoelectrons were then slowed down by the electromagnetic lenses and focused into the analyser. Only photoelectrons at the selected energies, the so-called pass energy, can pass through the concentric hemi-spherical analyser (CHA) before reaching the detector. It must be noted that the pass energy should be set consistently for each measurement so that fixed resolution across the spectrum can be achieved. Low pass energy usually improves the resolution of the spectrum but gives low intensity. A typical detector is composed of a multi-channel plate and a delay line detector (DLD) which is used to count the electron pulses.

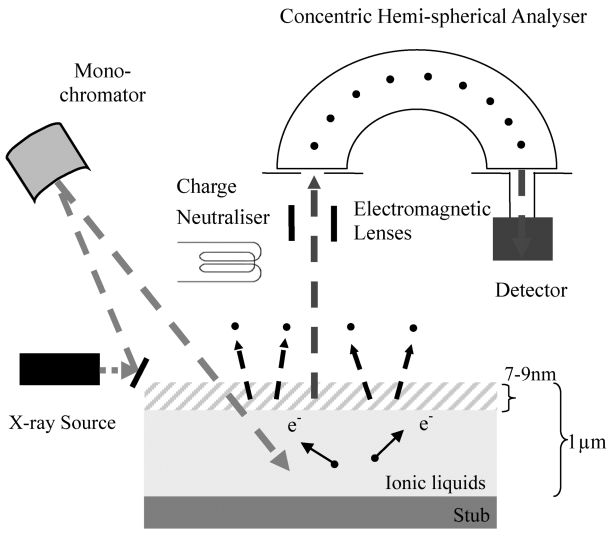

Figure 2.3 Schematic XPS experimental set-up

2.1.3 Vacuum environment

Ultra high vacuum is required for an XPS experiment to allow analysis of the emitted photoelectrons without impact from gas phase collisions. Consequently, a pressure between 10^{-8} and 10^{-9} mbar is utilised for XPS measurements. It should be noted that, in this work, initial pumping to high vacuum pressure was carried out in a preparation chamber. The pressure in the preparation airlock was 10^{-7} mbar. Pumping-times varied (1-3h total) depending upon the volume, volatile impurity content and viscosity of the sample, *i.e.* more viscous ionic liquids were found to require longer pumping times. The samples were then transferred to the main analysis chamber. Turbomolecular and sputter ion sublimation pumps are typically employed for the achievement of such an ultra high vacuum.

2.1.4 Charge neutralisation

As a consequence of photoelectron emission, a positive charging at the surface of the sample can occur. In the case of conductors, such a surface charge can be compensated directly by the earth, due to their high conductivity. However, in the case of non-conductors, the surface charge cannot be neutralised and thus causes the shift or broadening of the measured spectra. To overcome this effect, a charge neutralisation device is applied, which transfers low energy electrons to the analysis area and therefore stops the surface from charging up uncontrollably.

2.1.5 Data interpretation

An XP spectrum is plotted as number of counts/electrons in a unit time *versus* binding energy. A typical ionic liquid survey XP spectrum of $[C_8Py][Tf_2N]$ is presented, with labelled element orbitals in Figure 2.4.

2.1.5.1 Photoelectron lines

Photoelectron lines, which correspond to the photoemission from the core orbitals, are labelled in Figure 2.4 as F 1s, O 1s, N 1s, C 1s, S 2s and S 2p. Each element has a series of a characteristic set of binding energies which allows elemental identification. More detailed description about XPS analytical information is reported in *Section 2.2.5*.

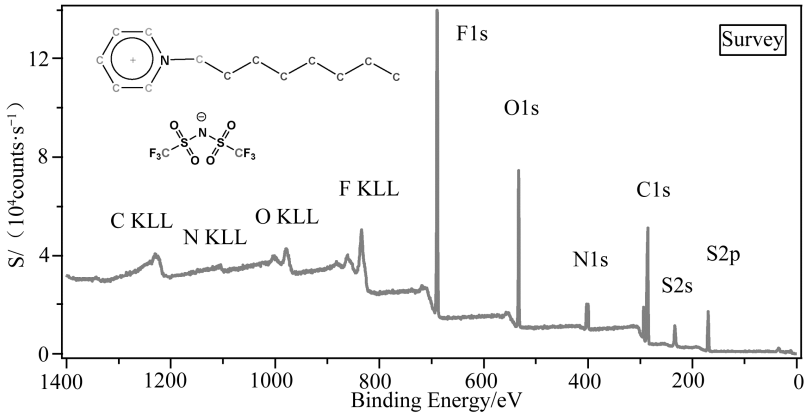

Figure 2.4 Typical XP survey spectrum of $[C_8Py][Tf_2N]$ with peaks labelled.

2.1.5.2 Auger lines

During the photoemission process, the atom is left in an excited state following the emission of photoelectrons. The relaxation of the atom occurs when an outer electron relaxes to the lower energy vacant core level. This process releases energy by either emitting a photon (light/UV/X-ray) or by causing the emission of a second outer electron. These emitted electrons, *i.e.* Auger electrons, can be observed between 1400 and 800 eV in an XP survey spectrum, as shown in Figure 2.4. The Auger process is shown schematically in Figure 2.5. Auger processes are independent of the incident photon energy and therefore are observed at fixed kinetic energies.

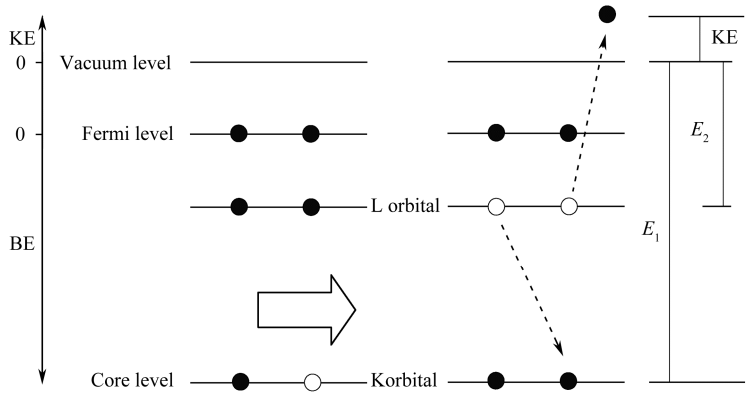

Figure 2.5 KLL Auger process

Each element has a characteristic Auger electron spectrum that can be used, along with photoelectron binding energies, to identify the existence of a given element, *i.e.* F KLL. The set of letters identify the quantum orbitals of the initial and final vacancies in the Auger process. For example, in the case of F KLL, the photoelectron originated from a K orbital (principal quantum number = 1) and the relaxed and emitted Auger electrons were both located in L orbitals (principal quantum number =2).

2.1.5.3 Valence band

In the low binding energy region, between 40 and 0 eV, lines with lower intensity can be observed. These lines are generated by photoelectron emission from molecular orbitals or valence bands. The valence band lines can be considered as a fingerprint of the sample being analysed and therefore can be used to distinguish between materials, specifically if the core orbital photoelectron lines are similar in shape and position.

2.2 XPS experiment

2.2.1 Instrument

All XP spectra were recorded using a Kratos Axis Ultra spectrometer (Figure 2.6) employing a focused, monochromated Al Kα source ($h\nu$ =1486.6 eV), hybrid (magnetic/electrostatic) optics, concentric hemispherical analyser (CHA) and a multi-channel plate and delay line detector (DLD)

with an X-ray incident angle of 30° and a collection angle of 0° (both relative to the surface normal).

All spectra were recorded using an entrance aperture of 300 × 700 μm^2 with a pass energy of 80 eV for survey spectra and 20 eV for high resolution spectra. The instrument sensitivity was 7.5 × 10^5 counts • s^{-1} when measuring the Ag $3d_{5/2}$ photoemission peak for a clean Ag sample recorded at a pass energy of 20 eV and 450 W emission power. Ag $3d_{5/2}$ full width half maximum (FWHM) was 0.55 eV for the same instrument settings. Binding energy calibration was made using Au $4f_{7/2}$ (83.96 eV), Ag $3d_{5/2}$ (368.21 eV) and Cu $2p_{3/2}$ (932.62 eV). Sample stubs were earthed *via* the instrument stage using a standard Bayonet Neill Concelman (BNC) connector. The experimental error in the acquisition of binding energies is ± 0.1 eV, as quoted by the instruments manufacturer (Kratos); consequently, any binding energies within 0.2 eV can be considered to be identical, within the experimental error.

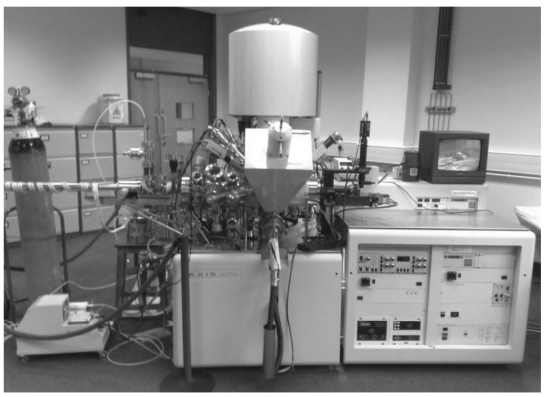

Figure 2.6 Kratos Axis Ultra spectrometer

Charge neutralisation was carried out by employing a system consisting of a filament which is coaxial with the electrostatic and magnetic transfer lenses, as well as a balance plate to create a potential gradient between the neutraliser and the sample. Usually the standard settings for solid samples are: 1.9 A filament current and 3.3 V balance voltage. It must be noted that for all of the ionic liquids which are liquids at room temperature, charge neutralisation was not employed in the measurement of XPS spectra.

An Ar^+ ion bombard of the samples was carried out by using a Kratos Minibeam III ion gun. The standard etching conditions are: 4 kV sputter energy and 10 mA emission current. The etched area is *ca.* 800 × 800 μm^2.

2.2.2 Sample preparation and transfer

Samples were prepared by placing a small drop (≈ 20 mg) of the ionic liquid into a depression on a stainless steel sample stub (designed for powders) or on a standard stainless steel multi-sample bar (both Kratos designs). The ionic liquid samples were presented as thin films (approx. thickness 0.5-1 mm), thereby avoiding experimental complications associated with variable sample height. Initial pumping to high vacuum pressure was carried out in a preparation chamber immediately after thin film preparation to avoid significant absorption of volatile impurities. Pumping of ionic liquids was carried out with care as the high viscosities associated with these samples meant that significant bubbling due to the removal of volatile impurities was observed. The pumping down process was consequently carried out slowly to avoid contamination of the UHV chamber by bumping/splashing of the ionic liquid samples. The preparation chamber pressure achieved was ≈ 10^{-7} mbar. Pumping-times varied (1-3 hours total) depending upon the volume, volatile impurity content and viscosity of the sample, *i.e.* viscous ionic liquids were found to require longer pumping times. The samples were then transferred to the main analytical vacuum chamber. The pressure in the main chamber remained $\leqslant 10^{-8}$ mbar during all XPS measurements.

2.2.3 Information depth

As highlighted in *Section 2.1.1*, the information depth (ID) may be defined as the depth, within the sample, from which 95% of the measured signal originates. ID is assumed to vary mainly with cos θ, where θ is the electron emission angle relative to the surface normal. If we assume that the inelastic mean free path of photoelectrons in organic compounds is of the order of 3 nm, at the kinetic energies measured here (~800-1300 eV), then we can estimate ID in XPS experiments. For θ=0°, ID = 7-9 nm. (Note: this value is also dependent upon the kinetic energy of the escaping photoelectron, and therefore the identity of the element probed). This suggests that we are effectively investigating bulk but not just surface information.

2.2.4 Data processing

For data interpretation, a two point linear or Shirley background subtraction was used; for $[Tf_2N]^-$-, based ionic liquids the C 1s spectra were subtracted by applying a spline linear background to allow the analysis of the -CF_3 substituent. Relative Sensitivity Factors (RSF) were

taken from the Kratos Library (RSF of F 1s = 1 by definition) and were used to determine atomic percentages.[6] Peaks were fitted using a GL(30) lineshape; a combination of a Gaussian (70%) and Lorentzian (30%).[2] This lineshape has been used consistently in the fitting of XP spectra, and has been found to match experimental lineshapes in ionic liquid systems.

Specifically for peak fitting, the number of components of an envelope was determined based on prior knowledge of the electronic environment of an atom in the chemical structure as well as ^{13}C NMR data. Assignment of each component to the related area of electronic environment was made referencing to the three main XPS databases[2, 3, 7] and other relevant literature. The full width at half maximum (FWHM), binding energy and peak area are constrained during the peak fitting. FWHM of each component was initially constrained to be $0.8 \leqslant FWHM \leqslant 1.5$ eV. The $C_{aliphatic}$ 1s component was constrained considerably larger due to the overlap of different carbon signals. Moreover the shake-up/off process was taken into account when constraining the area of the fitted peak, which is introduced in more detail in *Section 3.2.3*. The accuracy of each fitting model was checked by comparing the experimental area ratio of each component with a stoichiometry from chemical structure.

2.2.5 XP Spectrum

The spectra recorded from XPS are of two types: survey scan (wide scan) and high resolution scan. The survey scan gives the whole energy range of photoelectrons emitted from the sample and thus provides information about the elemental composition of the sample. The high resolution scan focuses on an energy area where measured signals originate from one element within the sample.

2.2.5.1 Survey scan

A survey scan is used to analyse all of the possible emission energies, for a monochromatic Al X-ray source ranging from 1400 to 0 eV, as has been shown in Figure 2.7. The survey scan is usually recorded with a pass energy of 80 eV and energy step of 0.5 eV, allowsy the acquisition of a higher intensity but poorly resolved spectrum. The spectrum consists of a series of photoelectron peaks of which signals originate from the elements present in the sample. Each element has a series of characteristic sets of binding energies which can be used to identify the existence of the element within the sample. Moreover, each element has its own most sensitive orbital, *i.e.* C 1s, S 2p, F 1s, O 1s and N 1s, as shown in Figure 2.7, which are used to determine the elemental composition of a sample.

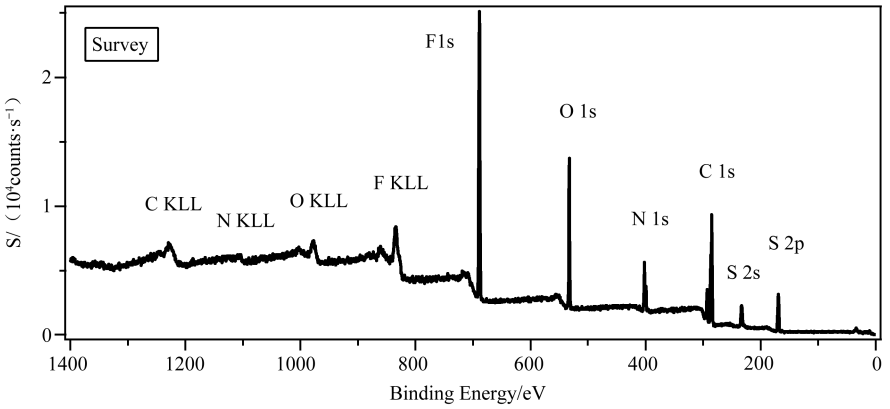

Figure 2.7 Survey scan for $[C_8C_1Im][Tf_2N]$

On the other hand, between 1400 to 800 eV, there are also other features, so-called Auger peaks, which are induced by the emission of electrons due to the relaxation of the ion after the photoemission, *i.e.* C KLL, N KLL, O KLL and F KLL, as shown in Figure 2.7. K and L represent the energetic orbitals which are involved in the Auger processes. The letters specify the initial and final vacancies which occur during the Auger transition.

Finally, at low energy (< 35 eV), several low intensity peaks can be observed. These peaks correspond to the valence band emission of the elements present in the sample.

2.2.5.2 High resolution scan

A high resolution scan focuses on an energy range where measured signals originate from an element present in the sample, *i.e.* the C 1s high resolution scan for $[C_8C_1Im][Tf_2N]$, as shown in Figure 2.8. The high resolution scan is recorded with a pass energy of 20 eV and energy step of 0.1 eV, giving the acquisition of a highly resolved spectrum. Consequently, more valuable information can be derived from the high resolution scan, *i.e.* the electronic environment of the element. It must be noted that the acquisition time of a high resolution scan depends upon the concentration and, more importantly, the RSF of the element. This will be discussed in more detail for ionic liquid-based metal solutions in *Chapters 4* and *5*.

Moreover, if a photoelectron spectrum consists of several unresolved peaks, it is important to fit components which correspond to different electronic environments. In this book, fitting models, in particular for C 1s spectra, have been developed for a series of ionic liquids,[8-11] as shown in Figure 2.8, C 1s for $[C_8C_1Im][Tf_2N]$ as an example. The high resolution scan can also be used to identify shake-up/off features, which will be discussed in more detail in *Section 3.2.3*.

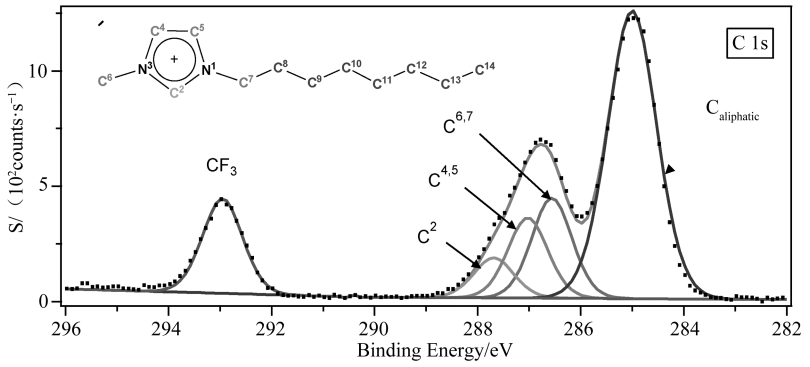

Figure 2.8 C 1s high resolution scan for $[C_8C_1Im][Tf_2N]$

2.2.6 XPS analysis

XPS can provide information about not only the elemental composition of the sample but also the electronic environment of a particular element. Each element has a series of a characteristic set of binding energies which allows elemental identification. The atomic concentration of all elements present in the sample can then be calculated from XPS by employing the RSF obtained from the Kratos Library for semi-quantitative analysis (accuracy of 10-20%).[6] The detection limit does vary amongst elements but in general 0.1 atomic % has been determined. Any element with a concentration lower than this limit will not result in resolved peaks in a survey spectrum.

Moreover, if an element is in several electronic environments, it can thus give rise to several photoelectron peaks corresponding to each possible photoemission orbital. This information can be extracted from the high resolution spectra. For the s-orbital, a single peak can be observed from the spectrum. Consequently, the observation of more than one peak can then indicate that the element is in more than one electronic environment. For p-, d- and f-orbitals, due to the effect of spin-orbital coupling, a doublet peak can be observed. The spin-orbital coupling energy difference is dependent on the element, but the area ratio of the coupling components is 1 : 2 for a p-orbital, 2 : 3 for a d-orbital and 3 : 4 for an f-orbital.

The electronic environment of an element can be determined by comparing the measured binding energies to those obtained in the literature. In this book, unless otherwise stated, the identification of the electronic environment for a given element is based upon three main databases.[2, 3, 7] It must be noted that the error associated with the measurement of binding energies is ± 0.1 eV.

2.2.6.1 Qualitative analysis

The XP spectrum is the summation of each individual signal from all elements within a sample. Each element has a series of a characteristic set of binding energies which allows elemental identification. Moreover, each element has a most sensitive photoemission orbital. Hydrogen and helium atoms with only one atomic orbital are the only two elements which cannot be detected by XPS.

2.2.6.2 Semi-quantitative analysis

The atomic concentration of all elements present in the sample can be calculated from XPS by employing the RSF obtained from the Kratos Library for semi-quantitative analysis (accuracy of 10-20%).[6] The detection limit does vary amongst elements but in general 0.1 atomic % has been determined. Any element with a concentration lower than this limit will not result in resolved peaks in a survey scan. Generally, the acquisition of a high resolution XP spectrum for a given element with low concentration is possible. The detection limit is found to be no less than 0.01 atomic %.

2.2.6.3 Electronic environment analysis

The binding energy of the photoelectron line is dependent upon the electronic environment of the atom. If an element is in several electronic environments, it can thus give rise to several photoelectron peaks corresponding to each possible photoemission orbital. The binding energy of a core orbital within an atom varies with chemical state, chemical bond type and inter- or intra-molecular interactions. Higher binding energy corresponds to a more electron poor atom, however lower binding energy means the atom is in a more electron rich environment. Consequently, XPS can provide information about different chemical state and electronic environment for a given element.

The electronic environment of an element can be determined by comparing the measured binding energies to those obtained in the main databases[2, 3, 7] and other literatures. It must be noted that the error associated with the measurement of binding energies is of the order ± 0.1 eV.

2.2.7 Charge correction

As mentioned in *Section 2.1.4*, a positive charging of the surface can occur during the measurement of XP spectra for non-conductors, as a consequence of the loss of electrons. This

effect can be overcome by charge neutralisation to avoid shift or broadening of photoelectron lines. However, charge neutralisation overcompensates leaving the spectra shifted to lower binding energies. Moreover, in the case of non-conductors, the Fermi levels of the instrument and the sample are not aligned.[12] Both factors give rise to a shift in the measured photoelectron lines.

All spectra measured for the same sample suffer the same charging situation and thus shift to the same direction by the same magnitude. Consequently, if the absolute binding energy for one of the peaks is available, all spectra can be calibrated relative to it. Reliable and comparable values can be then extracted with high level of confidence. This procedure, *i.e.* charge correction, is commonly applied during the analysis of XP spectra.

Amongst all of the charge correction methods, the use of an internal reference is thought to be the most reliable, as any charge created during an XP measurement will affect both the sample and the reference alive.[2, 13] Ionic liquids, containing a structurally aliphatic carbon moiety which is considered to be the most commonly used internal standard, are readily charge corrected, provided the aliphatic carbon moiety is long enough ($n \geqslant 8$). More detailed descriptions on the charge correction of imidazolium-, pyrrolidinium- and pyridinium- based ionic liquids are discussed in *Chapter 3*.

2.2.8 Auger Parameter

The experimental error associated with the measurement of binding energies is of the order ± 0.1 eV. Consequently, the determining of a binding energy shift which is no more than 0.2 eV is difficult. In this case, the Auger Parameter (AP) can be used to support the identification of the electronic environment information of an element.

AP was first reported by Wagner[14] in 1975 and was modified by Gaarenstroom and Winograd in 1977.[15] The modified AP was defined as the kinetic energy of the Auger line minus the kinetic energy of the photoelectron line of a given element plus the incident photo energy. Specifically for the Auger line applied in the definition of the AP, the most intense and sharpest feature is selected due to the ease of identification of the accurate kinetic energy.

The AP is characteristic of the electronic environment and the AP shift between two electronic environments is usually larger, theoretically calculated to be 3 times larger[16], than that obtained for the photoelectron line. Due to the larger shift in AP, it can be used in particular to determine the electronic environment difference when the measured binding energy shift is no more than 0.2 eV.

Moreover, the AP has an important advantage in the fact that it is not influenced by the charging formed during an XPS measurement. As shown in Eq. 2.2, during an XPS measurement, both of the kinetic energies will be influenced equally by the charging. Consequently, charge correction is no longer necessary.

$$AP_{modified} = KE_{auger} - KE_{photoelectron} + h\nu = KE_{auger} + BE_{photoelectron} \quad (2.2)$$

Although the AP has been widely used for identifying the electronic environment for a given element, it can only be applied for twenty-four elements.[17, 18] The main problem is the identification of the Auger line. The Auger process involves the valence electrons and thus the Auger line will be broad and not fully resolved. Unfortunately, with an Al Kα X-ray source, the AP is not applicable for the most commonly found elements present in ionic liquids, *i.e.* C, N, F, O, S, P and Cl.

Moreover, the measured intensities of the Auger lines is usually 15-40% of the photoelectron lines[19] which makes it impossible to use the AP for elements present in very low concentrations, *e.g.* a metal catalyst dissolved in an ionic liquid.

The use of AP as a support of the identification of the anion type for chlorostannate-based ionic liquids are not described in this book but has been demonstrated in detail in a recent publication.[20]

2.3 XPS of ionic liquids

There have been many attempts to apply UHV techniques for the characterisation of a liquid-vapour interface[21-24] over the past 40 years, with specific custom designed instruments being implemented.[25, 26] In all cases, the main problem which has to be overcome in the study of traditional liquids is their high vapour pressure. The fascinating properties of ionic liquids, *i.e.* negligible vapour pressure, provide an opportunity to analyse a liquid sample without the need of a modified experimental set up.

Actually, quaternary ammonium-based salts, if considered as ionic liquids in a wider sense of the concept but with slightly higher melting points, have been analysed by XPS for many years.[27, 28] Later, between the years 1999 and 2001, some groups attempted to analyse and purify ionic liquids under high vacuum conditions.[29, 30] In 2002, in a tribology study, XPS was used as a technique to

investigate the impact of lubrication by $[BF_4]^-$-based imidazolium ionic liquid on a steel/steel loaded contact. The XPS data in this work was focused upon load surfaces and not primarily on the ionic liquid itself and thus went unnoticed by chemists and materials scientists active in the field of ionic liquids.[31]

It was not until in 2005, when both Licence and Carporali almost simultaneously published XPS studies focused upon ionic liquid-based systems, great interest in this field was stimulated. It has since been shown that XPS can be used to characterise ionic liquids and provide information about their elemental composition, electronic environment and cation-anion interactions.[5] XPS has become a powerful analytical technique for the analysis of ionic liquids and ionic liquid-based systems. More detailed introductions regarding works in these fields will be reported in *Chapters 3*, *4* and *5* respectively.

The reaction performance of much homogeneous catalysis is dependent upon the electronic environment of the metal centre. XPS has been shown to provide information regarding the electronic environment at the metal centre. Since the application of negligible volatile ionic liquids, the investigation of solution state transition metal catalysts by XPS has become feasible.[32, 33] This method could potentially resolve several issues, such as whether the ionic liquid remains 'innocent' or can interact with the metal catalyst and how the ligand influences the electronic environment at the metal centre. These results are valuable for a proper understanding of metal centres in solution and the further design of ionic liquid-based catalytic systems to ensure the best application to a given catalytic process.[9, 20, 32, 34]

References

[1] HAGSTROM S B. Kai Manne Borje Siegbahn[J]. Physics Today，2007，60(11): 74.

[2] BRIGGS D，GRANT J T. Surface Analysis by Auger and X-ray Photoelectron Spectroscopy[M]. Manchester: IMPublications，2003.

[3] MOULDER J F，STICKLE W F，SOBOL P E，et al. Handbook of X-ray Photoelectron Spectroscopy: a reference book of standard spectra for identification and interpretation of XPS data[M]. Chanhassen: Physical Electronics，1995.

[4] MAIER F，CREMER T，KOLBECK C，et al. Insights into the surface composition and

enrichment effects of ionic liquids and ionic liquid mixtures[J]. Physical Chemistry Chemical Physics，2010，12(8): 1905-1915.

[5] LOVELOCK K R J，VILLAR-GARCIA I J，MAIER F，et al. Photoelectron Spectroscopy of Ionic Liquid-Based Interfaces[J]. Chemical Reviews，2010，110(9): 5158-5190.

[6] WAGNER C D，DAVIS L E，ZELLER M V，et al. Empirical Atomic Sensitivity Factors for Quantitative-Analysis by Electron-Spectroscopy for Chemical-Analysis[J]. Surface and Interface Analysis，1981，3(5): 211-225.

[7] BRIGGS D，BEAMSON G. The XPS of Polymers Database[M]. Manchester: SurfaceSpectra，2000.

[8] VILLAR-GARCIA I J，SMITH E F，TAYLOR A W，et al. Charging of ionic liquid surfaces under X-ray irradiation: the measurement of absolute binding energies by XPS[J]. Physical Chemistry Chemical Physics，2011，13(7): 2797-2808.

[9] MEN S，LOVELOCK K R J，LICENCE P. Directly probing the effect of the solvent on a catalyst electronic environment using X-ray photoelectron spectroscopy[J]. Rsc Advances，2015，5(45): 35958-35965.

[10] MEN S，LOVELOCK K R J，LICENCE P. X-ray Photoelectron Spectroscopy of Pyrrolidinium-Based Ionic Liquids: Cation-Anion Interactions and a Comparison to Imidazolium-Based Analogues[J]. Physical Chemistry Chemical Physics，2011，13(33): 15244-15255.

[11] MEN S，MITCHELL D S，LOVELOCK K R J，et al. X-ray Photoelectron Spectroscopy of Pyridinium-Based Ionic Liquids: Comparison to Imidazolium- and Pyrrolidinium-Based Analogues[J]. Chemphyschem，2015，16(10): 2211-2218.

[12] KELLY M A. Anaysing Insulators with XPS and AES[M]. Manchester: IMPublications，2003.

[13] LEWIS R T，KELLY M A. Binding-Energy Reference in X-ray Photoelectron-Spectroscopy of Insulators[J]. J. Electron Spectrosc. Relat. Phenom.，1980，20(1-2): 105-115.

[14] WAGNER C D. Chemical-Shifts of Auger Lines and Auger Parameter[J]. Faraday Discussions，1975，60: 291-300.

[15] GAARENSTROOM S W，WINOGRAD N. Initial and Final-State Effects in Eaca Spectra of Cadmium and Silver-Oxides[J]. Journal of Chemical Physics，1977，67(8): 3500-3506.

[16] WAGNER C D. New Approach to Identifying Chemical States，Comprising Combined Use of Auger and Photoelectron Lines[J]. Journal of Electron Spectroscopy and Related

Phenomena，1977，10(3): 305-315.

[17] WAGNER C D，JOSHI A. The Auger Parameter，Its Utility and Advantages-A Review[J]. Journal of Electron Spectroscopy and Related Phenomena，1988，47: 283-313.

[18] MORETTI G，PAPARAZZO E. Auger parameter studies of third-row chemical elements[J]. Surface and Interface Analysis，2006，38(4): 636-639.

[19] WAGNER C D，GALE L H，Raymond R H. 2-Dimensional Chemical-State Plots-Standardized Data Set for Use in Identifying Chemical-States by X-ray Photoelectron-Spectroscopy[J]. Analytical Chemistry，1979，51(4): 466-482.

[20] CURRIE M，ESTAGER J，LICENCE P，et al. Chlorostannate(II) Ionic Liquids: Speciation，Lewis Acidity，and Oxidative Stability[J]. Inorganic Chemistry，2013，52(4): 1710-1721.

[21] SIEGBAHN H，SIEGBAHN K. ESCA applied to liquids[J]. Journal of Electron Spectroscopy and related Phenomena，1973，2: 319-325.

[22] BALLARD R E，JONES J，SUTHERLAND E. Determination of the Liquid Surface-Composition of a Binary Mixture by Photoelectron-Spectroscopy - Adiponitrile and Tris (Dioxa-3,6-Heptyl)Amine[J]. Chemical Physics Letters，1984，112(5): 452-455.

[23] PANTFORDER J，POLLMANN S，ZHU J F，et al. New setup for in situ x-ray photoelectron spectroscopy from ultrahigh vacuum to 1 mbar[J]. Review of Scientific Instruments，2005，76(1): 014102.

[24] WINTER B，FAUBEL M. Photoemission from liquid aqueous solutions[J]. Chemical Reviews，2006，106(4): 1176-1211.

[25] SIEGBAHN H，SVENSSON S，LUNDHOLM M. A New Method for Esca Studies of Liquid-Phase Samples[J]. Journal of Electron Spectroscopy and related Phenomena，1981，24(2): 205-213.

[26] WILSON K R，RUDE B S，CATALANO T，et al. X-ray spectroscopy of liquid water microjets[J]. Journal of Physical Chemistry B，2001，105(17): 3346-3349.

[27] ESCARD J，MAVEL G，GUERCHAIS J E，et al. X-Ray Photoelectron-Spectroscopy Study of Some Metal(Ii) Halide and Pseudohalide Complexes[J]. Inorganic Chemistry，1974，13(3): 695-701.

[28] WAGNER C D. X-ray Photoelectron-Spectroscopy with X-ray Photos of Higher Energy[J]. J. Vac. Sci. Technol.，1978，15(2): 518-523.

[29] LAW G，WATSON P R，CARMICHAEL A J，et al. Molecular composition and orientation at the surface of room-temperature ionic liquids: Effect of molecular structure[J]. Physical

Chemistry Chemical Physics，2001，3(14): 2879-2885.

[30] BROWN R J C，DYSON P J，ELLIS D J，et al. 1-Butyl-3-methylimidazolium cobalt tetracarbonyl [bmim][$Co(CO)_4$]: a catalytically active organometallic ionic liquid[J]. Chemical Communications，2001(18): 1862-1863.

[31] LIU W，YE C，GONG Q，et al. Tribological performance of room-temperature ionic liquids as lubricant[J]. Tribology Letters，2002，13(2): 81-85.

[32] SMITH E F，VILLAR-GARCIA I J，BRIGGS D，et al. Ionic liquids in vacuo; solution-phase X-ray photoelectron spectroscopy[J]. Chemical Communications，2005(45): 5633-5635.

[33] MAIER F，GOTTFRIED J M，ROSSA J，et al. Surface enrichment and depletion effects of ions dissolved in an ionic liquid: an X-ray photoelectron spectroscopy study[J]. Angewandte Chemie-International Edition，2006，45(46): 7778-7780.

[34] MEN S，LOVELOCK K R J，LICENCE P. X-ray photoelectron spectroscopy as a probe of rhodium-ligand interaction in ionic liquids[J]. Chemical Physics Letters，2016，645: 53-58.

Chapter 3

XPS of Pure Ionic Liquids and Ionic Liquid Mixtures

3.1 Introduction

As highlighted in *Chapter 1*, ionic liquids have very low vapour pressures and therefore can be placed into a UHV chamber which enables the analysis ionic liguids of by XPS, without specific modification of the experimental set up at room temperature.[1, 2] XPS has become a widely used technique for the analysis of ionic liquids and ionic liquid-based systems. Generally, ionic liquids give well-resolved peaks in core level XP spectra.[1] As conducting samples, ionic liquids which are liquids at room temperature can dissipate the charge built up at the sample surface as a result of prolonged photoemission effect.[1, 3] Consequently, the effect of charging, as described in *Section 2.1.4,* is negligible and charge neutralisation is not normally necessary. However, as observed by Villar-Garcia *et al.*, measurable shifts in binding energy can still be observed for ionic liquids photoelectron peaks recorded over prolonged periods of time.[4] To overcome this potential problem and obtain comparable information between different spectra, standard charge correction methods should always be applied.[4] This procedure was introduced in *Section 2.2.7* and will be discussed experimentally in this chapter.

Since 2005, the majority of research concerned with UHV characterisation of ionic liquids has focused on dialkylimidazolium-based ionic liquids. In 2005, the Nottingham Ionic Liquids

group characterised $[C_2C_1Im][EtOSO_3]$ by XPS and established a fitting model for C 1s region.[5] In 2006, Carporali *et al*. characterised $[C_4C_1Im][Tf_2N]$ by XPS.[2] Höfft *et al*. also studied the surface structure of $[C_4C_1Im][Tf_2N]$ by XPS and a variety of other complementary surface sensitive techniques.[6] Later on, Gottfried *et al*. employed ARXPS to characterise the surface composition of $[C_2C_1Im][EtOSO_3]$.[7] In 2008, Lockett *et al*. studied $[C_nC_1Im][BF_4]$ ionic liquids by ARXPS and concluded that the carbon atomic concentration was higher in the top most layers of the surface.[8] XPS was subsequently used to determine the orientation and mutual location of ions at the surface of ionic liquids.[9] In 2009, Lovelock *et al*. investigated the influence of alkyl chain length and the anion on the surface composition using ARXPS.[10] Kolbeck *et al*. also applied ARXPS to investigate the influence of anions on surface composition of ionic liquids at near surface region.[11] In 2010, Maier *et al*. put their insight into the surface enrichment of the ionic liquids.[12] Meanwhile, Cremer *et al*. used XPS to illustrate very subtle trends in the binding energies of cation-based components, *i.e.* N_{cation}, as a function of the charge transferred from the anion to the cation and the hydrogen bond acceptor/donor abilities of corresponding anions.[13] In 2011, Villar-Garcia *et al*. summarised ongoing work in the Nottingham Ionic Liquids Group by reporting the XP spectra of a series of imidazolium-based ionic liquids with commonly used anions, and documented a robust method of charge correction.[4] Since then, a series of families of ionic liquid-based systems have been investigated by XPS, including halometallate-based ionic liquids,[14, 15] pyrrolidinium-based ionic liquids,[16, 17] pyridinium-based ionic liquids,[18] palladium-containing phosphineimidazolylidene systems[19] and ionic liquid mixtures.[20]

As described in *Chapter 1*, the principle aim of this work is to correlate XPS data with the reaction performance and to find a strategy for designing metal catalytic systems for given reactions. To obtain the absolute value of the binding energy for the metal catalyst dissolved in ionic liquids, the charge correction method is the key factor. In this *Chapter*, XPS is used to analyse pure ionic liquids. Ionic liquids families, *i.e.* imidazolium-, pyrrolidinium-and pyridinium-based ionic liquids with different anions are presented. The charge correction methods are discussed in detail for different families of ionic liquids. The same charge correction method will find application for the interpretation of XPS data measured for ionic liquids-based metal solutions.

3.2 Varying the cation

Binding energies derived from XPS can be regarded as a sensitive measurement of the electronic environment of each atom in a sample of interest. It can provide information about not only the formal chemical states of each element in a sample, but also subtle changes in the electronic environment resulting from changes in chemical bonding and both inter- and intra-molecular interactions. In order to obtain comparable measured binding energies for ionic liquids, and indeed solutes dissolved in ionic liquids, the application of an effective charge correction method becomes crucial.[4] Out of all possible charge correction methods, internal referencing using C 1s has been shown to be the most appropriate and consequently most widely employed, as any charging created during XPS measurement should influence all XP peaks equally, including the reference.[21]

3.2.1 Imidazolium-based ionic liquids

Previous work by the Nottingham Ionic Liquids group has primarily focused upon imidazolium- based ionic liquids.[4] Satisfactory fitting models for a series of imidazolium- based ionic liquids have been developed and were described in *Section 2.2.5.2.* This model is also used in *Chapters 4* and *5*.

The C 1s high resolution spectra of most imidazolium-based ionic liquids are composed of two distinct cation-based envelopes. However, the structure suggests that there are at least four different carbon-based components, each of which will appear at a different binding energy. A fitting model of the C 1s photoemission envelope is consequently important when binding energy is being extracted, specifically the $C_{aliphatic}$ 1s component. In the case of simple non-functionalised imidazolium-based ionic liquids, where the anion does not contain additional carbons, the C 1s high resolution spectra can be fitted using an established four-component model, which has been employed in previous studies[1, 4, 22, 23] (see Figure 3.1 for instance).

As the alkyl chain length is varied for simple non-functionalised imidazolium-based ionic liquids, the shape of the C 1s high resolution spectra changed significantly. In previous work by the Licence group, common anions (*i.e.* $[Tf_2N]^-$) were investigated with a series of cations by

increasing alkyl chain lengths from ethyl to dodecyl. The aliphatic moiety exhibits a higher binding energy when the alkyl substituent is changed from dodecyl to ethyl. This observation may be explained by the proximity to the charge positive imidazolium cation head group of the aliphatic carbon. Consequently, it was measured most obviously in short-chain ionic liquids by a shift of the $C_{aliphatic}$ 1s component to higher binding energy, see Figure 3.2 according to ref.[4] When $n \geqslant 8$, this effect was no longer observed and the $C_{aliphatic}$ tended to be a true binding energy value of 285.0 eV. Thus, for $n \geqslant 8$, the $C_{aliphatic}$ 1s component can be used as a reliable charge reference for imidazolium-based ionic liquids.[4]

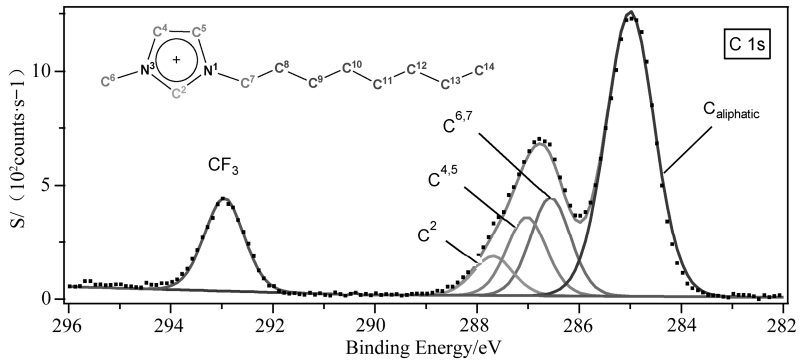

Figure 3.1 Fitting model of C 1s for $[C_8C_1Im][Tf_2N]$ with labelled structure: C^2, (C^4 + C^5), (C^6 + C^7) and (C^8 to C^{14}) = $C_{aliphatic}$. The XP spectrum was charge corrected by referencing the $C_{aliphatic}$ 1s component to 285.0 eV

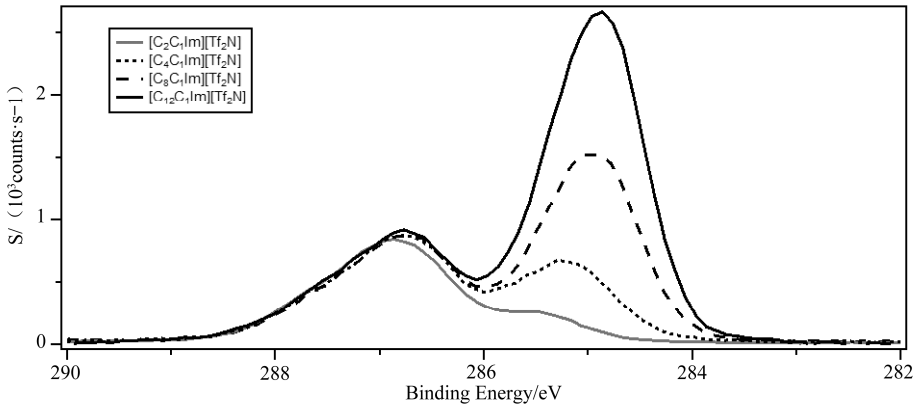

Figure 3.2 C 1s XP spectra for $[C_nC_1Im][Tf_2N]$ where n = 2 - 12.[4] The intensities are normalised to the intensity of the N_{cation} 1s fitted peak for $[C_8C_1Im][Tf_2N]$. For n = 8, XP spectra were charge corrected by referencing the $C_{aliphatic}$ 1s component to 285.0 eV. For other n values, XP spectra were charge corrected by referencing the N_{cation} 1s peak to the value for n = 8

It was then decided that C_8-based ionic liquids should always be selected to prepare metal catalyst solutions for ease of charge correction and thus obtain of reliable binding energy for the solute dissolved in ionic liquids. In *Chapters 4* and *5*, all ionic liquids-based metal solutions are prepared based upon using C_8-based ionic liquids. A more detailed description of the fitting model for acetate imidazolium-based ionic liquids will be given in *Section 3.3.1*.

3.2.2 Pyrrolidinium-based ionic liquids

As has been mentioned, the main emphasis of UHV characterisation, to date has been upon imidazolium-based ionic liquids,[22] simply because they are the materials most often used by synthetic chemists. However, interest in pyrrolidinium-based ionic liquids has increased, particularly amongst electrochemists, due to their varied, often superior, physico-chemical properties when compared to imidazolium-based ionic liquids. Pyrrolidinium-based ionic liquids have similar melting points[24] and slightly lower conductivities[25] and higher viscosities[26, 27] when compared to their imidazolium-based analogues. Pyrrolidinium-based ionic liquids typically have wider electrochemical window than their imidazolium-based analogues because there is no C^2 proton present and thus can be used to investigate a larger range of redox mediators, specifically the electrodeposition of group one alkali metals, *e.g.* Li.[28-31] Unsurprisingly, pyrrolidinium-based ionic liquids also find application as solvents in catalysis,[32] nanoparticle production[33] and liquid-liquid separation.[34]

The long-term thermal stability of pyrrolidinium-based ionic liquids has not yet been fully investigated.[35] Enthalpies of vaporisation, $\Delta_{vap}H_{298}$, have been measured for four pyrroli dinium-based ionic liquids, the $\Delta_{vap}H_{298}$ values obtained are all > 150 kJ • mol^{-1},[36, 37] indicating that they are vacuum stable and can be investigated using UHV techniques.

3.2.2.1 Fitting model of the C 1s regions

Upon inspection of the C 1s spectra of pyrrolidinium-based ionic liquids, it appears that there are two unresolved cation-based components present. Consequently, a two-component fitting model was initially developed.

To begin with, the focus will be upon $[C_2C_1Pyrr][Tf_2N]$, as shown in Figure 3.3. The carbon atoms are in two different electronic environments. The first component belongs to the carbon atoms bonded to nitrogen, labelled (C^2 + C^5 + C^6 + C^7), also labelled C_{hetero}. The second component represents the carbon atoms bonded to carbon and hydrogen only, labelled (C^3 + C^4 +

C^8), also labelled $C_{aliphatic}$. When fitting the C 1s region for $[C_2C_1Pyrr][Tf_2N]$ with two components, the area ratio was constrained to 4 : 3 as the nominal stoichiometry for $[C_2C_1Pyrr][Tf_2N]$ is C_{hetero} : $C_{aliphatic}$ = 4:3. The FWH maxima for the two components were very similar, with a ratio of 1 : 1.03, which confirmed that there are two distinct carbon electronic environments for $[C_2C_1Pyrr][Tf_2N]$. An accurate value for binding energy difference (C_{hetero} 1s – $C_{aliphatic}$ 1s) of 1.27 eV was obtained. The two-component fitting model gave a satisfactory fit for it as there are only two electronic environments present in $[C_2C_1Pyrr]^+$.

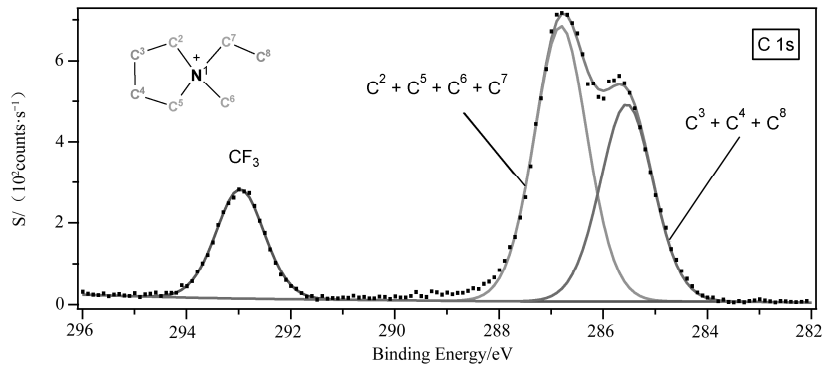

Figure 3.3 Fitting model of C 1s for $[C_2C_1Pyrr][Tf_2N]$ with labelled structure: ($C^2 + C^5 + C^6 + C^7$) = C_{hetero}, ($C^3 + C^4 + C^8$) = $C_{aliphatic}$ and CF_3. The XP spectra was charge corrected by referencing to N_{cation} 1s which was recorded for the standard $[C_8C_1Pyrr][Tf_2N]$ (402.7 eV)

However, for $n \geqslant 4$, although the two-component model can produce good agreement between experimental and fitted envelopes, it cannot provide a reliable value for the measured binding energy of $C_{aliphatic}$ 1s. The FWHM of the C_{hetero} 1s remains consistent as n increases from 4 to 10 (1.02 ± 0.03 eV), whereas the FWHM of the $C_{aliphatic}$ 1s increases as n increases, see Table 3.1. Therefore, the FWHM ratio for $C_{aliphatic}$: C_{hetero} increases along with the increasing of n. This trend shows that as more carbon atoms added to the alkyl chain, the variation of the electronic environment of the aliphatic carbons increases as well.

Table 3.1 Full width at half maxima for C_{hetero} 1s and $C_{aliphatic}$ 1s for $[C_nC_1Pyrr][Tf_2N]$ for the C 1s two-component fitting model

n for $[C_nC_1Pyrr][Tf_2N]$	FWHM		
	C_{hetero} 1s / eV	$C_{aliphatic}$ 1s / eV	($C_{aliphatic}$ 1s):(C_{hetero} 1s)
2	1.18	1.21	1.03
4	1.03	1.22	1.18

（To be continued）

Continued table

n for $[C_nC_1Pyrr][Tf_2N]$	FWHM		
	C_{hetero} 1s / eV	$C_{aliphatic}$ 1s / eV	($C_{aliphatic}$ 1s):(C_{hetero} 1s)
6	1.04	1.30	1.25
8	1.01	1.35	1.33
10	0.99	1.32	1.34

Generally, the carbon atoms located further away from the positively charged nitrogen atom are more likely to be 'normal' aliphatic carbons, *i.e*. carbons in simple molecules such as hexane. Therefore, for ionic liquids with smaller *n*, due to the electronic effect of the cation head group, the fitted $C_{aliphatic}$ 1s component does not represent the real aliphatic carbon atoms. Consequently, reliable binding energies cannot be obtained for pyrrolidinium-based ionic liquids using the two-component fitting model for the C 1s region, specifically in the case of short alkyl chain. Therefore, it was decided that a three-component fitting model for C 1s should be developed.

In this three-component fitting model, as shown in Figure 3.4, three cation-based components were defined. The first component belongs to the carbon atoms bonded to nitrogen, labelled (C^2 + C^5 + C^6 + C^7), also labelled C_{hetero}. The second component represents the carbon atoms β to nitrogen, labelled (C^3 + C^4 + C^8), also labelled C_{inter}. The last component indicates the carbon bonded to carbon and hydrogen only, labelled $C_{aliphatic}$.

When using the three-component fitting model for $[C_nC_1Pyrr][Tf_2N]$, the component areas, FWHM (C_{hetero} constrained to be equal to C_{inter}[38]) and the binding energy difference (C_{hetero} 1s - C_{inter} 1s) of 1.27 eV were constrained as it is assumed that the relative electronic environments of C_{hetero} and C_{inter} will not change significantly with increasing alkyl chain length. The application of these constraints gave rise to a satisfactory fit.[16]

The same fitting procedure was used when fitting other pyrrolidinium-based ionic liquids, *i.e.* in this book $[C_8C_1Pyrr]I$ and $[C_8C_1Pyrr][BF_4]$. It must be noted that the FWHM ratio of $C_{aliphatic}$: C_{hetero} was≈1.1 for all ionic liquids, illustrating that the carbon atoms labelled $C_{aliphatic}$ are all in very similar electronic environments. This is in agreement with the measurements obtained for imidazolium-based ionic liquids.[4]

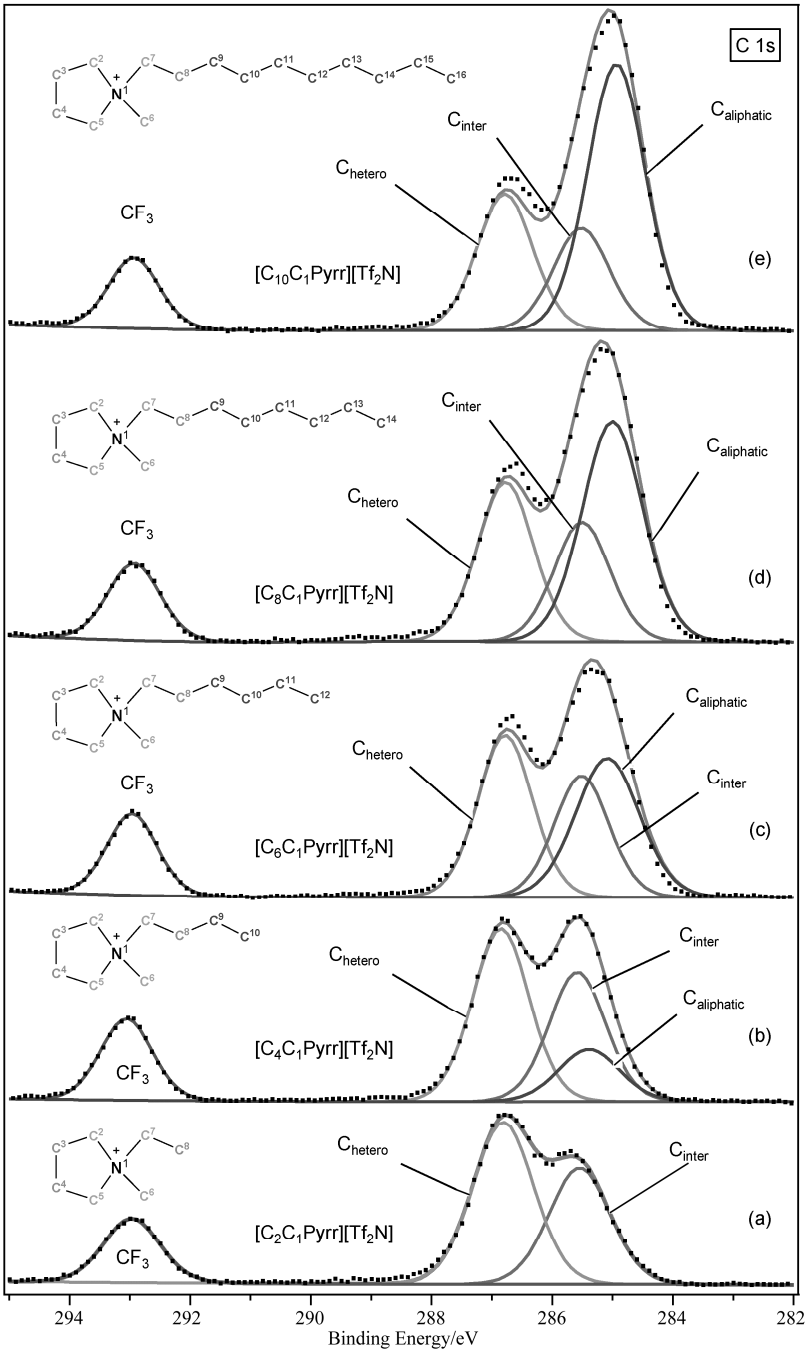

Figure 3.4 Fitting model of C 1s for (a) $[C_2C_1Pyrr][Tf_2N]$, (b)$[C_4C_1Pyrr][Tf_2N]$, (c) $[C_6C_1Pyrr][Tf_2N]$, (d) $[C_8C_1Pyrr][Tf_2N]$ and (e) $[C_{10}C_1Pyrr][Tf_2N]$. Labelled structure: $(C^2 + C^5 + C^6 + C^7) = C_{hetero}$, $(C^3 + C^4 + C^8) = C_{inter}$, CF_3 and $C_{aliphatic}$. When $n = 8$, the XP spectrum was charge corrected by referencing the $C_{aliphatic}$ 1s component to 285.0 eV. Other XP spectra were charge corrected by referencing to N_{cation} 1s which was recorded for $n = 8$

Moreover, the binding energy difference between C_{hetero} 1s and C_{inter} 1s is expected to vary according to the nature of the anion. As neither $[C_2C_1Pyrr][BF_4]$ nor $[C_2C_1Pyrr]I$ were studied in this book, a definitive binding energy difference between C_{hetero} 1s and C_{inter} 1s for these anions is not available. Consequently, no constraint was applied to the binding energy difference in these cases. The application of only FWHM ratios, along with area constraints, yielded satisfactory fits for these two ionic liquids. The binding energy difference (C_{hetero} 1s−C_{inter} 1s) was obtained to be 1.15 eV and 1.07 eV for $[C_8C_1Pyrr][BF_4]$ and $[C_8C_1Pyrr]I$ respectively. The binding energy difference (C_{hetero} 1s−C_{inter} 1s) was found to be 1.17 eV for the mixture of $[C_8C_1Pyrr][Tf_2N]$ and $[C_8C_1Pyrr]I$. The ionic liquid mixture is investigated in detail in *Section 3.4.2*.

3.2.2.2 Effect of alkyl chain length on the charge correction

In *Section 3.2.2.1*, we have described the development of a reliable three-component fitting model for the C 1s region of pyrrolidinium-based ionic liquids. The $C_{aliphatic}$ 1s component can be set equal to 285.0 eV as a robust internal charge reference. The binding energy of N_{cation} ls for n = 8 can then be used for the charge correction of all $[C_nC_1Pyrr][A]$ ionic liquids, where n = 2, 4, 6, 10 and $[A]^-$ is the same, as the electronic environment of N_{cation} is not expected to vary significantly with n.

Figure 3.5 shows the change of intensity of the $C_{aliphatic}$ 1s component as a function of alkyl chain length for $[C_nC_1Pyrr][Tf_2N]$. It must be noted that all spectra were normalised to the area of the N_{cation} 1s peak measured for $[C_8C_1Pyrr][Tf_2N]$. For n = 8 and 10, the binding energies of $C_{aliphatic}$ 1s are identical, within the error of the experiment. This observation shows that the $C_{aliphatic}$ 1s component for these ionic liquids is a good representation of the aliphatic carbon. When n = 6, the variety of the binding energy of $C_{aliphatic}$ 1s is still within the experimental error, however, confidence for this assumption is low. For n = 4, it is clear that the binding energy of the $C_{aliphatic}$ 1s component increases significantly when compared to that of n = 8, which indicates that the aliphatic carbons closer to the cation head group are much more electron poor than those which are further away from the cation. Consequently, $C_{aliphatic}$ 1s for n = 4 cannot be used for satisfactory charge correction. In general, it is clear that for pyrrolidinium-based ionic liquids with less basic anions, *i.e.* $[Tf_2N]^-$, when $n \geqslant 8$, the $C_{aliphatic}$ 1s component can be a reliable internal charge reference. However, as a suggestion throughout this *Section*, the binding energy of the $C_{aliphatic}$ 1s for n = 8 was set to 285.0 eV. Since the effect of altering n on the binding energy measured for the N_{cation} 1s peak is negligible, the value of N_{cation} 1s was used for the charge correction of $[C_nC_1Pyrr][A]$, where n = 2, 4, 6 and 10. It should be stressed that the binding energy for N_{cation} 1s varies between families of ionic liquids, *i.e.* different anions. Consequently, this procedure must be repeated for each individual ionic liquid family.

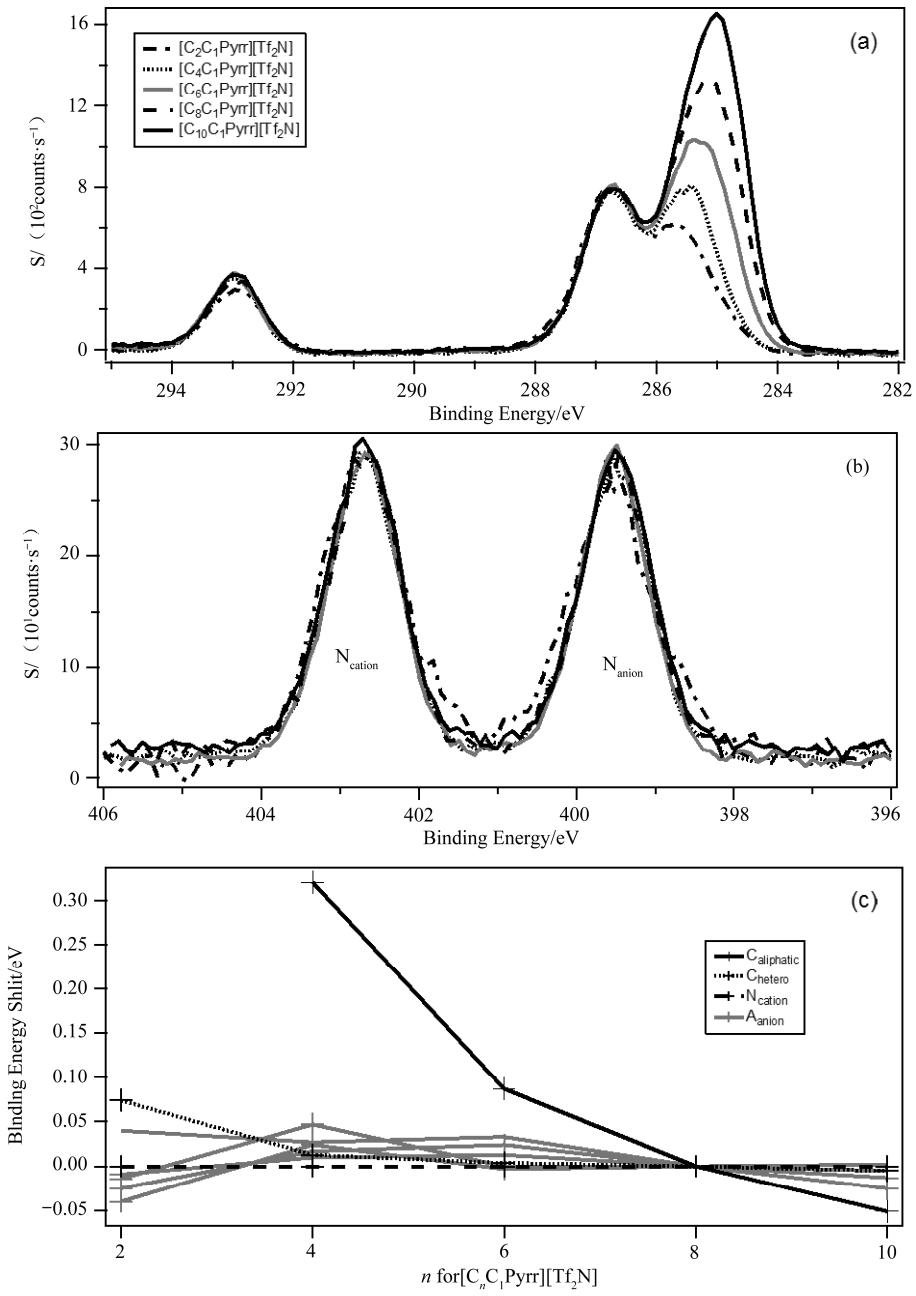

Figure 3.5 XP spectra for $[C_nC_1Pyrr][Tf_2N]$ where n = 2-10 for: (a) C 1s and (b) N 1s. The intensities are normalised to the intensity of the N_{cation} 1s fitted peak for $[C_8C_1Pyrr][Tf_2N]$. For n = 8, XP spectra were charge corrected by referencing the $C_{aliphatic}$ 1s component to 285.0 eV. Other XP spectra were charge corrected by referencing the N_{cation} 1s peak to the value for n = 8. (c) Binding energy shifts relative to $[C_8C_1Pyrr][Tf_2N]$ as a function of alkyl chain length, n = 2-10

3.2.2.3 Cation-anion interactions

It has been suggested that cation-anion interactions can be investigated by XPS.[13, 39] The binding energies of C_{hetero} 1s and N_{cation} 1s have been correlated to the basicity of the anion; for more basic anions, such as halides, more charge will be transferred from the anion to the cation, thus the binding energies are lower which means that the cation is more electron rich. The opposite is true for less basic anions such as $[Tf_2N]^-$.

This effect has been investigated in this section for three $[C_8C_1Pyrr][A]$ ionic liquids, where $[A]^- = [Tf_2N]^-$, $[BF_4]^-$ and I^- (see Figure 3.6). The binding energies for N 1s and C 1s peaks were charge corrected to $C_{aliphatic}$ 1s = 285.0 eV. The areas were normalised to the area of the N_{cation} 1s peak for $[C_8C_1Pyrr][Tf_2N]$. The binding energies for both N_{cation} 1s and C_{hetero} 1s components follow this trend: $[Tf_2N]^- > [BF_4]^- > I^-$. Since the lower binding energy corresponds to a more electron rich cation, more charge is transferred from anion to cation for the more basic anion, I^-. These results are in agreement with those obtained for imidazolium-based ionic liquids. [4, 13, 39]

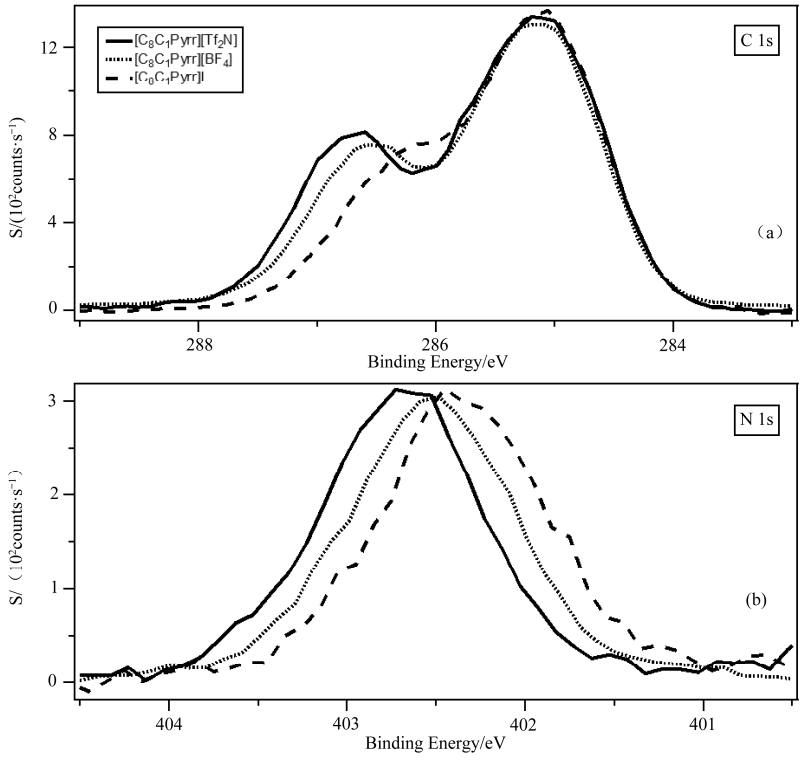

Figure 3.6 XP spectra for $[C_8C_1Pyrr][Tf_2N]$, $[C_8C_1Pyrr][BF_4]$ and $[C_8C_1Pyrr]I$ of (a) C 1s, (b) N 1s. The intensities are normalised to the intensity of the N_{cation} 1s fitted component for $[C_8C_1Pyrr][Tf_2N]$. All XP spectra were charge corrected by referencing the $C_{aliphatic}$ 1s component to 285.0 eV

The hydrogen bond acceptor ability, β, has been measured for a range of imidazolium-based ionic liquids and correlated to the measured binding energies of N_{cation}/C_{hetero} 1s component. Linear correlations are observed for imidazolium-based ionic liquids, which are introduced in more detail in *Section 3.3.2* and *Chapter 4*. At this stage, values are only available for a small number of pyrrolidinium-based ionic liquids[40, 41] as valid comparisons. However, it is expected that for pyrrolidinium-based ionic liquids, β values will follow a similar trend to imidazolium-based ionic liquids, as β is actually the anion-based parameter.

3.2.3 Pyridinium-based ionic liquids

Pyridinium-based ionic liquids have attracted more interest recently, mainly due to their potential as solvents for the capturing of CO_2 as well as offering a lower cost alternative to imidazolium-based ionic liquids.[42, 43] When compared to imidazolium-based analogues, pyridinium-based ionic liquids have higher stability, higher viscosities, slightly lower densities and similar surface tensions.[44] The excellent thermal stability is the huge advantage of pyridinium-based ionic liquids,[45] although only a handful of data is available to date, *i.e.* $\Delta_{vap}H_{298}$= 152 kJ • mol^{-1} for $[C_6Py][Tf_2N]$,[36] which also suggests that they may be investigated using UHV techniques.

3.2.3.1 Fitting model of the C 1s regions

There are three unresolved peaks in the C 1s XP spectrum for $[C_8Py][Tf_2N]$ due to the carbon signals from $[C_8Py]^+$ as shown in Figure 3.7, which differs from the imidazoloum- and pyrrolidinium-based ionic liquids discussed previously in *Section 3.2.1* and *3.2.2*[4, 16] (The peak at highest binding energy can be assigned to the -CF_3 group of the anion, as assigned previously for imidazolium and pyrrolidinium-based ionic liquids.[1, 10]) The three peaks at binding energies 287.2 to 286.6 eV, 286.4 to 285.8 eV and ~285 eV can be assigned to the three different electronic environments within the pyridinium cation head group, C_{hetero}, C_{inter} and $C_{aliphatic}$ respectively. C_{hetero} represents the carbon atoms bonded directly to the nitrogen atom, labelled (C^2 + C^6 + C^7). C_{inter} represents other carbons within the pyridinium ring, labelled (C^3 + C^4 + C^5). $C_{aliphatic}$ represents carbon atoms bonded to carbon and hydrogen only, labelled (C^8 to C^{14}). The three separate electronic environments of $[C_8Py]^+$ were shown in Figure 3.7(a).

It must be noted that the shake-up/off phenomenon is more pronounced in carbon (see Figure 3.7(a)) and nitrogen regions for pyridinium-based ionic liquids. The observation of a shake-up satellite is due to the π-π^* excitation of a valence electron after the photoemission involved in multiple bonding and aromatic compounds.[21, 46] During this process, the photoelectron will lose some of its kinetic energy, and thus shows higher binding energy. Moreover, in a process similar to "shake-up", the valence electrons can be ionised completely, *i.e.* excited into an unbound continuum state. This process, "shake-off", will leave an ion with vacancies in both core level and valence band. In "shake-off" process, no visible signal will be observed as in this case, the photoelectron will lose most of its kinetic energy and thus contribute to the inelastic baseline.[47] Shake-off occurs parallel to the shake-up process.[48, 49] Both shake-up and shake-off result in a loss in intensity of the main photoemission peaks of between 5-20%.[50, 51] The percentage of intensity loss depends on both the element and the chemical environment itself.[52]

For $[C_8C_1Im][Tf_2N]$, shake-up/off is obscured by the more intense signal from the photoelectrons of the $-CF_3$ group[4] (see Figure 3.7(b)). For $[C_8C_1Pyrr][Tf_2N]$ (see Figure 3.7(c)), no shake-up/off phenomenon could be observed as there is no multiple bond present and therefore the positive charge is localised on the nitrogen atom. For $[C_8Py][Tf_2N]$, it is apparent that a shoulder can be observed which overlaps with the signal from $-CF_3$ group (Figure 3.7(a)). The shake-up/off reduction was calculated from a series of pyridinium based-ionic liquids studied in this book, see Table 3.2. An average value of 10% was used to describe the shake-up/off losses and ensured that the area ratios of the components in the C 1s fitting model were accurate.

Taking into account the 10% shake-up/off loss, it is finally concluded that the area ratios of the three $[C_8Py]^+$-based components were constrained to C_{hetero} : C_{inter} : $C_{aliphatic}$ = 2.8:2.7:7. FWHM of C_{hetero} and C_{inter} were constrained to be equal as it is assumed that the relative electronic environments of C_{hetero} and C_{inter} will not change significantly as alkyl chain length increases.

When fitted other pyridinium-based ionic liquids, *i.e.* in this book $[C_8Py]Br$, $[C_8Py]I$, $[C_8Py][BF_4]$, $[C_8Py][TfO]$, $[C_8Py][PF_6]$ as well as $[C_nPy][Tf_2N]$ when n = 2, 4, 6 and 10, the same fitting model was applied. It must be noted that the FWHM ratio of $C_{aliphatic}$ 1s : C_{hetero} 1s was ≈1.1 in all cases, which indicates that all carbon atoms labelled as $C_{aliphatic}$ are in very similar electronic environments. The application of these constraints gave rise to satisfactory fits in all cases.

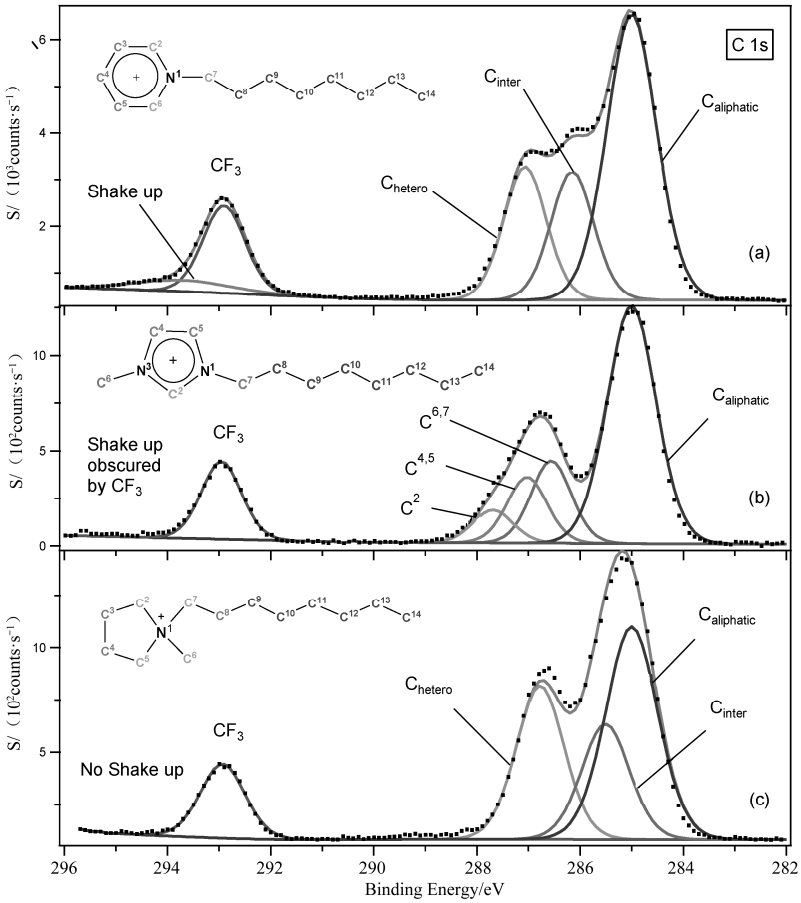

Figure 3.7 Fitting model of C 1s for (a) $[C_8Py][Tf_2N]$, (b) $[C_8C_1Im][Tf_2N]$ and (c) $[C_8C_1Pyrr][Tf_2N]$ with labelled structures. All XP spectra were charge corrected by referencing the $C_{aliphatic}$ 1s component to 285.0 eV

Table 3.2 Shake-up/off of C 1s and N 1s photoelectron losses for a series of pyridinium-based ionic liquids calculated from XP spectra

Cation	Anion	Shake-up/off % per Nitrogen atom	Shake-up/off % per Nitrogen atom
$[C_2Py]^+$	$[Tf_2N]^-$	12.3	9.7
$[C_4Py]^+$	$[Tf_2N]^-$	10.9	10.0
$[C_6Py]^+$	$[Tf_2N]^-$	9.7	10.2
$[C_8Py]^+$	$[Tf_2N]^-$	10.0	9.8
$[C_{10}Py]^+$	$[Tf_2N]^-$	9.3	8.4
$[C_8Py]^+$	$[PF_6]^-$	8.5	5.7
$[C_8Py]^+$	$[TfO]^-$	8.5	9.9
$[C_8Py]^+$	$[BF_4]^-$	8.6	7.7
$[C_8Py]^+$	I^-	10.5	8.3
$[C_8Py]^+$	Br^-	9.7	8.4
Average		9.8	8.8

3.2.3.2 Effect of alkyl chain length on the charge correction

As concluded in *Sections 3.2.1* and *3.2.2*, the $C_{aliphatic}$ 1s component could be used as a reliable internal charge reference when $n \geqslant 8$ for imidazolium-based ionic liquids and pyrrolidinium-based ionic liquids.

For pyridinium-based ionic liquids, the same result can be concluded when compared to pyrrolidinium analogues, see Figure 3.8. As has been highlighted in *Section 3.2.2.2*, it suggests that when n = 8, $C_{aliphatic}$ 1s was used as the internal charge reference. Whilst the N_{cation} 1s measured for n=8 was used for the charge reference of [C_nPy][A], where n = 2, 4, 6 and 10. This suggestion is applied throughout this book.

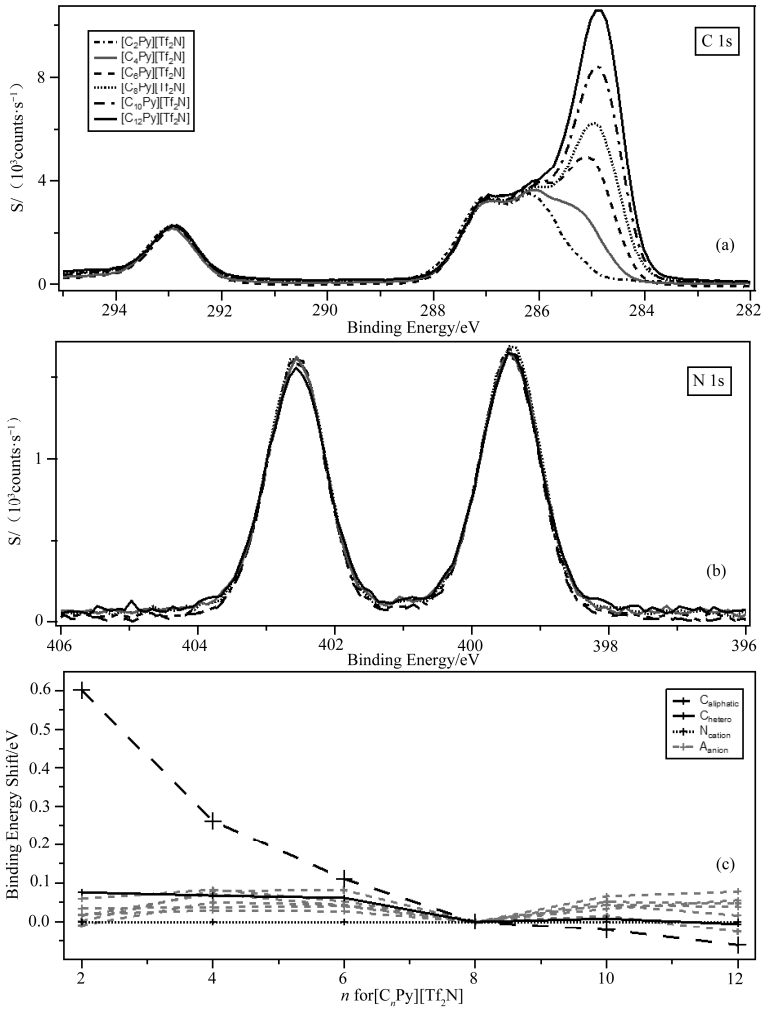

Figure 3.8 XP Spectra for [C_nPy][Tf_2N] where n = 2, 4, 6, 8 and 10 for: (a) C 1s and (b) N 1s. The intensities are normalised to the intensity of the N_{cation} 1s fitted peak for [C_8Py][Tf_2N]. For n = 8, XP spectra were charge corrected by referencing the $C_{aliphatic}$ 1s component to 285.0 eV. For other n values, XP spectra were charge corrected by referencing the N_{cation} 1s to the value for n = 8. (c) Binding energy shifts relative to [C_8Py][Tf_2N] as a function of aliphatic chain length, n = 2-10

3.2.4 Comparison of imidazolium, pyrrolidinium and pyridinium-based ionic liquids

A visual comparison amongst $[C_8Py][Tf_2N]$, $[C_8C_1Pyrr][Tf_2N]$ and $[C_8C_1Im][Tf_2N]$ for all regions is given in Figure 3.9. The XP spectra are all charge corrected to the binding energy of the $C_{aliphatic}$ 1s at 285.0 eV, and are normalised to the area of the F 1s peak since all ionic liquids contain six fluorine atoms. As could be predicted, the binding energies of all anion-based components match, within the error of the experiment (see Figure 3.9(a)-(e)). These observations indicate that changing the cation from imidazolium to pyrrolidinium or pyridinium has relatively little effect on the electronic environment of the anion.

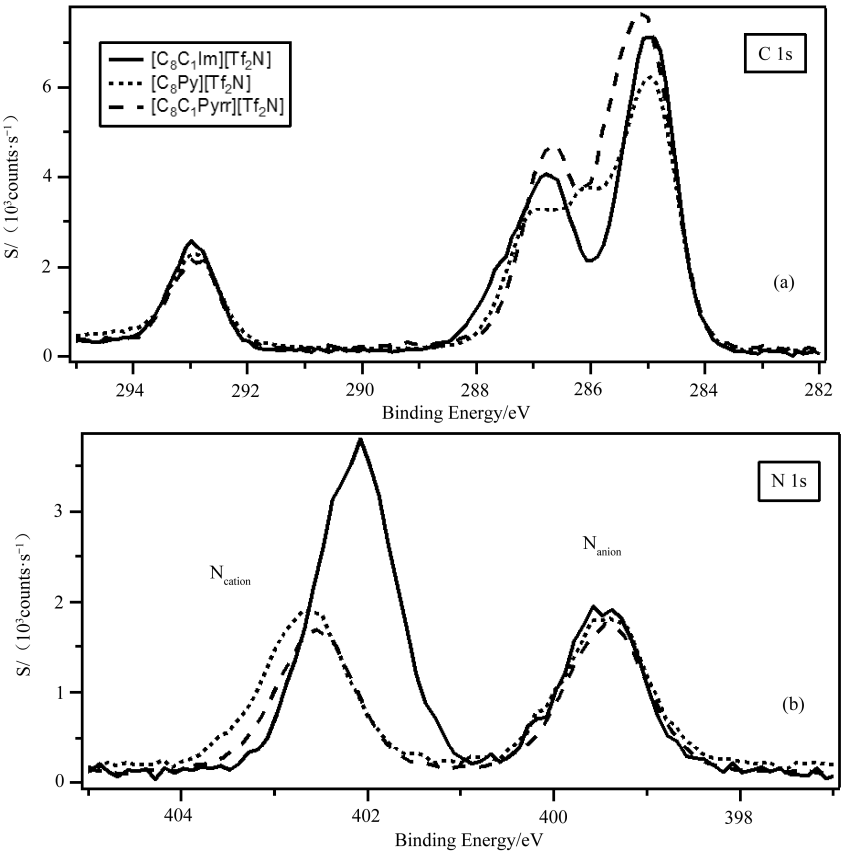

Figure 3.9 XP spectra of $[C_8Py][Tf_2N]$, $[C_8C_1Pyrr][Tf_2N]$ and $[C_8C_1Im][Tf_2N]$ for: (a) C 1s, (b) N 1s, (c) F 1s, (d) O 1s and (e) S 2p. The intensities are normalised to the intensity of the F 1s peak for $[C_8Py][Tf_2N]$. All XP spectra were charge corrected by referencing the $C_{aliphatic}$ 1s component to 285.0 eV

（To be continued）

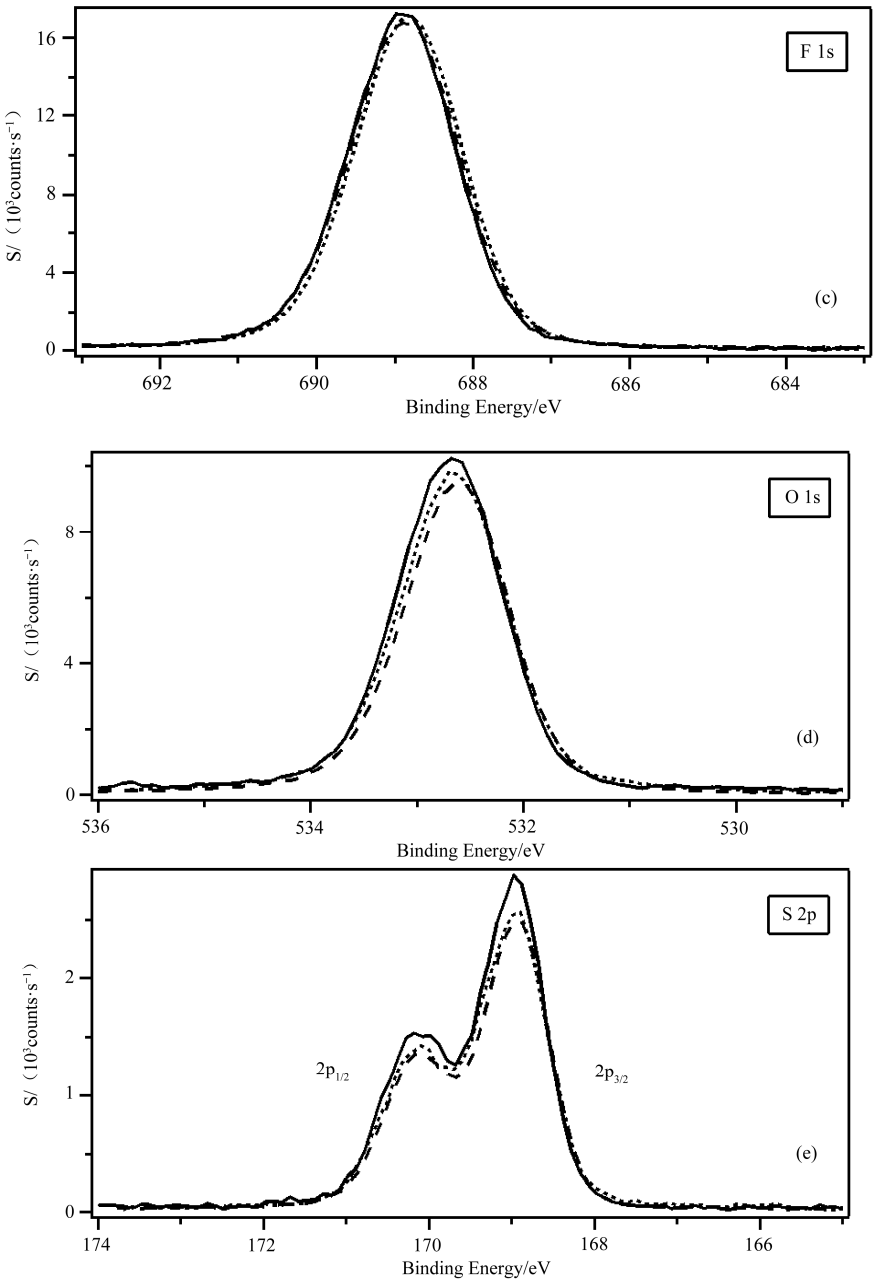

Figure 3.9 XP spectra of $[C_8Py][Tf_2N]$, $[C_8C_1Pyrr][Tf_2N]$ and $[C_8C_1Im][Tf_2N]$ for: (a) C 1s, (b) N 1s, (c) F 1s, (d) O 1s and (e) S 2p. The intensities are normalised to the intensity of the F 1s peak for $[C_8Py][Tf_2N]$. All XP spectra were charge corrected by referencing the $C_{aliphatic}$ 1s component to 285.0 eV

Continued figure

However, there are significant differences in spectra when comparing the binding energies of the peaks derived from the cations, see Figures 3.9(a) and (b). The binding energy of the N_{cation} 1s

for $[C_8Py][Tf_2N]$ is 402.6 eV, which is the same as that obtained for $[C_8C_1Pyrr][Tf_2N]$ (402.7 eV), within the experimental error, but different from that obtained for $[C_8C_1Im][Tf_2N]$ (402.1 eV). In general, N_{cation} 1s binding energies for $[C_8Py][A]$ and $[C_8C_1Pyrr][A]$ (where $[A]^- = [Tf_2N]^-$, $[BF_4]^-$ and I^-) are higher than those for $[C_8C_1Im][A]$, 0.5 ± 0.1 eV, when A is the same, see Table 3.3. The nitrogen atom in $[C_8C_1Pyrr][A]$ is in sp^3 hybridisation whereas sp^2 hybridisation in the cases of $[C_8Py][A]$ and $[C_8C_1Im][A]$. The similar binding energies measured for $[C_8C_1Pyrr][Tf_2N]$ and $[C_8Py][Tf_2N]$ indicate that the nitrogen atoms, regarding of hybridisation, are still in similar partial charge environments. Since there are two nitrogen atoms within the imidazolium cation, the distribution of the positive charge over two atoms gives rise to a noticeably higher electron density at each atom, and thus lower binding energy. The binding energies of the carbon atoms can also be compared. It is evident that $[C_8C_1Im][Tf_2N]$ contains a cation-based C 1s component with a higher binding energy than observed for $[C_8C_1Pyrr][Tf_2N]$ and $[C_8Py][Tf_2N]$ (Figure 3.9(a)). This component for $[C_nC_1Im][A]$ has been identified as the carbon within the imidazolium cation which is bonded to two nitrogen atoms, *i.e.* at the C^2 position.[1, 4] The C^2 atom of $[C_nC_1Im]^+$ is more electron poor than the C_{hetero} atoms of $[C_nC_1Pyrr]^+$ and $[C_nPy]^+$ when $[A]^-$ is common to all samples. For example, the binding energy of the C^2 component for $[C_8C_1Im][Tf_2N]$ is 287.7 eV,[4] whereas the binding energy of C_{hetero} 1s for $[C_8C_1Pyrr][Tf_2N]$ and $[C_8Py][Tf_2N]$ was found to be 286.8 and 287.0 eV respectively. The similar binding energies of the C_{hetero} 1s in both $[C_8C_1Pyrr][Tf_2N]$ and $[C_8Py][Tf_2N]$ further supports the hypothesis that the C_{hetero} atoms of $[C_8C_1Pyrr][Tf_2N]$ and $[C_8Py][Tf_2N]$ are in very similar partial charge environments. However, the binding energies of the C_{inter} atoms of $[C_8C_1Pyrr][Tf_2N]$ and $[C_8Py][Tf_2N]$ are very different from each other, 285.5 eV and 286.1 eV respectively. This observation illustrates that the C_{inter} atoms for $[C_8Py][Tf_2N]$ are in a more electron poor environment due to the sp^2 hybridisation and thus the delocalisation of the positive charge within the $[C_8Py]^+$ cation head group.

Pyrrolidinium-based ionic liquids have been investigated with a great deal of interest for use in electrochemistry due to their greater stability when compared to imidazolium-based ionic liquids, in terms of cation electrochemistry reduction.[53] Moreover, pyridinium-based ionic liquids have also been reported to be more thermally stable when compared to imidazolium analogues.[44] The differences in stability can be correlated to ease of removal of the C^2 proton within the imidazolium cation.[54, 55] XPS results here confirm that the C^2 carbon within the imidazolium cation is more electron poor than any carbon atom found within the pyrrolidinium and pyridinium cations. Consequently, in electrochemistry study, the C^2 proton can be easily removed. These results support the conclusion that pyrrolidinium- and pyridinium-based ionic liquids are more stable than their imidazolium analogues.

Table 3.3 Binding energies in eV for all regions of all ionic liquids in *Section 3.2*. It should be noted that the experimental error associated with the measurement of binding energies is ± 0.1 eV.

Ionic Liquid		Binding Energy / eV												
Cation	Anion	$C_{aliphatic}$1s	C_{hetero}1s	C_{inter} 1s	N_{cation} 1s	C_{CF3} 1s	N_{anion} 1s	O 1s	F 1s	S $2p_{3/2}$	P $2p_{3/2}$	I $3d_{5/2}$	B 1s	Br $3d_{5/2}$
$[C_2C_1Pyrr]^+$	$[Tf_2N]^-$		286.8	285.5	402.7	293.0	399.4	532.6	688.9	169.0				
$[C_4C_1Pyrr]^+$	$[Tf_2N]^-$	285.3	286.8	285.5	402.7	293.0	399.5	532.7	688.9	169.0				
$[C_6C_1Pyrr]^+$	$[Tf_2N]^-$	285.1	286.8	285.5	402.7	293.0	399.5	532.7	688.9	169.0				
$[C_8C_1Pyrr]^+$	$[Tf_2N]^-$	285.0	286.8	285.5	402.7	292.9	399.5	532.7	688.9	169.0				
$[C_{10}C_1Pyrr]^+$	$[Tf_2N]^-$	284.9	286.8	285.5	402.7	292.9	399.5	532.7	688.9	169.0				
$[C_8C_1Pyrr]^+$	$[BF_4]^-$	285.0	286.6	285.5	402.5				685.9				194.2	
$[C_8C_1Pyrr]^+$	I^-	285.0	286.4	285.3	402.4							618.4		
$[C_8C_1Pyrr]^+$	$[Tf_2N]^-$:I^-①	285.0	286.5	285.4	402.5	292.9	399.5	532.6	688.9	168.9		618.4		
$[C_2Py]^+$	$[Tf_2N]^-$	285.6	287.1	286.2	402.6	292.9	399.5	532.6	688.8	169.0				
$[C_4Py]^+$	$[Tf_2N]^-$	285.3	287.1	286.2	402.6	293.0	399.5	532.6	688.8	169.0				
$[C_6Py]^+$	$[Tf_2N]^-$	285.1	287.1	286.2	402.6	293.0	399.5	532.6	688.8	169.0				
$[C_8Py]^+$	$[Tf_2N]^-$	285.0	287.0	286.1	402.6	292.9	399.4	532.6	688.8	169.0				
$[C_{10}Py]^+$	$[Tf_2N]^-$	285.0	287.0	286.1	402.6	292.9	399.5	532.6	688.8	169.0				
$[C_8Py]^+$	$[PF_6]^-$	285.0	286.9	286.0	402.4				686.6		136.6			
$[C_8Py]^+$	$[TfO]^-$	285.0	286.9	286.0	402.4	292.5		532.0	688.6	168.4				
$[C_8Py]^+$	$[BF_4]^-$	285.0	286.9	286.0	402.4				685.9				194.2	
$[C_8Py]^+$	I^-	285.0	286.7	285.8	402.1							618.4		
$[C_8Py]^+$	Br^-	285.0	286.6	285.7	402.1									67.5
$[C_8Py]^+$	$[Tf_2N]^-$:I^-①	285.0	286.9	286.0	402.4	292.9	399.5	532.7	688.9	168.9		618.4		
$[C_8C_1Im]^+$	$[Tf_2N]^-$②	285.0	287.7	287.1/286.6	402.1	292.9	399.4	532.7	688.8	169.0				
$[C_8C_1Im]^+$	$[BF_4]^-$②	285.0	287.6	286.9/286.4	402.0				686.0				194.2	
$[C_8C_1Im]^+$	I^-	285.0	287.4	286.7/286.2	401.8							618.5		
$[C_8C_1Im]^+$	$[Tf_2N]^-$:I^-①	285.0	287.5	286.9/286.3	401.9	292.9	399.4	532.6	688.8	168.9				

①The molar ratios of corresponding pure ionic liquids were 1:1.

②Taken from ref [4]

3.3 Varying the anion

Unlike simple non-functionalised anions, those anions which contain additional carbon, *i.e.* $N(CN)_2^-$, $[EtOSO_3]^-$ and $[OAc]^-$, contribute to the acquired C 1s photoemission envelope. These anions require a modified C 1s fitting model to ensure the reliable identification of the $C_{aliphatic}$ 1s component and therefore enable valid and robust comparisons between binding energies.

3.3.1 Acetate-based imidazolium ionic liquids

As highlighted in *Section 3.2.1*, in the case of simple non-functionalised imidazolium-based

ionic liquids, the high resolution C 1s spectra can be fitted using a four-component model. Structural variation of ionic liquids, normally by changing the combination of cation and anion, can require the use of distinct fitting models, which are in turn dependent upon the number of additional electronic environments which contribute to the C 1s spectra.

The presence of additional carbons in $[OAc]^-$ results in an overlap of the anion and cation contributions, which complicates the fitting of each respective photoemission envelope, particularly the C 1s and potentially the O 1s. In this *Section*, a modified fitting model which is specific to acetate-based imidazolium ionic liquids is described. This new fitting model has been developed based upon the same principles as those used for simple non-functionalised imidazolium-based ionic liquids, where individual contributions corresponding to different electronic environments are included in a summation model with appropriate constraint of FWHM or binding energy.

3.3.1.1 Fitting model of C 1s regions

The $[OAc]^-$ comprises new carbon contributions, labelled C^{15} and C^{16}, see structure in Figure 3.10. Upon closer analysis of their electronic environments, the anion-based carbon atoms are distinct from one another but have similar electronic environments to those found in the imidazolium head group, *i.e.* C^{16} is similar to C^2 as they are both bonded to electronegative atoms, and C^{15} is similar to $C_{aliphatic}$.[56] Consequently, their additional contributions have been included in the fitting model for simple imidazolium-based ionic liquids by amending the appropriate weighting to the existing components. The resulting model is in high agreement with the measured experimental data, see for example the C 1s spectrum for $[C_8C_1Im][OAc]$ in Figure 3.10.

Moreover, as described in *Section 3.2.3.1*, shake up/off phenomenon could be observed typically in the atoms of delocalised systems with multiple bond or aromatic compounds. Consequently, photoelectrons originating from the π-bonded imidazolium cation and carboxylate group are susceptible to shake-up/off.[47] In the case of $[C_8C_1Im][OAc]$, shake-up feature is observed between 291-295 eV. The proportion of each component to shake-up/off must be adjusted to reflect such reduction.[22] Consequently, the relative area ratios for the four C 1s components are set to 1.6:1.6:2.0:8.0 for (C^2+C^{16}): (C^4+C^5): (C^6+C^7): $C_{aliphatic}$ respectively (20% reduction was applied of (C^2+C^{16}) and (C^4+C^5) components to compensate for the shake-up/off processes in the sp^2 hybirdisation components[4]). FWHM values are set to be equal for (C^4+C^5) and (C^6+C^7). FWHM of the $C_{aliphatic}$ 1s component is set separately to be typically ~0.2 eV broader.[4] FWHM for (C^2+C^{16}) is also set ~0.2 eV broader due to the overlap of the two signals of carbons from similar electronic environments (N-C-N and O-C-O). The modified fitting model shows good agreement with measured experimental spectra.

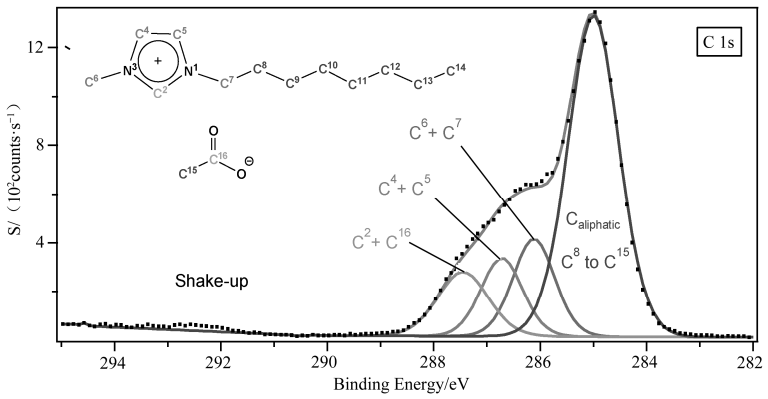

Figure 3.10 Fitting model of C 1s for $[C_8C_1Im][OAc]$, labelled structure: ($C^4 + C^5$), ($C^6 + C^7$), ($C^2 + C^{16}$) and (C^8 to C^{15}) = $C_{aliphatic}$. XP spectrum was charge corrected by referencing the $C_{aliphatic}$ 1s component to 285.0 eV. It must be noted that due the shake-up/off reduction, ($C^4 + C^5$) and ($C^2 + C^{16}$) components were fitted considerably smaller than that of ($C^6 + C^7$) which will be described in detail as below

The same fitting procedure was used when fitting other acetate-based ionic liquids, *i.e.* $[C_2C_1Im][OAc]$, $[C_4C_1Im][OAc]$ and $[C_{12}C_1Im][OAc]$. As shown in Figure 3.11, good agreement was noted in each case.

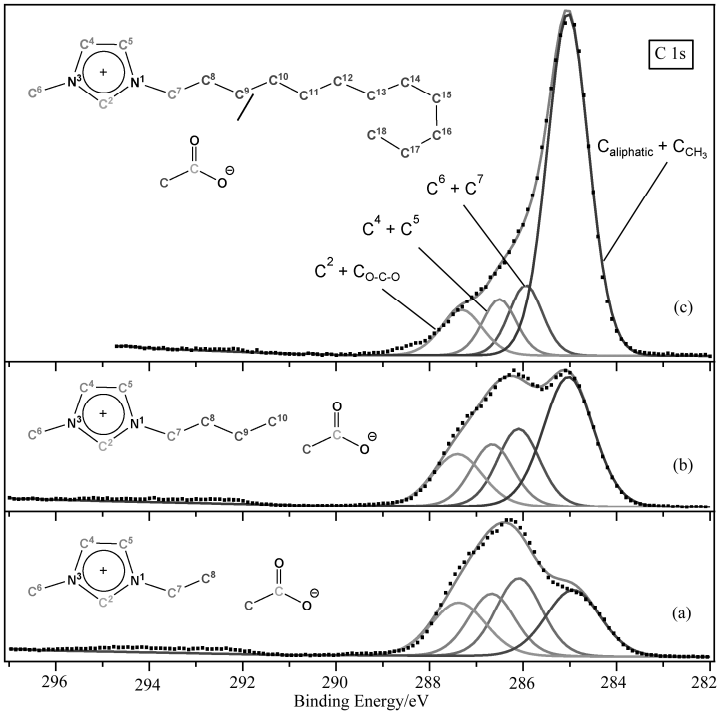

Figure 3.11 Fitting model of C 1s for (a) $[C_2C_1Im][OAc]$, (b) $[C_4C_1Im][OAc]$ and (c) $[C_{12}C_1Im][OAc]$. All XP spectra were charge corrected by referencing the N 1s to the value for $[C_8C_1Im][OAc]$

3.3.1.2 Effect of alkyl chain length on the charge correction

Figure 3.12 shows the change in intensity of the $C_{aliphatic}$ 1s component as a function of alkyl chain length for $[C_nC_1Im][OAc]$, where n = 2-12. All spectra were normalised to the area of the N 1s peak measured for $[C_8C_1Im][OAc]$. It is obvious that for all n values, the binding energies of $C_{aliphatic}$ 1s are identical, within the experimental error. The binding energies of all elements in actetate-based ionic liquids are also shown in Table 3.4.

Table 3.4 Binding energies in eV for all regions of $[C_nC_1Im][OAc]$ (n = 2, 4, 8 and 12). For n = 8, XP spectra were charge corrected by referencing the aliphatic C 1s photoemission peak ($C_{aliphatic}$ 1s) to 285.0 eV. For other values of n, XP spectra were charge corrected by referencing the Nis peak to the value measured for n = 8. It should be noted that the experimental error associated with the measurement of binding energies is of the order ± 0.1 eV

$[C_nC_1Im][OAc]$	$C_{aliphatic}$ 1s	(C^6+C^7) 1s	(C^4+C^5) 1s	C_{hetero} 1s	N_{cation}1s	O_{anion} 1s
2	284.9	286.1	286.7	287.4	401.6	530.3
4	285.0	286.1	286.7	287.4	401.6	530.3
8	285.0	286.1	286.7	287.4	401.6	530.3
12	285.0	286.0	286.6	287.3	401.6	530.4

As highlighted in *Section 3.2.1*,[4] for simple non-functionalised imidazolium-based ionic liquids, when $n \geqslant 8$, we expect the binding energies of $C_{aliphatic}$ 1s to act as a reliable charge reference. As the alkyl chain length decreased, the $C_{aliphatic}$ is located sufficiently close to the imidazolium cation head group, such that the electron withdrawing effect of the imidazolium cation head group becomes significant. With the electron withdrawing influence of the positive charged imidazolium cation head group, the $C_{aliphatic}$ 1s component should be in a more electron poor environment if the alkyl chain is changed from dodecyl to ethyl. Consequently, the $C_{aliphatic}$ 1s component should exhibit a higher binding energy. For imidazolium-based ionic liquids with less basic anions, *i.e.* $[Tf_2N]^-$, the data is in good agreement with this trend.[4] For this reason, the charge correction method using the $C_{aliphatic}$ 1s component could only be achieved when $n \geqslant 8$.

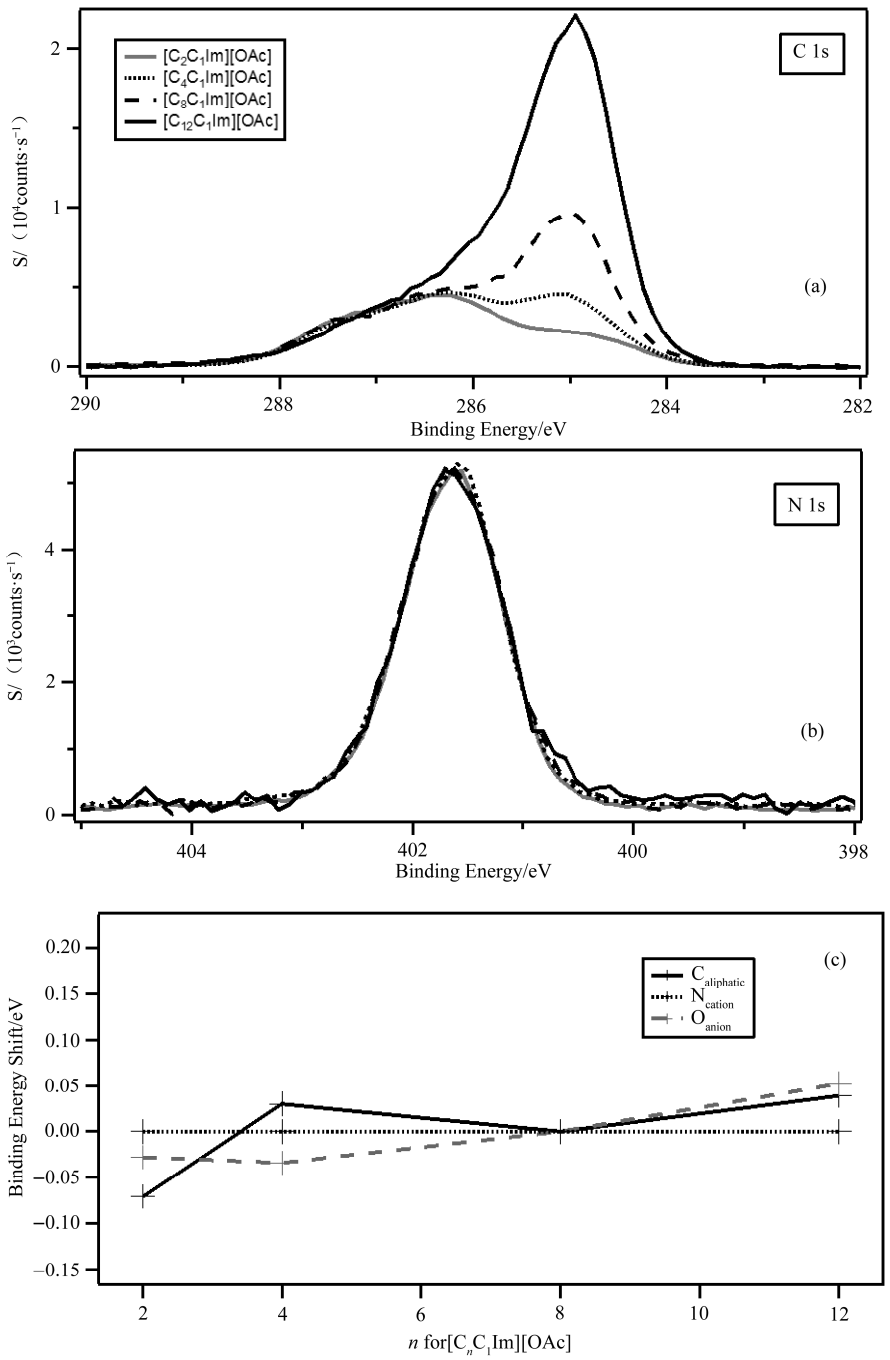

Figure 3.12 XP Spectra for $[C_nC_1Im][OAc]$ (n = 2, 4, 8, 12) for: (a) C 1s and (b) N 1s. The intensities are normalised to the intensity of the N_{cation} 1s fitted peak for $[C_8C_1Im][OAc]$. For n = 8, XP spectra were charge corrected by referencing the $C_{aliphatic}$ 1s component to 285.0 eV. For other n values, XP spectra were charge corrected by referencing the N 1s to the value for n = 8. (c) Binding energy shifts relative to $[C_8C_1Im][OAc]$ as a function of aliphatic chain length, n =2-12

It is important to note that in the case of $[OAc]^-$-based imidazolium ionic liquids, XPS data reveals that the binding energy of the crucial $C_{aliphatic}$ 1s component does not move as a function of alkyl chain length. This observation is in junction position to the analogous family of $[Tf_2N]^-$. A direct comparison of these two analogous ionic liquid families can be seen in Figure 3.13.

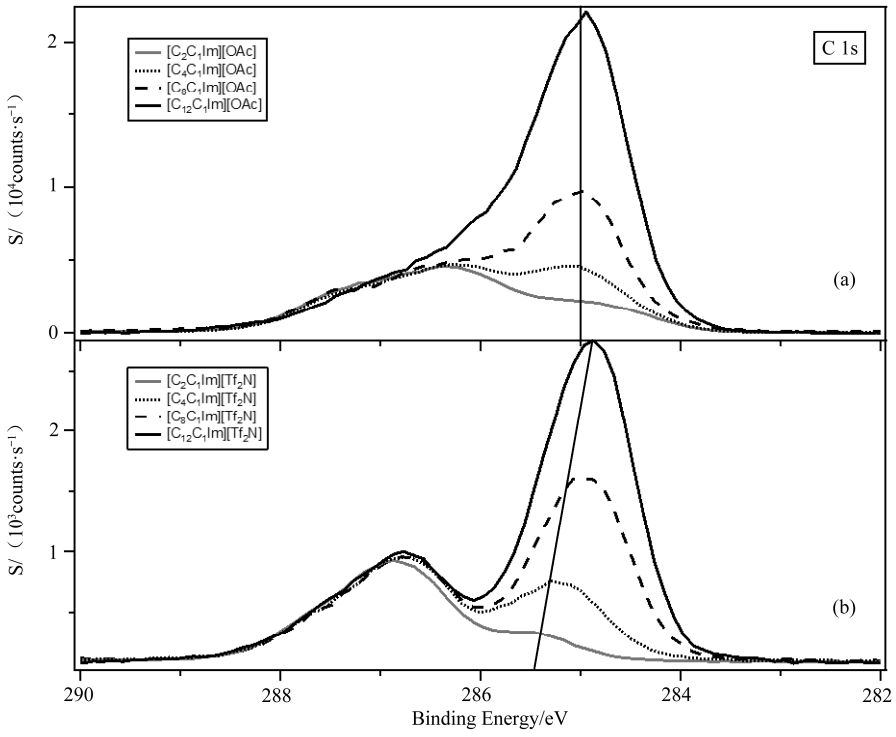

Figure 3.13 C 1s XP Spectra for (a) $[C_nC_1Im][OAc]$ and (b) $[C_nC_1Im][Tf_2N]$ (data according to ref [4]) (n = 2, 4, 8, 12). The intensities are normalised to the intensity of the N_{cation} 1s peak for $[C_8C_1Im][OAc]$ and $[C_8C_1Im][Tf_2N]$ respectively for the two families. For n = 8, XP spectra were charge corrected by referencing the $C_{aliphatic}$ 1s component to 285.0 eV. For other n values, XP spectra were charge corrected by referencing the N_{cation} 1s to the value for n = 8. It should be noted that the experimental error associated with the measurement of binding energies is of the order ± 0.1 eV

This observation suggests that there are significant differences in the cation-anion interactions of these two series of ionic liquids, essentially the alkyl chain is acting as a reporter to these interactions. The measured binding energy for $C_{aliphatic}$ 1s is dependent upon not only the alkyl chain length substituted onto the imidazolium cation head group but also on the nature of the anion, which interacts with the cation head group in the ionic liquid. This may be interpreted as the summation of two sets of interactions which both lead to donation of electron density to the

positively charged cation head group:

(i) Charge transfer from anion to cation;

(ii) Withdrawal of electron density from alkyl substituent (induction).

Clearly the magnitude of charge transferred from the anion to the cation will impact upon XPS signals of the positively charged cation head group, *i.e.* C_{hetero} or N_{cation}. The amount of charge transferred from the anion to the cation gives rise to the difference in measured binding energies for C_{hetero} and N_{cation}. Low basicity anions, *i.e.* $[Tf_2N]^-$, transfer less charge; whereas the opposite is true for high basicity anions such as $[OAc]^-$.

The "charge transfer" model now allows us to explain the apparent change in inductive effects which cause changes to the measured binding energy of the $C_{aliphatic}$ 1s of ionic liquids. This concept is best described by defining two extreme cases, a low basicity anion ($[Tf_2N]^-$) where negligible charge transfer is expected, and a high basicity anion ($[OAc]^-$) where significant electron density can be donated to the electron deficient cation.

1）Low basicity anion

Since the charge transferred from the anion to the cation is negligible, the cation head group is electron deficient. This causes the strongly inductive effect and thus large change in measured $C_{aliphatic}$ binding energy, as shown in Figure 3.14.

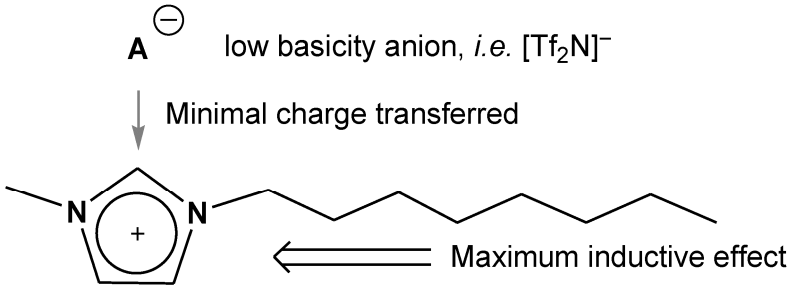

Figure 3.14 Proposed charge transfer mechanism for low basicity anion. Grey arrow represents the charge transferred from the anion to the cation, black arrow corresponds the inductive effect of the alkyl chain

2）High basicity anion

In this case, the charge transferred from anion to cation is significant which increases the electron density of the cation head group.

This effectively reduces the magnitude of the positive charge on the cation head group and thus the "pull" of electron from the alkyl chain. Consequently, the inductive effect is weak which

means only the subtle change in measured $C_{aliphatic}$ binding energy can be observed, as shown in Figure 3.15.

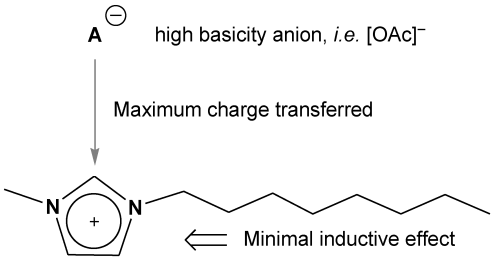

Figure 3.15 Proposed charge transfer mechanism for high basicity anion. Grey arrow represents the charge transferred from the anion to the cation, black arrow corresponds the inductive effect of the alkyl chain

3.3.2 Effect of the anion on the cation

The data presented in *Section 3.3.1* demonstrates that cation-anion interactions can be studied by XPS. For high basicity anions, such as $[OAc]^-$ or halides, the measured binding energies are lower which suggests that the cation head group is more electron rich. Thus, more charge has been transferred from anion to cation. The opposite is true for low basicity anions such as $[Tf_2N]^-$.

A series of simple non-functionalised imidazolium-based ionic liquids with commonly used anions have been investigated by the Nottingham Ionic Liquids group. Based upon previous work ($[Tf_2N]^-$, $[PF_6]^-$, $[TfO]^-$, $[BF_4]^-$ I^-, Br^- and Cl^-)[4] and the work in this chapter ($[OAc]^-$),[19] the binding energies for both C_{hetero} and N_{cation} are shown in Figure 3.16. The investigation of $[SnCl_3]^-$ [14], $[Sn_2Cl_5]^-$[14] ,$[I_3]$ [57] and $[IB_{r2}]$ [57] are not described in this book but can be found in recent publications.

The measured binding energies for C_{hetero} 1s and N_{cation} 1s have been shown to correlate with the anion basicity, hydrogen bond acceptor ability (β).[4, 16, 18] Figure 3.17 shows the linear correlation between binding energy and β. Indeed, β uses a dye to investigate the basicity of the anions. The result shown in Figure 3.17 indicates that XPS can be used to investigate the basicity of the anions in the absence of dyes. The concept of charge transfer is a key factor in understanding ionic liquid anion basicity and thus the measured binding energies for the cation-based components. This concept is even more important when considering the effect of ionic liquids on a metal centre towards ylidene formation and ligand interactions. These will be described in more detail in *Chapters 4* and *5*.

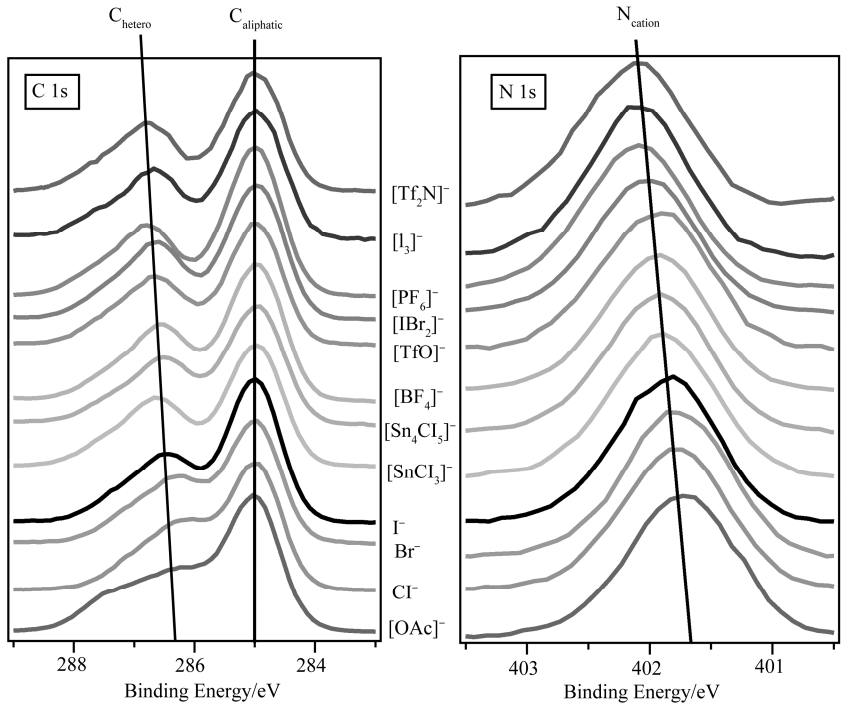

Figure 3.16 Binding energies for C_{hetero} 1s and N_{cation} 1s for a series of imidazolium-based ionic liquids. All XP spectra were charge corrected by referencing the $C_{aliphatic}$ 1s component to 285.0 eV

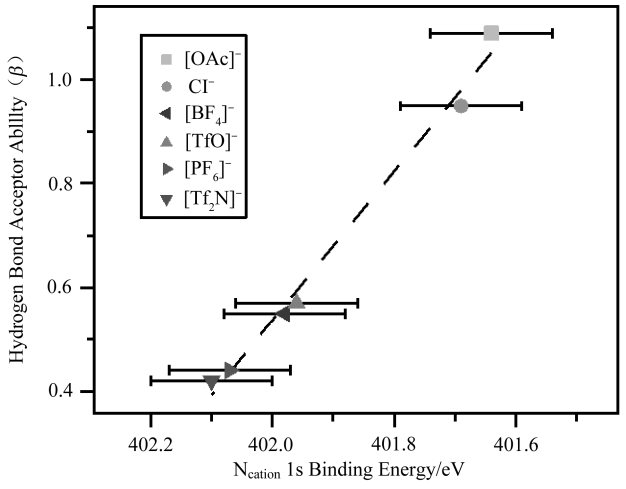

Figure 3.17 Binding energy for N_{cation} 1s compared with hydrogen bond acceptor ability (β) for a series of imidazolium-based ionic liquids. All XP spectra were charge corrected by referencing the $C_{aliphatic}$ 1s component to 285.0 eV

3.4 Ionic liquid mixture

XPS has been used to study ionic liquid mixtures for both elemental composition[12] and subtle binding energy shifts as as result of the different electronic environment within the mixture.[20] As highlighted in *Section 2.2.3*, XPS in the normal emission angle (θ) can be viewed as bulk sensitive (7-9 nm).[12] Consequently, bulk electronic environment of ionic liquid mixture can be effectively probed by normal XPS.

As described in *Section 3.3.2*, the electronic environment of the cation-based component can be significantly influenced by the basicity of the anion. Apart from simply changing the anion, the basicity can also be tuned by applying the mixture anions, *i.e.* the mixture of $[Tf_2N]^-$ and $[OAc]^-$. Consequently, it is worth to investigate the ionic liquid mixtures.

The basicity of the anions used to prepare the mixture should be significantly different such that differences in binding energies of C_{hetero} 1s and N_{cation} 1s are larger than the error of the experiment. Therefore, $[Tf_2N]^-$ and $[OAc]^-$ should be used for all cases. However, in this book, neither $[C_8C_1Pyrr][OAc]$ nor $[C_8Py][OAc]$ is available. Moreover, both $[C_8C_1Pyrr]Cl$ and $[C_8C_1Pyrr]Br$ are unstable under X-ray irradiation which caused surface damage during analysis. Consequently, it was decided that I^- was used for the study of the ionic liquid mixture as halides have the similar high basicity with $[OAc]^-$.

3.4.1 Imidazolium-based ionic liquid mixture

A 1：1 mixture of $[C_8C_1Im][Tf_2N]/[C_8C_1Im]I$ was investigated in this *Section*. As commented in the *Section 3.3.1*, the nature of the anion has a significant impact upon the binding energies of atoms within the cation headgroup due to changes in the amount of charge transfered to the cation. Basic anions, such as I^-, donate more electron density to the cation than less basic ones such as $[Tf_2N]^-$. Therefore, the magnitude of the positive charge associated with the cation headgroup is lower for ionic liquids containing more basic anions. This lower positive charge, and therefore increase in electron density, in the cation can be clearly observed in the binding energies of the N_{cation} 1s and C_{hetero} 1s components. The data presented in Figure 3.18 clearly demonstrates this

difference in binding energy due to different charge transfer between anions and cations. Pure $[C_8C_1Im]I$ exhibits lower measured binding energy values for both C_{hetero} 1s and N_{cation} 1s, 286.7 (taken from the $C^{4,5}$ component) and 401.8 eV respectively.

Similar data for pure $[C_8C_1Im][Tf_2N]$ is also included for comparison; clearly both photoemission envelopes appear at higher binding energies, 287.1 and 402.1 eV respectively. These data confirm again that the cation of $[C_8C_1Im][Tf_2N]$ is significantly more electron deficient than that of $[C_8C_1Im]I$, consistent with the fact that $[Tf_2N]^-$ is less basic and poorly coordinating and not likely to participate in charge transfer towards the cationic moiety. The peaks for the $[C_8C_1Im]I/[C_8C_1Im][Tf_2N]$(1:1) mixture, give rise to remarkably simple XP spectra, sharp, apparently single component spectra are observed with measured binding energies in between those of the two pure ionic liquids. It should be noted that the FWH maxima of the photoemission envelopes in the mixture spectra were comparable to those exhibited by the neat ionic liquid spectra, see Appedix. This observation clearly illustrates that the spectrum of the mixture is not composed of a superposition of the XP spectra of each neat ionic liquid, but a new signal corresponding to a series of entirely new electronic environments.

This set of data agrees with the well reported structure of ionic liquid mixtures consisting of a randomly distributed mixture of all component ions. Consequently, the cation in the ionic liquid mixture is interacting with a statistically similar environment which is composed of an average number of both anions at the same time. As a result of this mixed interaction, the net amount of charge transferred to each cation in the mixture is identical, *i.e.* the electronic environment of the cation is now distinct to that of the two pure ionic liquids. The binding energies acquired for the C_{hetero} 1s and N_{cation} peaks (286.9 and 401.9 eV respectively) suggest that the final average electron density associated with the cation is a weighted average of the electron densities of the same cation in the two pure ionic liquids, where the weighting is reflective of the molar ratio of the two pure ionic liquids employed.

The I $3d_{5/2}$ peak in the $[C_8C_1Im]I/[C_8C_1Im][Tf_2N]$(1:1) mixture is observed at 618.5 eV, which is consist with that of pure $[C_8C_1Im]I$. There is no significant perturbation in the measured binding energies of the elements within the $[Tf_2N]^-$ in the mixtures, *i.e.* any change in electron density is too small to be measured directly by XPS.

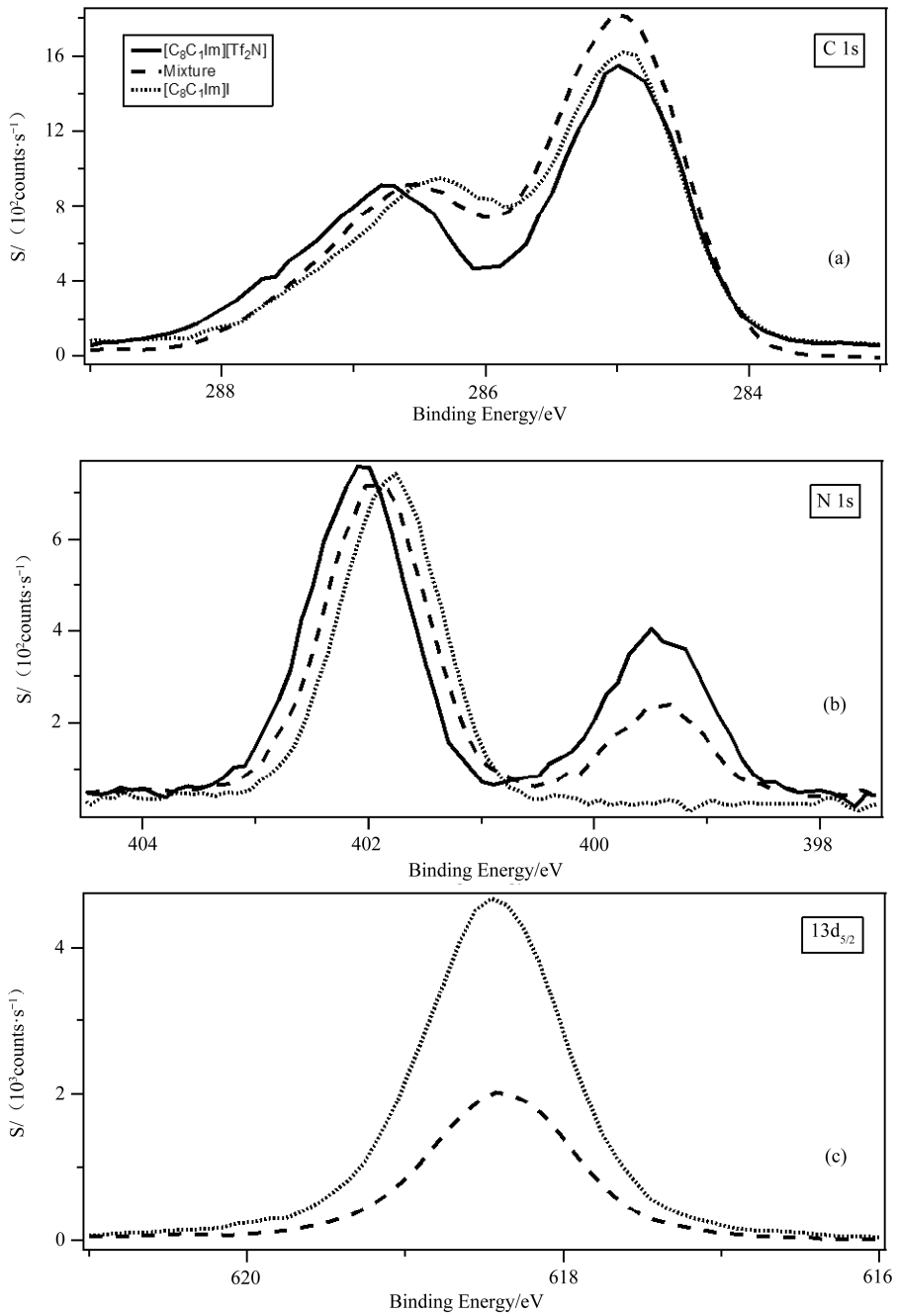

Figure 3.18 XP spectra for a 1:1 mixture of $[C_8C_1Im][Tf_2N]$/$[C_8C_1Im]I$ as well as pure ionic liquids $[C_8C_1Im][Tf_2N]$ and $[C_8C_1Im]I$: (a) C 1s, (b) N 1s and (c) I $3d_{5/2}$. The intensities were normalised to the intensity of the N_{cation} 1s fitted component for $[C_8C_1Im][Tf_2N]$. All XP spectra were charge corrected by referencing the $C_{aliphatic}$ 1s component to 285.0 eV

3.4.2 Pyrrolidinium-based ionic liquid mixture

A 1:1 mixture of $[C_8C_1Pyrr][Tf_2N]$/$[C_8C_1Pyrr]I$ was investigated in this section. A similar observation compared to the imidazolium-based mixtures can be found in Figure 3.19. The results indicate that the electronic environment of the cation-based components can be desired by changing the proportion of different anions.

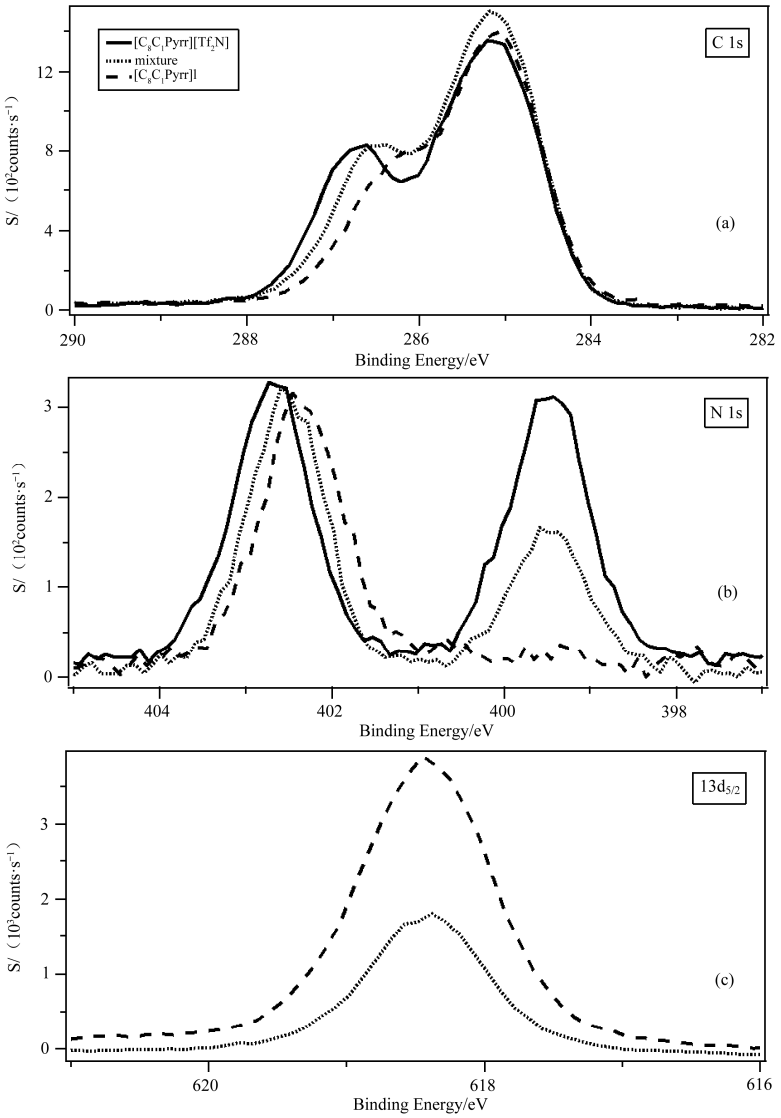

Figure 3.19 XP spectra for a 1∶1 mixture of $[C_8C_1Pyrr][Tf_2N]$/$[C_8C_1Pyrr]I$ as well as pure ionic liquids $[C_8C_1Pyrr][Tf_2N]$ and $[C_8C_1Pyrr]I$: (a) C 1s, (b) N 1s, (c) I $3d_{5/2}$. The intensities were normalised to the intensity of the N_{cation} 1s fitted component for $[C_8C_1Pyrr][Tf_2N]$. All XP spectra were charge corrected by referencing the $C_{aliphatic}$ 1s component to 285.0 eV

3.4.3 Pyridinium-based ionic liquid mixture

A 1:1 mixture of $[C_8Py][Tf_2N]$/$[C_8Py]I$ was also studied in this section as instance. The similar observation as concluded in *Sections 3.4.1 and 3.4.2* can be found in Figure 3.20.

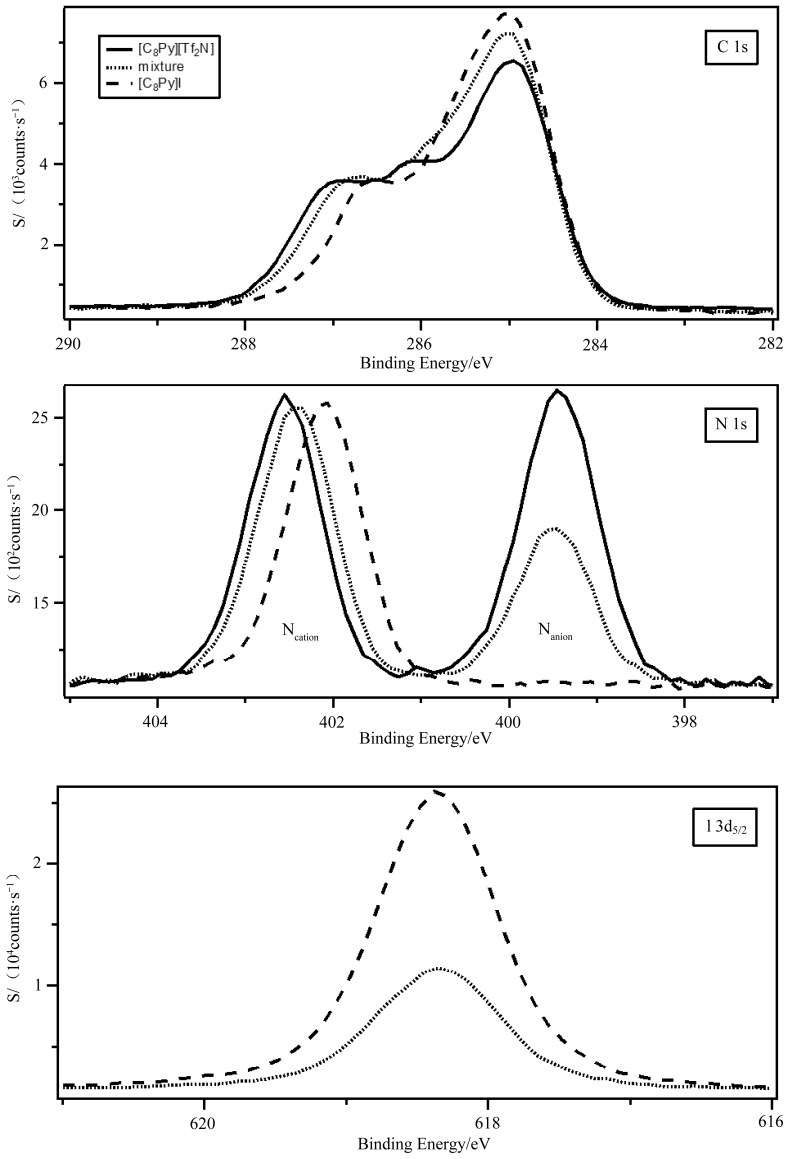

Figure 3.20 XP spectra for a 1:1 mixture of $[C_8Py][Tf_2N]$/$[C_8Py]I$ as well as pure ionic liquids $[C_8Py][Tf_2N]$ and $[C_8Py]I$: (a) C 1s, (b) N 1s, (c) I $3d_{5/2}$. The intensities were normalised to the intensity of the N_{cation} 1s fitted component for $[C_8Py][Tf_2N]$. All XP spectra were charge corrected by referencing the $C_{aliphatic}$ 1s component to 285.0 eV

It was concluded that for all imidazolium-, pyrrolidinium- and pyridinium-based ionic liquid mixtures, the cation is surrounded by both of anions, not pockets of the cation with one specific type of anion. The significant influence of the anion on the electronic environment of the cation can be used for the design of the cation, specifically by using the appropriate mixture of different anions. The conclusion even inspired the idea of tuning the cation-based component (metal centre) within the phosphineimidazolylidene cation to a desired binding energy value and will be introduced in more detail in *Chapter 4*.

3.5 Conclusions

The results presented in this chapter demonstrate a detailed description about the C 1s fitting model used for pyrrolidinium- and pyridinium-based ionic liquids as well as $[OAc]^-$-based imidazolium ionic liquids. The method for charge correction is extensively discussed and the conclusion is that for low basicity anions, *i.e.* $[Tf_2N]^-$, when the alkyl chain length is$\geqslant$8, we expect the $C_{aliphatic}$ 1s component to be a reliable charge reference; for high basicity anions, *i.e.* $[OAc]^-$, the $C_{aliphatic}$ 1s component cannot be electronically influenced by the cation head group and thus is always a reliable charge reference. It was then decided that C_8-based ionic liquids should be always selected to prepare metal catalyst solutions for ease of charge correction and thus obtain of reliable and comparable binding energy for the solute dissolved in ionic liquids.

Moreover, the cation-anion interaction is a key factor which influences the measured binding energies obtained for cation-based components. This interaction has been correlated to the measured binding energy of the N_{cation} peak for three pyrrolidinium-based ionic liquids. The work in this area by the Nottingham Ionic Liquids group has been summarised for a series of imidazolium-based ionic liquids and it can be concluded that low basicity anions lead to a higher measured N_{cation} 1s binding energy; the opposite is also true. The research based upon analysis of ionic liquid mixtures in this book concludes that in the mixture, the cation is always surrounded by both of the anions. This observation allows the design of cation electronic environment by using mixture of anions.

References

[1] SMITH E F，RUTTEN F J M，VILLAR-GARCIA I J，et al. Ionic liquids in vacuo: Analysis of liquid surfaces using ultra-high-vacuum techniques[J]. Langmuir， 2006， 22(22): 9386-9392.

[2] CAPORALI S，BARDI U，LAVACCHI A. X-ray photoelectron spectroscopy and low energy ion scattering studies on 1-buthyl-3-methyl-imidazolium bis(trifluoromethane) sulfonimide[J]. Journal of Electron Spectroscopy and Related Phenomena，2006，151(1): 4-8.

[3] MAIER F，GOTTFRIED J M，ROSSA J，et al. Surface enrichment and depletion effects of ions dissolved in an ionic liquid: an X-ray photoelectron spectroscopy study[J]. Angewandte Chemie-International Edition，2006，45(46): 7778-7780.

[4] VILLAR-GARCIA I J，SMITH E F，TAYLOR A W，et al. Charging of ionic liquid surfaces under X-ray irradiation: the measurement of absolute binding energies by XPS[J]. Physical Chemistry Chemical Physics，2011，13(7): 2797-2808.

[5] SMITH E F，VILLAR-GARCIA I J，BRIGGS D，et al. Ionic liquids in vacuo；solution-phase X-ray photoelectron spectroscopy[J]. Chemical Communications，2005(45): 5633-5635.

[6] HOFFT O，BAHR S，HIMMERLICH M，et al. Electronic structure of the surface of the ionic liquid [EMIM][Tf2N] studied by metastable impact electron spectroscopy (MIES)，UPS，and XPS[J]. Langmuir，2006，22(17): 7120-7123.

[7] GOTTFRIED J M，MAIER F，ROSSA J，et al. Surface studies on the ionic liquid 1-ethyl-3-methylimidazolium ethylsulfate using X-ray photoelectron spectroscopy[J]. Zeitschrift Fur Physikalische Chemie-International Journal of Research in Physical Chemistry & Chemical Physics，2006，220(10-11): 1439-1453.

[8] LOCKETT V，SEDEV R，BASSELL C，et al. Angle-resolved X-ray photoelectron spectroscopy of the surface of imidazolium ionic liquids[J]. Physical Chemistry Chemical Physics，2008，10(9): 1330-1335.

[9] LOCKETT V，SEDEV R，HARMER S，et al. Orientation and mutual location of ions at the surface of ionic liquids[J]. Physical Chemistry Chemical Physics， 2010， 12(41): 13816-13827.

[10] LOVELOCK K R J，KOLBECK C，CREMEr T，et al. Influence of Different Substituents on the Surface Composition of Ionic Liquids Studied Using ARXPS[J]. Journal of Physical

Chemistry B，2009，113(9): 2854-2864.

[11] KOLBECK C，CREMER T，LOVELOCK K R J，et al. Influence of Different Anions on the Surface Composition of Ionic Liquids Studied Using ARXPS[J]. Journal of Physical Chemistry B，2009，113(25): 8682-8688.

[12] MAIER F，CREMER T，KOLBECK C，et al. Insights into the surface composition and enrichment effects of ionic liquids and ionic liquid mixtures[J]. Physical Chemistry Chemical Physics，2010，12(8): 1905-1915.

[13] CREMER T，KOLBECK C，LOVELOCK K R J，et al. Towards a Molecular Understanding of Cation-Anion Interactions-Probing the Electronic Structure of Imidazolium Ionic Liquids by NMR Spectroscopy，X-ray Photoelectron Spectroscopy and Theoretical Calculations[J]. Chemistry-a European Journal，2010，16(30): 9018-9033.

[14] CURRIE M，ESTAGER J，LICENCE P，et al. Chlorostannate(II) Ionic Liquids: Speciation，Lewis Acidity and Oxidative Stability[J]. Inorganic Chemistry，2013，52(4): 1710-1721.

[15] TAYLOR A W，MEN S，CLARKE C J，et al. Acidity and basicity of halometallate-based ionic liquids from X-ray photoelectron spectroscopy[J]. Rsc Advances，2013，3(24): 9436-9445.

[16] MEN S，LOVELOCK K R J，LICENCE P. X-ray Photoelectron Spectroscopy of Pyrrolidinium-Based Ionic Liquids: Cation-Anion Interactions and a Comparison to Imidazolium-Based Analogues[J]. Physical Chemistry Chemical Physics，2011，13(33): 15244-15255.

[17] MEN S，HURISSO B B，LOVELOCK K R J，et al. Does the influence of substituents impact upon the surface composition of pyrrolidinium-based ionic liquids? An angle resolved XPS study[J]. Physical Chemistry Chemical Physics，2012，14(15): 5229-5238.

[18] MEN S，MITCHELL D S，LOVELOCK K R J，et al. X-ray Photoelectron Spectroscopy of Pyridinium-Based Ionic Liquids: Comparison to Imidazolium- and Pyrrolidinium-Based Analogues[J]. Chemphyschem，2015，16(10): 2211-2218.

[19] MEN S，LOVELOCK K R J，LICENCE P. Directly probing the effect of the solvent on a catalyst electronic environment using X-ray photoelectron spectroscopy[J]. Rsc Advances，2015，5(45): 35958-35965.

[20] VILLAR-GARCIA I J，LOVELOCK K R J，MEN S，et al. Tuning the electronic environment of cations and anions using ionic liquid mixtures[J]. Chemical Science，2014，5(6): 2573-2579.

[21] BRIGGS D，GRANT J T. Surface Analysis by Auger and X-ray Photoelectron Spectroscopy[M]. Manchester: IMPublications，2003.

[22] LOVELOCK K R J，VILLAR-GARCIA I J，MAIER F，et al. Photoelectron Spectroscopy of Ionic Liquid-Based Interfaces[J]. Chemical Reviews，2010，110(9): 5158-5190.

[23] BERNARDI F，SCHOLTEN J D，FECHER G H，et al. Probing the chemical interaction between iridium nanoparticles and ionic liquid by XPS analysis[J]. Chemical Physics Letters，2009，479(1-3): 113-116.

[24] FORSYTH S A，BATTEN S R，DAI Q，et al. Ionic liquids based on imidazolium and pyrrolidinium salts of the tricyanomethanide anion[J]. Australian Journal of Chemistry，2004，57(2): 121-124.

[25] JOHANSSON P，FAST L E，MATIC A，et al. The conductivity of pyrrolidinium and sulfonylimide-based ionic liquids: A combined experimental and computational study[J]. Journal of Power Sources，2010，195(7): 2074-2076.

[26] GHATEE M H，ZARE M，ZOLGHADR A R，et al. Temperature dependence of viscosity and relation with the surface tension of ionic liquids[J]. Fluid Phase Equilibria，2010，291(2): 188-194.

[27] GARDAS R L，COUTINHO J A P. A group contribution method for viscosity estimation of ionic liquids[J]. Fluid Phase Equilibria，2008，266(1-2): 195-201.

[28] HOWLETT P C，BRACK N，HOLLENKAMP A F，et al. Characterization of the lithium surface in N-methyl-N-alkylpyrrolidinium bis(trifluoromethanesulfonyl) amide room-temperature ionic liquid electrolytes[J]. Journal of the Electrochemical Society，2006，153(3): A595-A606.

[29] BHATT A I，BEST A S，HUANG J H，et al. Application of the N-propyl-N-methyl-pyrrolidinium Bis(fluorosulfonyl)imide RTIL Containing Lithium Bis(fluorosulfonyl)imide in Ionic Liquid Based Lithium Batteries[J]. Journal of the Electrochemical Society，2010，157(1): A66-A74.

[30] MACFARLANE D R，PRINGLE J M，HOWLETT P C，et al. Ionic liquids and reactions at the electrochemical interface[J]. Physical Chemistry Chemical Physics，2010，12(8): 1659-1669.

[31] CASTIGLIONE F，RAGG E，MELE A，et al. Molecular Environment and Enhanced Diffusivity of Li^+ Ions in Lithium-Salt-Doped Ionic Liquid Electrolytes[J]. Journal of Physical Chemistry Letters，2011，2(3): 153-157.

[32] FAVRE F，OLIVIER-BOURBIGOU H，COMMEREUC D，et al. Hydroformylation of 1-hexene with rhodium in non-aqueous ionic liquids: how to design the solvent and the ligand to the reaction[J]. Chemical Communications，2001(15): 1360-1361.

[33] CUI Y，BIONDI I，CHAUBEY M，et al. Nitrile-functionalized pyrrolidinium ionic liquids as solvents for cross-coupling reactions involving in situ generated nanoparticle catalyst reservoirs[J]. Physical Chemistry Chemical Physics，2010，12(8): 1834-1841.

[34] JUNG S，PALGUNADI J，KIM J H，et al. Highly efficient metal-free membranes for the separation of acetylene/olefin mixtures: Pyrrolidinium-based ionic liquids as acetylene transport carriers[J]. Journal of Membrane Science，2010，354(1-2): 63-67.

[35] WOOSTER T J，JOHANSON K M，FRASER K J，et al. Thermal degradation of cyano containing ionic liquids[J]. Green Chemistry，2006，8(8): 691-696.

[36] DEYKO A，LOVELOCK K R J，CORFIELD J A，et al. Measuring and predicting Delta(vap)H298 values of ionic liquids[J]. Physical Chemistry Chemical Physics，2009，11(38): 8544-8555.

[37] CHAMBREAU S D，VAGHJIANI G L，TO A，et al. Heats of Vaporization of Room Temperature Ionic Liquids by Tunable Vacuum Ultraviolet Photoionization[J]. Journal of Physical Chemistry B，2010，114(3): 1361-1367.

[38] BRIGGS D，BEAMSON G. The XPS of Polymers Database[M]. Manchester: SurfaceSpectra，2000.

[39] HURISSO B B，LOVELOCK K R J，LICENCE P. Amino Acid-Based Ionic Liquids: Using XPS to Probe the Electronic Environment via Binding Energies[J]. Physical Chemistry Chemical Physics，2011，13: 17737-17748.

[40] CROWHURST L，FALCONE R，LANCASTER N L，et al. Using Kamlet-Taft solvent descriptors to explain the reactivity of anionic nucleophiles in ionic liquids[J]. Journal of Organic Chemistry，2006，71(23): 8847-8853.

[41] LEE J M，PRAUSNITZ J M. Polarity and hydrogen-bond-donor strength for some ionic liquids: Effect of alkyl chain length on the pyrrolidinium cation[J]. Chemical Physics Letters，2010，492(1-3): 55-59.

[42] YUNUS N M，MUTALIB M I A，MAN Z，et al. Thermophysical properties of 1-alkylpyridinum bis(trifluoromethylsulfonyl)imide ionic liquids[J]. Journal of Chemical Thermodynamics，2010，42(4): 491-495.

[43] CADENA C，ZHAO Q，SNURR R Q，et al. Molecular modeling and experimental studies

of the thermodynamic and transport properties of pyridinium-based ionic liquids[J]. Journal of Physical Chemistry B，2006，110(6): 2821-2832.

[44] SANCHEZ L G，ESPEL J R，ONINK F，et al. Density，Viscosity，and Surface Tension of Synthesis Grade Imidazolium，Pyridinium，and Pyrrolidinium Based Room Temperature Ionic Liquids[J]. Journal of Chemical and Engineering Data，2009，54(10): 2803-2812.

[45] CROSTHWAITE J M，MULDOON M J，DIXON J K，et al. Phase transition and decomposition temperatures，heat capacities and viscosities of pyridinium ionic liquids[J]. Journal of Chemical Thermodynamics，2005，37(6): 559-568.

[46] BEAMSON G，BRIGGS D. High-Resolution Monochromated X-Ray Photoelectron-Spectroscopy of Organic Polymers - a Comparison between Solid-State Data for Organic Polymers and Gas-Phase Data for Small Molecules[J]. Molecular Physics，1992，76(4): 919-936.

[47] MOULDER J F，STICKLE W F，SOBOL P E，et al. Handbook of X-ray Photoelectron Spectroscopy: a reference book of standard spectra for identification and interpretation of XPS data[M]. Chanhassen: Physical Electronics，1995.

[48] YARZHEMSKY V，NEFEDOV V I，TRZHASKOVSKAYA M B，et al. The influence of core hole relaxation on the main-line intensities in X-ray photoelectron spectra[J]. J. Electron Spectrosc. Relat. Phenom.，2002，123(1): 1-10.

[49] SVENSSON S，ERIKSSON B，MARTENSSON N，et al. Electron Shake-up and Correlation Satellites and Continuum Shake-off Distributions in X-ray Photoelectron-Spectra of The Rare-Gas Atoms[J]. J. Electron Spectrosc. Relat. Phenom.，1988，47: 327-384.

[50] BRIGGS D，BEAMSON G. XPS Studies of The Oxygen-1s and Oxygen-2s Levels in A Wide-Range of Functional Polymers[J]. Analytical Chemistry，1993，65(11): 1517-1523.

[51] SJOGREN B，SVENSSON S，DEBRITO A N，et al. The C 1s Core Shake-up Spectra of Alkene Molecules - An Experimental and Theoretical-Study[J]. Journal of Chemical Physics，1992，96(9): 6389-6398.

[52] ROBERT T. Correlation Between Chemical Bonding and Satellite Lines in X-ray Photoelectron Spectra of Transition-Metal Compounds[J]. Chemical Physics，1975，8(1-2): 123-135.

[53] WIBOWO R，Jones S E W，Compton R G. Investigating the Electrode Kinetics of the Li/Li+ Couple in a Wide Range of Room Temperature Ionic Liquids at 298 K[J]. Journal of Chemical and Engineering Data，2010，55(3): 1374-1376.

[54] KROON M C，BUIJS W，PETERS C J，et al. Decomposition of ionic liquids in electrochemical processing[J]. Green Chemistry，2006，8(3): 241-245.

[55] BONHOTE P，DIAS A P，PAPAGEORGIOU N，et al. Hydrophobic，highly conductive ambient-temperature molten salts[J]. Inorganic Chemistry，1996，35(5): 1168-1178.

[56] SITKOFF D，SHARP K A，HONIG B. Accurate calculation of hydration free-energies using macroscopic solvent models[J]. Journal of Physical Chemistry，1994，98(7): 1978-1988.

[57] MEN S，LOVELOCK K R J，LICENCE P. X-ray photoelectron spectroscopy of trihalide ionic liquids: Comparison to halide-based analogues，anion basicity and beam damage[J]. Chemical Physics Letters，2017，679: 207-211.

Chapter 4

XPS of Solute-solvent Interaction in Ionic Liquids

4.1 Introduction

To date, the role which ionic liquids play in chemical reactions, in particular in homogeneous catalytic processes, has been a topic of great discussion. The properties of ionic liquids, for example their associated low volatility, is advantageous in terms of immobilising homogeneous catalysts and separating products post reaction. In addition, exchanging traditional organic reaction solvents for ionic liquids can give rise to an acceleration of catalytic reaction.[1, 2] The *in situ* formation of metal-containing ylidene-based catalytic species, in many homogeneous catalytic processes, *e.g.* the Heck coupling reaction,[3] telomerisation,[4] oligomerisation[5] and the Suzuki cross coupling reaction,[2, 6] have been shown to be more effective in ionic liquids. It has been found that a large range of transformations can be carried out by employing transition metals to form metal-containing ylidene complexes, *e.g.* zirconium,[5] silver,[7, 8] copper,[9, 10] platinum,[11, 12] rhodium,[7, 13, 14] iridium[15, 16] and palladium.[17, 18]

The Suzuki cross coupling reaction has been widely studied, using ionic liquids as the reaction solvent, the reaction is typically catalysed by Tetrakis (triphenylphosphine) palladium(0) ($[Pd(PPh_3)_4]$). The formation of the metal-containing ylidene complex, *i.e.* a phosphin eimidazol ylidene palladium complex, is responsible for the acceleration in reaction rate, when carried out in imidazolium-based ionic liquids.[3, 6]

The analysis of the catalyst in solution is of utmost importance in order to be able to understand the role of ionic liquids in homogeneous catalytic reactions. Several techniques have been used to characterise the catalyst in solution. MS can provide with the spectrometric evidence of the catalyst especially when charged catalyst are involved (ESI-MS)[19] and EXAFs can provide the first coordination shell of the catalyst in solution and bond distances.[20] IR,[21] UV-Vis[22] and EPR[23] spectra can also be used to identify its spectroscopic finger prints in solution. One of the main factors controlling the outcome of these reactions is the electronic environment of the metal centre of the catalysts. This information can, potentially, be indirectly obtained from NMR analysis of the ligand characteristic atoms or the IR metal-ligand bonds signals or directly measured by UV-Vis spectra (energy gap) or NMR analysis of the metal centre. UV-Vis and IR analysis have been routinely used to assess the donating ability of ligands to metal centres. These techniques could be potentially used to observe the effect of other ligands or the existence of new ionic liquid-metal centre interactions. However, for UV-Vis and IR analysis, the acquisition of this information is dependent on the catalyst producing an observable (and not obscured by the ionic liquid) spectroscopic signal. For NMR, only diamagnetic complexes can be analysed, which in practice prevents the analysis of many systems. These are most probably the reasons for the scarcity of such studies in ionic liquid systems.[24]

XPS is a powerful analytical tool that allows investigations of the bulk electronic environment of both solids and solvents/solutes. XPS of solid catalysts has been used for years to characterise the metal oxidation state. However, studies of the electronic environment of metal centres in solution have been limited by experimental challenges as most solvents are too volatile to be studied using conventional XPS apparatus.[25, 26] XPS offers a unique spectroscopic opportunity to investigate the presence of solvent-solute interactions that may promote the *in situ* formation of new catalytic species that may otherwise not easily be characterised by more traditional solution spectroscopic methods.

Over the past decade, the use of XPS in the investigation of ionic liquid-based systems has greatly increased.[27] XPS can give information on both the electronic environment of ionic liquids[28-30] and the ionic liquid/gas surface composition.[28, 30-33] XPS can be used to monitor the liquid-phase organic reactions,[34, 35] chemical state of metal catalysts in ionic liquids[36-38] and the electronic contribution of a substituent towards the stabilisation of the cationic charge.[28, 29] XPS can reveal very subtle trends in the binding energies of cation-based components[28] and the hydrogen bond acceptor abilities of corresponding anions.[30, 39, 40] Recent studies have highlighted

that the XPS signals can act as reporters to tune the electronic environment of cations and anions using ionic liquid mixtures.[39, 41]

In this chapter, we extend this method to investigate if XPS may be used to probe solute-solvent interactions in catalytic systems. We highlight the formation of a palladium-containing complex, which is employed as a probe of the solvation environment in five $[C_8C_1Im]^+$-based ionic liquids and $[C_8Py][BF_4]$. The effect of anion basicity on the electronic environment of the cation-based components has been investigated for five phosphineimi dazolylidene palladium containing solutions, where the anions are $[OAc]^-$, Cl^-, $[BF_4]^-$, $[TfO]^-$ and $[Tf_2N]^-$, as a sequence of basicity from highest to lowest.[42, 43]

The formation of a new phosphineimidazolylidene palladium complex is confirmed using high-resolution Pd 3d XP spectra, and the binding energy of the Pd-containing probe is shown to be sensitive to the ionic liquid solvent across a range of compositions. The impact of anion composition upon the electronic environment of the new Pd carbene species is investigated; our data is correlated to the Kamlet-Taft hydrogen bond acceptor ability, β. Furthermore, in the case of the deliberate investigation of simple ionic liquid based mixtures, where a common cation is probed in the presence of mixed anions, the probe appears to experience a single "average" environment which suggests that the ions form a single anisotropic mixture as opposed to discrete yet intimately mixed pockets of differing anion/cation combinations which could initiate segregation and preferential solute clustering.

Our data suggests that ionic liquids can contribute to catalytic processes and are much more than mere spectators in chemical reactions. Interactions of this nature can be correlated to reaction performance providing essential information for the design of more efficient catalytic systems for the future. This hypothesis is tested experimentally by comparison of catalyst turnover frequencies (TOFs) for a series of standard benchmark reactions, *i.e.* the Pd-catalysed Suzuki reaction, carried out in a range of ionic liquids that were chosen to offer a range of both measured Pd 3d binding energies and Kamlet-Taft β values.

4.2 Formation of a phosphineimidazolylidene palladium complex

The $[Pd(PPh_3)_4]$ catalysed Suzuki cross coupling reaction is accelerated dramatically when

ionic liquids are employed as solvents.[2] The reason for this observation has been investigated and it has been concluded that the interaction between the palladium catalyst and the ionic liquid, which Subsequently causes the formation of a new palladium species in the solution, increases the reaction rate. The *in situ* formation of phosphineimidazolylidene palladium complexes results in a more thermally stable, catalytically active species in ionic liquids. In literature, the phosphineimidazolylidene palladium complex has been observed in the case of the $[BF_4]^-$-based system by ESI-MS and NMR spectroscopy, with the successful determination of a crystal structure highlighted in Figure 4.1.[17] It must be noted that, the formation of the 1-octyl-3-methyl phosphineimidazolylidene palladium complex in all cases investigated in this chapter has been confirmed by ESI-MS and XPS.

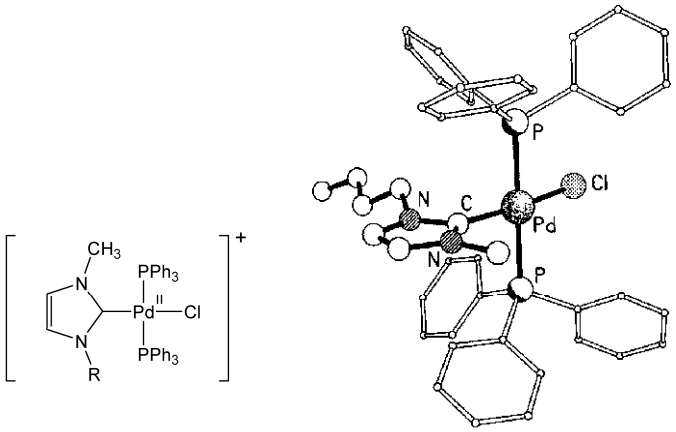

Figure 4.1 Structure of the phosphineimidazolylidene palladium complex cation formed *in situ* during the Pd catalysed Suzuki cross coupling reaction conducted in imidazolium-based ionic liquids[17]

Generally, the acquisition of a high resolution XP spectrum for a given element with low concentration is possible. The detection limit is dependent on the element but is found to be no less than 0.01 atomic %. Unfortunately, in the case of real catalysis, the concentration of the catalyst in solution will be below such a detection limit, which means that Pd 3d photoemission cannot be observed due to the low signal to noise ratio. Consequently, in this chapter, all palladium-containing samples were prepared in higher concentration in a "model" Suzuki system, with Pd concentration around 0.1 atomic %, as described in *Section 2.2.6*. Table 4.1 shows the palladium concentration in palladium-containing solutions prepared in 'model' Suzuki systems for XPS measurement, as well as in Suzuki reactions which is reported in more detail in *Section 4.6*.

Table 4.1 Pd atomic % in XPS samples and in Suzuki reaction for $[C_8C_1Im][A]$

A for $[C_8C_1Im][A]$	[Pd] / atomic % in XPS samples	[Pd] / atomic % in Suzuki reaction
$[Tf_2N]^-$	0.14	3.5×10^{-3}
$[TfO]^-$	0.12	
$[BF_4]^-$	0.10	3.4×10^{-3}
Cl^-	0.09	
$[OAc]^-$	0.10	3.5×10^{-3}
$[Tf_2N]^-:Cl^-$ (1:1)	0.10	3.4×10^{-3}

The RSF of Pd 3d is relative high, 5.356, compared to those of C 1s and F 1s, 0.278 and 1.000 respectively.[44] This means that high quality Pd 3d XP spectra are more readily acquired compared to C 1s or F 1s spectra. The difference in RSFs provides a possibility that high resolved Pd 3d XP spectra can be recorded but the contribution of C 1s signals from the low concentration of phosphineimidazolylidene palladium complex, *i.e.* around 0.1 atomic %, is negligible. Consequently, when analysing XP spectra, the $C_{aliphatic}$ 1s component can still be used as a reliable charge correction.

Initially, $[C_8C_1Im][BF_4]$ was used as a case study as it has been previously reported that the phosphineimidazolylidene palladium complex can be formed in this solvent.[17] Survey and high resolution XP spectra of each of the elements measured for the phosphineimidazolylidene palladium complex in $[C_8C_1Im][BF_4]$ are shown in Figure 4.2. From the survey spectrum, photoelectron peaks were observed for all expected elements except Pd, as was the case for each of the ionic liquid solutions presented herein. Furthermore, it showed that neither surface segregated impurities, *e.g.* silicone, nor hydrocarbon/oxygenated impurities were present for any of the ionic liquid solutions studied. The Pd photoelectron line, *i.e.* Pd 3d at 334-346 eV, is too low in intensity to extract any useful scientific data from this particular data set. High resolution spectra for each element are also presented. It should be noted that the C 1s envelope was fitted according to the previously developed fitting model for simple imidazolium-based ionic liquids (see *Section 2.2.5.2*).[30] A high quality Pd 3d spectrum can be observed by setting the acquisition time to be considerably longer (t=4800s for Pd 3d, compared to 600 s for all other spectra) to compensate for the low concentration of palladium in the solution.

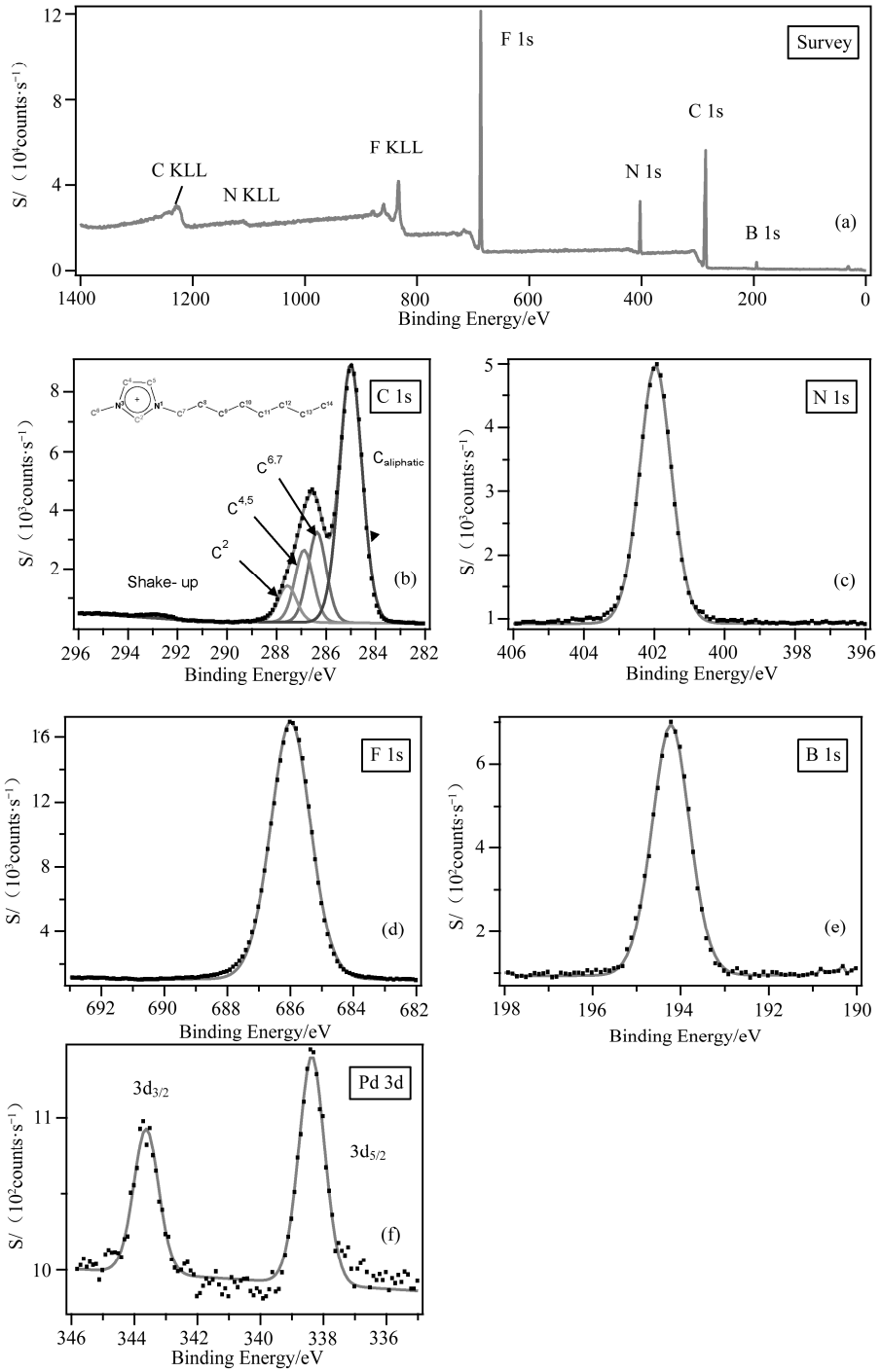

Figure 4.2 XP spectra of each component present in a sample of $[C_8C_1Im][BF_4]$ containing the *in situ* generated phosphineimidazolylidene palladium complex, (a) survey (b) C 1s (c) N 1s (d) F 1s (e) B 1s (f) Pd 3d. All XP spectra were charge corrected by referencing the $C_{aliphatic}$ 1s component to 285.0 eV

Surface enrichment of low concentrations of a metal element in metal-containing ionic liquid solutions has been observed by several research groups.[45, 46] In some cases, when the metal complex only acts as the solute in an ionic liquid, surface enhancement can be observed by XPS. Quantitative analysis of the Pd-containing solutions is presented in Table 4.2. These data show no evidence of surface enhancement of the Pd-containing ylidene complex which indicates that we are investigating the bulk nature.

Table 4.2 Pd atomic % measured by XPS and theoretically calculated from solution preparation for $[C_8C_1Im][A]$. It must be note that the error of XPS as a semi-quantitative method is ± 20%

A for $[C_8C_1Im][A]$	Measured [Pd] / atomic %	Theoretical [Pd] / atomic %
$[Tf_2N]^-$	0.04 ± 0.01	0.14
$[TfO]^-$	0.05 ± 0.01	0.12
$[BF_4]^-$	0.05 ± 0.01	0.10
Cl^-	0.03 ± 0.01	0.09
$[OAc]^-$	0.05 ± 0.01	0.10
$[Tf_2N]^-:Cl^-$ (1:1)	0.05 ± 0.01	0.10

Figures 4.3(a) and (b) show a comparison between the Pd 3d XP spectra for solid $[Pd(PPh_3)_4]$ and a typical solution sample of palladium-containing ylidene complex in $[C_8C_1Im][BF_4]$. Upon first inspection, it is clear that the XP spectrum of the solution sample is much sharper than that of the solid $[Pd(PPh_3)_4]$. Indeed, the FWHM for the Pd $3d_{5/2}$ component of the spectra are 1.0 and 1.8 respectively. This observation may be explained as a result of charging at the surface of the non-conducting solid sample[30, 47, 48] or, more probably, as a consequence of the photo-physics involved during the photoelectron emission. It is well known that FWHM is proportional to the lifetime of the vacancy that is left as a result of photoelectron emission (FWHM ~ h/τ, where τ is the vacancy lifetime and h is Planck's constant). The vacancy lifetime is, in turn determined by Auger processes. In the case of Pd, this mainly involves the 5s orbital, to form an $M_{4,5}VV$ Auger process. The valence electron configuration of molecular Pd, in solution, is $4d^{10}5s^0$. However in the case of solid samples, as we move from discrete mono-metallic molecular species through to the formation of small clusters and eventually on to the bulk metal, s-d hybridisation can occur which causes a change in the electronic configuration from $4d^{10}5s^0$ to $4d^{10-\varepsilon}5s^{\varepsilon}$. This increase in 5s orbital electron density gives rise to a shorter Pd 3d vacancy lifetime and, consequently, larger FWHM.[49]

The Pd 3d high resolution spectrum is composed of a doublet peak which originates from the 3d orbital with a spin-orbital coupling energy difference of 5.26 eV[50] and area ratio of $3d_{5/2}$:$3d_{3/2}$ is 3:2 as expected from theory (see Figure 4.3). In this *Chapter*, unless otherwise stated, the $3d_{5/2}$ component is selected to ensure valid comparisons, simply because the intensity for this component is higher. The Pd $3d_{5/2}$ component in the solid sample shows a binding energy at 336.4 eV (obtained after charge corrected to the benzene carbon signal, $C_{benzene}$ 1s = 284.7 eV[51]) which indicates that the Pd is in the (0) oxidation state (see Figure 4.3(a)). The measured binding energy is consistent with values found in the literature.[50, 52] By contrast, the Pd $3d_{5/2}$ component with a binding energy at 338.4 eV measured for a solution sample in $[C_8C_1Im][BF_4]$ indicates that the Pd is in the (+2) oxidation state and the phosphineimidazolylidene palladium complex is formed in the ionic liquid, see Figure 4.3(b).

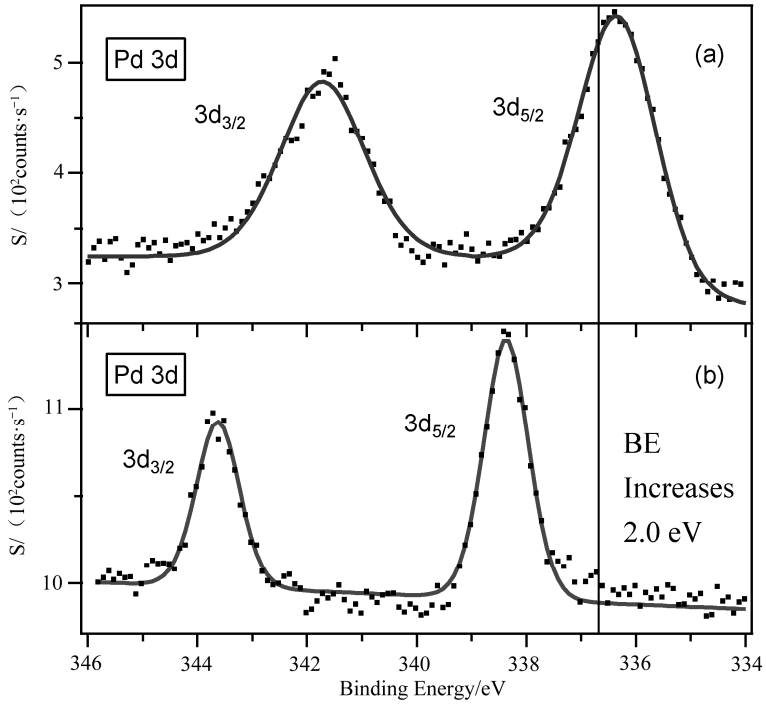

Figure 4.3 Pd 3d spectra of (a) solid $[Pd(PPh_3)_4]$, (b) the phosphineimidazolylidene palladium complex in $[C_8C_1Im][BF_4]$. The XP spectrum obtained for solid $[Pd(PPh_3)_4]$ was charge corrected to $C_{benzene}$ 1s at 284.7 eV.[51] The other XP spectrum was charge corrected by referencing to $C_{aliphatic}$ 1s at 285.0 eV

Moreover, the measured binding energy of Pd $3d_{5/2}$ for the sample of $[Pd(PPh_3)_4]$ dissolved in $[C_8Py][BF_4]$ is found to be 336.5 eV which is the same as that of solid $[Pd(PPh_3)_4]$, within the

experimental error, as shown in Figure 4.4(a). It must be noted that $[C_8C_1Pyrr][BF_4]$ is a solid at room temperature. Consequently, a similar solution sample cannot be prepared in this ionic liquid. In this section, a 1:1 mixture of $[C_8C_1Pyrr][BF_4]$/$[C_8C_1Pyrr][Tf_2N]$ is used to prepare the solution sample to ensure valid comparison. As shown in Figure 4.4(b), the binding energy of Pd $3d_{5/2}$ measured for such sample is 336.5 eV, which is also the same as that of solid $[Pd(PPh_3)_4]$, within the experimental error. As has been highlighted in *Chapter 3*, the reason why imidazolium-based ionic liquids show lower electrochemical stabilities than pyrrolidinium- and pyridinium-based analogues is mainly due to ease of removal of the C^2 proton. In pyrrolidinium- and pyridinium-based ionic liquids, since no palladium-containing ylidene complex is formed, the electronic environment of the Pd centre is left unchanged and the measured binding energy of Pd $3d_{5/2}$ is similar to that of solid $[Pd(PPh_3)_4]$. These Pd 3d binding energies, measured for different catalysts can be correlated to the catalytic performance. A closer correlation of reaction performance and XPS data could open up a new method for the design of ionic liquid-based catalytic systems.

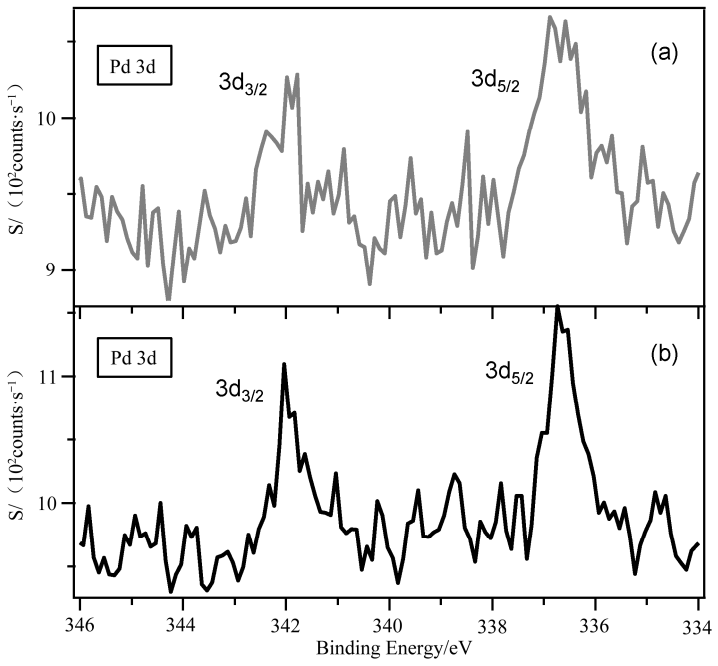

Figure 4.4 Pd 3d spectra of (a) $Pd(PPh_3)_4$ dissolved in $[C_8Py][BF_4]$ and (b) $Pd(PPh_3)_4$ dissolved in the mixture of $[C_8C_1Pyrr][BF_4]$/$[C_8C_1Pyrr][Tf_2N]$ (1:1). All XP spectra were charge corrected by referencing to $C_{aliphatic}$ 1s at 285.0 eV

4.3 Pd as a probe of solute–solvent interactions

Previous studies have suggested that cation-anion interactions can be investigated by XPS. In 2010, Cremer *et al*. showed that binding energies of cation-based components, *i.e.* C_{hetero} 1s and N_{cation} 1s could be correlated to the basicity of the anions for imidazolium-based ionic liquids.[53] In *Chapter 3*, we highlighted that the XPS signals associated with the charge carried cation-based component, *i.e.* C_{hetero} 1s/N_{cation} 1s acted as reporters of cation-anion interactions and hence a measurement of anion basicity for imidazolium- and pyrrolidinium-based ionic liquids.[39, 54] A mechanism detailed cation-anion charge transfer process was proposed and clear differences between high basicity and low basicity anions were highlighted, see *Section 3.3.1*. Here we extend this concept to investigate if XPS may be used to probe solute-solvent interactions in catalytic systems.

The effect of anion basicity on the electronic environment at the cation-based components has been investigated for five phosphineimidazolylidene palladium containing solutions, where the anions are $[OAc]^-$, Cl^-, $[BF_4]^-$, $[TfO]^-$ and $[Tf_2N]^-$ (see Figure 4.5). The measured binding energies of Pd $3d_{5/2}$ for each sample are also listed in Table 4.3.

Table 4.3 Binding Energies and FWHM of the Pd $3d_{5/2}$ peak for solid $[Pd(PPh_3)_4]$, $[Pd(PPh_3)_4]$ dissolved in $[C_8Py][BF_4]$, $[Pd(PPh_3)_4]$ dissolved in $[C_8C_1Pyrr][BF_4]$/ $[C_8C_1Pyrr][Tf_2N]$ (1:1) and the phosphineimidazolylidene palladium complexes in a range of $[C_8C_1Im]^+$-based ionic liquids (including a mixed anion system). This data is correlated to proton affinity, interaction energy and hydrogen bond acceptor ability (β). The binding energy of Pd $3d_{5/2}$ for solid $[Pd(PPh_3)_4]$ was obtained after charge corrected to $C_{benzene}$ 1s at 284.7 eV. All other peaks were charge corrected by referencing the $C_{aliphatic}$ 1s component to 285.0 eV. The error in binding energies is ± 0.1 eV

Ionic liquid Cation	Anion	Binding Energy Pd $3d_{5/2}$ / eV	FWHM / eV	Proton Affinity① /(kJ mol^{-1})	Interaction Energy② /(kJ mol^{-1})	Hydrogen Bond Acceptor Ability (β)③
	Solid Sample	336.4	1.8			

（To be continued）

Continued table

Ionic liquid Cation	Anion	Binding Energy Pd $3d_{5/2}$ / eV	FWHM / eV	Proton Affinity① /(kJ mol^{-1})	Interaction Energy② /(kJ mol^{-1})	Hydrogen Bond Acceptor Ability (β)③
$[C_8Py]^+$	$[BF_4]^-$	336.5	1.1			
$[C_8C_1Pyrr]^+$	$[BF_4]^-$:$[Tf_2N]^-$ (1:1)	336.5	1.0			
$[C_8C_1Im]^+$	$[Tf_2N]^-$	338.7	1.1	−556.6	−329.7	0.42
$[C_8C_1Im]^+$	$[TfO]^-$	338.5	0.9	−580.0	−345.6	0.57
$[C_8C_1Im]^+$	$[BF_4]^-$	338.4	1.0		−356.5	0.55
$[C_8C_1Im]^+$	Cl^-	338.2	0.8	−706.5	−369.9	0.95
$[C_8C_1Im]^+$	$[OAc]^-$	337.6	1.0	−757.9	−421.7	1.09
$[C_8C_1Im]^+$	$[Tf_2N]^-$:Cl^- (1:1)	338.4	0.9			

① data available for $[Tf_2N]^-$, $[TfO]^-$, Cl^- and $[OAc]^-$ anions[60]

② data available for $[C_2C_1Im][Tf_2N]$,[55] $[C_2C_1Im][TfO]$,[55] $[C_2C_1Im][BF_4]$,[55] $[C_4C_1Im]Cl$[62] and $[C_4C_1Im]$ $[OAc]$[67]

③ data available for $[C_4C_1Im]^+$-based $[Tf_2N]^-$[42], $[TfO]^-$[42], $[BF_4]^-$ [42], Cl^-[42] and $[OAc]^-$[43] anions

As shown in Figure 4.5, the binding energies of Pd $3d_{5/2}$ follow the trend $[OAc]^- < Cl^- < [BF_4]^- \sim [TfO]^- < [Tf_2N]^-$. The lower binding energy corresponds to a more electron rich cation head group, *i.e.* palladium centre, which indicates that more charge has been transferred from the anion to the palladium centre for the high basicity anions, such as $[OAc]^-$. These results are in good agreement with those for pure imidazolium- and pyrrolidinium-based ionic liquids.[30, 39]

Based upon the huge difference in catalytic performance between $[Pd(PPh_3)_4]$ and the phosphineimidazolylidene palladium complex generated in the $[BF_4]^-$-based ionic liquid, it is expected that, in the Suzuki cross coupling reaction, a more electron poor palladium centre would be more catalytically active. Such a correlation between XPS data and catalytic reaction performance makes it possible for the design of metal-based catalytic systems. This is discussed in more detail in *Section 4.6*.

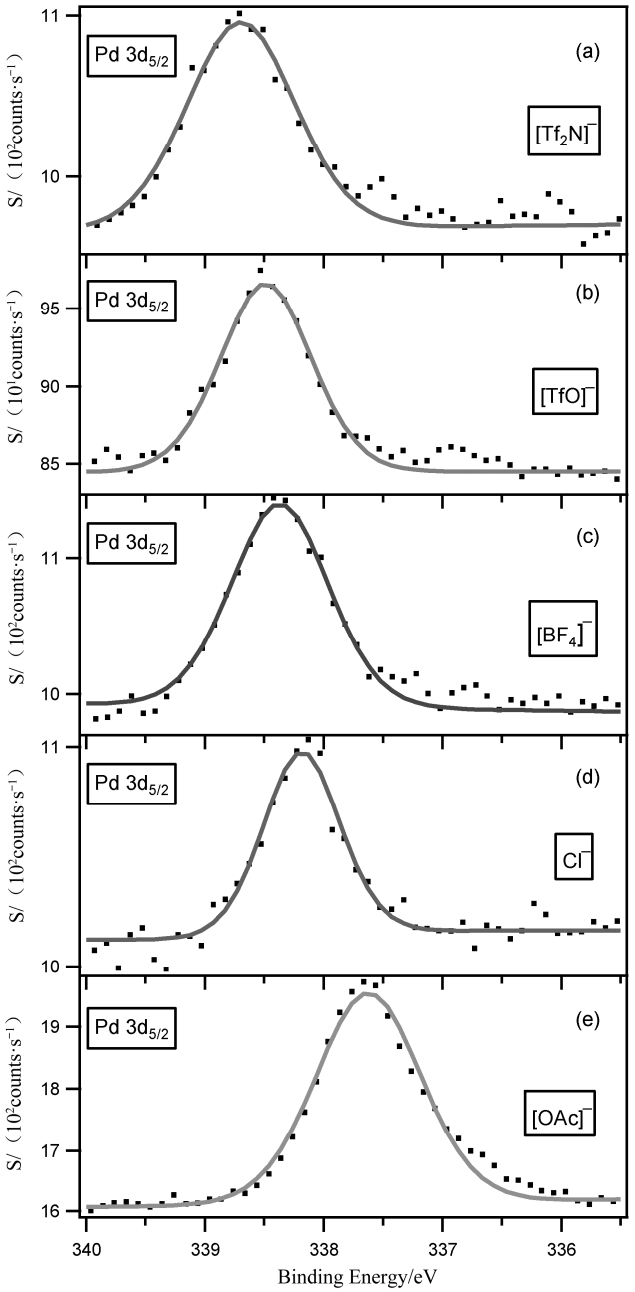

Figure 4.5 XP spectra of Pd $3d_{5/2}$ for phosphineimidazolylidene palladium complexes in a range of $[C_8C_1Im]^+$-based ionic liquids, (a) $[Tf_2N]^-$ (b) $[TfO]^-$ (c) $[BF_4]^-$ (d) Cl^- and (e) $[OAc]^-$. All XP spectra were charge corrected by referencing the $C_{aliphatic}$ 1s component to 285.0 eV

4.4 Selection of anions: correlation of binding energy to established metrics

Intermolecular interactions are one of the key factors, which determine the structure[55, 56] and properties of ionic liquids, *e.g.* viscosity and conductivity.[57] Based upon such a correlation, the selection of a specific anion for a particular task is preceded by considering the delivery of a liquid that can provide the desired physico-chemical properties. However, in terms of quantifying such a selection process, it has to revolve around the prediction of the cation-anion interaction.

Charge distribution and ion pair availability is intrinsic to the formation of hydrogen-bonded networks involving both the cation and solute components. The direct quantification of these interactions in the case of a single specific ion is not straightforward. Indeed, a number of metrics have been proposed including proton affinity, dissociation energy and interaction energies, all of which are based upon semi-empirical, single molecule calculations, which omit multi-point interactions.

The delocalisation of negative charge within anions is inherent to the formation of hydrogen-bonded networks surrounding both the cation and, in turn, the solute. To date, a number of metrics have been proposed aiming to examine the degree of delocalisation, such as dissociation energy[56, 58, 59] and proton affinity.[60, 61]

According to proton affinities (see Figure 4.6), the degree of charge delocalisation for different anions follows this trend, $[OAc]^- < Cl^- < [TfO]^- < [Tf_2N]^-$. Interestingly, the measured Pd $3d_{5/2}$ binding energies for the palladium-containing ylidene complexes in these four ionic liquids follow the same trend.

It must be noted that a valid value is not available for the $[BF_4]^-$ anion. However, the similar correlation can be made to the dissociation energies calculated by Hunt *et al.*[56] The dissociation energies available for $[C_8C_1Im]Cl$, $[C_8C_1Im][BF_4]$ and $[C_8C_1Im][Tf_2N]$ follow the trend $[C_8C_1Im]Cl < [C_8C_1Im][BF_4] < [C_8C_1Im][Tf_2N]$. The strength of the interactions depends upon the delocalisation of the negative charge. For an anion which shows lower negative charge delocalisation, *e.g.* Cl^-, strong networks will form around the cation head group; whilst weak and

disordered networks surround the cation head group in the case of anions with a higher negative charge delocalisation such as $[Tf_2N]^-$. It is found that the negative charge delocalisation of $[BF_4]^-$ lies between Cl^- and $[Tf_2N]^-$, according to the dissociation energy values. The measured binding energies of Pd $3d_{5/2}$ for the palladium-containing ylidene complexes in these three ionic liquids follow the same trend.

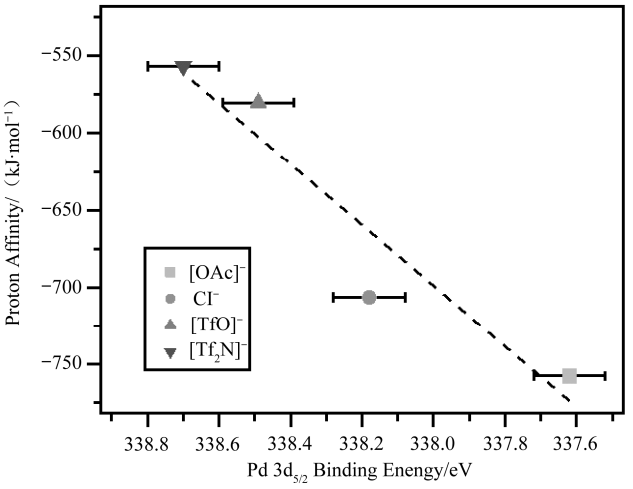

Figure 4.6 Pd $3d_{5/2}$ binding energies for phosphineimidazolylidene palladium complexes in different $[C_8C_1Im]^+$-based ionic liquids compared with proton affinity. All binding energies obtained were charge corrected by referencing the $C_{aliphatic}$ 1s component to 285.0 eV. It must be noted that the experimental error associated with the XPS measurement is of the order ± 0.1 eV

The intermolecular interaction energy has been obtained for a variety of ionic liquids.[55, 62] According to the available literature values, $[Tf_2N]^-$ has the largest interaction energies; $[OAc]^-$ and Cl^- the lowest, with $[TfO]^-$ and $[BF_4]^-$ in between. This can be used to explain the deviation in measured binding energies of Pd $3d_{5/2}$ for palladium-containing ylidene complexes in different cation-anion combinations. The intermolecular interaction energy values (see Figure 4.7) of these five ionic liquids follow the same sequence as the measured binding energies of Pd $3d_{5/2}$ for palladium-containing ylidene complexes in these ionic liquids.

The correlation, indeed between binding energy and simulated neutral ion pair (NIP) metrics, *i.e.* proton affinity and interaction energy, provides a method to predict the interaction between the metal centre and ionic liquids. However, those simulated NIP metrics do not include multi-point interactions and consequently can not reflect real experimental systems.

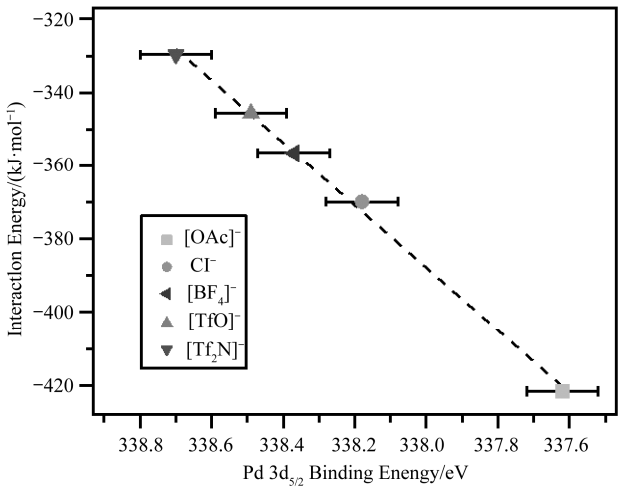

Figure 4.7 Pd $3d_{5/2}$ binding energies for phosphineimidazolylidene palladium complexes in different $[C_8C_1Im]^+$-based ionic liquids compared with interaction energy. All binding energies obtained were charge corrected by referencing the $C_{aliphatic}$ 1s component to 285.0 eV. It must be noted that the experimental error associated with the XPS measurement is of the order ± 0.1 eV

Kamlett-Taft parameters provide information about the interactions within a solvent and therefore describe liquid phase properties of ionic liquids. In the literature, the Kamlett-Taft hydrogen bond acceptor ability (β) has been used to indicate the basicity of the corresponding anions of ionic liquids. β was found to follow the trend $[Tf_2N]^- < [TfO]^- \sim [BF_4]^- < Cl^- < [OAc]^-$.[42, 43] This observation is in good agreement with the trend of measured binding energies of Pd $3d_{5/2}$ for palladium-containing ylidene complexes in the corresponding pure ionic liquids, see Figure 4.8. Such an observation confirmed the conclusion highlighted in *Section 3.3.2,* the basicity of the anions can influence the measured binding energies obtained for the cation-based components.[30, 39]

It can be concluded that the electronic environment of the palladium centre can be tuned by manipulating the basicity of the anion. In *Chapter 3*, we highlighted that the electronic environment of cation-based components can be designed by simply varying the amounts of different anions of a mixture. If it is also true for the palladium-containing ylidene complex, the ionic liquid mixture would find application in terms of generating the desired electronic environment of the palladium centre in the solvent.

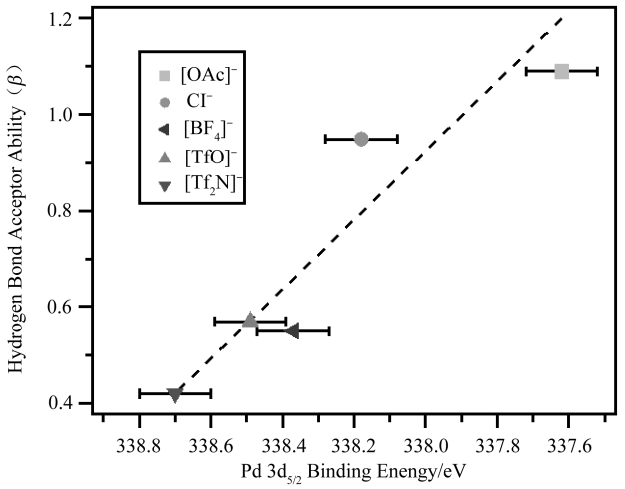

Figure 4.8 Pd $3d_{5/2}$ binding energies for phosphineimidazolylidene palladium complexes in different $[C_8C_1Im]^+$-based ionic liquids compared with hydrogen bond acceptor ability (β). All binding energies obtained were charge corrected by referencing the $C_{aliphatic}$ 1s component to 285.0 eV. It must be noted that the experimental error associated with the XPS measurement is of the order ± 0.1 eV

4.5 Can the solvent environment be tuned?

XPS has been used to study ionic liquid mixtures for both elemental composition[63] and subtle changes in binding energy.[39-41] Indeed the tunability of ionic liquids is one of the most interesting topics.[64] To properly understand the properties of ionic liquid mixtures will find application on selection of the most suitable ionic liquid for a specific task.[65, 66] Here we analysed the phosphineimidazolylidene palladium complex, as a solution in a mixture of $[C_8C_1Im]Cl$ and $[C_8C_1Im][Tf_2N]$ (1:1). The difference in basicity for the two anions is sufficiently large that the difference between the measured binding energies of Pd $3d_{5/2}$ is larger than the error of the experiment.

The high resolution spectrum of Pd $3d_{5/2}$ for the solute in the ionic liquid mixture is presented in Figure 4.9(b). At first glance, the XP spectrum for the solute in the mixture is different to the spectra obtained for the solute in both of the corresponding pure ionic liquids (see Figures 4.9(a) and (c)). A single, well-resolved Pd $3d_{5/2}$ peak with a FWHM of 0.9 eV can be observed. It should be noted that the FWHM for the solute in the two corresponding pure ionic liquids, $[C_8C_1Im]Cl$

and $[C_8C_1Im][Tf_2N]$, are 0.8 eV and 1.0 eV respectively. If the spectrum was simply an overlap of both of the spectra for the solute in the corresponding pure ionic liquids, *i.e.* if the solution was composed of discrete pockets of both ionic liquids, we would expect to observe an XP spectrum with a broad, partially resolved envelope. Even in the case where resolution of the two components cannot be achieved, an increase in the FWHM should be observed. It is clear from the data in this *Section* that such discrete pockets are not formed. The solute is surrounded by both corresponding anions in the mixture and therefore experiences a new solution environment which is characteristic of the weighting of the two corresponding pure ionic liquids employed.

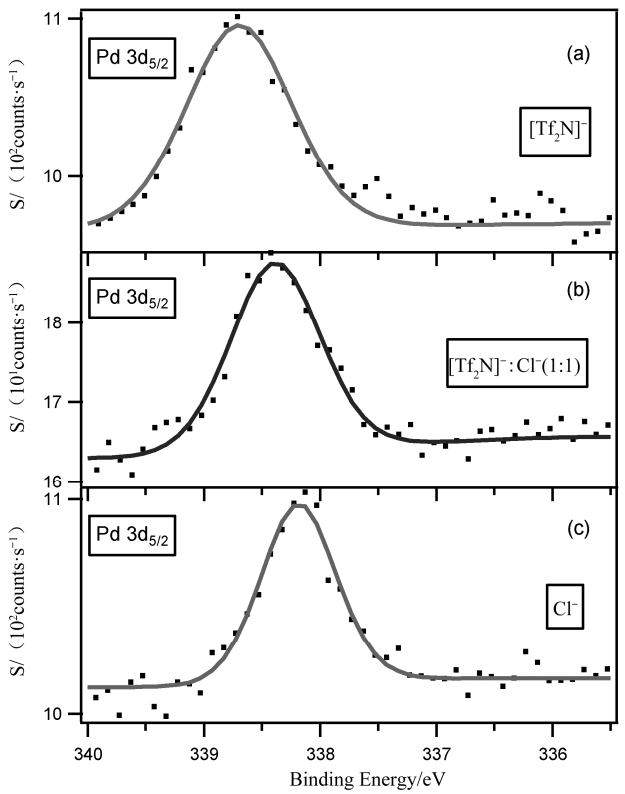

Figure 4.9 XP spectra of Pd $3d_{5/2}$ for phosphineimidazolylidene palladium complexes in a range of $[C_8C_1Im]^+$-based ionic liquids (including a mixed anion system), (a) $[Tf_2N]^-$ (b) $[Tf_2N]^-$:Cl^- (1:1) and (c) Cl^-. All XP spectra were charge corrected by referencing the $C_{aliphatic}$ 1s component to 285.0 eV

Moreover, the measured binding energy of Pd $3d_{5/2}$ for the solute in the mixture is found to be 338.4 eV which lies in between those obtained for the solute in both of the corresponding pure ionic liquids, 338.2 eV and 338.7 eV for $[C_8C_1Im]Cl$ and $[C_8C_1Im][Tf_2N]$ respectively (see Table 4.3 and Table 4.4). This obseivation shows good agreement with those obtained for simple

imidazolium- and pyrrolidinium-based ionic liquid mixtures.[30, 39] We can conclude that the cation head group, *i.e.* the palladium centre, is surrounded by both Cl^- and $[Tf_2N]^-$, not pockets of the cation and one type of anion, with other pockets of the cation and the other anion.[60]

The results shown in this section indicate that the electronic environment of the cation-based component can be tuned to a desired value by simply varying the amounts of different anions of a mixture, as anion can significantly influence the electronic environment of the cation head group. This knowledge can be used to design the metal centre of a catalyst with a desired binding energy, in particular by using the appropriate mixture of different anions. This subject has often been suggested but until now not achieved experimentally. However, the catalytic activity of the palladium centre in ionic liquid mixtures, in particular compared to simple pure ionic liquids, still needs to be further investigated and debated, this is investigated in *Section 4.6.3*.

Table 4.4 Binding Energies of all elements for $[Pd(PPh_3)_4]$ dissolved in $[C_8Py][BF_4]$, $[Pd(PPh_3)_4]$ dissolved in $[C_8C_1Pyrr][BF_4]/[C_8C_1Pyrr][Tf_2N]$ (1:1) and the phosphineimidazolylidene palladium complexes in a range of $[C_8C_1Im]^+$-based ionic liquids (including a mixed anion system). All XP spectra were charge corrected by referencing the $C_{aliphatic}$ 1s component to 285.0 eV. It must be noted that the experimental error associated with measurement of binding energies is ± 0.1 eV

Ionic Liquid		Binding Energy / eV												
Cation	Anion	Pd $3d_{5/2}$	$C_{aliphatic}$ 1s	C^2 1s (C_{hetero})	$C^{4,5}$ 1s	$C^{6,7}$ 1s (C_{inter})	N_{cation} 1s	C_{CF3} 1s	N_{anion} 1s	O 1s	F 1s	S $2p_{3/2}$	B 1s	Cl $2p_{3/2}$
$[C_8Py]^+$	$[BF_4]^-$	336.5	285.0	286.9		286.0	402.4				686.0		194.2	
$[C_8C_1Pyrr]^+$	$[BF_4]^-$:$[Tf_2N]^-$	336.5	285.0	286.7		285.6	402.6	292.9	399.5	532.7	688.9	168.9	194.2	
	(1:1)										686.0			
$[C_8C_1Im]^+$	$[Tf_2N]^-$	338.7	285.0	287.7	287.0	286.4	402.1	292.8	399.5	532.6	688.8	168.9		
$[C_8C_1Im]^+$	$[TfO]^-$	338.5	285.0	287.6	286.9	286.4	402.0			532.0	688.5	168.4		
$[C_8C_1Im]^+$	$[BF_4]^-$	338.4	285.0	287.6	286.9	286.4	402.0				686.0		194.2	
$[C_8C_1Im]^+$	Cl^-	338.2	285.0	287.2	286.6	286.0	401.6							197.0
$[C_8C_1Im]^+$	$[OAc]^-$	337.6	285.0	287.4	286.6	286.0	401.6			530.3				
$[C_8C_1Im]^+$	$[Tf_2N]^-$:Cl^-(1:1)	338.4	285.0	287.6	286.9	286.3	401.9	292.9	399.5	532.6	688.9	168.9		197.1

4.6 Can anion basicity impact on the reaction rate?

As mentioned previously, the Suzuki cross coupling reaction has been widely studied,

employing ionic liquids as reaction media.[2, 3, 6, 68-72] Switching from traditional organic solvents to ionic liquids can give rise to a dramatic increase in reaction rate due to the formation of a new, more reactive palladium-containing ylidene complex.[2, 6] XPS of ionic liquid-based solutions offers a unique opportunity to probe this process and investigate the influence of the anion chemistry.[41, 73]

In this section, we investigate the impact of anion basicity on the tuning of a catalytic system. In principle, such data could inform the systematic design of a new, more active catalyst which will deliver high productivity in terms of reaction rate or selectivity. We report a simple palladium catalysed Suzuki crossing coupling reaction, processed in ionic liquids, see Scheme 4.1.

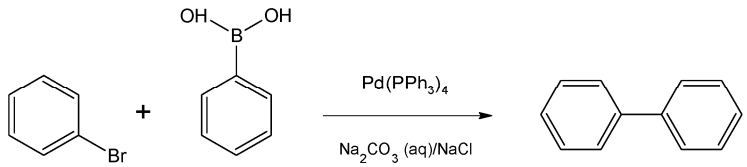

Scheme 4.1 Suzuki cross coupling reaction of bromobenzene and benzeneboronic acid

4.6.1 Suzuki cross coupling reaction

A mixture of NaCl (38 mg, 0.67 mmol), phenylboronic acid (0.58 g, 4.76 mmol) and $[Pd(PPh_3)_4]$ (5.5 mg, 4.76×10^{-3} mmol) in $[C_8C_1Im][BF_4]$ (2 ml) was stirred at 110 ℃. Into this mixture, a solution of Na_2CO_3 (83 mg, 0.783 mmol) in water (3 ml) and bromobenzene (0.5 ml, 4.76 mmol) were injected. The reaction was allowed to proceed at 110℃ for 10 min. Immediately after this time, the mixture was cooled using liquid nitrogen to stop reaction. The same procedure was carried out for $[C_8C_1Im][Tf_2N]$, $[C_8C_1Im][OAc]$ as well as the mixture of $[C_8C_1Im]$ $[Tf_2N]$ and $[C_8C_1Im]Cl$ (1:1).

4.6.2 Correlation of binding energy with reaction rate

The reaction conversion (Conv.) in all cases was monitored by ^1H NMR. The proton signals from both of the starting materials and the product show similar chemical shift (δ), between 7.65 and 7.15 ppm. However, the two ortho-protons within phenylboronic acid show higher δ at around 8.00 ppm, as shown in Figure 4.10, and can be easily integrated to quantify the conversion.

The reaction conversion calculated by integrating the desired ^1H NMR peaks was

consequently used to calculate the *Turnover of Frequency* (TOF) of the reaction. It was given by Eq.(4.1).

$$\mathrm{TOF} = \frac{\text{mol of starting material converted}}{\text{mol of catalyst} \cdot t} = \frac{\text{conversion}}{0.1\,\% \cdot t} \qquad (4.1)$$

It must be noted that the TOF was given by assuming that no side reaction was carried out during the reaction, and thus the starting materials will only be converted to the desired product. NMR spectroscopy suggests that this assumption is valid as all observed peaks can be assigned to the starting materials, product or the solvent.

Moreover, as concluded earlier, the measured binding energies of Pd $3d_{5/2}$ for the phosphineimidazolylidene palladium complexes in different ionic liquids follow a trend. In this *Section*, three ionic liquids, with different basicity of anions, $[C_8C_1Im]$ $[Tf_2N]$, $[C_8C_1Im]$ $[BF_4]$ and $[C_8C_1Im][OAc]$, were selected as the reaction solvents. This is mainly because the basicity of these three anions are significantly different, *i.e.* $[Tf_2N]^-$ is the least basic anion whilst $[OAc]^-$ the most basic anion with $[BF_4]^-$ lying in between. A mixture of $[C_8C_1Im][Tf_2N]$ and $[C_8C_1Im]Cl$ (1:1) was also employed as the reaction solvent. The reaction rates are shown in Table 4.5.

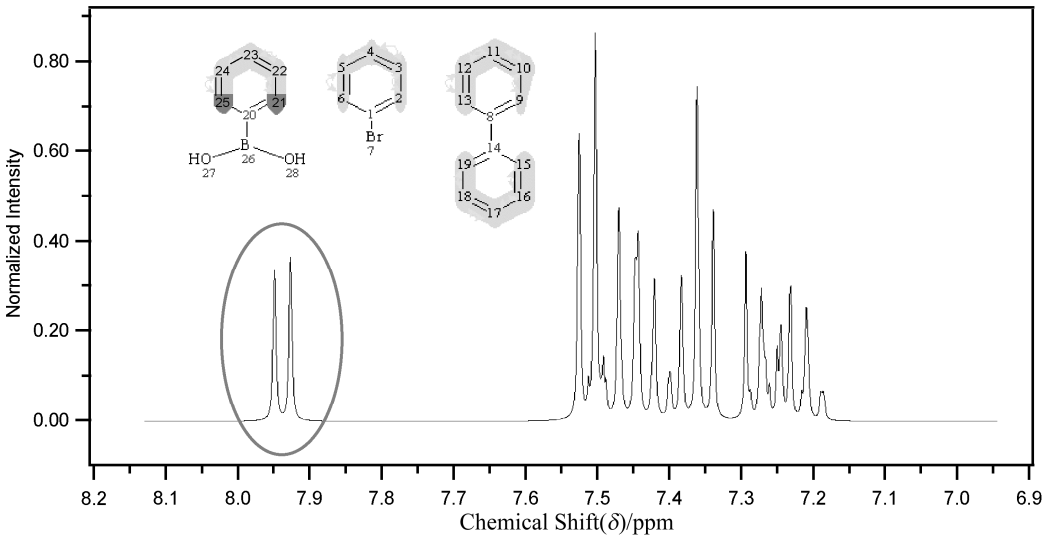

Figure 4.10 ^{1}H NMR spectrum for the mixture of starting materials and product for Suzuki reaction conducted in this section

Table 4.5 [$Pd(PPh_3)_4$] catalysed Suzuki cross coupling reaction of bromobenzene and benzeneboronic acid in ionic liquids①

Ionic Liquids	Pd[mol %]	Pd $3d_{5/2}$ BindingEnergy / eV	Conv.②/ %	TOF / h^{-1}
$[C_8C_1Im][Tf_2N]$	0.1	338.7	64.1	3845
$[C_8C_1Im][BF_4]$	0.1	338.4	56.4	3384
$[C_8C_1Im][OAc]$	0.1	337.6	32.9	1973
$[C_8C_1Im][Tf_2N]$:$[C_8C_1Im]Cl$ (1:1)	0.1	338.4	48.7	2923

①reaction conditions: 110℃, 10 mins, 0.1 mol % $[Pd(PPh_3)_4]$, 13.5 mol % NaCl, 2 equiv $NaCO_3$ (aq)

②conversion calculated based upon ^1H NMR data

The measured binding energy of Pd $3d_{5/2}$ for the palladium-containing ylidene complex in $[C_8C_1Im][Tf_2N]$ is found to be 338.7 eV, which is higher than any other binding energy obtained for the palladium centre in corresponding ionic liquids. The reaction rate monitored for this Suzuki cross coupling reaction, in $[C_8C_1Im][Tf_2N]$, is also the largest which confirms that, for such a catalytic system, a more electron poor palladium centre is more catalytically active. The less basic the anion, the more electron poor the palladium centre, and thus the faster the reaction. The opposite is also true in the case of higher basicity anions, *e.g.* $[C_8C_1Im][OAc]$. In the case of $[C_8C_1Im][BF_4]$, since the basicity of $[BF_4]^-$ lies in between $[Tf_2N]^-$ and $[OAc]^-$, the monitored reaction rate in this ionic liquid was also found to be in the middle of those obtained for $[Tf_2N]^-$ and $[OAc]^-$.

It must be noted that due to the formation of HF in the $[C_8C_1Im][BF_4]$, the catalytic activity of the Pd centre in such ionic liquid may be influenced. In this section, such influence on the measured TOF was ignored. However, for future work, it is worth to investigate the method aiming to minimise the effect of HF on the catalytic reaction rate.

The conclusion can then be made that, in this Suzuki cross coupling reaction, a more electron poor palladium centre is more catalytically active and thus gives rise to a faster reaction. Figure 4.11 shows the correlation between the measured binding energy of Pd $3d_{5/2}$ for the palladium-containing ylidene complex with the TOF. Although insufficient data has been available to quantify the effect of binding energy on the reaction rate, this is the first time that we have successfully correlated binding energy to reaction rate, which could allow us to specifically design a metal catalytic system to enhance catalytic reaction.

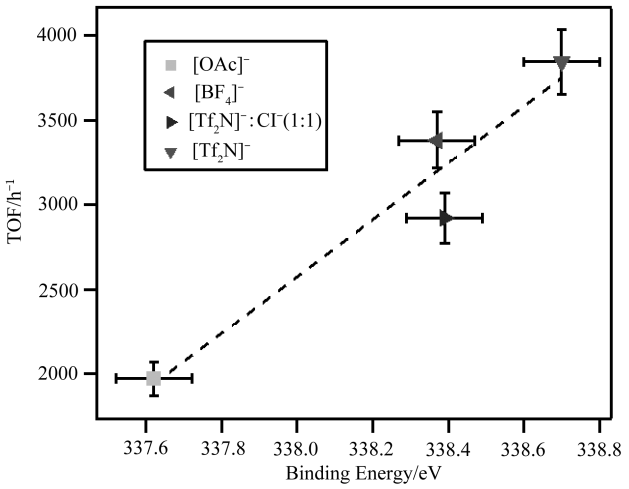

Figure 4.11 Correlation of reaction rate to Pd $3d_{5/2}$ binding energy for a Suzuki cross coupling reaction

4.6.3 The catalytic activity of the palladium centre in ionic liquid mixture

It has been highlighted in *Section 4.5* that the measured binding energy of Pd $3d_{5/2}$ for the palladium-containing ylidene complex in the mixture of $[C_8C_1Im][Tf_2N]$: $[C_8C_1Im]Cl$ (1:1) is 338.4 eV which is the same as that of the palladium-containing ylidene complex in $[C_8C_1Im][BF_4]$. As predicted, a similar electronic environment of the palladium centre will probably give rise to a similar catalytic activity in such a Sukuzi cross coupling reaction. The monitored TOFs are 3384 h^{-1} and 2923 h^{-1} in $[C_8C_1Im][BF_4]$ and the mixture of $[C_8C_1Im][Tf_2N]$:$[C_8C_1Im]Cl$ (1:1), respectively. Taking into account the experimental error associated with the measurement of binding energies, which is ± 0.1 eV, as well as the error with integrated ^1H NMR peak area, which is ± 5%, these data fit the trend very well (see Figure 4.11). It indicates that the palladium centre in ionic liquid mixture has the similar catalytic activity compared to that of simple pure ionic liquid.

4.7 Conclusions

We have successfully measured the XP spectra of a range of phosphineimidazolylidene palladium complexes in different ionic liquids. A comparison of the binding energies obtained for solid $[Pd(PPh_3)_4]$ and phosphineimidazolylidene palladium complex, in $[C_8C_1Im][BF_4]$, revealed a significant difference. The palladium centre in the phosphineimidazolylidene palladium complex

was found to be more electron poor, which could be correlated to reaction rate and thus allow the improvement of a particular ionic liquid-based homogeneous catalytic system. Moreover, the binding energies of Pd $3d_{5/2}$ measured for $[Pd(PPh_3)_4]$ dissolved in $[C_8Py][BF_4]$ and $[C_8C_1Pyrr][BF_4]$/ $[C_8C_1Pyrr][Tf_2N]$ (1:1) are the same as that of the solid $[Pd(PPh_3)_4]$. This observation further confirmed that the Pd (II) centre was not formed in pyrrolidinium- and pyridinium-based ionic liquids.

Comparisons of charge corrected binding energies of Pd 3d for the phosphineimidazolylidene palladium complexes, when the anion is varied, were carried out. The binding energy for Pd $3d_{5/2}$ decreases as the basicity of the anion increases, indicating that more charge is transferred from the anion to the cation for higher basicity anions such as C^- and $[OAc]^-$.

The Pd $3d_{5/2}$ binding energies measured for different ionic liquid solutions could be correlated to proton affinity, interaction energy and β. It has been found that the measured binding energies for palladium-containing ylidene complexes in different ionic liquids are proportional to the values of proton affinities and β for the corresponding anions, as well as the cation-anion interaction energies for the corresponding pure ionic liquids.

Mixtures of anions can be used to tune the electronic environ ment of the palladium centre within the phosphineimidazolylidene cation. The tuned electronic environment of the palladium centre with anion mixture can posses the similar catalytic activity to that of single anion.

References

[1] WELTON T. Room-temperature ionic liquids. Solvents for synthesis and catalysis[J]. Chemical Reviews，1999，99(8): 2071-2083.

[2] YANG C，TAI C，HUANG Y，et al. Ionic liquid promoted palladium-catalyzed Suzuki cross-couplings of N-contained heterocyclic chlorides with naphthaleneboronic acids[J]. Tetrahedron，2005，61(20): 4857-4861.

[3] XU L，CHEN W，XIAO J. Heck reaction in ionic liquids and the in situ identification of N-heterocyclic carbene complexes of palladium[J]. Organometallics，2000，19(6): 1123-1127.

[4] CLEMENT N D，ROUTABOUL L，GROTEVENDT A，et al. Development of palladium-carbene catalysts for telomerization and dimerization of 1,3-dienes: From basic research to

industrial applications[J]. Chemistry-a European Journal，2008，14(25): 7408-7420.

[5] MCGUINNESS D. Alkene oligomerisation and polymerisation with metal-NHC based catalysts[J]. Dalton Transactions，2009(35): 6915-6923.

[6] MATHEWS C J，SMITH P J，WELTON T. Palladium catalysed Suzuki cross-coupling reactions in ambient temperature ionic liquids[J]. Chemical Communications，2000(14): 1249-1250.

[7] HANNIG F，KEHR G，FROHLICH R，et al. Formation of chiral ionic liquids and imidazol-2-ylidene metal complexes from the proteinogenic aminoacid L-histidine[J]. Journal of Organometallic Chemistry，2005，690(24-25): 5959-5972.

[8] TALISMAN I J，KUMAR V，RAZZAGHY J，et al. O-Glycosidation reactions promoted by in situ generated silver N-heterocyclic carbenes in ionic liquids[J]. Carbohydrate Research，2011，346(7): 883-890.

[9] OKAMOTO M，YAMAMOTO Y，SAKAGUCHI S. A new approach to switching of enantioselectivity in NHC-Cu-catalyzed conjugate addition of alkylzincs to cyclic enones[J]. Chemical Communications，2009(47): 7363-7365.

[10] DEUTSCH C，LIPSHUTZ B H，KRAUSE N. (NHC)CuH-Catalyzed Entry to Allenes via Propargylic Carbonate SN_2-Reductions[J]. Organic Letters，2009，11(21): 5010-5012.

[11] MCGUINNESS D S，CAVELL K J，YATES B F. Unprecedented C-H bond oxidative addition of the imidazolium cation to Pt-0: a combined density functional analysis and experimental study[J]. Chemical Communications，2001(4): 355-356.

[12] TAIGE M A，AHRENS S，STRASSNER T. Platinum(II)-bis-(N-heterocyclic carbene) complexes: synthesis，structure and catalytic activity in the hydrosilylation of alkenes[J]. Journal of Organometallic Chemistry，2011，696(17): 2918-2927.

[13] BITTERMANN A，HERDTWECK E，HARTER P，et al. Rhodium(I)，a Carbene-Transfer Transition-Metal Ion and a Synthetic Route to Symmetrical and Asymmetrical Substituted trans-RhCl(CO)(NHC)(NHC) Complexes[J]. Organometallics，2009，28(24): 6963-6968.

[14] GONZALEZ I，PLA-QUINTANA A，ROGLANS A. Rhodium N-Heterocyclic Carbene Complexes as Effective Catalysts for [2+2+2]-Cycloaddition Reactions[J]. Synlett，2009(17): 2844-2848.

[15] HINTERMAIR U，GUTEL T，SLAWIN A M Z，et al. Direct in situ synthesis of cationic N-heterocyclic carbene iridium and rhodium complexes from neat ionic liquid: Application in catalytic dehydrogenation of cyclooctadiene[J]. Journal of Organometallic Chemistry，

2008，693(14): 2407-2414.

[16] NICHOL G S，RAJASEELAN J，ANNA L J，et al. N-Heterocyclic Carbene Complexes of Rhodium and Iridium: Steric Effects on Molecular Conformation[J]. European Journal of Inorganic Chemistry，2009(28): 4320-4328.

[17] MATHEWS C J，SMITH P J，WELTON T，et al. In situ formation of mixed phosphine-imidazolylidene palladium complexes in room-temperature ionic liquids[J]. Organometallics，2001，20(18): 3848-3850.

[18] HAUWERT P，BOERLEIDER R，WARSINK S，et al. Mechanism of Pd(NHC)-Catalyzed Transfer Hydrogenation of Alkynes[J]. Journal of the American Chemical Society，2010，132(47): 16900-16910.

[19] BROWN R J C，DYSON P J，ELLIS D J，et al. 1-Butyl-3-methylimidazolium cobalt tetracarbonyl [bmim][$Co(CO)_4$]: a catalytically active organometallic ionic liquid[J]. Chemical Communications，2001(18): 1862-1863.

[20] ZHONG C M，SASAKI T，TADA M，et al. Ni ion-containing ionic liquid salt and Ni ion-containing immobilized ionic liquid on silica: Application to Suzuki cross-coupling reactions between chloroarenes and arylboronic acids[J]. Journal of Catalysis，2006，242(2): 357-364.

[21] SILVA S M，BRONGER R P J，FREIXA Z，et al. High pressure infrared and nuclear magnetic resonance studies of the rhodium-sulfoxantphos catalysed hydroformylation of 1-octene in ionic liquids[J]. New Journal of Chemistry，2003，27(9): 1294-1296.

[22] WEBER C F，VAN ELDIK R. Influence of solvent on ligand-substitution reactions of Pt-II complexes as function of the pi-acceptor properties of the spectator chelate[J]. European Journal of Inorganic Chemistry，2005(23): 4755-4761.

[23] KUCHEROV A V，VASNEV A V，GREISH A A，et al. Catalytically active species in new metathesis systems [Wn+(Mon+)-ionic liquid-olefin]: A quantitative ESR study[J]. Journal of Molecular Catalysis a-Chemical，2005，237(1-2): 165-171.

[24] CREMER T，KILLIAN M，GOTTFRIED J M，et al. Physical Vapor Deposition of [EMIM][Tf_2N]: A New Approach to the Modification of Surface Properties with Ultrathin Ionic Liquid Films[J]. Chemphyschem，2008，9(15): 2185-2190.

[25] BOKMAN F，BOHMAN O，SIEGBAHN H O G. Esca Studies Of Phase-Transfer Catalysts In Solution .2. Surface Ion-Pairing and Salting-Out Effects[J]. Journal of Physical Chemistry，1992，96(5): 2278-2283.

[26] WINTER B，FAUBEL M. Photoemission from liquid aqueous solutions[J]. Chemical Reviews，2006，106(4): 1176-1211.

[27] LOVELOCK K R J，VILLAR-GARCIA I J，MAIER F，et al. Photoelectron Spectroscopy of Ionic Liquid-Based Interfaces[J]. Chemical Reviews，2010，110(9): 5158-5190.

[28] CREMER T，KOLBECK C，LOVELOCK K R J，et al. Towards a Molecular Understanding of Cation-Anion Interactions-Probing the Electronic Structure of Imidazolium Ionic Liquids by NMR Spectroscopy，X-ray Photoelectron Spectroscopy and Theoretical Calculations[J]. Chemistry-a European Journal，2010，16(30): 9018-9033.

[29] KOLBECK C，NIEDERMAIER I，TACCARDI N，et al. Monitoring of Liquid-Phase Organic Reactions by Photoelectron Spectroscopy[J]. Angewandte Chemie-International Edition，2012，51(11): 2610-2613.

[30] VILLAR-GARCIA I J，SMITH E F，TAYLOR A W，et al. Charging of ionic liquid surfaces under X-ray irradiation: the measurement of absolute binding energies by XPS[J]. Physical Chemistry Chemical Physics，2011，13(7): 2797-2808.

[31] MAIER F，GOTTFRIED J M，ROSSA J，et al. Surface enrichment and depletion effects of ions dissolved in an ionic liquid: an X-ray photoelectron spectroscopy study[J]. Angewandte Chemie-International Edition，2006，45(46): 7778-7780.

[32] KOLBECK C，PAAPE N，CREMER T，et al. Ligand Effects on the Surface Composition of Rh-Containing Ionic Liquid Solutions Used in Hydroformylation Catalysis[J]. Chemistry-a European Journal，2010，16(40): 12083-12087.

[33] LOVELOCK K R J. Influence of the ionic liquid/gas surface on ionic liquid chemistry[J]. Physical Chemistry Chemical Physics，2012，14(15): 5071-5089.

[34] PAAPE N，WEI W，BOSMANN A，et al. Chloroalkylsulfonate ionic liquids by ring opening of sultones with organic chloride salts[J]. Chemical Communications，2008(33): 3867-3869.

[35] TACCARDI N，NIEDERMAIER I，MAIER F，et al. Cyclic Thiouronium Ionic Liquids: Physicochemical Properties and their Electronic Structure Probed by X-Ray Induced Photoelectron Spectroscopy[J]. Chemistry-a European Journal，2012，18(27): 8288-8291.

[36] QIU F，TAYLOR A W，MEN S，et al. An ultra high vacuum-spectroelectrochemical study of the dissolution of copper in the ionic liquid (N-methylacetate)-4-picolinium bis (trifluoromethylsulfonyl)imide[J]. Physical Chemistry Chemical Physics，2010，12(8): 1982-1990.

[37] TAYLOR A W，QIU F，VILLAR-GARCIA I J，et al. Spectroelectrochemistry at ultrahigh vacuum: in situ monitoring of electrochemically generated species by X-ray photoelectron spectroscopy[J]. Chemical Communications，2009(39): 5817-5819.

[38] TAYLOR A W，MEN S，CLARKE C J，et al. Acidity and basicity of halometallate-based ionic liquids from X-ray photoelectron spectroscopy[J]. Rsc Advances，2013，3(24): 9436-9445.

[39] MEN S，LOVELOCK K R J，LICENCE P. X-ray Photoelectron Spectroscopy of Pyrrolidinium-Based Ionic Liquids: Cation-Anion Interactions and a Comparison to Imidazolium-Based Analogues[J]. Physical Chemistry Chemical Physics，2011，13(33): 15244-15255.

[40] MEN S，MITCHELL D S，LOVELOCK K R J，et al. X-ray Photoelectron Spectroscopy of Pyridinium-Based Ionic Liquids: Comparison to Imidazolium- and Pyrrolidinium-Based Analogues[J]. Chemphyschem，2015，16(10): 2211-2218.

[41] VILLAR-GARCIA I J，LOVELOCK K R J，MEN S，et al. Tuning the electronic environment of cations and anions using ionic liquid mixtures[J]. Chemical Science，2014，5(6): 2573-2579.

[42] LUNGWITZ R，STREHMEL V，SPANGE S. The dipolarity/polarisability of 1-alkyl-3-methylimidazolium ionic liquids as function of anion structure and the alkyl chain length[J]. New Journal of Chemistry，2010，34(6): 1135-1140.

[43] PALGUNADI J，HONG S Y，LEE J K，et al. Correlation between Hydrogen Bond Basicity and Acetylene Solubility in Room Temperature Ionic Liquids[J]. Journal of Physical Chemistry B，2011，115(5): 1067-1074.

[44] WAGNER C D，DAVIS L E，ZELLER M V，et al. Empirical Atomic Sensitivity Factors for Quantitative-Analysis by Electron-Spectroscopy for Chemical-Analysis[J]. Surface and Interface Analysis，1981，3(5): 211-225.

[45] MAIER F，GOTTFRIED J M，ROSSA J，et al. Surface enrichment and depletion effects of ions dissolved in an ionic liquid: an X-ray photoelectron spectroscopy study[J]. Angewandte Chemie-International Edition，2006，45(46): 7778-7780.

[46] KOLBECK C，PAAPE N，CREMER T，et al. Ligand Effects on the Surface Composition of Rh-Containing Ionic Liquid Solutions Used in Hydroformylation Catalysis[J]. Chemistry-a European Journal，2010，16(40): 12083-12087.

[47] SMITH E F，RUTTEN F J M，VILLAR-GARCIA I J，et al. Ionic liquids in vacuo: Analysis of liquid surfaces using ultra-high-vacuum techniques[J]. Langmuir，2006，22(22): 9386-9392.

[48] FAIRLEY N，CARRICK A. The Casa Cookbook[M]. Knutsford: Acolyte Science，2005.

[49] LAI X C，PUSHKIN M A，TROYAN V I. XPS study of Cu/substrate systems obtained by pulsed laser deposition[J]. Surface and Interface Analysis，2004，36(8): 1199-1202.

[50] MOULDER J F，STICKLE W F，SOBOL P E，et al. Handbook of X-ray Photoelectron Spectroscopy: a reference book of standard spectra for identification and interpretation of XPS data[M]. Chanhassen: Physical Electronics，1995.

[51] BRIGGS D，BEAMSON G. The XPS of Polymers Database[M]. Manchester: Surface-Spectra，2000.

[52] BRIGGS D，GRANT J T. Surface Analysis by Auger and X-ray Photoelectron Spectroscopy[M]. Manchester: IMPublications，2003.

[53] CREMER T，KOLBECK C，LOVELOCK K R J，et al. Towards a Molecular Understanding of Cation-Anion Interactions-Probing the Electronic Structure of Imidazolium Ionic Liquids by NMR Spectroscopy，X-ray Photoelectron Spectroscopy and Theoretical Calculations[J]. Chemistry-a European Journal，2010，16(30): 9018-9033.

[54] HURISSO B B，LOVELOCK K R J，LICENCE P. Amino Acid-Based Ionic Liquids: Using XPS to Probe the Electronic Environment via Binding Energies[J]. Physical Chemistry Chemical Physics，2011，13: 17737-17748.

[55] TSUZUKI S，TOKUDA H，HAYAMIZU K，et al. Magnitude and directionality of interaction in ion pairs of ionic liquids: Relationship with ionic conductivity[J]. Journal of Physical Chemistry B，2005，109(34): 16474-16481.

[56] HUNT P A，GOULD I R，KIRCHNER B. The structure of imidazolium-based ionic liquids: Insights from ion-pair interactions[J]. Australian Journal of Chemistry，2007，60(1): 9-14.

[57] TOKUDA H，TSUZUKI S，SUSAN M，et al. How ionic are room-temperature ionic liquids? An indicator of the physicochemical properties[J]. Journal of Physical Chemistry B，2006，110(39): 19593-19600.

[58] HOLLOCZKI O，NYULASZI L. Neutral species from "non-protic" N-heterocyclic ionic liquids[J]. Organic & Biomolecular Chemistry，2011，9(8): 2634-2640.

[59] FERNANDES A M，ROCHA M A A，FREIRE M G，et al. Evaluation of Cation-Anion Interaction Strength in Ionic Liquids[J]. Journal of Physical Chemistry B，2011，115(14):

4033-4041.

[60] IZGORODINA E I，FORSYTH M，MACFARLANE D R. Towards a better understanding of 'delocalized charge' in ionic liquid anions[J]. Australian Journal of Chemistry，2007，60(1): 15-20.

[61] NEWTON K A，HE M，AMUNUGAMA R，et al. Selective cation removal from gaseous polypeptide ions: proton vs. sodium ion abstraction via ion/ion reactions[J]. Physical Chemistry Chemical Physics，2004，6(10): 2710-2717.

[62] TSUZUKI S，KATOH R，MIKAMI M. Analysis of interactions between 1-butyl-3-methy limidazolium cation and halide anions (Cl^-，Br^- and I^-) by ab initio calculations: anion size effects on preferential locations of anions[J]. Molecular Physics，2008，106(12-13): 1621-1629.

[63] MAIER F，CREMER T，KOLBECK C，et al. Insights into the surface composition and enrichment effects of ionic liquids and ionic liquid mixtures[J]. Physical Chemistry Chemical Physics，2010，12(8): 1905-1915.

[64] PLECHKOVA N V，SEDDON K R. Applications of ionic liquids in the chemical industry[J]. Chemical Society Reviews，2008，37(1): 123-150.

[65] FLETCHER K A，BAKER S N，BAKER G A，et al. Probing solute and solvent interactions within binary ionic liquid mixtures[J]. New Journal of Chemistry，2003，27(12): 1706-1712.

[66] BALTAZAR Q Q，LEININGER S K，ANDERSON J L. Binary ionic liquid mixtures as gas chromatography stationary phases for improving the separation selectivity of alcohols and aromatic compounds[J]. Journal of Chromatography A，2008，1182(1): 119-127.

[67] XUAN X，GUO M，PEI Y，et al. Theoretical study on cation-anion interaction and vibrational spectra of 1-allyl-3-methylimidazolium-based ionic liquids[J]. Spectrochimica Acta Part a-Molecular and Biomolecular Spectroscopy，2011，78(5): 1492-1499.

[68] CALO V，NACCI A，MONOPOLI A. Effects of ionic liquids on Pd-catalysed carbon-carbon bond formation[J]. European Journal of Organic Chemistry，2006(17): 3791-3802.

[69] PHAN N T S，VAN DER SLUYS M，JONES C W. On the nature of the active species in palladium catalyzed Mizoroki-Heck and Suzuki-Miyaura couplings - Homogeneous or heterogeneous catalysis，a critical review[J]. Advanced Synthesis & Catalysis，2006，348(6): 609-679.

[70] SATO Y，YOSHINO T，MORI M. N-heterocyclic carbenes as ligands in palladium-catalyzed Tsuji-Trost allylic substitution[J]. Journal of Organometallic Chemistry，2005，

690(24-25): 5753-5758.

[71] SINGH R，NOLAN S P. An efficient and mild protocol for the alpha-arylation of ketones mediated by an (imidazol-2-ylidene)palladium(acetate) system[J]. Journal of Organometallic Chemistry，2005，690(24-25): 5832-5840.

[72] MARION N，NOLAN S P. Well-Defined N-Heterocyclic Carbenes-Palladium(II) Precatalysts for Cross-Coupling Reactions[J]. Accounts of Chemical Research，2008，41(11): 1440-1449.

[73] MEN S，LOVELOCK K R J，LICENCE P. Directly probing the effect of the solvent on a catalyst electronic environment using X-ray photoelectron spectroscopy[J]. Rsc Advances，2015，5(45): 35958-35965.

Chapter 5

XPS of Metal-ligand Interaction in Ionic Liquids

5.1 Introduction

Homogeneous catalysis is a large field of activity within the area of ionic liquids and has attracted a lot of interest over the past decade.[1-4] Since ionic liquids exhibit such a range of fascinating properties, *i.e.* low volatility and good solvating ability, they have shown huge potential for the replacement of traditional organic solvents.[2,5] As has been summarised in *Chapter 1*, many ionic liquids can dissolve organometallic compounds, allowing them to act as suitable solvents for transition metal based catalysis. In many cases, they have been found to be better solvents when compared to traditional organic solvents, as well as water.[1] Ionic liquids have been successfully applied to many homogeneous catalytic reactions such as hydrogenation,[6] hydroformylation,[3] oxidation,[3] oligomerization[3] as well as coupling reactions, *i.e.* Heck reaction[7, 8] and Suzuki reaction.[8, 9] Using ionic liquids as reaction solvents can give rise to a different chemical activity of the system[10-17] and thus an acceleration[8, 9] or better selectivity towards the desired product,[18, 19] which renders them more valuable.

XPS which is able to characterise the elemental composition and subtle binding energy shifts of samples, has been used to analyse heterogeneous metal catalysts for many years.[20, 21] Due to the low volatility of ionic liquids, the Licence group at the University of Nottingham published the first paper about the XPS analysis of a metal catalyst in solution, illustrating the monitoring of the

reduction of a palladium catalyst in 2005.[22] Almost at the same time, Mikkola *et al.* detected a palladium centre in different chemical environments in a supported ionic liquid catalytic system.[23, 24] These works pioneered the method of using XPS to analyse a metal catalyst in solution. It not only opened the door to a new technique for the analysis of ionic liquid-based solutions but also provided an opportunity to further understand the processes involved when a metal catalyst is dissolved in ionic liquids, *e.g.* the metal-ligand interaction.

Since then, there have been lots of publications from all over the word focusing on the use of XPS to analyse ionic liquid-based metal catalytic systems.[25, 26] In 2006, Maier *et al.* used angle resolved XPS (ARXPS) to analyse a platinum catalyst in $[C_2C_1Im][EtSO_4]$ and for the first time showed surface enrichment of the cation of the catalyst.[27] In 2008, Neatu *et al*. proved the chemical state of Au in an ionic liquid mixture using an XPS Au 4f high resolution spectrum together with EXAFS measurements. In the same year, Nguyen *et al.* investigated the reduction of Fe in halometallate-based ionic liquids with the anions $[FeCl_4]^-$ and $[Fe_2Cl_7]^-$.[28] In 2009, Tao *et al.* analysed the presence of Pd（Ⅱ）nanoparticles in ionic liquid-based catalytic systems on sepiolite.[29] Shortly after, the Licence group monitored the *in situ* electrochemical generation of an Fe（Ⅲ） species in an ionic liquid system using XPS with a special EC-XPS set up.[30] In 2010, the same group also investigated the *in situ* dissolution of copper into ionic liquids by XPS.[31] Later in the same year, Kolbeck *et al.* investigated the ligand effect on the surface composition of Rh-containing ionic liquid systems by XPS.[32] In the same year, Apperley *et al.* analysed chloroindate-based ionic liquids by XPS together with EXAFS and found that there is indium chloride power suspended in the neutral tetrachloroindate ionic liquid.[33] Recent studies have highlighted that the XPS signals can act as reporters to tune the electronic environment of metal atoms in halometallate-based ionic liquids[34, 35] and as probes of solvent-solute interactions in ionic liquid-based palladium systems.[36, 37]

Since binding energies obtained from XPS are sensitive to changes in electronic environment, they can be used to reflect differences in activity towards catalytic performance for a given metal catalyst. The activity of catalytic reactions strongly depends on the electronic environment at the metal centre in combination with, (a) interactions between the “catalyst” and the surrounding solvents,[38] and (b) the ligands that surround it. Consequently, a proper understanding of such interactions becomes crucial.[17, 39-46]

The role of ionic liquids in catalytic reaction systems needs to be studied. In *Chapter 4*, we have already discussed about the solute-solvent interaction in ionic liquids. However, the inner sphere

change, *i.e.* metal-ligand interaction, is still not properly investigated. Several questions need to be resolved in an attempt to clarify aspects of inner sphere change at the metal centre, such as:

（1）Can we detect ligand substitution by XPS?

（2）What is the effect of the ligands on the electronic environment at the metal centre? Can this be quantified?

（3）Do ionic liquids influence the metal-ligand interaction? If so, how?

In this chapter, the use of XPS as an effective technique to investigate the ligand effect on the electronic environment at the rhodium centre for a widely used catalyst, (Acetylacetonato) dicarbonylrhodium(I) ([Rh(acac)$(CO)_2$]) is explored. The formation of phosphine rhodium complex es based upon addition of phoshine ligands is confirmed by XP spectra. The different reaction selectivity of such catalytic system towards metal-ligand interaction is correlated to the measured binding energies of Rh $3d_{5/2}$. The influence of anion basicity on the formation of different phosphine rhodium complexes is also investigated.

5.2 Detection of the rhodium centre in solution

Rhodium based catalysts have been successfully applied to hydroformylation reactions in a biphasic ionic liquid/$scCO_2$ systems where the catalyst was firstly dissolved in ionic liquid phase and the product is extracted by $scCO_2$.[47-49] In the case of reactions catalysed by [Rh(acac)$(CO)_2$], a potential problem is that the catalyst can be also extracted out of the ionic liquid phase. To overcome such problem, phosphine ligands were added to enhance the solubility of the catalyst in ionic liquid phase. Such a procedure aims to avoid leaching of the rhodium catalyst from ionic liquid phase.

As highlighted in *Chapter 3*, for low basicity anion-based imidazolium ionic liquids, when $n \geqslant 8$ we expect the $C_{aliphatic}$ 1s component to be a reliable charge reference. Consequently, in this chapter, C_8-based ionic liquids have been used to prepare ionic liquid-based metal catalyst solutions for ease of charge correction and to obtain reliable and comparable binding energies.

A solution of [Rh(acac)$(CO)_2$] dissolved in [C_8C_1Im][Tf_2N] was prepared and analysed by XPS. The survey spectrum and all high resolution spectra are shown in Figure 5.1. Specifically in

the Rh 3d high resolution spectrum, a signal from the rhodium catalyst can be observed. The Rh 3d spectrum shows the characteristic doublet peak with a spin-orbital coupling energy difference of 4.74 eV and area ratio $3d_{5/2}$: $3d_{3/2}$ of 3 : 2.[50] In this chapter, unless otherwise stated, $3d_{5/2}$ component is selected to ensure valid comparisons, simply because the intensity for this component is higher. The measured binding energy of Rh $3d_{5/2}$ is 309.9 eV which is the same as that obtained previously for the solid $[Rh(acac)(CO)_2]$.[51, 52]

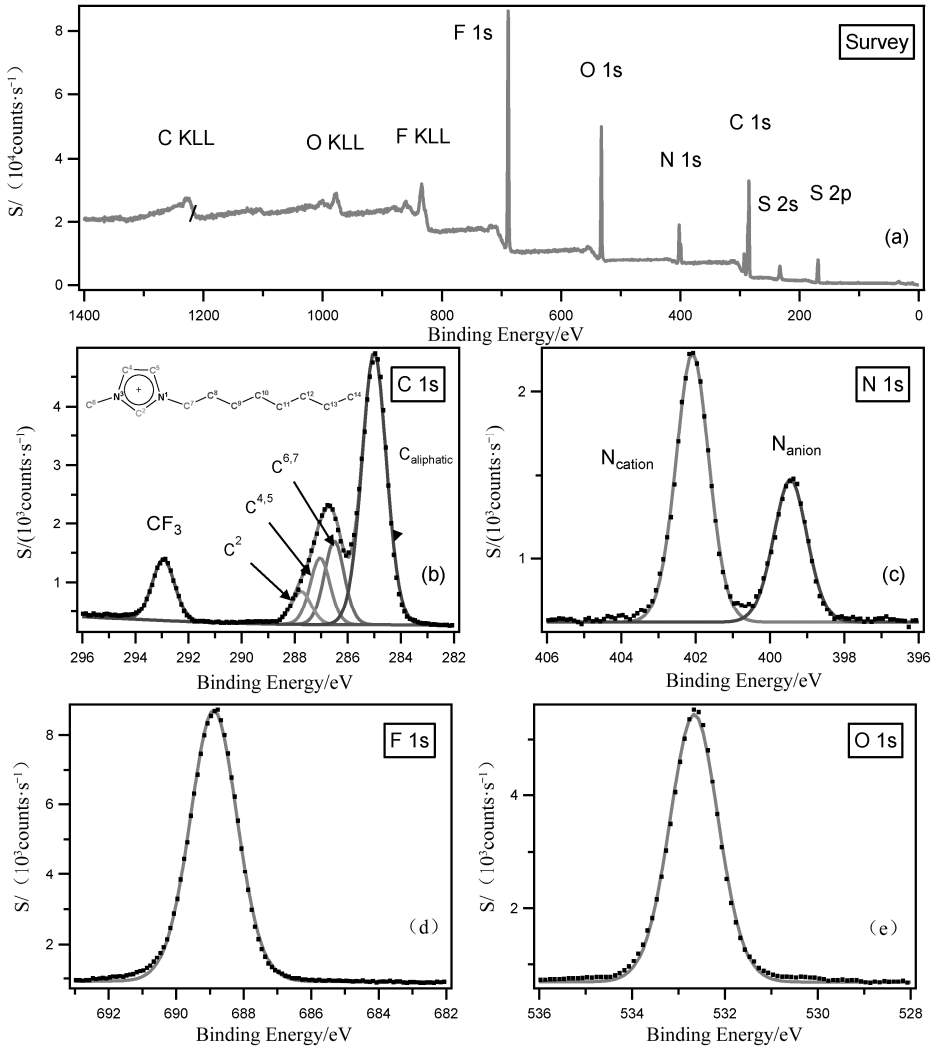

Figure 5.1 XP spectra of $[Rh(acac)(CO)_2]$ in $[C_8C_1Im][Tf_2N]$ for (a) survey, (b) C 1s, (c) N 1s, (d) F 1s, (e) O 1s, (f) S 2p and (g) Rh 3d. All XP spectra were charge corrected by referencing the $C_{aliphatic}$ 1s component to 285.0 eV

（To be continued）

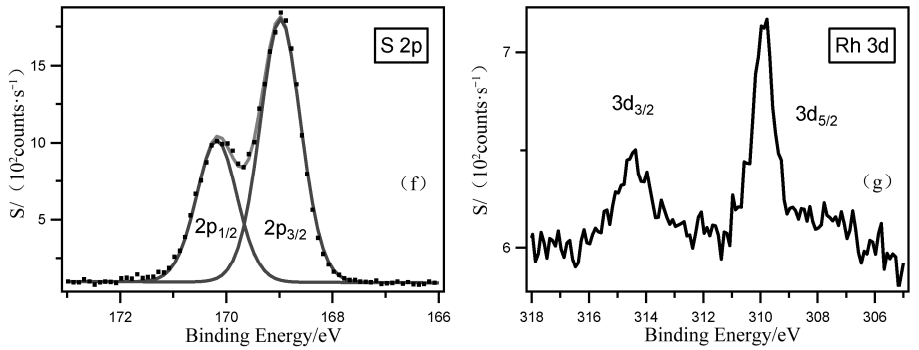

Figure 5.1 XP spectra of $[Rh(acac)(CO)_2]$ in $[C_8C_1Im][Tf_2N]$ for (a) survey, (b) C 1s, (c) N 1s, (d) F 1s, (e) O 1s, (f) S 2p and (g) Rh 3d. All XP spectra were charge corrected by referencing the $C_{aliphatic}$ 1s component to 285.0 eV

Continued figure

It must be noted that the signal to noise ratio of the Rh 3d spectrum is relatively low when compared to the other spectra. This is due to the relatively low concentration of $[Rh(acac)(CO)_2]$ in the ionic liquid solution, *i.e.* lower than 0.02 atomic %. Indeed, in this work, Rh 3d spectrum with good quality can only be obtained for $[Tf_2N]^-$-based solution. The poor solubility of the $[Rh(acac)(CO)_2]$ in ionic liquids makes it impossible to compare Rh 3d spectra for different ionic liquid-based solutions.

As has been summarised in *Chapter 2*, the solubility of neutral metal compounds[47, 53, 54] is generally much lower than ionic metal complexes[6, 55] in ionic liquids. In order to achieve a high concentration for neutral metal compounds, different approaches have been successfully applied, *i.e.* the use of task specific ionic liquids[54, 56, 57] and the addition of ligands.[58, 59] In this chapter, phosphine ligands were used to enhance the solubility of the $[Rh(acac)(CO)_2]$ to valid comparison of Rh 3d spectra in different ionic liquids. This work is introduced in detail in *Section 5.3*.

Moreover, as shown in Figure 5.2 the comparison of Rh 3d high resolution spectra for solid $[Rh(acac)(CO)_2]$ and $[Rh(acac)(CO)_2]$ dissolved in $[C_8C_1Im][Tf_2N]$, it is clear that the spectrum of the solution-based sample is much sharper than that of the solid sample. The FWHM for the $3d_{5/2}$ component of each spectrum are 1.9 and 1.0 respectively. Actually, the FWHM of solid samples are found to be broader than those of liquid samples. This observation may be explained as a result of charging at the surface of the non-conducting solid sample[60-64] or more probably, as a consequence of the photo-physics involved during the photoelectron process. Such a photo-physical effect was extensively discussed in *Section 4.2*. The measured binding energies of

Rh $3d_{5/2}$ for the two samples are the same, within the experimental error of XPS measurement.

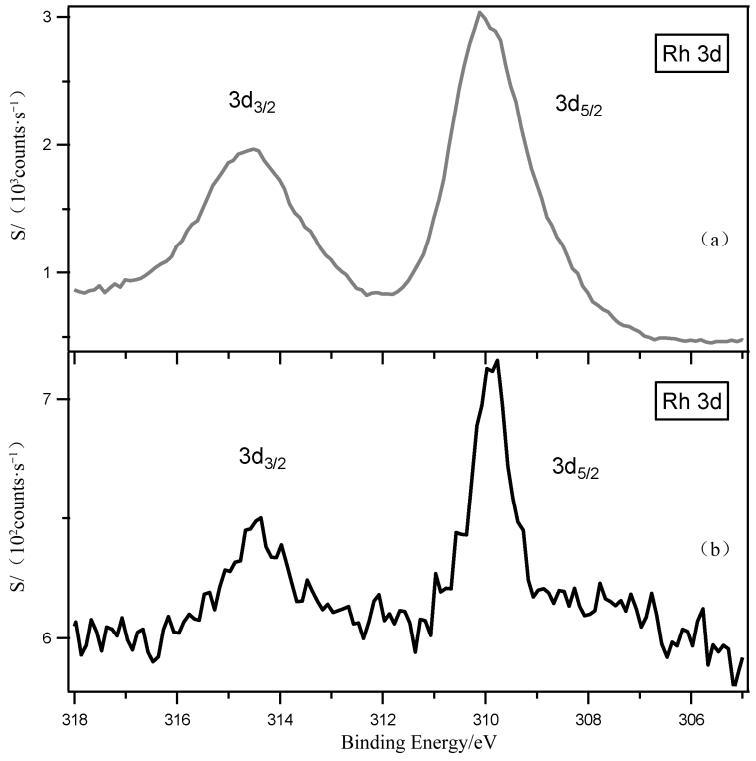

Figure 5.2 Rh 3d high resolution XP spectra of (a) solid $[Rh(acac)(CO)_2]$ and (b) $[Rh(acac)(CO)_2]$ in $[C_8C_1Im][Tf_2N]$. XP spectrum of solid sample was charge corrected by referencing the C_{CO} 1s component to 287.7 eV.[51] XP spectrum of solution sample was charge corrected by referencing the $C_{aliphatic}$ 1s component to 285.0 eV

5.3 Formation of the mono−phosphine rhodium complex

It is well known that $[Rh(acac)(CO)_2]$ can react with phosphine ligands at room temperature in ionic liquids and thus form a new rhodium catalytic system, as according to Scheme 5.1.[32, 65]

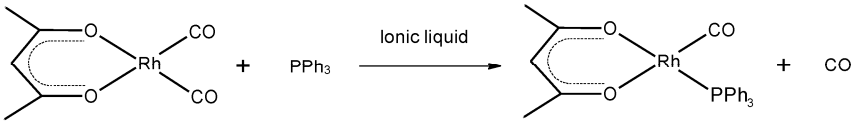

Scheme 5.1 Reaction of $[Rh(acac)(CO)_2]$ with PPh_3 in ionic liquids

The coordination of the phosphine ligand to the rhodium centre affects its electronic environment and thus reflects the shift of its measured binding energy. One equivalent of a phosphine ligand, triphenylphosphine (PPh_3), was added to the Rh-containing ionic liquid solution and the new system was analysed by XPS.

A comparison of the Rh $3d_{5/2}$ high resolution spectra of $[Rh(acac)(CO)_2]$ and the new PPh_3-containing complex is shown in Figure 5.3. The XP spectrum indicates how the Rh 3d binding energy shifts upon the addition of the new ligand. The measured binding energy of Rh $3d_{5/2}$ for the ligand-containing solution is 308.7 eV which is 1.2 eV lower than the reference $[Rh(acac)(CO)_2]$ solution. This observation suggests that the ligand is coordinated to the rhodium centre. Phosphine ligands are well known to be electron donors.[66] The electronic donating effect of the ligand gives rise to a rhodium centre in a more electron rich environment, which is observed at a lower binding energy.

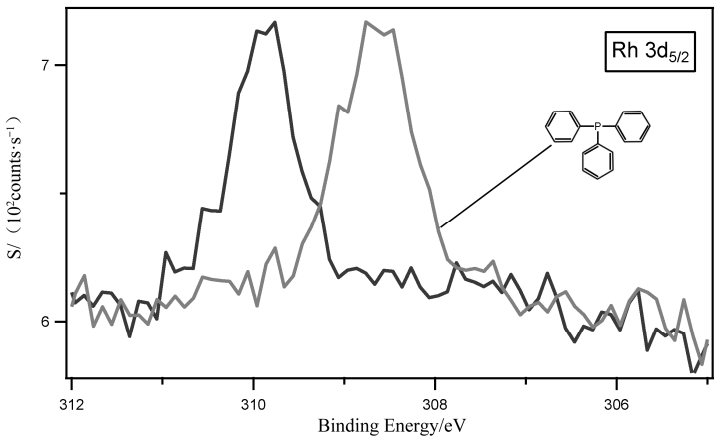

Figure 5.3 XP spectra of Rh $3d_{5/2}$ for $[Rh(acac)(CO)_2]$ in $[C_8C_1Im][Tf_2N]$ and $[Rh(acac)(CO)_2]$ plus PPh_3 in $[C_8C_1Im][Tf_2N]$. All XP spectra were charge corrected by referencing the $C_{aliphatic}$ 1s component to 285.0 eV

The ligand-containing ionic liquid solutions were prepared in a range of different $[C_8C_1Im]^+$-based ionic liquids with commonly used anions. Figure 5.4 shows XP spectra of all Rh 3d high resolution spectra. It is apparent that the reaction outlined in Scheme 5.1 occurred in all $[C_8C_1Im]^+$-based ionic liquids. The measured binding energies of Rh $3d_{5/2}$ in all $[C_8C_1Im]^+$-based ionic liquids are the same (see Table 5.1), which indicates that ionic liquid components are spectators and have no impact on the electronic environment of the rhodium centre.

This observation is very different to the data presented in *Chapter 4*. However, it is quite easily explained. In the case of Pd-containing ylidene complexes, the ionic liquid anion was the anion of the Pd-containing ylidene cation. Consequently, the interaction is more truly. The observation in this chapter indicates that ionic liquids have no impact on inner sphere electronic

change at the metal centre and may be considered as spectators in neutral solute systems.

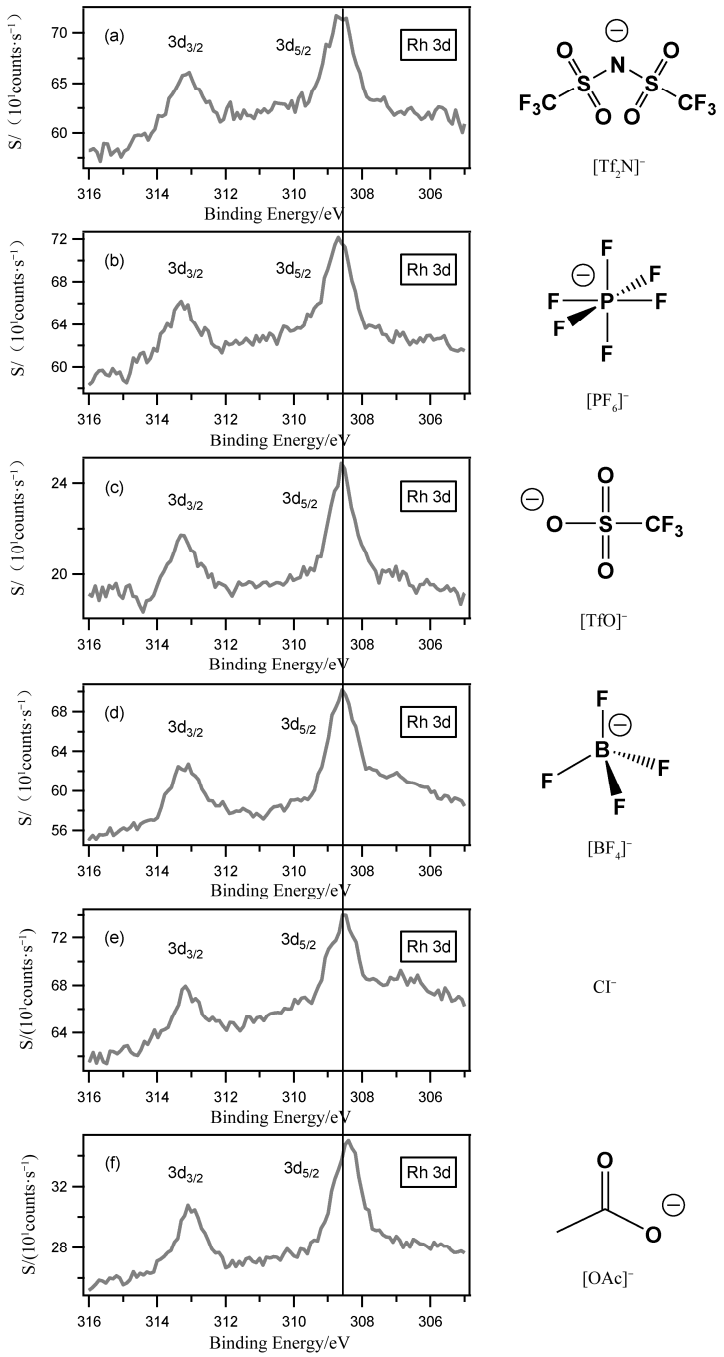

Figure 5.4 XP spectra of Rh 3d for $[Rh(acac)(CO)_2]$ plus PPh_3 in $[C_8C_1Im]^+$-based ionic liquids (a) $[Tf_2N]^-$, (b) $[PF_6]^-$, (c) $[TfO]^-$, (d) $[BF_4]^-$, (e) Cl^- and (f) $[OAc]^-$. All XP spectra were charge corrected by referencing the $C_{aliphatic}$ 1s component to 285.0 eV

Table 5.1 Binding energies in eV for all regions of all Rh-containing solutions. It should be noted that the experimental error associated with the measurement of binding energies is of the order ± 0.1 eV. The molar ratio of Rh : Ligand was 1 : 1

Ionic Liquid		Ligand	Binding Energy / eV													
Cation	Anion		Rh $3d_{5/2}$	$C_{aliphatic}$ 1s	C^{2} 1s	$C^{4,5}$ 1s	$C^{6,7}$ 1s	N_{cation} 1s	C_{CF3} 1s	N_{anion} 1s	O 1s	F 1s	S $2p_{3/2}$	P $2p_{3/2}$ ①	Cl $2p_{3/2}$	B 1s
Solid		None	309.9	285.1	287.7	285.9					531.9					
$[C_8C_1Im]$	$[Tf_2N]^-$	None	309.9	285.0	287.8	287.1	286.5	402.1	292.9	399.5	532.7	688.9	169.0			
$[C_8C_1Im]$	$[Tf_2N]^-$	PPh_3	308.7	285.0	287.7	287.0	286.5	402.1	292.9	399.5	532.6	688.8	169.0			
$[C_8C_1Im]$	$[PF_6]^-$	PPh_3	308.7	285.0	287.8	287.1	286.5	402.1				686.8		136.6		
$[C_8C_1Im]$	$[TfO]^-$	PPh_3	308.6	285.0	287.6	286.9	286.3	402.0	292.5		532.0	688.5	168.4			
$[C_8C_1Im]$	$[BF_4]^-$	PPh_3	308.7	285.0	286.9	286.6	286.4	402.0				688.0				194.2
$[C_8C_1Im]$	Cl^-	PPh_3	308.6	285.0	287.2	286.6	286.0	401.7							197.0	
$[C_8C_1Im]$	$[OAc]^-$	PPh_3	308.6	285.0	287.4	286.6	286.0	401.6			530.3					
$[C_8C_1Im]$	$[Tf_2N]^-$	dppf	308.6	285.0	287.8	287.1	286.5	402.1	292.9	399.5	532.7	688.9	168.9			
$[C_8C_1Im]$	$[TfO]^-$	dppf		285.0	287.6	286.9	286.4	402.0	292.5		532.0	688.5	168.4			
$[C_8C_1Im]$	$[OAc]^-$	dppf	307.9	285.0	287.4	286.6	286.0	401.7			530.4					

① It must be noted that the P 2p signals for the ligands were not observed due to the low concentration

5.4 Investigation of the chelated diphosphine rhodium complex

Since there is coordination between $[Rh(acac)(CO)_2]$ and phosphine ligands,[32, 65] the presence of a diphoshine ligand, *i.e.* 1,1′-bis(diphenylphosphino)- ferrocene (dppf), could result in a more complicated coordination scenario.[67] Upon addition of the phosphine ligand, immediately, the first CO group within $[Rh(acac)(CO)_2]$ will be substituted to form a mono-phosphine rhodium complex. However, by simply heating or evacuating, the second CO group could eventually be substituted to form a diphosphine rhodium complex, see Scheme 5.2.

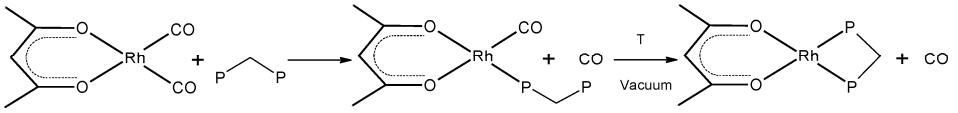

Scheme 5.2 Reaction of $[Rh(acac)(CO)_2]$ with diphosphine ligand in ionic liquids

As highlighted in *Section 3.2.2*, the basicity of the anion is a key factor in determining the charge transferred from the anion to the cation, and thus the measured binding energy for cation-based components. It also influences the physical or chemical properties of the ionic liquids, *i.e.* dipolarity or polarisability.[68] Consequently, it is assumed that during the processes of CO

group substitution using ionic liquids as the reaction solvents, perhaps a degree of reactive control could be afforded by carefully selecting/tuning of the reaction solvent.

Three dppf-containing solutions in different basicity anion-based ionic liquids, *i.e.* $[C_8C_1Im][Tf_2N]$, $[C_8C_1Im][TfO]$ and $[C_8C_1Im][OAc]$, were prepared and analysed by XPS. As shown in Figure 5.5(a), in low basicity anion-based ionic liquids, *i.e.* $[C_8C_1Im][Tf_2N]$, XPS data suggests that only a mono-phosphine rhodium complex is formed with a measured binding energy for Rh $3d_{5/2}$ of 308.7 eV, which is consistent with those obtained for PPh_3-containing solutions. This observation was confirmed by Infrared (IR) Spectroscopy. In the IR spectrum, only one CO group stretching vibration[69] at 2012 cm^{-1} was observed for the dppf-containing solution in $[C_8C_1Im][Tf_2N]$, which replaced the two CO stretching vibrations for $[Rh(acac)(CO)_2]$ (2075, 2015 cm^{-1}).

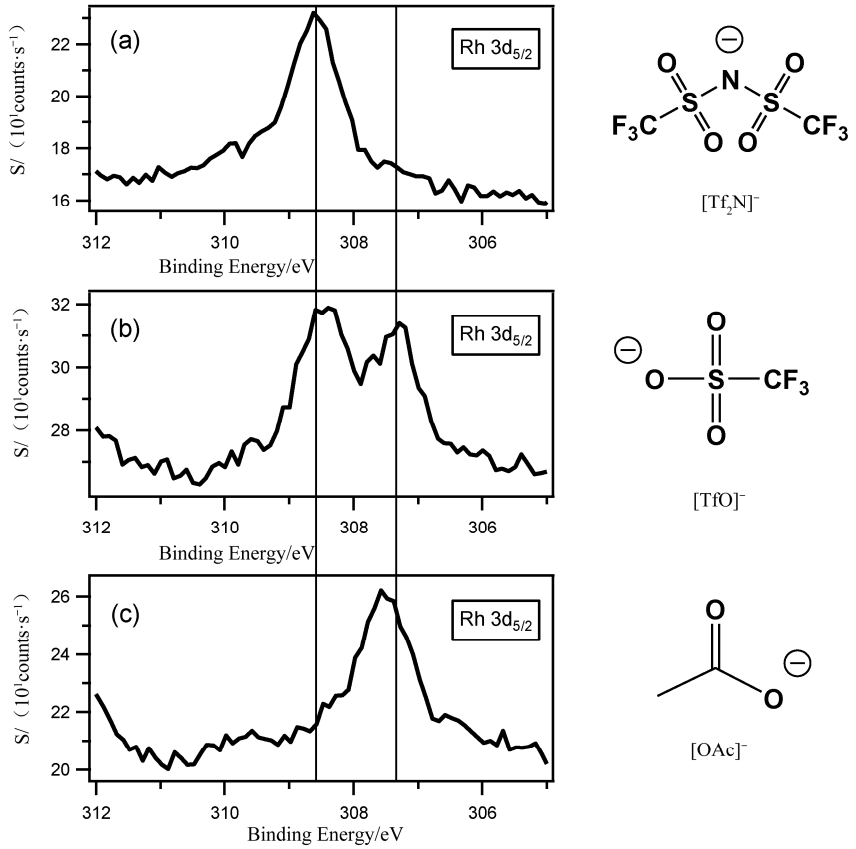

Figure 5.5 XP spectra of Rh $3d_{5/2}$ for $[Rh(acac)(CO)_2]$ plus dppf in $[C_8C_1Im]^+$-based ionic liquids (a) $[Tf_2N]^-$, (b) $[TfO]^-$ and (c) $[OAc]^-$. All XP spectra were charge corrected by referencing the $C_{aliphatic}$ 1s component to 285.0 eV.

In high basicity anion-based ionic liquids, *i.e.* $[C_8C_1Im][OAc]$, it is apparent that only a diphosphine rhodium complex is formed, with a measured binding energy for Rh $3d_{5/2}$ of 307.9 eV, see Figure 5.5(c). Moreover, in the IR spectrum, no CO group stretching vibration was observed, confirming the formation of the chelated diphosphine rhodium complex.

In the case of $[C_8C_1Im][TfO]$, since the basicity of $[TfO]^-$ is in between that of $[Tf_2N]^-$ and $[OAc]^-$, the XP spectrum indicates two different Rh environments, see Figure 5.5(b). The higher binding energy component is very similar, certainly within the experimental error to that obtained for the singly coordinated dppf-containing complex in $[Tf_2N]^-$-based solution. The lower binding energy is consistent to that obtained for the chelated bidentate dppf-containing in $[OAc]^-$-based solution. This suggests that both mono- and chelated diphosphine rhodium complexes are formed in $[C_8C_1Im][TfO]$. The results in this section suggest that ionic liquids can impact upon the coordination of a ligand to the rhodium centre in $[Rh(acac)(CO)_2]$, specifically the substitute of the second CO group.

5.5 Correlation of reaction selectivity and binding energy

As mentioned earlier, ionic liquids can be used as solvents for hydroformylation reactions.[3] When different phosphine ligands are applied to the $[Rh(acac)(CO)_2]$ catalysed hydroformylation of 1-octene in ionic liquids (see Scheme 5.3), they are found to improve the solubility of the catalyst, and also show different reaction selectivity towards the desired linear product, *i.e.* n-nonanal (see Table 5.2).[19]

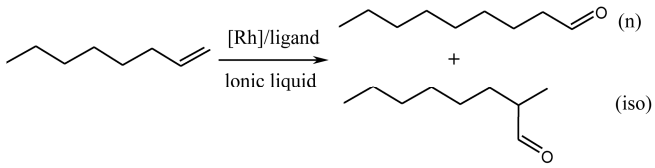

Scheme 5.3 The hydroformylation of 1-octene in ionic liquid

The reason different phosphine ligands show different reaction selectivity towards the desired linear product in the hydroformylation reaction may be due to the formation of different rhodium complexes in ionic liquids. In *Sections 5.3* and *5.4*, the formation of different types of rhodium complexes by addition of different ligands, *i.e.* PPh_3 and dppf, in high basicity anion-based ionic

liquids, *i.e.* [C_8C_1Im][OAc], has been illustrated.

Table 5.2 A comparison of different phosphine ligands in the [Rh(acac)$(CO)_2$] catalysed hydroformylation reaction of 1-octene in ionic liquid according to ref [19]

Ligand	n/iso	S (n)①/%
PPh_3	2.6	72
dppf	3.8	79

t = 1 h, *T* = 373 K, *p* = 10 bar, 1-octene/Rh = 1000

① S (n) = selectivity to n-nonanal in the product

Figure 5.6 shows the Rh $3d_{5/2}$ high resolution XP spectra for the solutions of [Rh(acac)$(CO)_2$] plus two ligands with a 1∶1 molar equivalent (catalyst : ligand) in [C_8C_1Im][OAc]. It is evident that the measured Rh $3d_{5/2}$ binding energies for both solutions are lower than that obtained for [Rh(acac)$(CO)_2$] (309.9 eV, see Table 5.1). This suggests that both of the ligands have coordinated to the rhodium centre and thus influenced its electronic environment. The binding energy of Rh $3d_{5/2}$ for the dppf-containing solution shifts as much as 0.8 eV lower when compared to that obtained for the PPh_3-containing solution. The lower binding energy of Rh $3d_{5/2}$ for the dppf-containing solution means that the corresponding Rh centre is more electron rich when compared to the PPh_3-containing analogue. XPS can thus be used to quantify the difference in the amount of charge transferred to the rhodium centre.

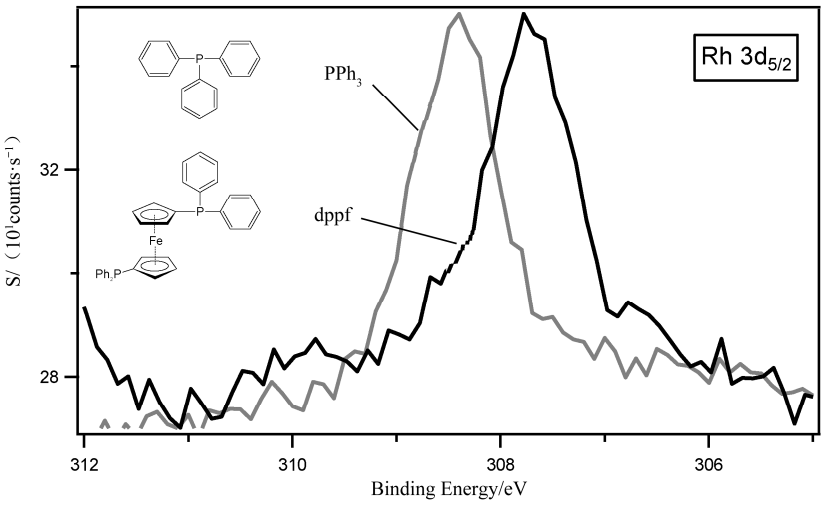

Figure 5.6 XP spectra of Rh $3d_{5/2}$ for [Rh(acac)$(CO)_2$] plus PPh_3 and dppf in [C_8C_1Im][OAc]. All XP spectra were charge corrected by referencing the $C_{aliphatic}$ 1s component to 285.0 eV

It can be concluded that XPS can provide useful information about the effect of ligands on a

metal centre and furthermore can even be used to quantify the difference in the amount of charge transferred to the metal centre. The reaction selectivity for the hydroformylation reaction can be correlated to the measured binding energies for the metal centres of the catalytic systems. The correlation between reaction performance and the binding energy of the metal centre concludes that the electronic environment of the catalyst greatly affects the reaction. Based upon such conclusion, it is worth to employ more types of phosphine ligands in the future work, *e.g.* $P(Me)_3$ and dppe. Such correlation also inspired the idea of designing a metal catalyst to enhance reaction selectivity for the future work.

5.6 Conclusions

In this chapter, XPS has been used as an effective method for the analysis of ionic liquid-based metal catalyst solutions. Rh-containing ionic liquid-based solutions, with a variety of ligands, for the use in the hydroformylation reaction were analysed and the reaction selectivity data were correlated to the binding energies of the Rh centre. The differences in electronic environment were quantified for different Rh centres in solution. Moreover, the formation of Rh-containing complexes was monitored by XPS. In the case of the mono-phosphine ligand, *i.e.* PPh_3, the binding energies of Rh 3d for all Rh-containing solutions are the same, within the experimental error. In the case of diphosphine ligands, *i.e.* dppf, the influence of anion basicity on the formation of diphosphine rhodium complex was discussed and confirmed by XPS in conjunction with IR spectrocopy. It was concluded that in low basicity anion-based ionic liquids, *i.e.* $[Tf_2N]^-$, only a mono-phosphine rhodium complex can be formed; but in high basicity anion-based ionic liquids, *i.e.* $[OAc]^-$, only a diphosphine rhodium complex is observed.

It has been shown in this chapter that XPS is able to provide valuable information about the effect of ligands on the electronic environment of the metal centre. An important question to ask is : how does a ligand affect the electronic environment of the catalytic metal centre in solution? The binding energy derived from the XPS measurement can be used to help answer this question.

In general, the results shown in this chapter summarise the method of using XPS to analyse ionic liquid-based catalytic solutions. XPS data has been used to correlate with catalytic reaction selectivity. Such a correlation provides a better understanding of homogeneous catalytic processes

and shows the potential of this method for the prediction, control and even design of catalytic systems in future.[70]

References

[1] WASSERSCHEID P，WELTON T. Ionic Liquids in Synthesis[M]. Weinheim: WILEY-VCH，2007.

[2] PARVULESCU V I，HARDACRE C. Catalysis in ionic liquids[J]. Chemical Reviews，2007，107(6): 2615-2665.

[3] WELTON T. Ionic liquids in catalysis[J]. Coordination Chemistry Reviews，2004，248 (21-24): 2459-2477.

[4] FORSYTH S A，PRINGLE J M，MACFARLANE D R. Ionic liquids - An overview[J]. Australian Journal of Chemistry，2004，57(2): 113-119.

[5] EARLE M J，KATDARE S P，SEDDON K R. Paradigm confirmed: The first use of ionic liquids to dramatically influence the outcome of chemical reactions[J]. Organic Letters，2004，6(5): 707-710.

[6] CHAUVIN Y，MUSSMANN L，OLIVIER H. A novel class of versatile solvents for two-phase catalysis: Hydrogenation，isomerization，and hydroformylation of alkenes catalyzed by rhodium complexes in liquid 1,3-dialkylimidazolium salts[J]. Angewandte Chemie-International Edition，1995，34(23-24): 2698-2700.

[7] WAN Q，LIU Y，CAI Y. A Hybrid P,N-Ligand Functionalized Imidazolium Salt for Palladium-Catalyzed Heck Reactions in Ionic Liquid Solution[J]. Catalysis Letters，2009，127(3-4): 386-391.

[8] XU L，CHEN W，XIAO J. Heck reaction in ionic liquids and the in situ identification of N-heterocyclic carbene complexes of palladium[J]. Organometallics，2000，19(6): 1123-1127.

[9] MATHEWS C J，SMITH P J，WELTON T. Palladium catalysed Suzuki cross-coupling reactions in ambient temperature ionic liquids[J]. Chemical Communications，2000(14): 1249-1250.

[10] WELTON T. Room-temperature ionic liquids. Solvents for synthesis and catalysis[J]. Chemical Reviews，1999，99(8): 2071-2083.

[11] JAIN N，KUMAR A，CHAUHAN S，et al. Chemical and biochemical transformations in ionic liquids[J]. Tetrahedron，2005，61(5): 1015-1060.

[12] ZHAO D，WU M，KOU Y，et al. Ionic liquids: applications in catalysis[J]. Catalysis Today，2002，74(1-2): 157-189.

[13] DUPONT J，DE SOUZA R F，SUAREZ P A Z. Ionic liquid (molten salt) phase organometallic catalysis[J]. Chemical Reviews，2002，102(10): 3667-3691.

[14] WASSERSCHEID P，KEIM W. Ionic liquids - New "solutions" for transition metal catalysis[J]. Angewandte Chemie-International Edition，2000，39(21): 3772-3789.

[15] WILKES J S. Properties of ionic liquid solvents for catalysis[J]. Journal of Molecular Catalysis a-Chemical，2004，214(1): 11-17.

[16] OLIVIER-BOURBIGOU H，MAGNA L. Ionic liquids: perspectives for organic and catalytic reactions[J]. Journal of Molecular Catalysis a-Chemical，2002，182(1): 419-437.

[17] POOLE C F. Chromatographic and spectroscopic methods for the determination of solvent properties of room temperature ionic liquids[J]. Journal of Chromatography A，2004，1037(1-2): 49-82.

[18] HERRMANN W A，BOHM V P W. Heck reaction catalyzed by phospha-palladacycles in non-aqueous ionic liquids[J]. Journal of Organometallic Chemistry，1999，572(1): 141-145.

[19] BRASSE C C，ENGLERT U，SALZER A，et al. Ionic phosphine ligands with cobaltocenium backbone: Novel ligands for the highly selective，biphasic，rhodium-catalyzed hydroformylation of 1-octene in ionic liquids[J]. Organometallics，2000，19(19): 3818-3823.

[20] VENEZIA A M. X-ray photoelectron spectroscopy for catalysts characterization[J]. Catalysis Today，2003，77(4): 359-370.

[21] NIEMANTSVERDRIET J W. Spectroscopy in Catalysis[M]. Weinheim: WILEY-VCH，2007.

[22] SMITH E F，VILLAR-GARCIA I J，BRIGGS D，et al. Ionic liquids in vacuo；solution-phase X-ray photoelectron spectroscopy[J]. Chemical Communications，2005(45): 5633-5635.

[23] MIKKOLA J P，VIRTANEN P，KARHU H，et al. Supported ionic liquids catalysts for fine chemicals: citral hydrogenation[J]. Green Chemistry，2006，8(2): 197-205.

[24] MIKKOLA J P，VIRTANEN P，KORDAS K，et al. SILCA-supported ionic liquid catalysts for fine chemicals[J]. Applied Catalysis a-General，2007，328(1): 68-76.

[25] KWON J H，YOUN S W，KANG Y C. XPS investigation of A^3 coupling reaction in room temperature ionic liquids[J]. Bulletin of the Korean Chemical Society，2006，27(11): 1851-1853.

[26] SILVESTER D S，BRODER T L，ALDOUS L，et al. Using XPS to determine solute solubility in room temperature ionic liquids[J]. Analyst，2007，132(3): 196-198.

[27] MAIER F，GOTTFRIED J M，ROSSA J，et al. Surface enrichment and depletion effects of ions dissolved in an ionic liquid: an X-ray photoelectron spectroscopy study[J]. Angewandte Chemie-International Edition，2006，45(46): 7778-7780.

[28] NGUYEN M D，NGUYEN L V，JEON E H，et al. Fe-containing ionic liquids as catalysts for the dimerization of bicyclo[2.2.1]hepta-2,5-diene[J]. Journal of Catalysis，2008，258(1): 5-13.

[29] TAO R，MIAO S，LIU Z，et al. Pd nanoparticles immobilized on sepiolite by ionic liquids: efficient catalysts for hydrogenation of alkenes and Heck reactions[J]. Green Chemistry，2009，11(1): 96-101.

[30] TAYLOR A W，QIU F，VILLAR-GARCIA I J，et al. Spectroelectrochemistry at ultrahigh vacuum: in situ monitoring of electrochemically generated species by X-ray photoelectron spectroscopy[J]. Chemical Communications，2009(39): 5817-5819.

[31] QIU F，TAYLOR A W，MEN S，et al. An ultra high vacuum-spectroelectrochemical study of the dissolution of copper in the ionic liquid (N-methylacetate)-4-picolinium bis (trifluoromethylsulfonyl)imide[J]. Physical Chemistry Chemical Physics，2010，12(8): 1982-1990.

[32] KOLBECK C，PAAPE N，CREMER T，et al. Ligand Effects on the Surface Composition of Rh-Containing Ionic Liquid Solutions Used in Hydroformylation Catalysis[J]. Chemistry-a European Journal，2010，16(40): 12083-12087.

[33] APPERLEY D C，HARDACRE C，LICENCE P，et al. Speciation of chloroindate(III) ionic liquids[J]. Dalton Transactions，2010，39(37): 8679-8687.

[34] CURRIE M，ESTAGER J，LICENCE P，et al. Chlorostannate(II) Ionic Liquids: Speciation，Lewis Acidity，and Oxidative Stability[J]. Inorganic Chemistry，2013，52(4): 1710-1721.

[35] TAYLOR A W，MEN S，CLARKE C J，et al. Acidity and basicity of halometallate-based ionic liquids from X-ray photoelectron spectroscopy[J]. Rsc Advances，2013，3(24): 9436-9445.

[36] MEN S，LOVELOCK K R J，LICENCE P. Directly probing the effect of the solvent on a

catalyst electronic environment using X-ray photoelectron spectroscopy[J]. Rsc Advances，2015，5(45): 35958-35965.

[37] VILLAR-GARCIA I J，LOVELOCK K R J，MEN S，et al. Tuning the electronic environment of cations and anions using ionic liquid mixtures[J]. Chemical Science，2014，5(6): 2573-2579.

[38] CHIAPPE C，PIERACCINI D. Ionic liquids: solvent properties and organic reactivity[J]. Journal of Physical Organic Chemistry，2005，18(4): 275-297.

[39] SHIM Y，JEONG D，MANJARI S，et al. Solvation，solute rotation and vibration relaxation，and electron-transfer reactions in room-temperature ionic liquids[J]. Acc. Chem. Res.，2007，40(11): 1130-1137.

[40] KOBRAK M N. A comparative study of solvation dynamics in room-temperature ionic liquids[J]. Journal of Chemical Physics，2007，127(18): 184507.

[41] HARDACRE C，HOLBREY J D，NIEUWENHUYZEN M，et al. Structure and solvation in ionic liquids[J]. Acc. Chem. Res.，2007，40(11): 1146-1155.

[42] CROWHURST L，MAWDSLEY P R，PEREZ-ARLANDIS J M，et al. Solvent-solute interactions in ionic liquids[J]. Physical Chemistry Chemical Physics，2003，5(13): 2790-2794.

[43] CASTNER E W，WISHART J F，SHIROTA H. Intermolecular dynamics，interactions，and solvation in ionic liquids[J]. Acc. Chem. Res.，2007，40(11): 1217-1227.

[44] CADENA C，ANTHONY J L，SHAH J K，et al. Why is CO2 so soluble in imidazolium-based ionic liquids?[J]. Journal of the American Chemical Society，2004，126(16): 5300-5308.

[45] ANDERSON J L，DING J，WELTON T，et al. Characterizing ionic liquids on the basis of multiple solvation interactions[J]. Journal of the American Chemical Society，2002，124(47): 14247-14254.

[46] ABRAHAM M H，ZISSIMOS A M，HUDDLESTON J G，et al. Some novel liquid partitioning systems: Water-ionic liquids and aqueous biphasic systems[J]. Industrial & Engineering Chemistry Research，2003，42(3): 413-418.

[47] SELLIN M F，WEBB P B，COLE-HAMILTON D J. Continuous flow homogeneous catalysis: hydroformylation of alkenes in supercritical fluid-ionic liquid biphasic mixtures[J]. Chemical Communications，2001(8): 781-782.

[48] WEBB P B，SELLIN M F，KUNENE T E，et al. Continuous flow hydroformylation of

alkenes in supercritical fluid-ionic liquid biphasic systems[J]. Journal of the American Chemical Society，2003，125(50): 15577-15588.

[49] HINTERMAIR U，ZHAO G Y，SANTINI C C，et al. Supported ionic liquid phase catalysis with supercritical flow[J]. Chemical Communications，2007(14): 1462-1464.

[50] MOULDER J F，STICKLE W F，SOBOL P E，et al. Handbook of X-ray Photoelectron Spectroscopy: a reference book of standard spectra for identification and interpretation of XPS data[M]. Chanhassen: Physical Electronics，1995.

[51] EVANS J，HAYDEN B E，NEWTON M A. A comparison of the chemistry of $Rh(I)(acac)(CO)_2$ and $Rh(I)(CO)_2Cl$ adsorbed on TiO_2[110]: development of particulate Rh and oxidative disruption by CO[J]. Surface Science，2000，462(1-3): 169-180.

[52] JUEL M，SAMUELSEN B T，KILDEMO M，et al. Surface alloy formation after deposition of Ce on Rh(110)[J]. Surface Science，2007，601(14): 2917-2923.

[53] CHAUVIN Y，OLIVIERBOURBIGOU H. Nonaqueous Ionic Liquids as Reaction Solvents[J]. Chemtech，1995，25(9): 26-30.

[54] NOCKEMANN P，THIJS B，PITTOIS S，et al. Task-specific ionic liquid for solubilizing metal oxides[J]. Journal of Physical Chemistry B，2006，110(42): 20978-20992.

[55] EINLOFT S，DIETRICH F K，DESOUZA R F，et al. Selective two-phase catalytic ethylene dimerization by Ni-II complexes/$AlEtCl_2$ dissolved in organoaluminate ionic liquids[J]. Polyhedron，1996，15(19): 3257-3259.

[56] FEI Z，GELDBACH T J，ZHAO D，et al. From dysfunction to bis-function: On the design and applications of functionalised ionic liquids[J]. Chemistry-a European Journal，2006，12(8): 2123-2130.

[57] LEE S G. Functionalized imidazolium salts for task-specific ionic liquids and their applications[J]. Chemical Communications，2006(10): 1049-1063.

[58] WASSERSCHEID P，WAFFENSCHMIDT H，MACHNITZKI P，et al. Cationic phosphine ligands with phenylguanidinium modified xanthene moieties - a successful concept for highly regioselective，biphasic hydroformylation of 1-octene in hexafluorophosphate ionic liquids[J]. Chemical Communications，2001(5): 451-452.

[59] FAVRE F，OLIVIER-BOURBIGOU H，COMMEREUC D，et al. Hydroformylation of 1-hexene with rhodium in non-aqueous ionic liquids: how to design the solvent and the ligand to the reaction[J]. Chemical Communications，2001(15): 1360-1361.

[60] SMITH E F，RUTTEN F J M，VILLAR-GARCIA I J，et al. Ionic liquids in vacuo: Analysis

of liquid surfaces using ultra-high-vacuum techniques[J]. Langmuir，2006，22(22): 9386-9392.

[61] MEN S，LOVELOCK K R J，LICENCE P. X-ray Photoelectron Spectroscopy of Pyrrolidinium-Based Ionic Liquids: Cation-Anion Interactions and a Comparison to Imidazolium-Based Analogues[J]. Physical Chemistry Chemical Physics，2011，13(33): 15244-15255.

[62] VILLAR-GARCIA I J，SMITH E F，TAYLOR A W，et al. Charging of ionic liquid surfaces under X-ray irradiation: the measurement of absolute binding energies by XPS[J]. Physical Chemistry Chemical Physics，2011，13(7): 2797-2808.

[63] FAIRLEY N，CARRICK A. The Casa Cookbook[M]. Knutsford: Acolyte Science，2005.

[64] HURISSO B B，LOVELOCK K R J，LICENCE P. Amino Acid-Based Ionic Liquids: Using XPS to Probe the Electronic Environment via Binding Energies[J]. Physical Chemistry Chemical Physics，2011，13: 17737-17748.

[65] PRUCHNIK F P，SMOLENSKI P，WAJDA-HERMANOWICZ K. Rhodium(I) acetylacetonato complexes with functionalized phosphines[J]. Journal of Organometallic Chemistry，1998，570(1): 63-69.

[66] KUHL O. Predicting the net donating ability of phosphines - do we need sophisticated theoretical methods?[J]. Coordination Chemistry Reviews，2005，249(5-6): 693-704.

[67] VAN ROOY A，KAMER P C J，VAN LEEUWEN P，et al. Bulky diphosphite-modified rhodium catalysts: Hydroformylation and characterization[J]. Organometallics，1996，15(2): 835-847.

[68] LUNGWITZ R，STREHMEL V，SPANGE S. The dipolarity/polarisability of 1-alkyl-3-methylimidazolium ionic liquids as function of anion structure and the alkyl chain length[J]. New Journal of Chemistry，2010，34(6): 1135-1140.

[69] LIN-VIEN D，COLTHUP N B，FATELEY W G，et al. Infrared and Raman Characteristic frequencies of Organic Molecules[M]. London: Academic Press，Inc.，1991.

[70] MEN S，LOVELOCK K R J，LICENCE P. X-ray photoelectron spectroscopy as a probe of rhodium-ligand interaction in ionic liquids[J]. Chemical Physics Letters，2016，645: 53-58.

Appendix A

XP Spectra

1 XP spectra with component fittings of $[C_8C_1Im][Tf_2N]$ for: (a) survey, (b) C 1s, (c) N 1s, (d) F 1s, (e) O 1s and (f) S 2p.

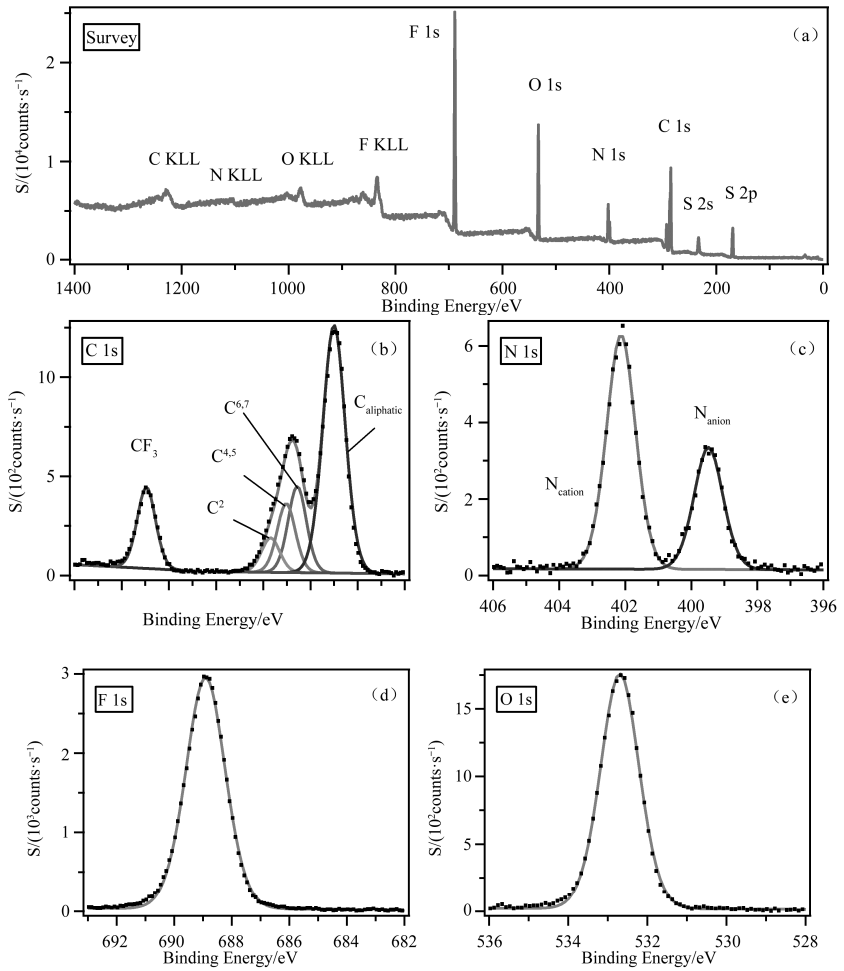

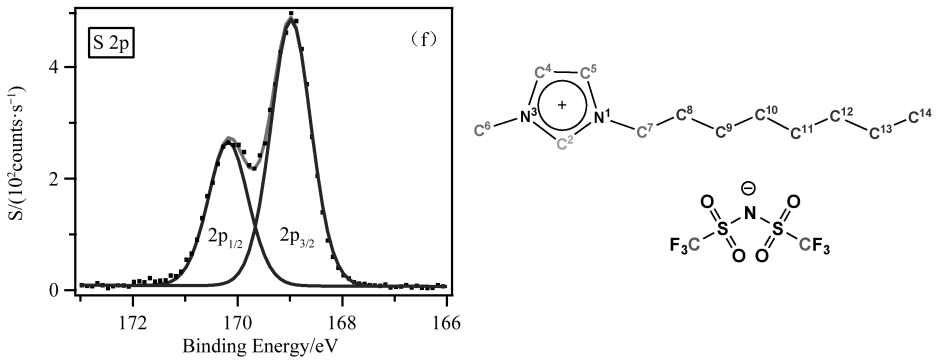

XP spectra with component fittings of $[C_8C_1Im][I_3]$ for: (a) survey, (b) C 1s, (c) N 1s and (d) I 3d.

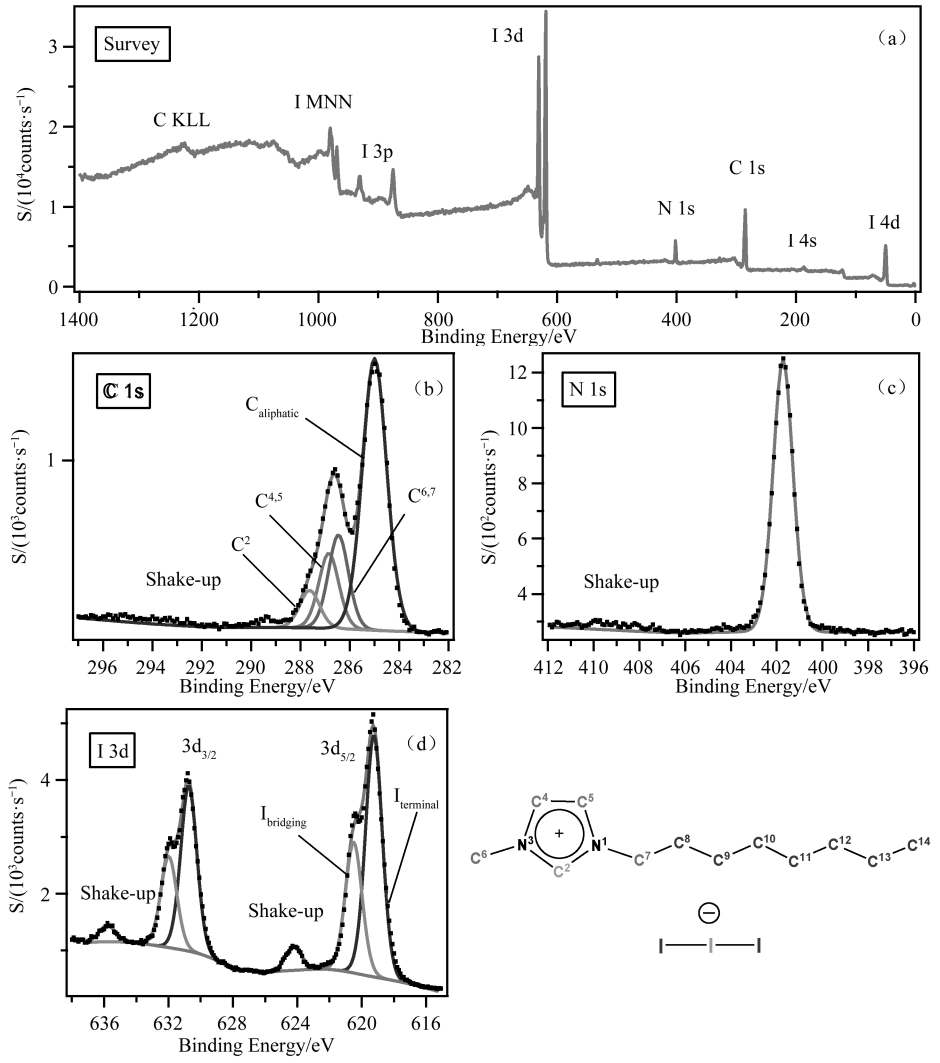

XP spectra with component fittings of $[C_8C_1Im][IBr_2]$ for: (a) survey, (b) I 3d5/2 (c) Br 3d, (d)C 1s and (e) N 1s.

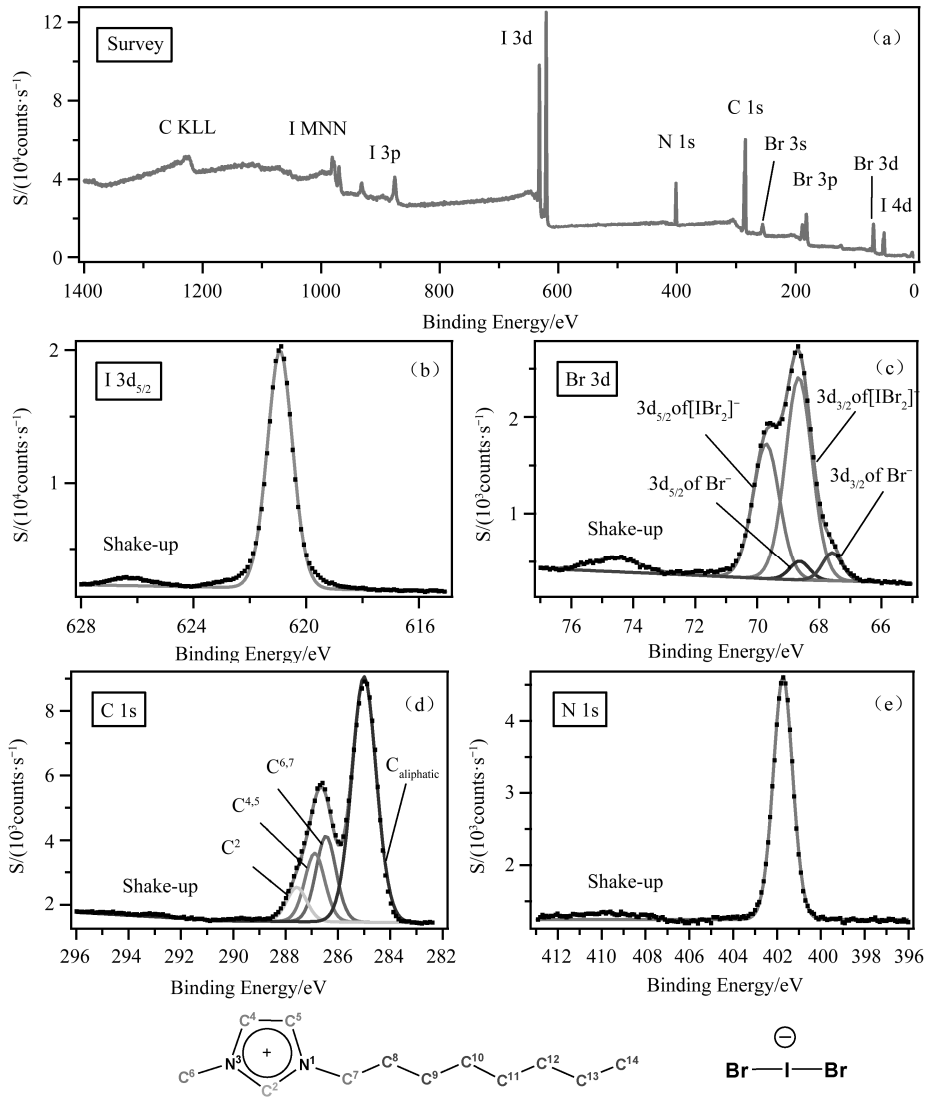

2 XP spectra with component fittings of [C_8C_1Im][OAc] for: (a) survey, (b) C 1s, (c) N 1s and (d) O 1s.

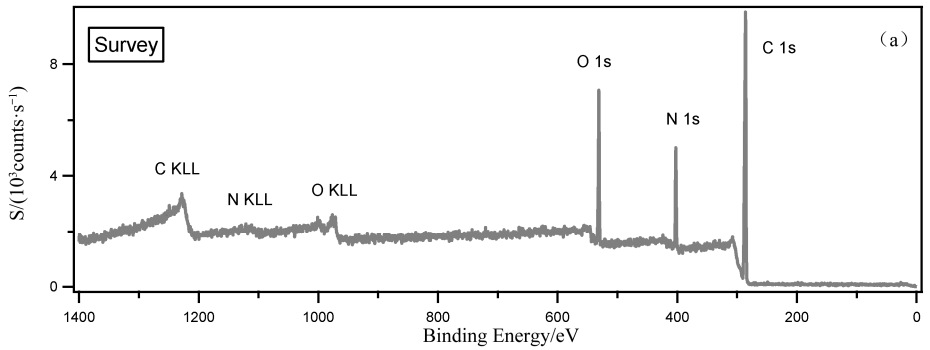

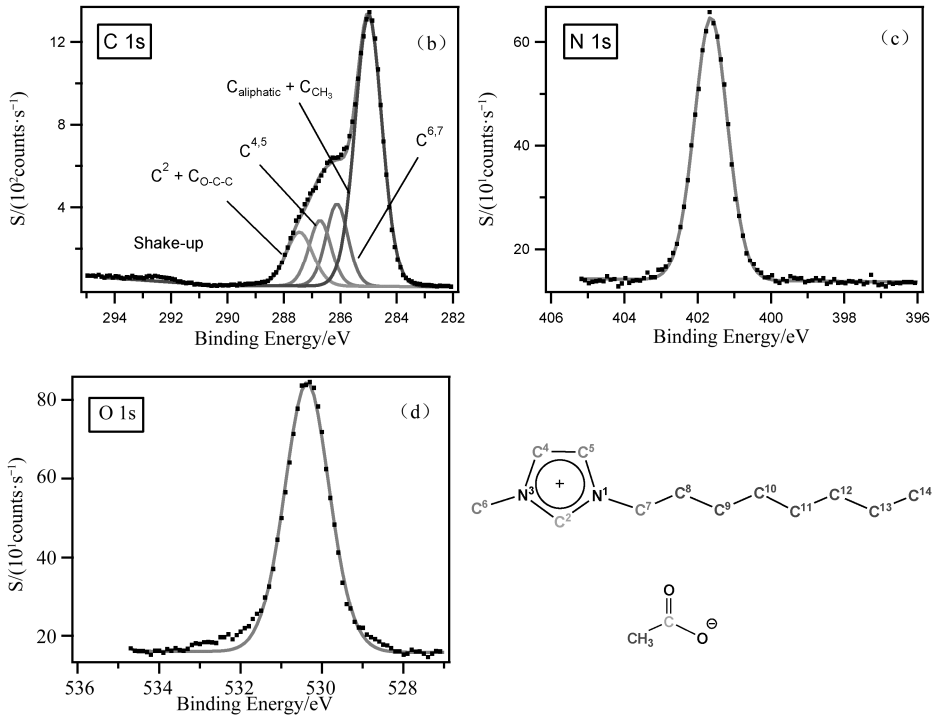

3 XP spectra with component fittings of $[C_8C_1Pyrr][Tf_2N]$ for: (a) survey, (b) C 1s, (c) N 1s, (d) F 1s, (e) O 1s and (f) S 2p.

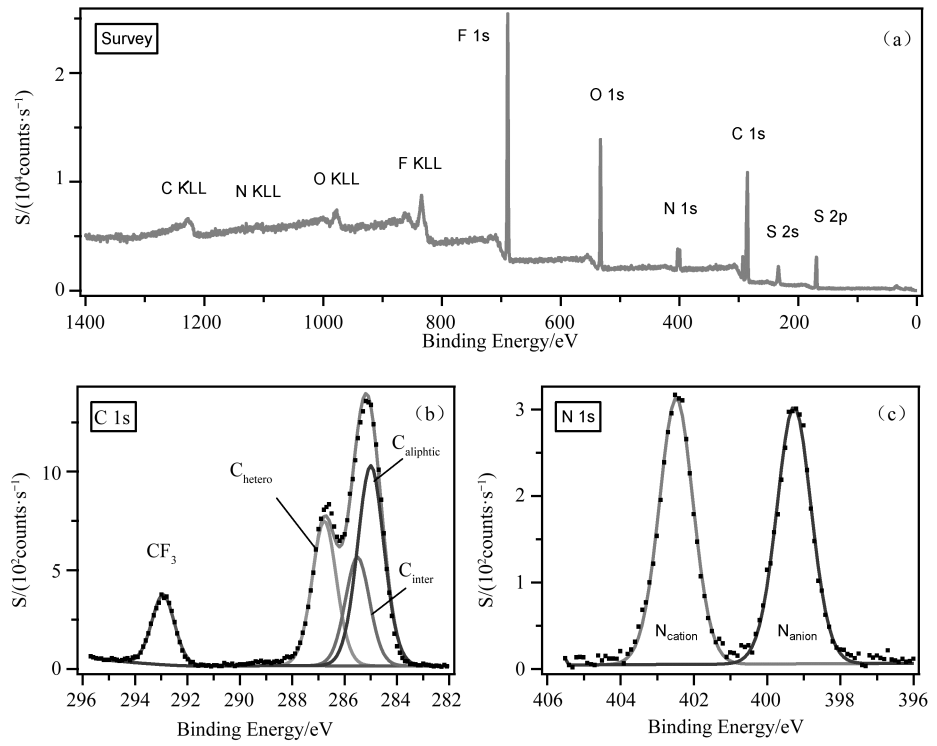

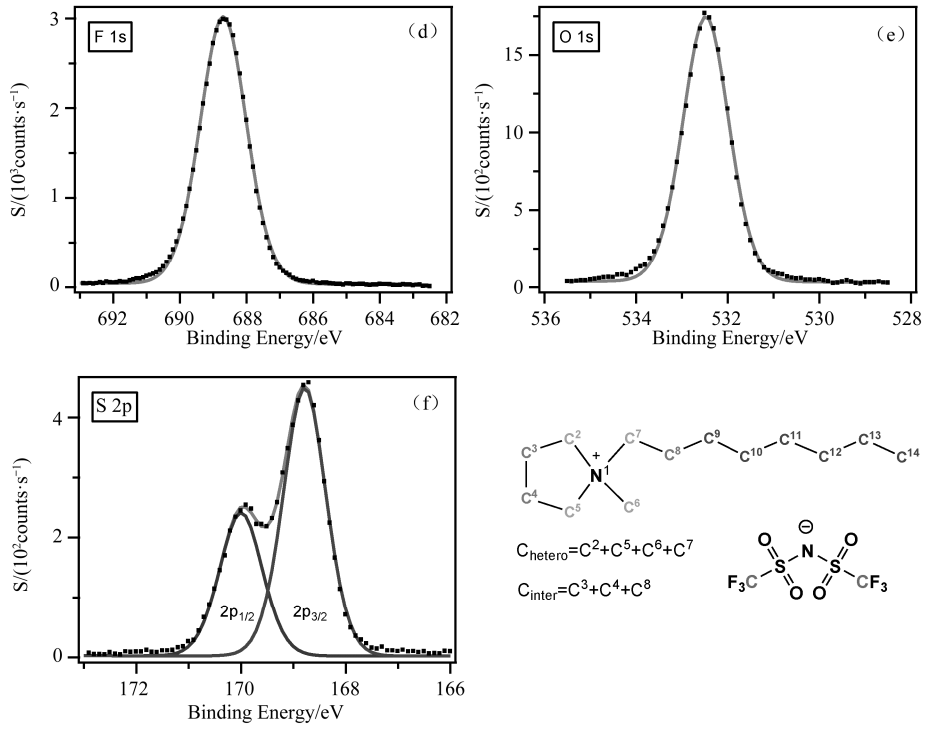

4 XP spectra with component fittings of $[C_8C_1Pyrr][BF_4]$ for: (a) survey, (b) C 1s, (c) N 1s, (d) F 1s and (e) B 1s.

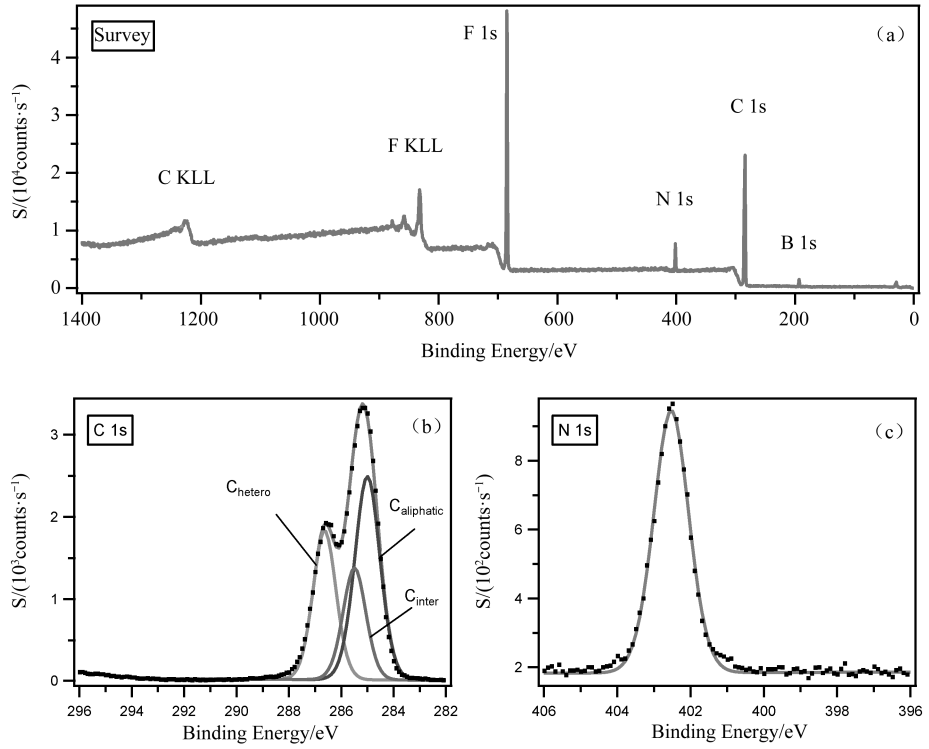

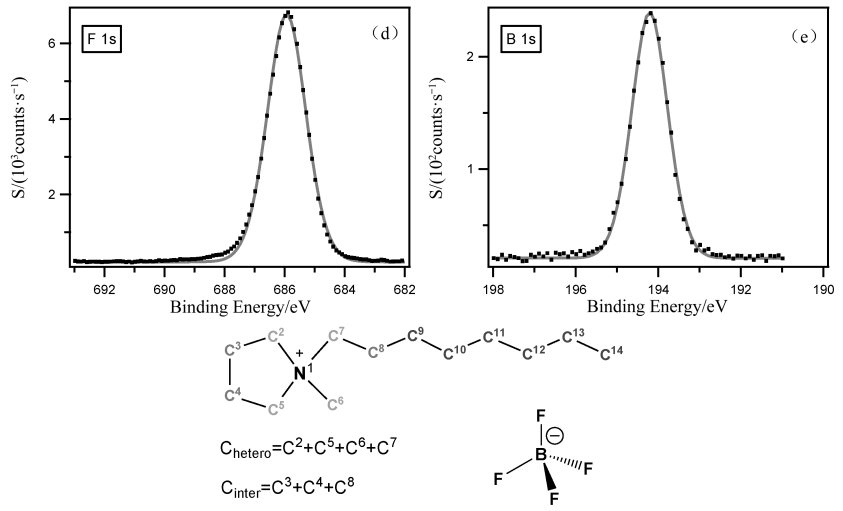

5 XP spectra with component fittings of $[C_8C_1Pyrr]I$ for: (a) survey, (b) C 1s, (c) N 1s and (d) I 3d.

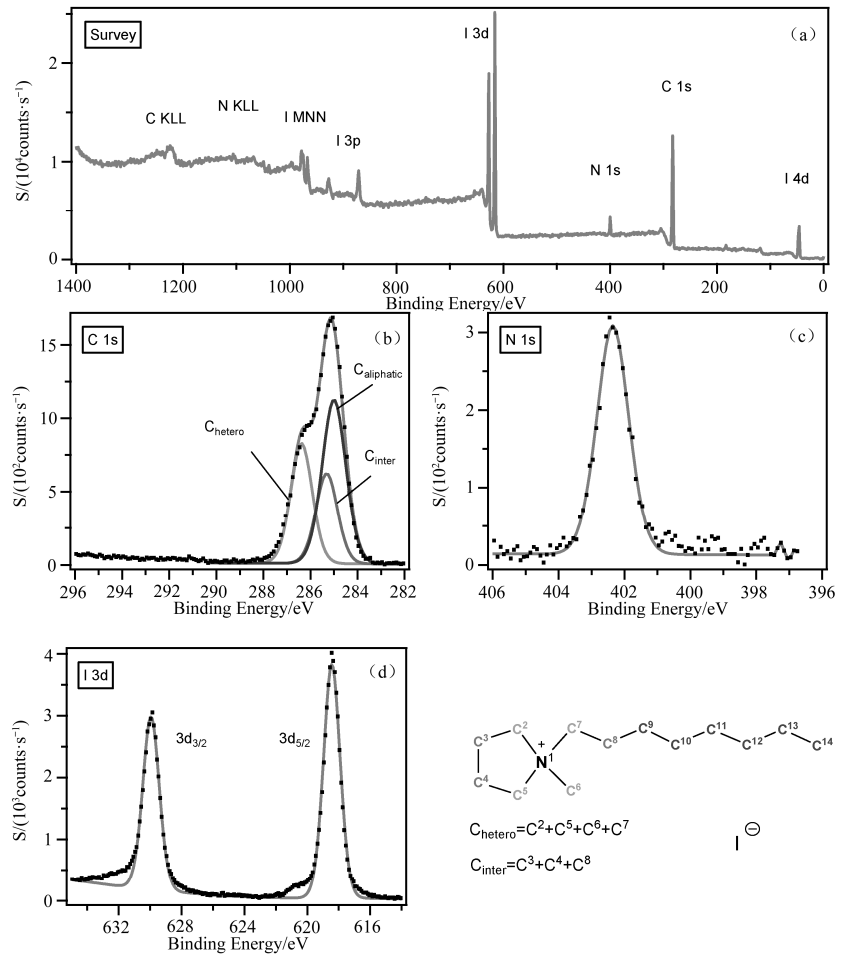

6 XP spectra with component fittings of $[C_8Py][Tf_2N]$ for: (a) survey, (b) C 1s, (c) N 1s, (d) F 1s, (e) O 1s and (f) S 2p.

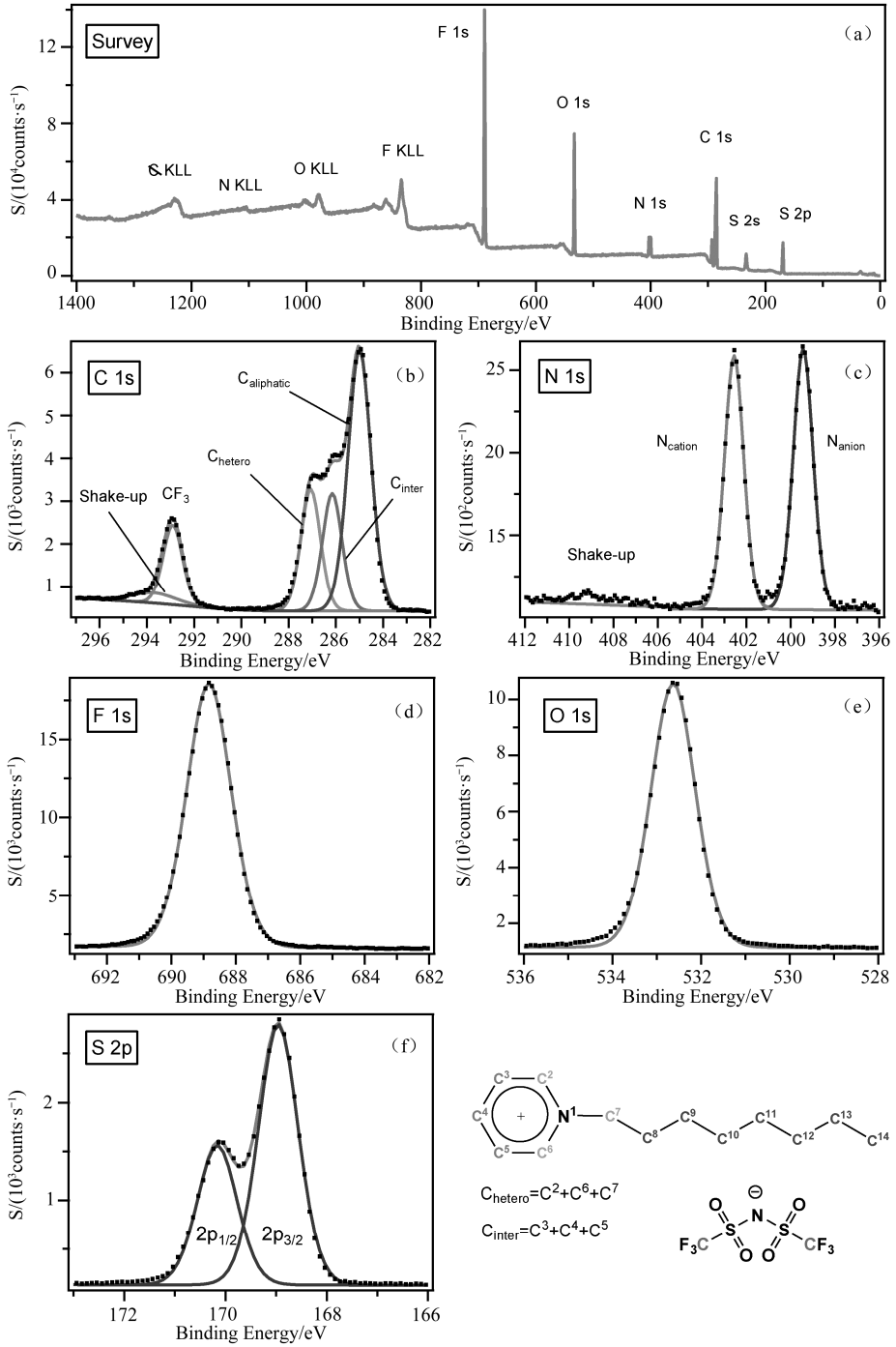

7 XP spectra with component fittings of $[C_8Py][PF_6]$ for: (a) survey, (b) C 1s, (c) N 1s, (d) F 1s, (e) P 2p.

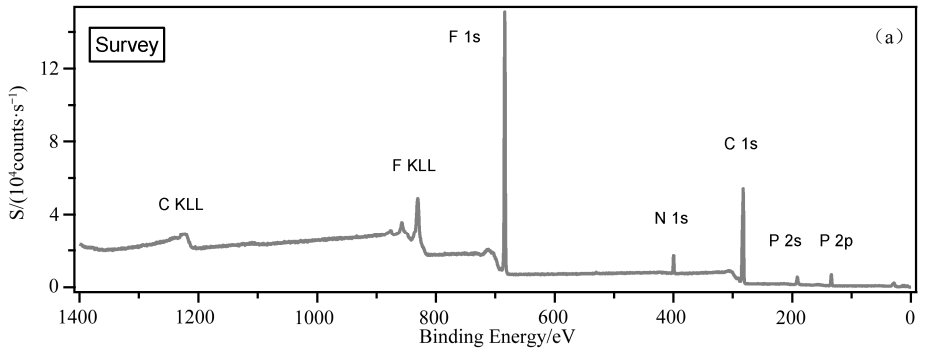

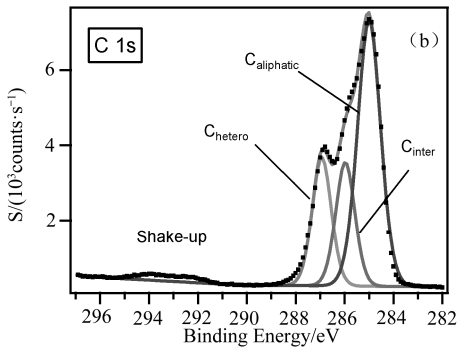

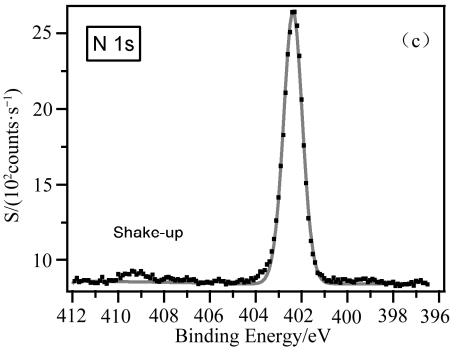

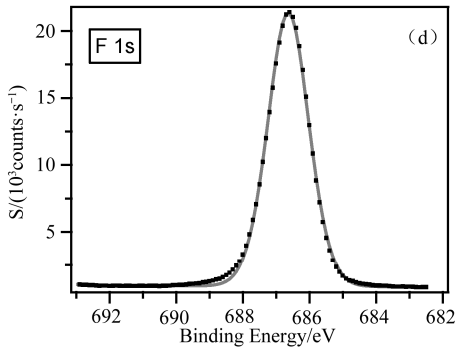

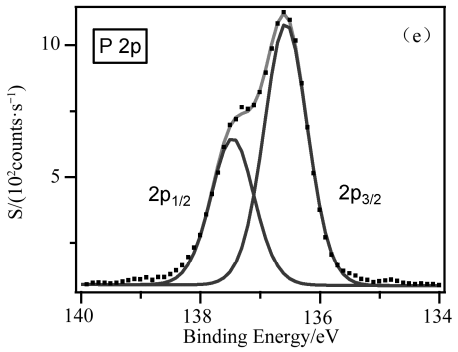

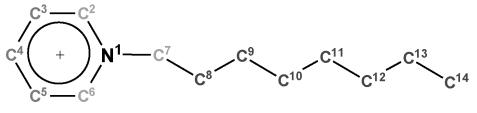

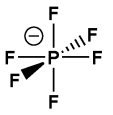

$C_{hetero}=C^2+C^6+C^7$

$C_{inter}=C^3+C^4+C^5$

8 XP spectra with component fittings of $[C_8Py][TfO]$ for: (a) survey, (b) C 1s, (c) N 1s, (d) F 1s, (e) O 1s and (f) S 2p.

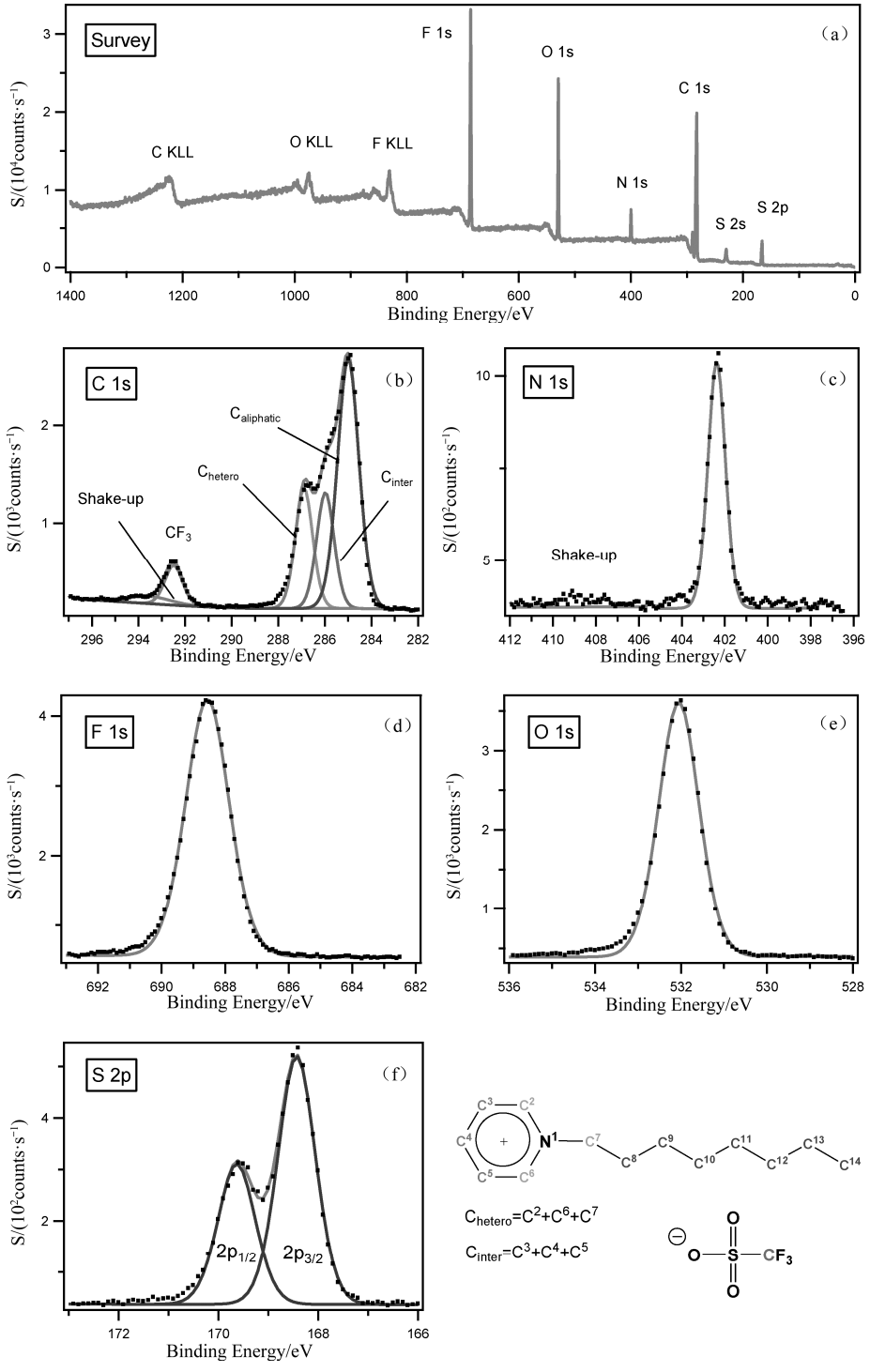

9 XP spectra with component fittings of $[C_8Py][BF_4]$ for: (a) survey, (b) C 1s, (c) N 1s, (d) F 1s and (e) B 1s.

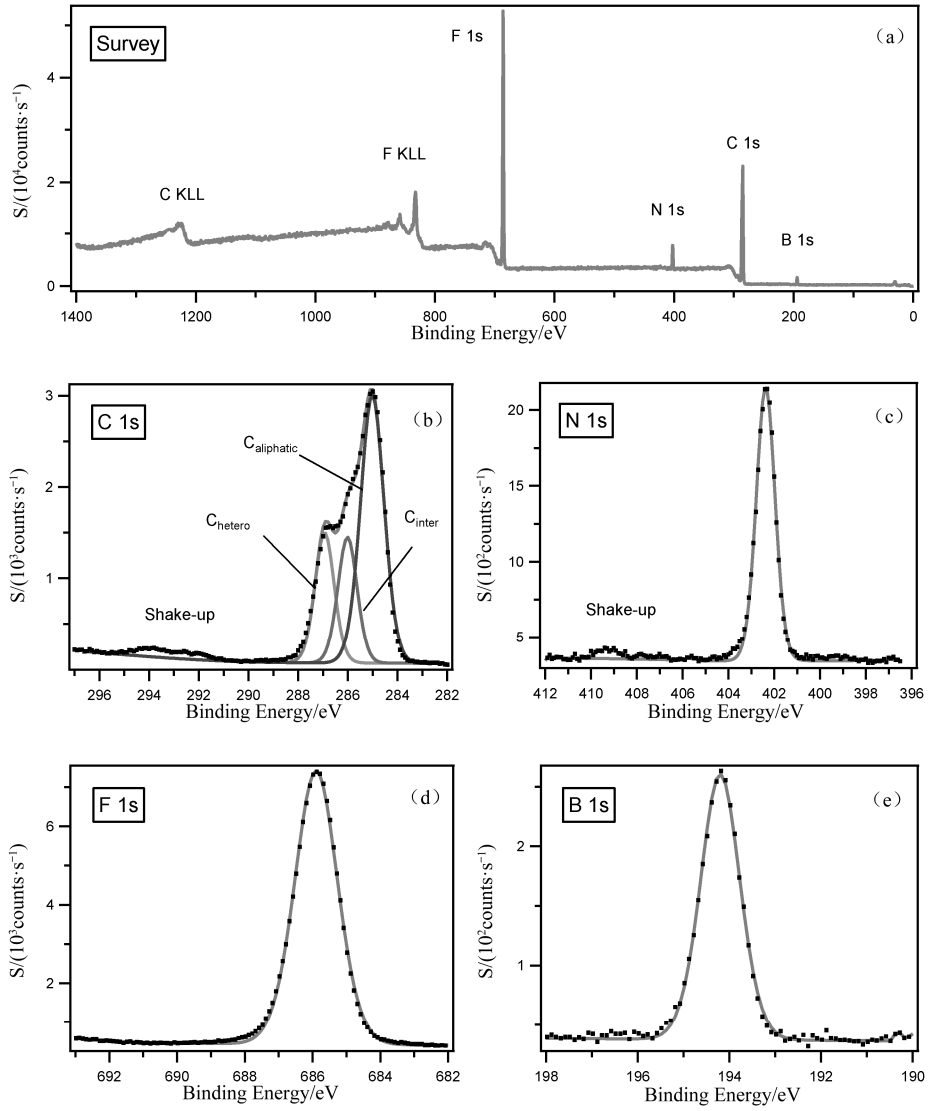

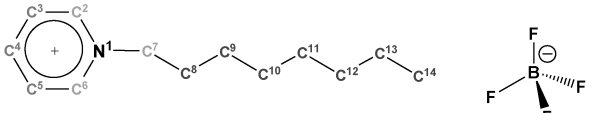

$C_{hetero}=C^2+C^6+C^7$

$C_{inter}=C^3+C^4+C^5$

10 XP spectra with component fittings of [C_8Py]I for: (a) survey, (b) C 1s, (c) N 1s and (d) I 3d.

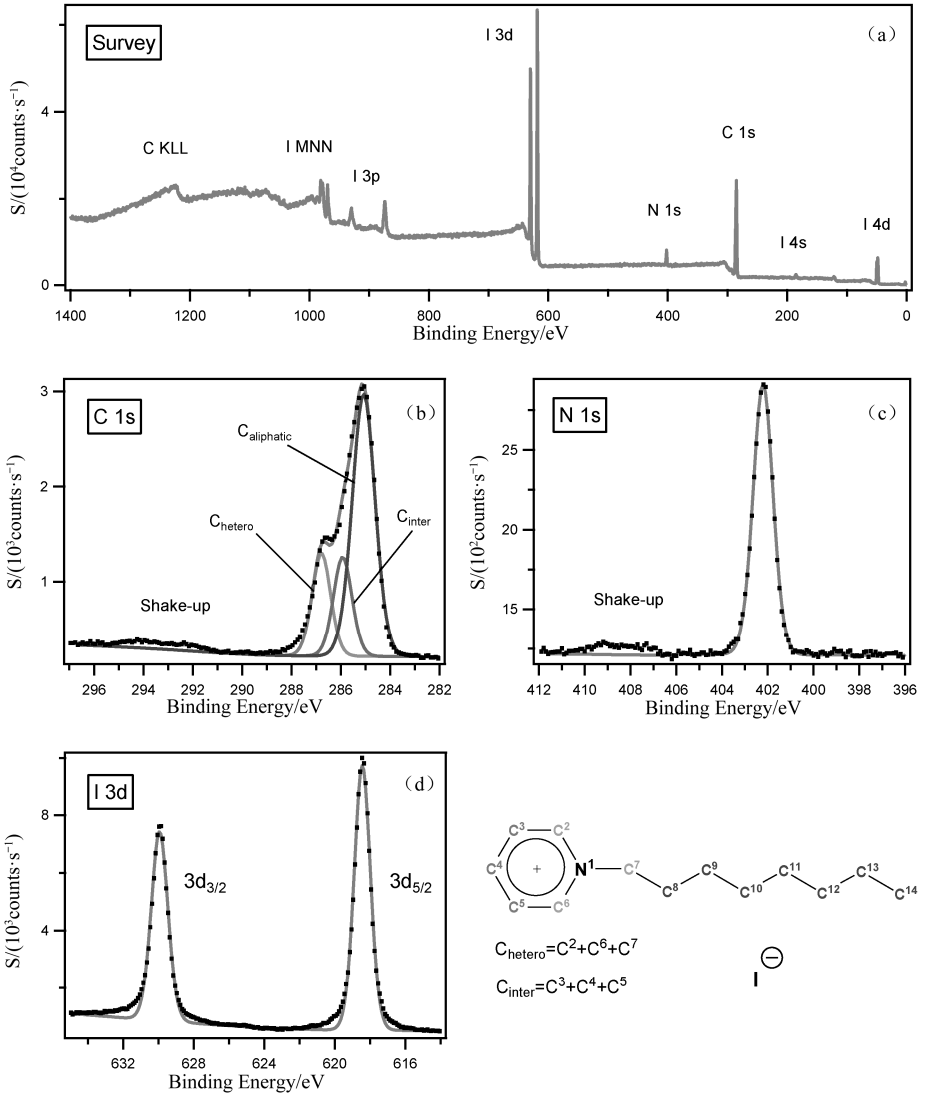

11 XP spectra with component fittings of [C_8Py]Br for: (a) survey, (b) C 1s, (c) N 1s, (d) Br 3d.

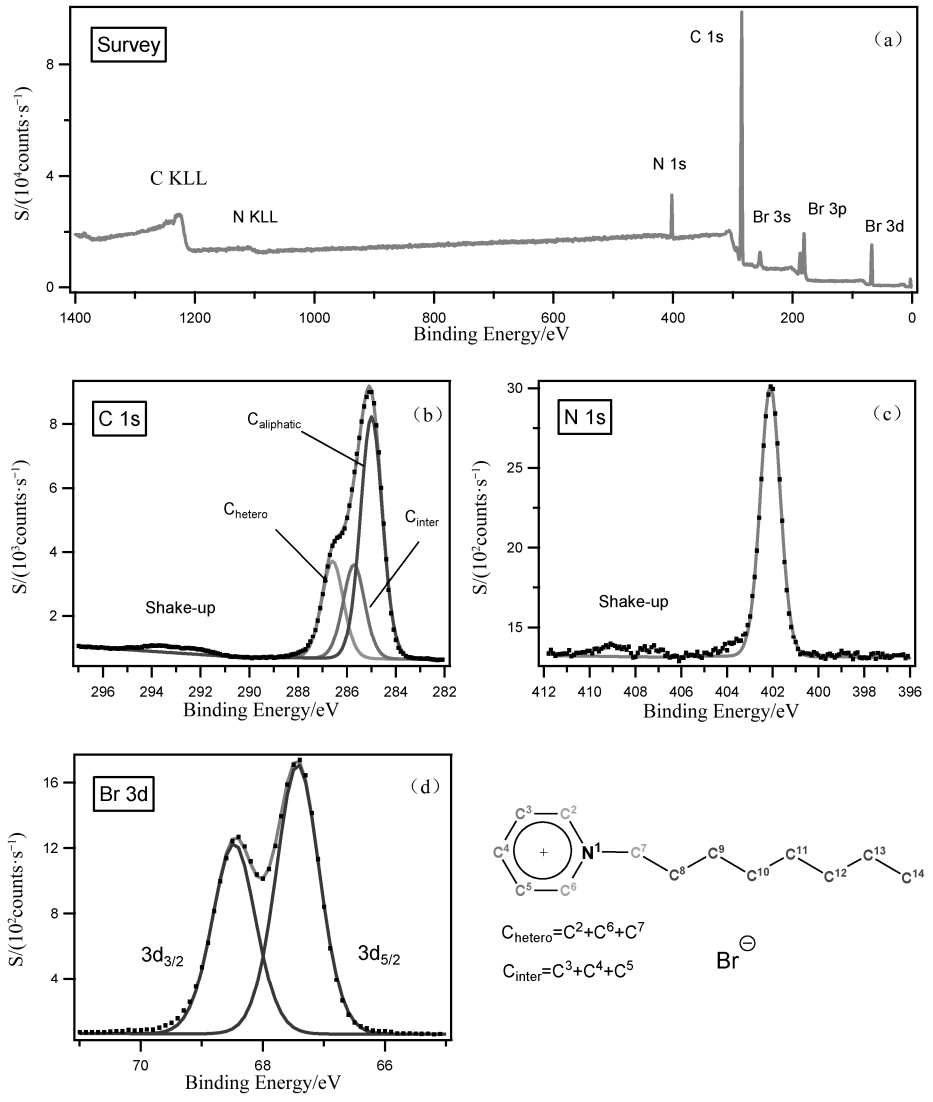

12 XP spectra with component fittings of phoshineimidazolylidene palladium complex in $[C_8C_1Im][Tf_2N]$ for : (a) survey, (b) C 1s, (c) N 1s, (d) F 1s, (e) O 1s, (f) S 2p and (g) Pd 3d.

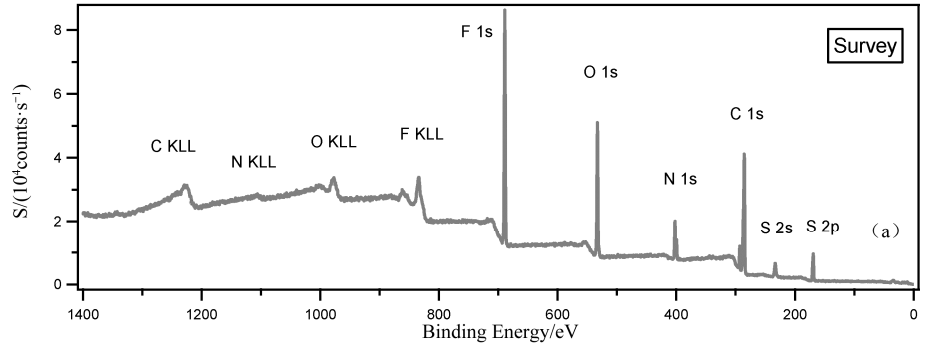

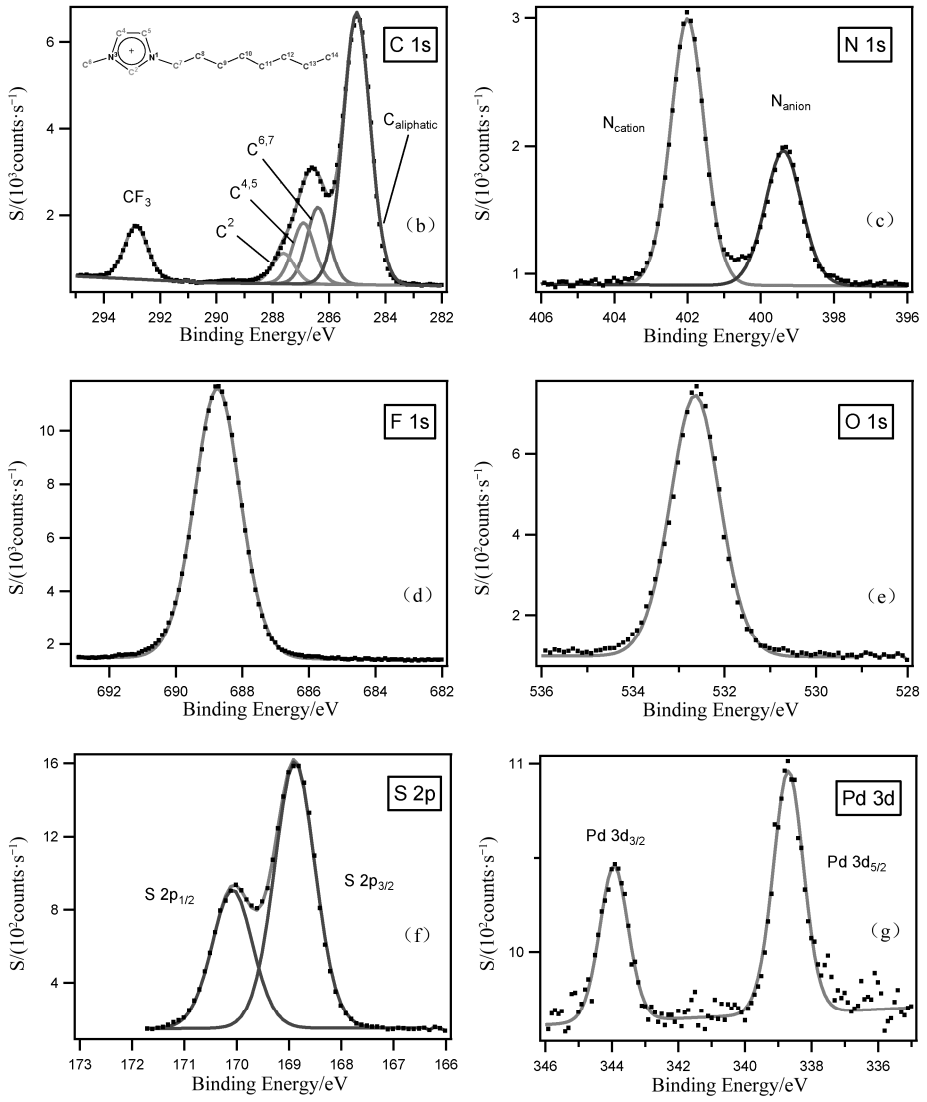

13 XP spectra with component fittings of phoshineimidazolylidene palladium complex in $[C_8C_1Im][TfO]$ for : (a) survey, (b) C 1s, (c) N 1s, (d) F 1s, (e) O 1s, (f) S 2p and (g) Pd 3d.

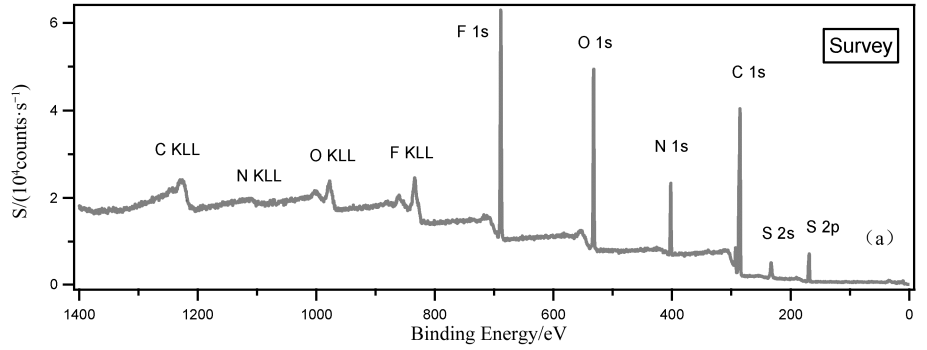

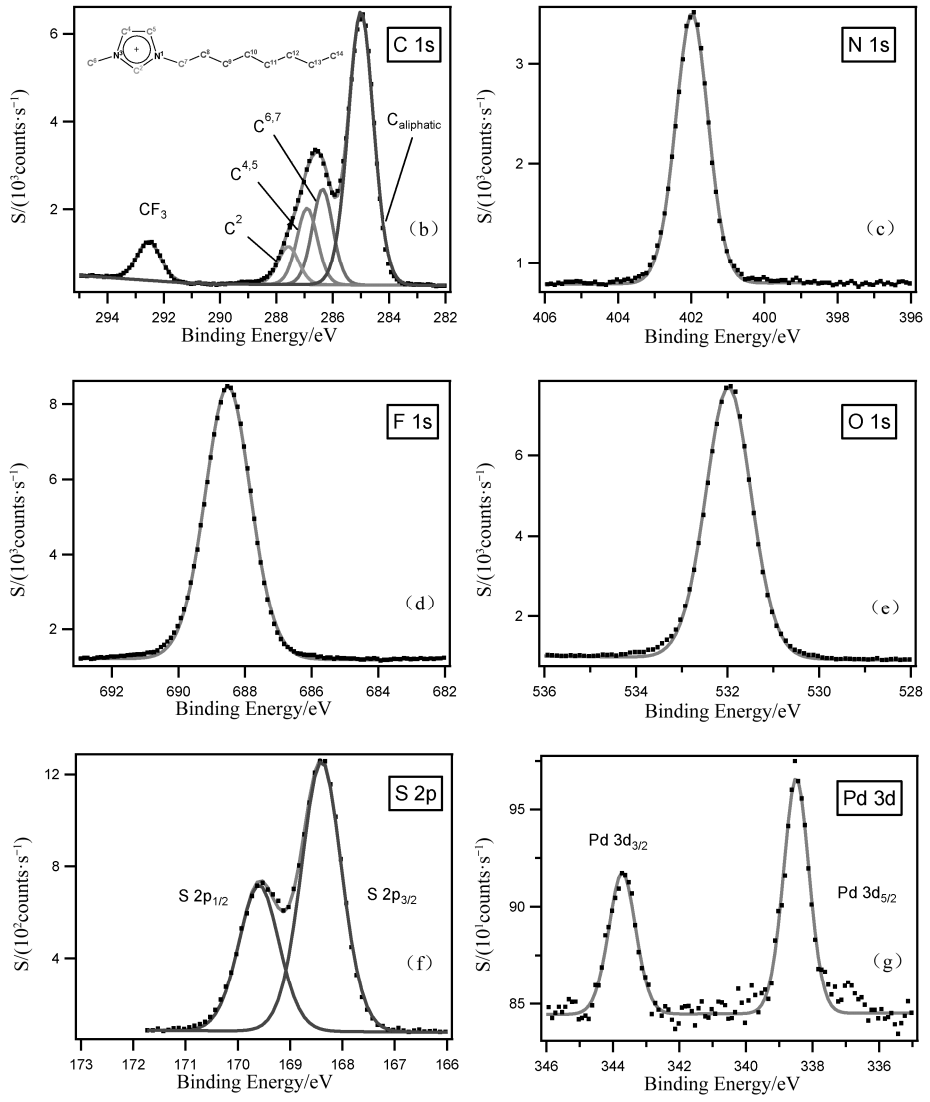

14 XP spectra with component fittings of phoshineimidazolylidene palladium complex in $[C_8C_1Im][BF_4]$ for : (a) survey, (b) C 1s, (c) N 1s, (d) F 1s, (e) B 1s and (f) Pd 3d.

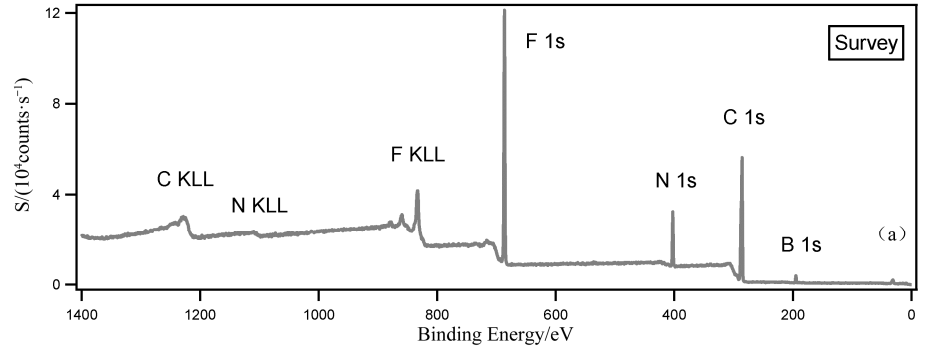

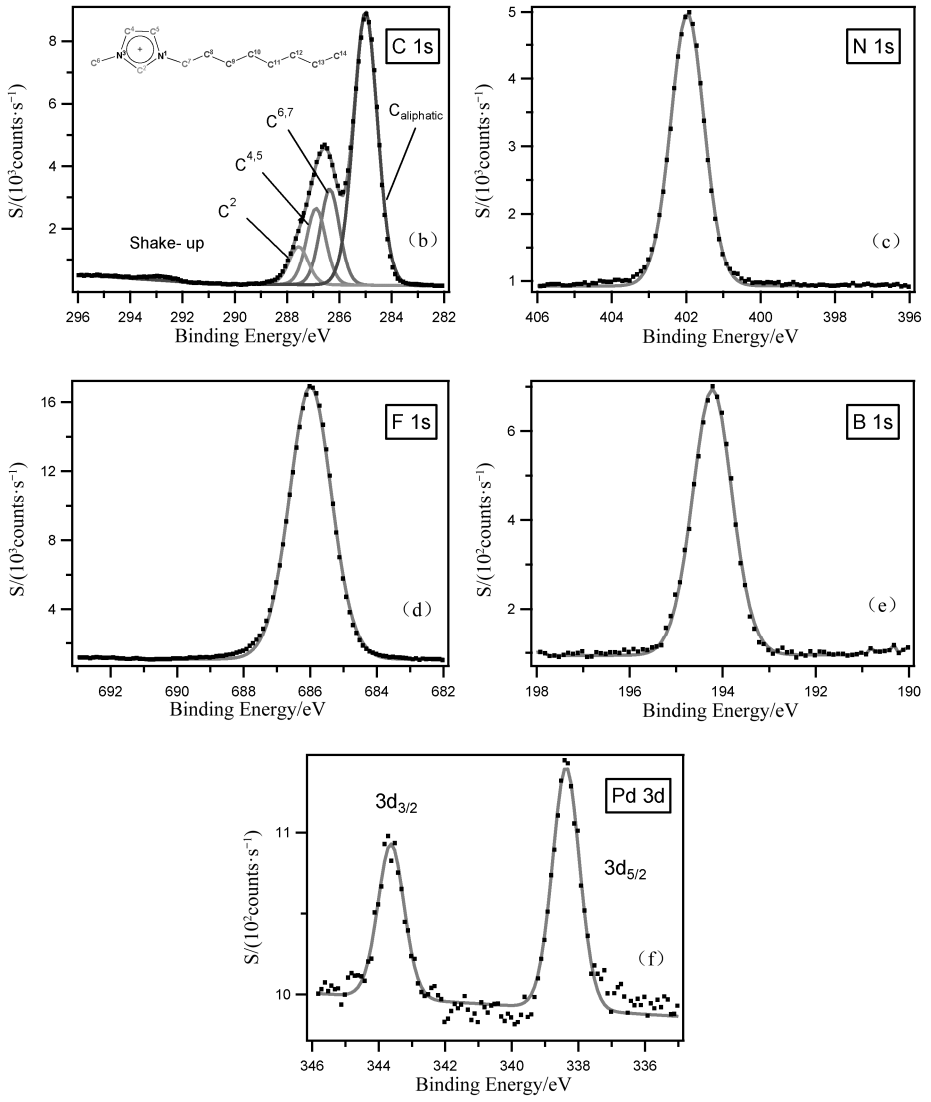

15 XP spectra with component fittings of phoshineimidazolylidene palladium complex in $[C_8C_1Im]Cl$ for : (a) survey, (b) C 1s, (c) N 1s, (d) Cl 2p and (e) Pd 3d.

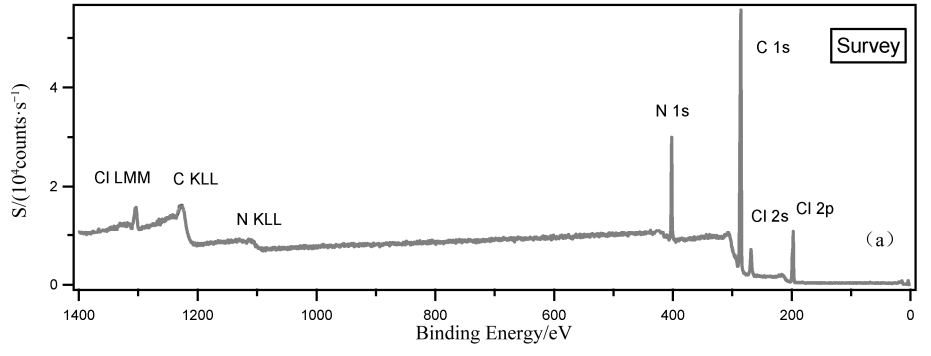

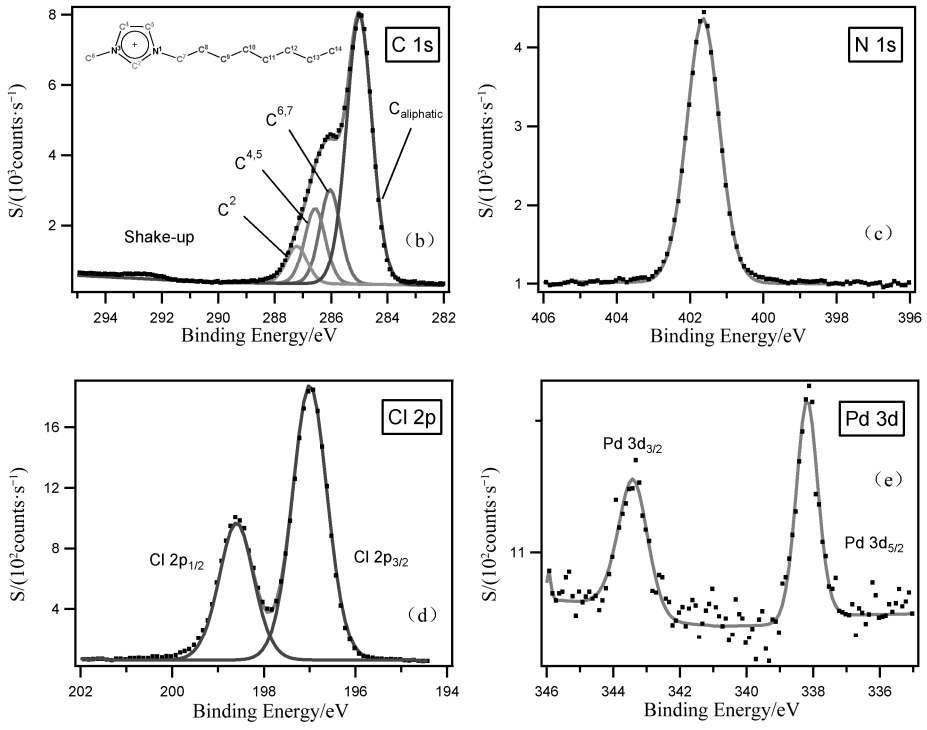

16 XP spectra with component fittings of phoshineimidazolylidene palladium complex in $[C_8C_1Im][OAc]$ for : (a) survey, (b) C 1s, (c) N 1s, (d) O 1s and (e) Pd 3d.

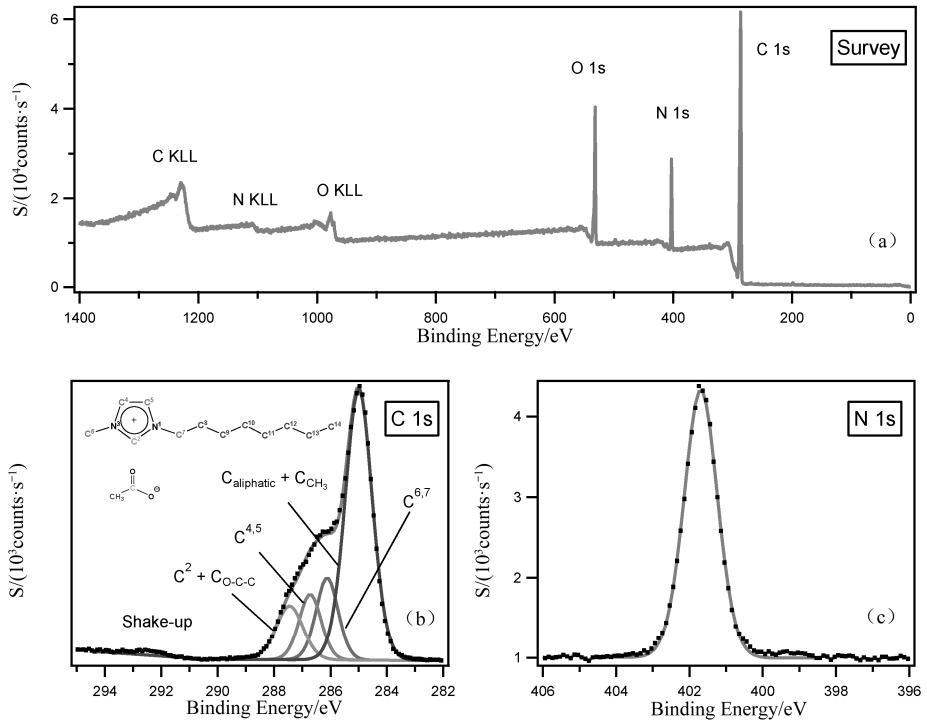

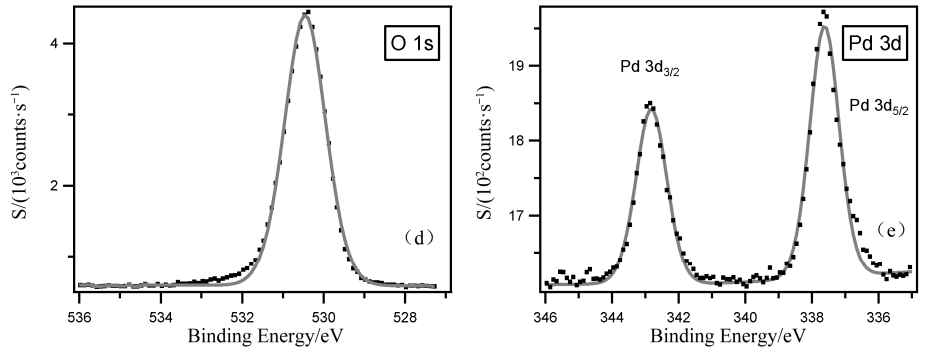

17 XP spectra with component fittings of $[Rh(acac)(CO)_2]$ plus PPh_3 in $[C_8C_1Im][Tf_2N]$ for: (a) survey, (b) C 1s, (c) N 1s, (d) F 1s, (e) O 1s (f) S 2p and (g) Rh 3d.

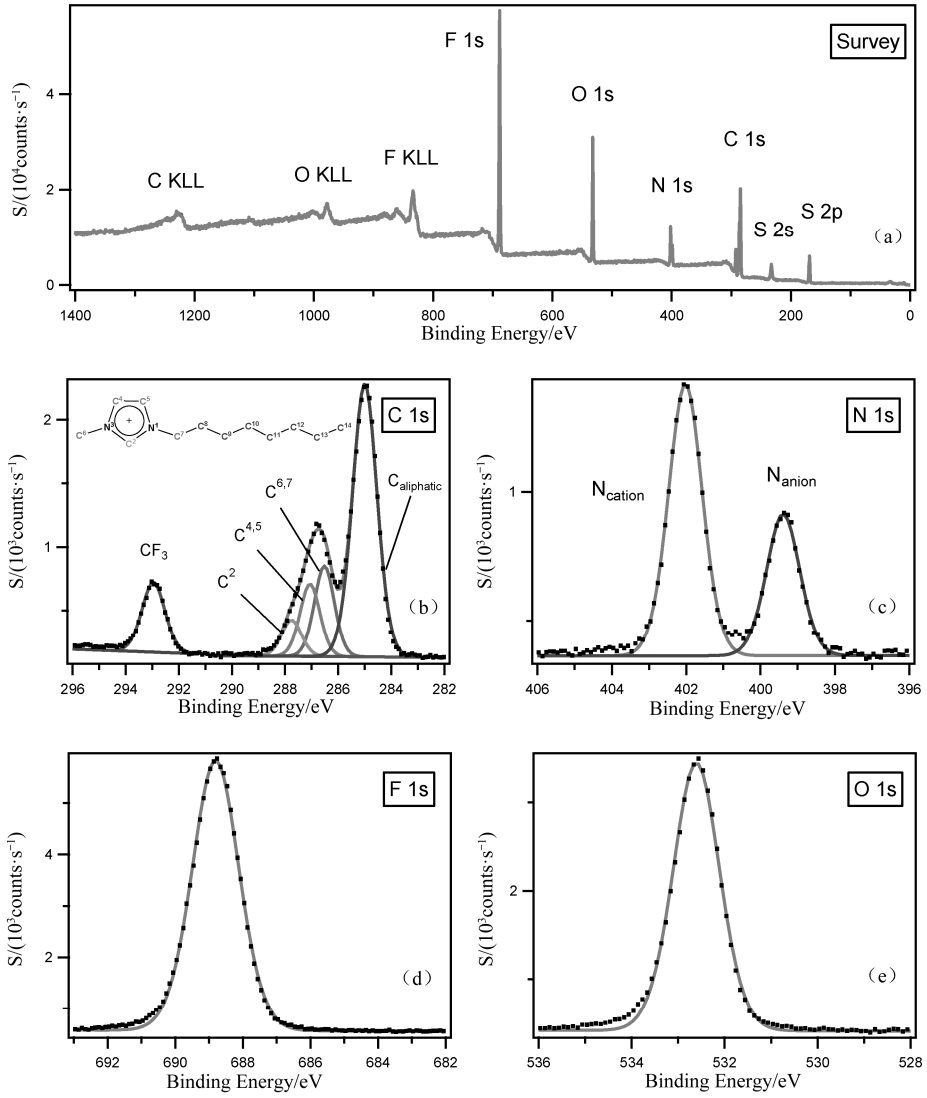

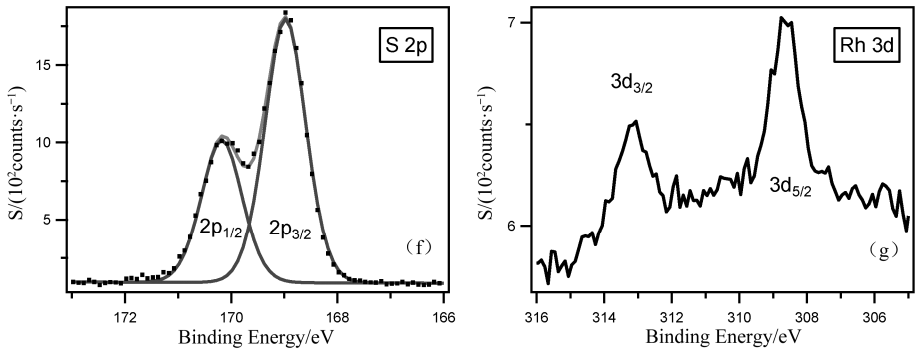

18 XP spectra with component fittings of $[Rh(acac)(CO)_2]$ plus PPh_3 in $[C_8C_1Im][PF_6]$ for: (a) survey, (b) C 1s, (c) N 1s, (d) F 1s, (e) P 2p and (f) Rh 3d.

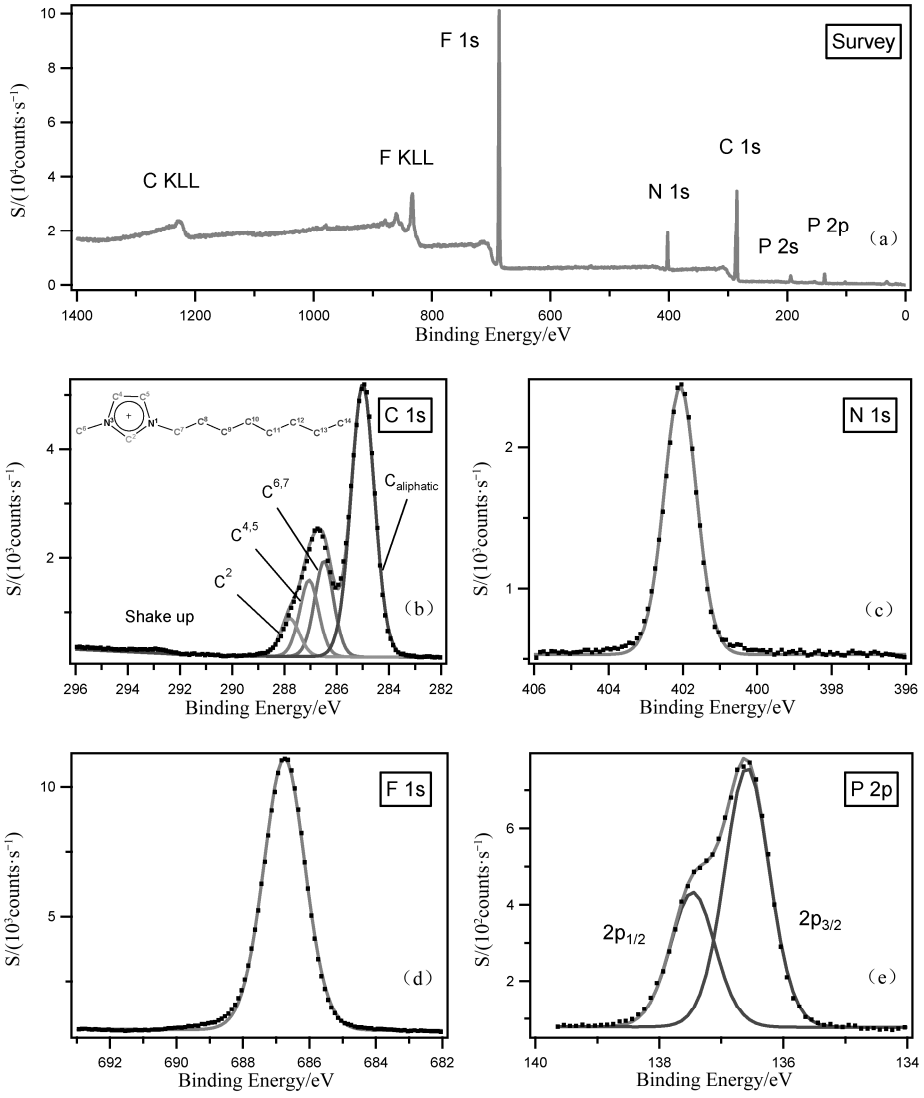

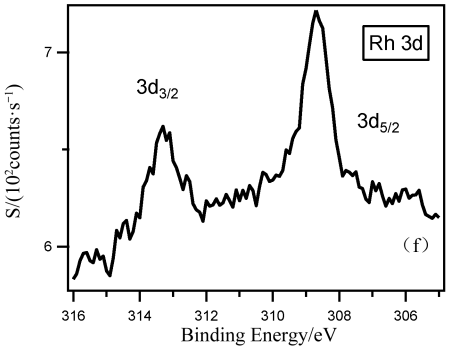

19 XP spectra with component fittings of [Rh(acac)(CO)$_2$] plus PPh_3 in [C_8C_1Im][TfO] for: (a) survey, (b) C 1s, (c) N 1s, (d) F 1s, (e) O 1s (f) S 2p and (g) Rh 3d.

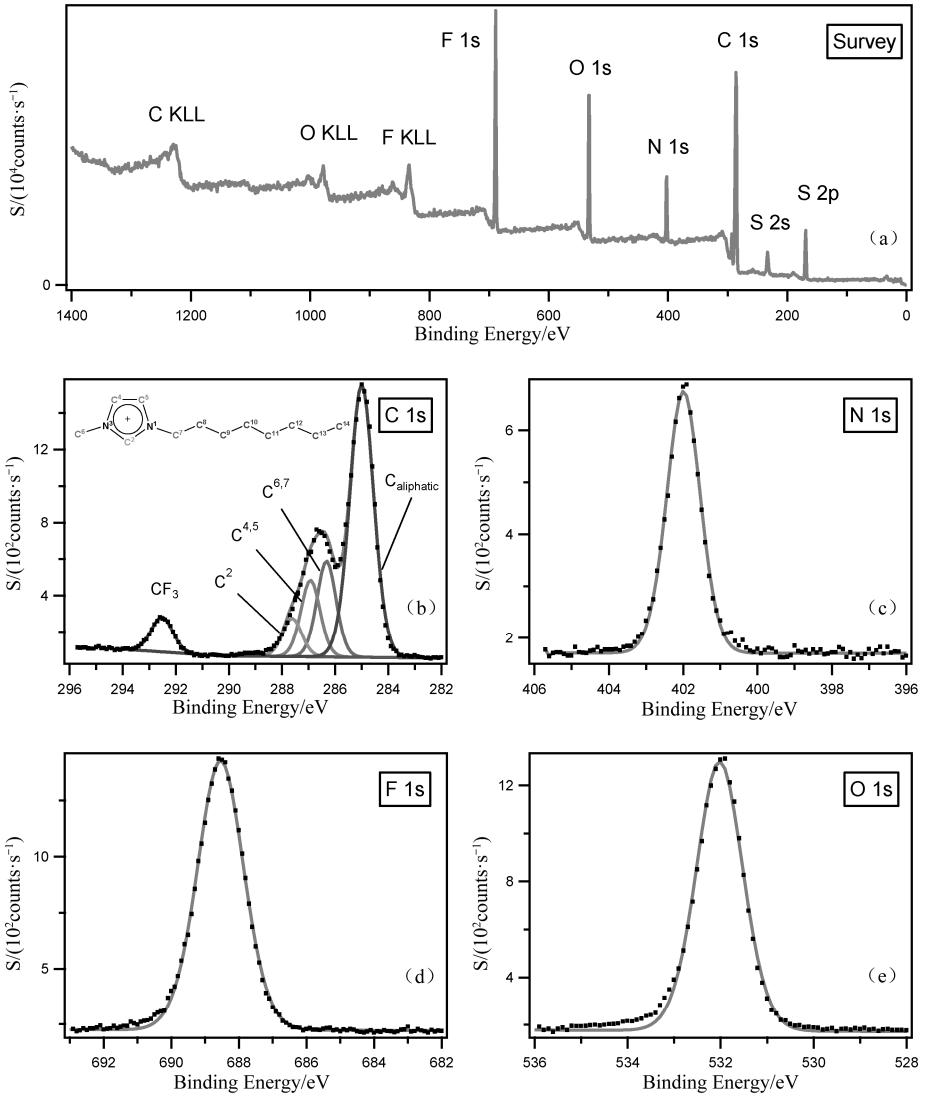

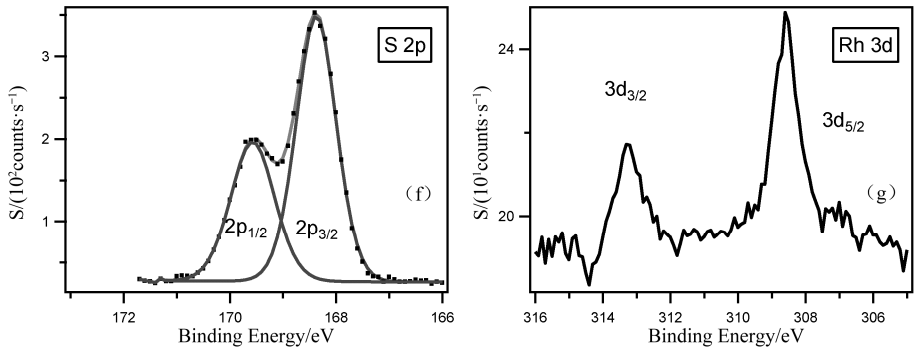

20 XP spectra with component fittings of $[Rh(acac)(CO)_2]$ plus PPh_3 in $[C_8C_1Im][BF_4]$ for: (a) survey, (b) C 1s, (c) N 1s, (d) F 1s, (e) B 1s and (f) Rh 3d.

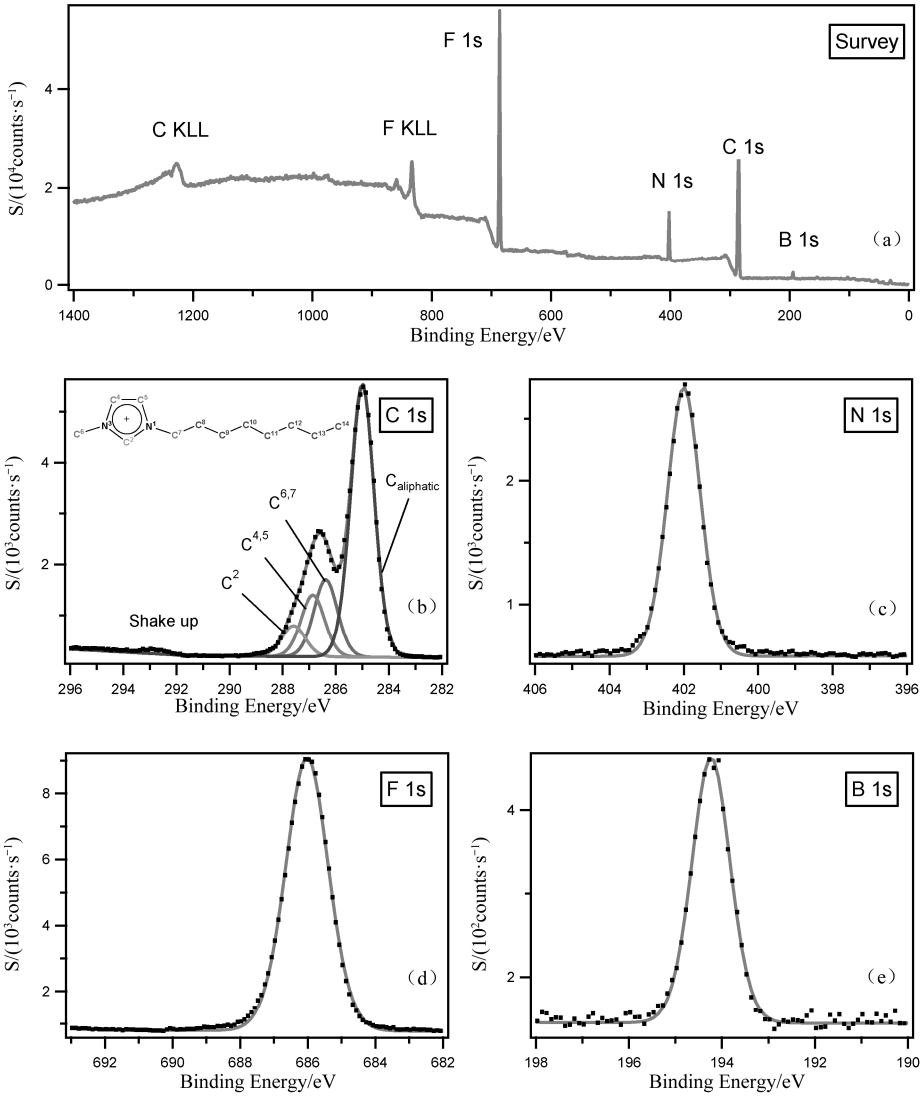

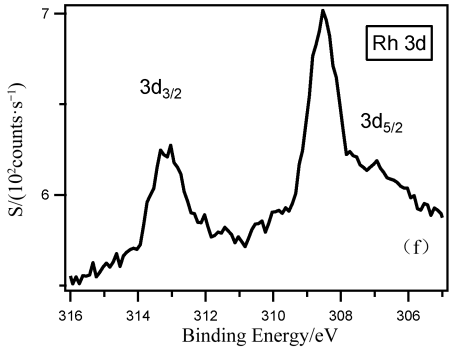

21 XP spectra with component fittings of [Rh(acac)$(CO)_2$] plus PPh_3 in [C_8C_1Im]Cl for: (a) survey, (b) C 1s, (c) N 1s, (d) Cl 2p and (e) Rh 3d.

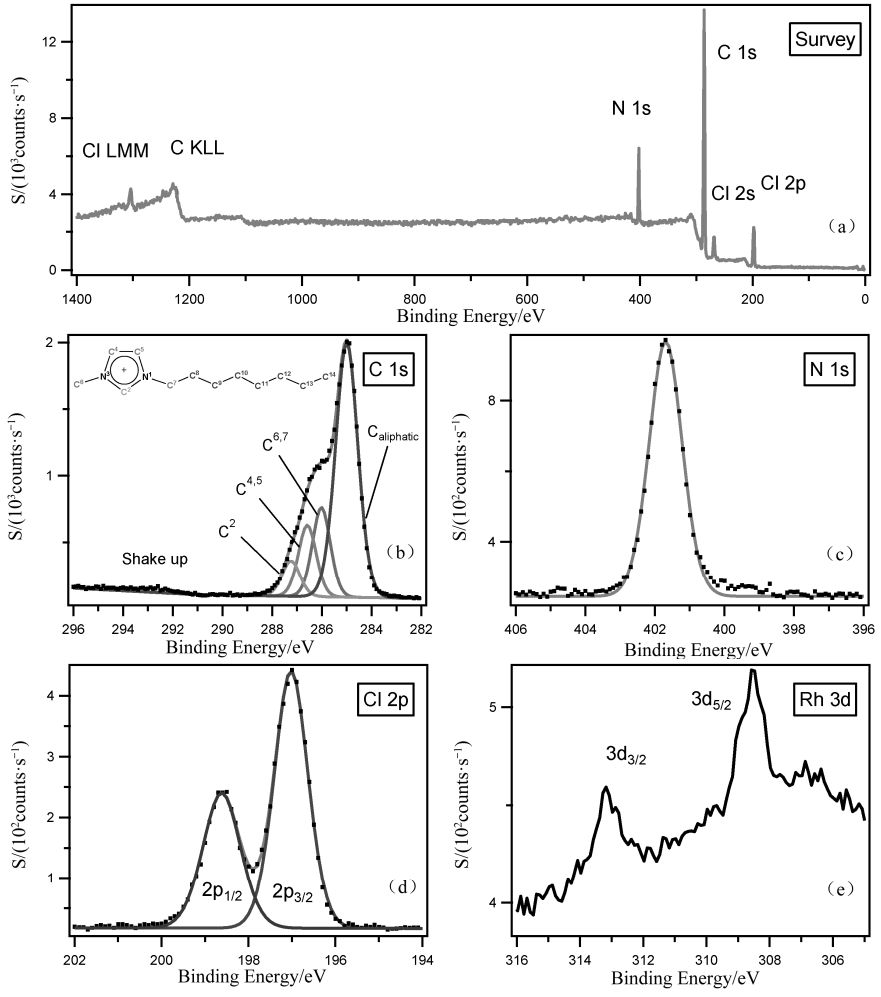

22 XP spectra with component fittings of [Rh(acac)$(CO)_2$] plus PPh_3 in [C_8C_1Im][OAc] for: (a) survey, (b) C 1s, (c) N 1s, (d) O 1s and (e) Rh 3d.

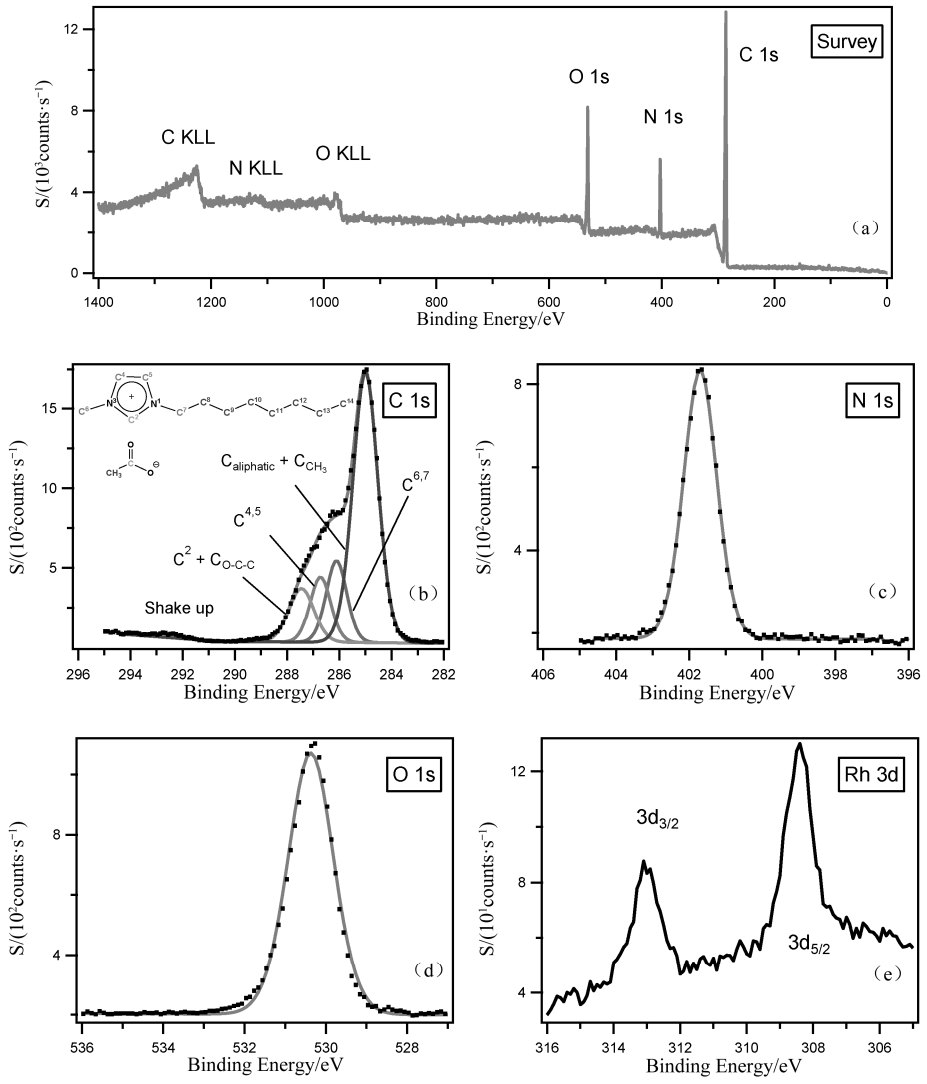

23 XP spectra with component fittings of [Rh(acac)(CO)$_2$] plus dppf in [C_8C_1Im][TfO] for: (a) survey, (b) C 1s, (c) N 1s, (d) F 1s, (e) O 1s, (f) S 2p and (g) Rh 3d.

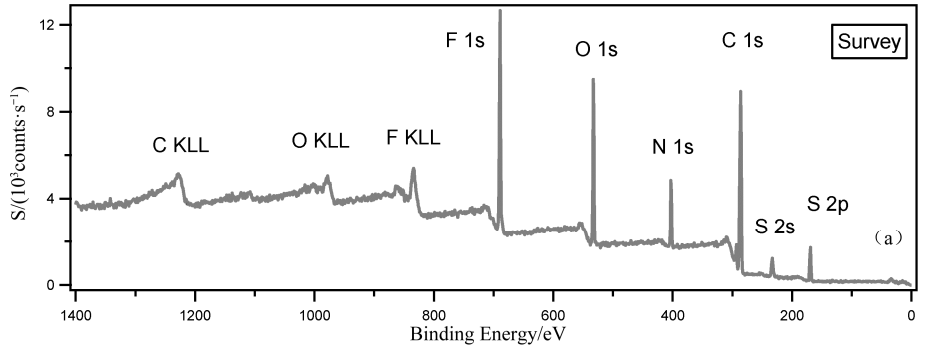

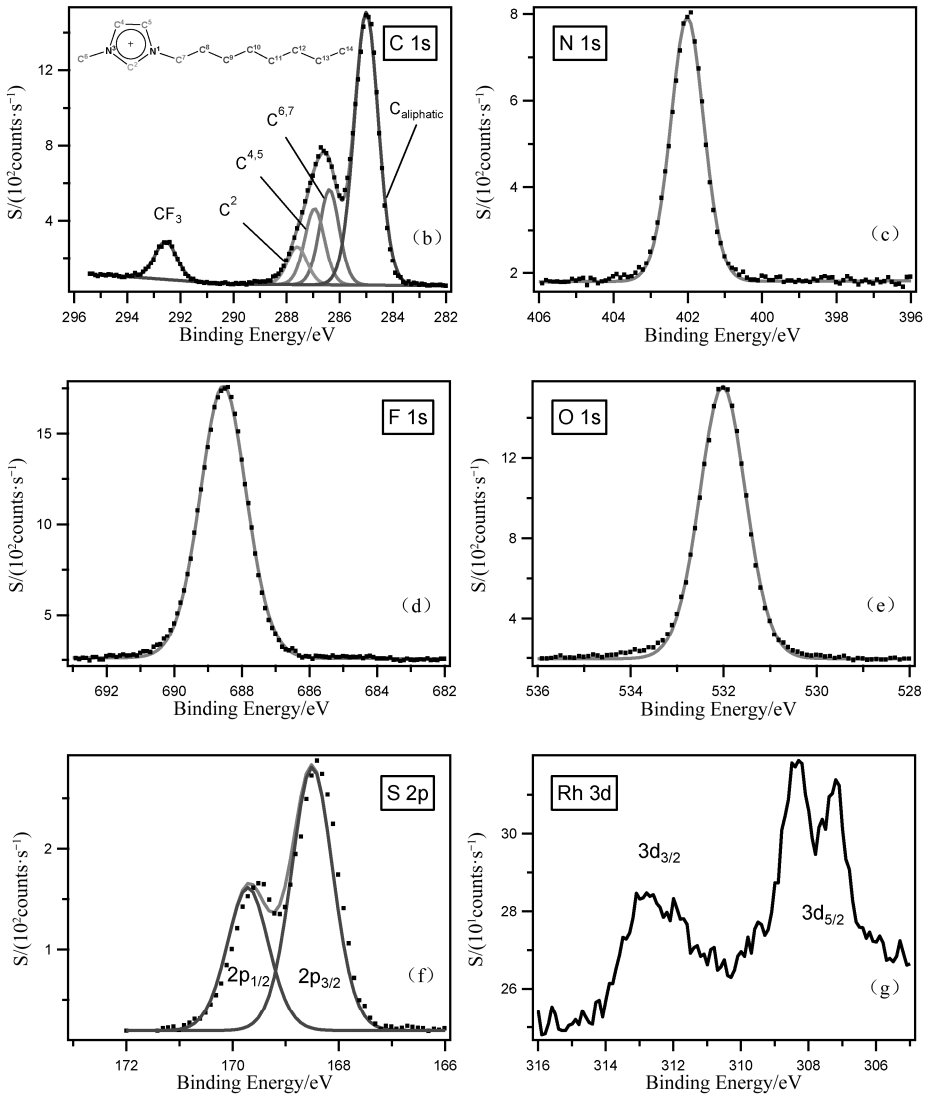
C 1s
N 1s
F 1s
O 1s
S 2p
Rh 3d
CF3
C2
C4,5
C6,7
Caliphatic
2p1/2
2p3/2
3d3/2
3d5/2
(b)
(c)
(d)
(e)
(f)
(g)
S/(10²counts·s⁻¹)
S/(10¹counts·s⁻¹)
Binding Energy/eV

反侵权盗版声明